PUSHOVER ANALYSIS OF R/C SETBACK BUILDING FRAMES

A THESIS

Submitted by

RASMITA TRIPATHY (609 CE 302)

In partial fulfillment of the requirements for
the award of the degree of

MASTER OF TECHNOLOGY (RESEARCH)

Department of Civil Engineering
National Institute of Technology Rourkela
Orissa -769 008, India

August 2012

THESIS CERTIFICATE

This is to certify that the thesis entitled "**PUSHOVER ANALYSIS OF R/C SETBACK BUILDING FRAMES"** submitted by **RASMITA TRIPATHY** to the National Institute of Technology Rourkela for the award of the degree of Master of Technology (Research) is a bonafide record of research work carried out by her under my supervision. The contents of this thesis, in full or in parts, have not been submitted to any other Institute or University for the award of any degree or diploma.

Rourkela – 769 008
Date:

Dr Pradip Sarkar
Department of Civil Engineering

ACKNOWLEDGEMENTS

I would like to express my sincere gratitude to my thesis supervisor Professor Pradip Sarkar, Department of Civil Engineering, National Institute of Technology Rourkela, for his guidance, inspiration, moral support and affectionate relationship throughout the course of this research. I consider myself as very fortunate to get this opportunity to work under his guidance. Without his invaluable guidance and support, this thesis would not have been possible.

My sincere thanks to Prof. N. Roy, Prof. M. Panda and Prof. S.P. Singh, National Institute of Technology Rourkela, for their suggestions and encouragement.

The support received from Department of Science and Technology, Govt. of India funded project at NIT Rourkela (CE- CSB) is gratefully acknowledged.

I would like to thank my parents, sister and brother for their continuous support and encouragement throughout my life. I also extend my sincere thanks to my husband Mihir for his understanding, patience and inspiration.

Last but not the least; I thank my colleagues and friends for their encouragement and help.

RASMITA TRIPATHY

ABSTRACT

KEYWORDS: *setback building; pushover analysis; irregularity; target displacement; lateral load profile; time history analysis.*

The behaviour of a multi-storey framed building during strong earthquake motions depends on the distribution of mass, stiffness, and strength in both the horizontal and vertical planes of the building. In multi-storeyed framed buildings, damage from earthquake ground motion generally initiates at locations of structural weaknesses present in the lateral load resisting frames. Further, these weaknesses tend to accentuate and concentrate the structural damage through plastification that eventually leads to complete collapse. In some cases, these weaknesses may be created by discontinuities in stiffness, strength or mass between adjacent storeys. Such discontinuities between storeys are often associated with sudden variations in the frame geometry along the height. There are many examples of failure of buildings in past earthquakes due to such vertical discontinuities. Irregular configurations either in plan or elevation were often recognised as one of the main causes of failure during past earthquakes. A common type of vertical geometrical irregularity in building structures arises from abrupt reduction of the lateral dimension of the building at specific levels of the elevation. This building category is known as the setback building. Many investigations have been performed to understand the behaviour of irregular structures as well as setback structures and to ascertain method of improving their performance.

Pushover analysis is a nonlinear static analysis used mainly for seismic evaluation of framed building. Conventional pushover analysis outlined in FEMA 356:2000 and ATC 40:1996 is limited for the buildings with regular geometry. It may not be possible to evaluate the seismic performance of setback building accurately using conventional nonlinear static (pushover)

analysis outlined in FEMA 356:2000 and ATC 40:1996, because of its limitations for the irregular structures with significant higher modes effects. There is no research effort found in the literature to use this analysis procedure for setback building. It is instructive to study the performance of conventional pushover analysis methodology as well as other alternative pushover methodologies for setback buildings and to suggest improvements suitable for setback buildings.

In the present study an improved procedure for estimating target displacement of setback buildings is proposed. This proposal is a simple modification of the displacement coefficient method as outlined in FEMA 356: 2000. A parametric study is also carried out to understand the applicability of existing lateral load patterns on the pushover analysis of setback building. It is found that mass proportional uniform load pattern is most suitable amongst others for pushover analysis of setback buildings. The results of the study show that pushover analysis carried out by mass proportional uniform load pattern and proposed modification in target displacement estimation procedure consistently predicting the results close to that of nonlinear dynamic analyses.

TABLE OF CONTENTS

Title ..... Page No.

ACKNOWLEDGEMENTS i

ABSTRACT ii

TABLE OF CONTENTS iv

LIST OF TABLES vii

LIST OF FIGURES viii

ABBREVIATIONS xiv

NOTATION xv

CHAPTER 1 INTRODUCTION

1.1 Background and Motivation 1

1.2 Objectives of the Thesis 4

1.3 Scope of the Study 6

1.4 Methodology 6

1.5 Organisation of the Thesis 7

CHAPTER 2 LITERATURE REVIEW

2.1 Introduction 9

2.2 Research on Setback Building 10

2.3 Research on Performance Based Seismic Engineering and Pushover Analysis 12

2.4 Pushover Analysis – An Overview 14

2.4.1 Pushover Analysis Procedure 15

2.4.2 Lateral Load Profile 17

2.4.3 Target displacement 20

2.4.4 Pushover Analysis of Buildings with Non-orthogonal frames 26

2.5 Shortcomings of the Pushover Analysis 27

2.6 Alternate Pushover Analysis Procedures 29
2.6.1 Modal pushover analysis 29
2.6.2 Modified modal pushover analysis 34
2.6.3 Upper-bound pushover analysis 38
2.6.4 Adaptive pushover analysis 41
2.7 Improvement over Conventional Pushover Analysis 43
2.8 Summary 46

CHAPTER 3 STRUCTURAL MODELLING

3.1 Introduction 47
3.2 Computational Model 47
3.2.1 Material properties 48
3.2.2 Structural elements 48
3.3 Building Geometry 49
3.4 Modelling of Flexural Plastic Hinges 53
3.4.1 Stress-strain characteristics for concrete 54
3.4.2 Stress-strain characteristics for reinforcing steel 56
3.4.3 Moment-curvature relationship 57
3.4.4 Modelling of moment-curvature in RC sections 59
3.4.5 Moment-rotation parameters for Beams 61
3.4.6 Moment-rotation parameters for Columns (PMM Hinges) 65
3.5 Modelling of shear hinges for beams and columns 66
3.6 Nonlinear Time History Analysis 69
3.6.1 Natural record of earthquake ground motion 72
3.7 Summary 72

CHAPTER 4 RESULTS AND DISCUSSIONS

4.1 Introduction 73

4.2 Study on Invariant Load Patterns....73

4.2.1 Comparison of the shape of available Load Patterns....74

4.2.2 Comparison of the Load Patterns for their Applicability to Setback Buildings....99

4.3 Study on Target Displacement....126

4.3.1 Proposed procedure of Target Displacements estimation for setback Buildings....127

4.4 Performance of proposed Pushover analysis....138

4.5 Summary....141

CHAPTER 5 SUMMARY AND CONCLUSIONS

5.1 Summary....142

5.2 Conclusions....146

5.3 Scope of Future study....148

APPENDIX A....150

APPENDIX B....159

REFERENCES....171

LIST OF TABLES

Table No.	Title	Page No.
2.1	Values of C_0 factor for shear building as per FEMA 356	23
3.1	The range of natural periods of the selected building models	51
3.2	Characteristics of the selected ground motion	71
4.1	Comparison of estimated target displacement using different procedures	139

LIST OF FIGURES

Figure No.	Title	Page No.
1.1	The Paramount Building at New York, United States	2
1.2	Typical Setback Building at India	3
2.1	Schematic representation of pushover analysis procedure	17
2.2	Lateral load pattern for pushover analysis as per FEMA 356	20
2.3	Schematic representation of Displacement Coefficient Method (FEMA 356)	21
2.4	Schematic representation of Capacity spectrum Method (ATC 40)	24
2.5	Effective damping in Capacity Spectrum Method (ATC 40)	25
2.6	Properties of the nth-mode inelastic SDOF system from the pushover curve	33
2.7	First-, second- and third- mode pushover curves for a typical building and corresponding target roof displacement (Chopra and Goel, 2004)	36
2.8	Adaptive pushover analysis (Papanikolaou *et. al*., 2005)	42
3.1	Use of end offsets at beam-column joint	48
3.2	Typical building models used in the present study	49
3.3	Fundamental period versus overall height variation of all the selected frames	50
3.4	The coordinate system used to define the flexural and shear hinges	53
3.5	Typical stress-strain curve for M-20 grade concrete (Panagiotakos and Fardis 2001)	56
3.6	Stress-strain relationship for reinforcement – IS 456 (2000)	57
3.7	Curvature in an initially straight beam section	58
3.8	(a) cantilever beam, (b) Bending moment distribution, and (c) Curvature distribution (Park and Paulay, 1975)	62
3.9	Idealised moment-rotation curve of RC beam sections	64
3.10	PMM Interaction Surface	65

3.11 Idealised moment-rotation curve of RC elements 66
3.12 Typical shear force- deformation curves to model shear hinges 67
4.1 Lateral load patterns for R-8-4 building frame 75
4.2 Lateral load patterns for S1-8-4 building frame 75
4.3 Lateral load patterns for S2-8-4 building frame 76
4.4 Lateral load patterns for S3-8-4 building frame 76
4.5 Lateral load patterns for R-8-8 building frame 77
4.6 Lateral load patterns for S1-8-8 building frame 77
4.7 Lateral load patterns for S2-8-8 building frame 78
4.8 Lateral load patterns for S3-8-8 building frame 78
4.9 Lateral load patterns for R-8-12 building frame 79
4.10 Lateral load patterns for S1-8-12 building frame 79
4.11 Lateral load patterns for S2-8-12 building frame 80
4.12 Lateral load patterns for S3-8-12 building frame 80
4.13 Lateral load patterns for R-12-4 building frame 81
4.14 Lateral load patterns for S1-12-4 building frame 81
4.15 Lateral load patterns for S2-12-4 building frame 82
4.16 Lateral load patterns for S3-12-4 building frame 82
4.17 Lateral load patterns for R-12-8 building frame 83
4.18 Lateral load patterns for S1-12-8 building frame 83
4.19 Lateral load patterns for S2-12-8 building frame 84
4.20 Lateral load patterns for S3-12-8 building frame 84
4.21 Lateral load patterns for R-12-12 building frame 85
4.22 Lateral load patterns for S1-12-12 building frame 85
4.23 Lateral load patterns for S2-12-12 building frame 86
4.24 Lateral load patterns for S3-12-12 building frame 86
4.25 Lateral load patterns for R-16-4 building frame 87

4.26 Lateral load patterns for S1-16-4 building frame 87
4.27 Lateral load patterns for S2-16-4 building frame 88
4.28 Lateral load patterns for S3-16-4 building frame 88
4.29 Lateral load patterns for R-16-8 building frame 89
4.30 Lateral load patterns for S1-16-8 building frame 89
4.31 Lateral load patterns for S2-16-8 building frame) 90
4.32 Lateral load patterns for S3-16-8 building frame 90
4.33 Lateral load patterns for R-16-12 building frame 91
4.34 Lateral load patterns for S1-16-12 building frame 91
4.35 Lateral load patterns for S2-16-12 building frame 92
4.36 Lateral load patterns for S3-16-12 building frame 92
4.37 Lateral load patterns for R-20-4 building frame 93
4.38 Lateral load patterns for S1-20-4 building frame 93
4.39 Lateral load patterns for S2-20-4 building frame 94
4.40 Lateral load patterns for S3-20-4 building frame 94
4.41 Lateral load patterns for R-20-8 building frame 95
4.42 Lateral load patterns for S1-20-8 building frame 95
4.43 Lateral load patterns for S2-20-8 building frame 96
4.44 Lateral load patterns for S3-20-8 building frame 96
4.45 Lateral load patterns for R-20-12 building frame 97
4.46 Lateral load patterns for S1-20-12 building frame 97
4.47 Lateral load patterns for S2-20-12 building frame 98
4.48 Lateral load patterns for S3-20-12 building frame 98
4.49 Pushover curve for different load patterns for R-8-4 building category.....100
4.50 Pushover curve for different load patterns for S1-8-4 building category 100
4.51 Pushover curve for different load patterns for S2-8-4 building category 101
4.52 Pushover curve for different load patterns for S3-8-4 building category 101

4.53 Pushover curve for different load patterns for R-8-8 building category.....102

4.54 Pushover curve for different load patterns for S1-8-8 building category 102

4.55 Pushover curve for different load patterns for S2-8-8 building category 103

4.56 Pushover curve for different load patterns for S3-8-8 building category 103

4.57 Pushover curve for different load patterns for R-8-12 building category.....104

4.58 Pushover curve for different load patterns for S1-8-12 building category ...104

4.59 Pushover curve for different load patterns for S2-8-12 building category ...105

4.60 Pushover curve for different load patterns for S3-8-12 building category ...105

4.61 Pushover curve for different load patterns for R-12-4 building category.....106

4.62 Pushover curve for different load patterns for S1-12-4 building category ...106

4.63 Pushover curve for different load patterns for S2-12-4 building category ...107

4.64 Pushover curve for different load patterns for S3-12-4 building category ...107

4.65 Pushover curve for different load patterns for R-12-8 building category.....108

4.66 Pushover curve for different load patterns for S1-12-8 building category ...108

4.67 Pushover curve for different load patterns for S2-12-8 building category ...109

4.68 Pushover curve for different load patterns for S3-12-8 building category ...109

4.69 Pushover curve for different load patterns for R-12-12 building category...110

4.70 Pushover curve for different load patterns for S1-12-12 building category.....110

4.71 Pushover curve for different load patterns for S2-12-12 building category.....111

4.72 Pushover curve for different load patterns for S3-12-12 building category.....111

4.73 Pushover curve for different load patterns for R-16-4 building category.....112

4.74 Pushover curve for different load patterns for S1-16-4 building category ...112

4.75 Pushover curve for different load patterns for S2-16-4 building category ...113

4.76 Pushover curve for different load patterns for S3-16-4 building category ...113

4.77 Pushover curve for different load patterns for R-16-8 building category.....114

4.78 Pushover curve for different load patterns for S1-16-8 building category ...114

4.79 Pushover curve for different load patterns for S2-16-8 building category ...115

4.80 Pushover curve for different load patterns for S3-16-8 building category ...115

4.81 Pushover curve for different load patterns for R-16-12 building category...116

4.82 Pushover curve for different load patterns for S1-16-12 building category.....116

4.83 Pushover curve for different load patterns for S2-16-12 building category.....117

4.84 Pushover curve for different load patterns for S3-16-12 building category.....117

4.85 Pushover curve for different load patterns for R-20-4 building category.....118

4.86 Pushover curve for different load patterns for S1-20-4 building category ...118

4.87 Pushover curve for different load patterns for S2-20-4 building category ...119

4.88 Pushover curve for different load patterns for S3-20-4 building category ...119

4.89 Pushover curve for different load patterns for R-20-8 building category.....120

4.90 Pushover curve for different load patterns for S1-20-8 building category ...120

4.91 Pushover curve for different load patterns for S2-20-8 building category ...121

4.92 Pushover curve for different load patterns for S3-20-8 building category ...121

4.93 Pushover curve for different load patterns for R-20-12 building category...122

4.94 Pushover curve for different load patterns for S1-20-12 building category.....122

4.95 Pushover curve for different load patterns for S2-20-12 building category.....123

4.96 Pushover curve for different load patterns for S3-20-12 building category.....123

4.97 Correlation between maximum roof displacements of regular frames to the spectral displacement for corresponding equivalent SDOF system.....128

4.98 Correlation between maximum roof displacements of setback frames (S1) to the spectral displacement for corresponding equivalent SDOF system 129

4.99 Correlation between maximum roof displacements of setback frames (S2) to the spectral displacement for corresponding equivalent SDOF system 130

4.100 Correlation between maximum roof displacements of setback frames (S3) to the spectral displacement for corresponding equivalent SDOF system 130

4.101 Variation of C_0-Factor with bay numbers for 8-storey building variants 131

4.102 Variation of C_0-Factor with bay numbers for 12-storey building variants ...132

4.103 Variation of C_0-Factor with bay numbers for 16-storey building variants ...132

4.104 Variation of C_0-Factor with bay numbers for 20-storey building variants ...133

4.105 Variation of C_0-Factor with storey numbers for 4-bay building variants 133

4.106 Variation of C_0-Factor with storey numbers for 8-bay building variants 134

4.107 Variation of C_0-Factor with storey numbers for 12-bay building variants ...134

4.108 Variation of C_0-Factor with percentage setback for 20- storey building variants 135

4.109 Variation of C_0-Factor with percentage setback for 16- storey building variants 135

4.110 Variation of C_0-Factor with percentage setback for 12- storey building variants 136

4.111 Variation of C_0-Factor with percentage setback for 8- storey building variants 136

4.112 Comparison of mean time-history results and the proposed function 137

ABBREVIATIONS

ACI	-	American Concrete Institute
ATC	-	Applied Technology Council
BS	-	British Standard
CQC	-	Complete Quadratic Combination
CSM	-	Capacity Spectrum Method
DCM	-	Displacement Coefficient Method
EC	-	Eurocode
FEMA	-	Federal Emergency Management Agency
IS	-	Indian Standard
MDOF	-	Multi Degree of Freedom
MMPA	-	Modified Modal Pushover Analysis
MODE 1	-	Fundamental Mode Shape as Load Pattern
MPA	-	Modal Pushover Analysis
PGA	-	Peak Ground Acceleration
RC	-	Reinforced Concrete
SAP	-	Structural Analysis Program
SDOF	-	Single Degree of Freedom
SRSS	-	Square Root of Sum of the Squares
TRI	-	Triangular Load Pattern
UBPA	-	Upper Bound Pushover Analysis

NOTATION

English Symbols

a	-	regression constant
c	-	classical damping
C_0	-	factor for MDOF displacement
C_1	-	factor for inelastic displacement
C_2	-	factor for strength and stiffness degradation
C_3	-	factor for geometric nonlinearity
d	-	effective depth of the section
d_b	-	diameter of the longitudinal bar
d_p	-	spectral displacement corresponding to performance point
D	-	overall depth of the beam.
$D_n(t)$	-	displacement response for an equivalent SDOF system,
E_c	-	short-term modulus of elasticity of concrete
E_D	-	energy dissipated by damping
E_s	-	modulus of elasticity of steel rebar
E_S	-	maximum strain energy
E_{sec}	-	elastic secant modulus
EI	-	flexural rigidity of beam
f_c	-	concrete compressive stress
f'_{cc}	-	compressive strength of confined concrete
f'_{co}	-	unconfined compressive strength of concrete
f_{ck}	-	characteristic compressive strength of concrete
F_e	-	elastic strength
$\{f_s(t)\}$	-	lateral load vector

$\{f_{s,UB}\}$ - force vector in upper bound pushover analysis

f_y - yield stress of steel rebar

F_y - defines the yield strength capacity of the SDOF

f_{yh} - grade of the stirrup reinforcement

G - shear modulus of the reinforced concrete section

h - overall building height (in m)

k - lateral stiffness

k_e - confinement effectiveness coefficient

K_{eq} - equivalent stiffness

K_i - initial stiffness

l - length of frame element

l_p - equivalent length of plastic hinge

m - storey mass

M_n^* - modal mass for n^{th} mode

N - number of modes considered

$P_{eff}(t)$ - effective earthquake force

$q_n(t)$ - the modal coordinate for n^{th} mode

R - Regular frame considered for study

S1 - Type- 1 setback frame considered for study

S2 - Type- 2 setback frame considered for study

S3 - Type- 3 setback frame considered for study

$\{s\}$ - height-wise distribution of effective earthquake force

S_a - spectral acceleration

S_d - spectral displacement

$\{s_n\}$ - n^{th} mode contribution in $\{s\}$

SR_A - spectral reduction factor at constant acceleration region

SR_V - spectral reduction factor at constant velocity region

T - fundamental natural period of vibration

T_{eq} - equivalent time period

T_i - initial elastic period of the structure

T_n - n^{th} mode natural period

$\ddot{u}_g(t)$ - earthquake ground acceleration

$u_{n,roof}(t)$ - displacement at the roof due to n^{th} mode

$u_{no,roof}$ - peak value of the roof displacement due to n^{th} mode

$u_{roof}(t)$ - roof displacement at time 't'

[illegible] - target roof displacement in upper bound pushover analysis

V_{Bn} - base shear capacity for n^{th} mode pushover analysis

x - strain ratio

Greek Symbols

α - post-yield stiffness ratio

β_{eq} - equivalent damping

β_i - initial elastic damping

β_s - damping due to structural yielding

δ_t - target displacement

ε_{sm} - steel strain at maximum tensile stress

$\{\phi_n\}$ - n^{th} mode shape of the structure

$\phi_{n,roof}$ - value of the n^{th} mode shape at roof

φ_u - ultimate curvature

φ_y - yield curvature

κ - an adjustment factor to approximately account for changes in hysteretic behaviour in reinforced concrete structures

μ - displacement ductility ratio

θ_p - plastic rotation

θ_u - ultimate rotation

θ_y - yield rotation

ρ_s - volumetric ratio of confining steel

ω_n - n^{th} mode natural frequency

ξ_n - n^{th} mode damping ratio

Γ_n - modal participation factor of the n^{th} mode

CHAPTER 1

INTRODUCTION

1.1 BACKGROUND AND MOTIVATION

In multi-storeyed framed buildings, damage from earthquake ground motion generally initiates at locations of structural weaknesses present in the lateral load resisting frames. This behaviour of multi-storey framed buildings during strong earthquake motions depends on the distribution of mass, stiffness, and strength in both the horizontal and vertical planes of buildings. In some cases, these weaknesses may be created by discontinuities in stiffness, strength or mass between adjacent storeys. Such discontinuities between storeys are often associated with sudden variations in the frame geometry along the height. There are many examples of failure of buildings in past earthquakes due to such vertical discontinuities. Structural engineers have developed confidence in the design of buildings in which the distributions of mass, stiffness and strength are more or less uniform. But there is a less confidence about the design of structures having irregular geometrical configurations.

A common type of vertical geometrical irregularity in building structures arises is the presence of setbacks, *i.e*. the presence of abrupt reduction of the lateral dimension of the building at specific levels of the elevation. This building category is known as ‘setback building’. This building form is becoming increasingly popular in modern multi-storey building construction mainly because of its functional and aesthetic architecture. In particular, such a setback form provides for adequate daylight and ventilation for the

lower storeys in an urban locality with closely spaced tall buildings. This type of building form also provides for compliance with building bye-law restrictions related to ‘floor area ratio’ (practice in India). Figs 1.1 to 1.2 show typical examples of setback buildings. Setback buildings are characterised by staggered abrupt reductions in floor area along the height of the building, with consequent drops in mass, strength and stiffness.

Fig. 1.1: The Paramount Building at New York, United States

Height-wise changes in stiffness and mass render the dynamic characteristics of these buildings different from the ‘regular’ building. It has been reported in the literature (Athanassiadou, 2008) that higher mode participation is significant in these buildings. Also, the inter-storey drifts for setback building are expected to be more in the upper floors and less in the lower floors, compared to regular buildings without setback.

Fig. 1.2: Typical Setback building at India

Many investigations have been performed to understand the behaviour of irregular structures as well as setback structures and to ascertain method of improving their performance.

It may not be possible to evaluate the seismic performance of setback building accurately using conventional nonlinear static (pushover) analysis outlined in FEMA 356 (2000) and ATC 40 (1996), because of its limitations for the irregular structures with significant higher modes effects. There have been a number of efforts reported in literature to extend the pushover analysis procedure to include different irregular building categories. However, so far, setback buildings have not been addressed in this regard. It is instructive to study the performance of conventional pushover analysis methodology as well as other alternative pushover methodologies for

setback buildings and to suggest improvements suitable for setback buildings. This is the primary motivation underlying the present study.

1.2 OBJECTIVES OF THE THESIS

A detailed literature review is carried out to define the objectives of the thesis. This is discussed in detail in Chapter 2 and briefly summarised here. Design codes have not given particular attention to the setback building form. The research papers on setback buildings conclude that the displacement demand is dependent on the geometrical configuration of frame and concentrated in the neighbourhood of the setbacks for setback buildings. The higher modes significantly contribute to the response quantities of structure. Also conventional pushover analysis seems to be underestimating the response quantities in the upper floors of the irregular frames.

Prestandard and Commentary for the Seismic Rehabilitation of Buildings: FEMA 356:2000, American Society of Civil Engineers, USA describes the non-linear static analysis or pushover analysis procedure to estimate the seismic demand and capacity of the existing structure. In this procedure the magnitude of lateral load is increased monotonically along the height of the building. The building is displaced up to the target displacement or until the collapse of the building. A curve is drawn between base shear and roof displacement known as the pushover curve or capacity curve. The generation of capacity curve defines the capacity of the building for an assumed force distribution and displacement pattern. A point on the curve defines a specific damage state for the structure. By correlating this capacity curve to the seismic demand generated by a specific earthquake ground motion, a point can be found on the capacity curve that

estimates the maximum displacement of the building the earthquake will cause. This defines the performance point or target displacement. The location of this performance point relative to the performance levels defined by the capacity curve indicates whether or not the performance objective is met. This analysis, as explained in FEMA 356, is primarily meant for regular buildings with dominant fundamental mode participation.

There are many alternative approaches of pushover analysis reported in the literature to make it applicable for different categories of irregular buildings. These comprise (i) *modal pushover analysis* (Chopra and Goel, 2001), (ii) *modified modal pushover analysis* (Chopra *et. al*., 2004), (iii) *upper bound pushover analysis* (Jan *et. al*., 2004), and (iv) *adaptive pushover analysis*, etc. However, none of these methods have been tested for setback buildings.

Based on the literature review presented later, the salient objectives of the present study have been identified as follows:

1. To assess different pushover methodologies available in literature for their applicability to setback buildings.
2. To propose improvements in existing pushover analysis techniques for Setback buildings, supported by nonlinear time history analyses.

The principal objective of the proposed research is to extend the conventional pushover analysis procedure (FEMA-356), which retains the conceptual simplicity and computational attractiveness of current procedures with invariant force distribution, but provide superior accuracy in estimating seismic demands on setback building.

1.3 SCOPE OF THE STUDY

The present study is limited to reinforced concrete (RC) multi-storeyed building frames with setbacks. Setback buildings up to 20 storeys with different degrees of irregularity are considered. The buildings are assumed to have setback only in one direction.

The plan asymmetry arising out of the vertical geometric irregularity strictly calls for three-dimensional analysis to account properly for torsion effects. This is not considered in the present study, which is limited to analysis of plane setback frames. Although different storey numbers (up to 20 storeys), bay numbers (up to 12 bays) and irregularity are considered, the bay width is restricted, to 6m and storey height to 3m.

It will be appropriate to consider adaptive load pattern in pushover analysis in order to include the effect of progressive structural yielding. However, for the present study only fixed load distribution shapes are planned to utilise in pushover analysis, in order to keep the procedure computationally simple and attractive for design office environment. Soil-structure interaction effects are not considered.

1.4 METHODOLOGY

The steps undertaken in the present study to achieve the above-mentioned objectives are as follows:

a) Carry out extensive literature review, to establish the objectives of the research work.

b) Select an exhaustive set of setback building frame models with different heights (8 to 20 storeys), widths (4 to 12 bays) and different irregularities (limit to 48 setback frame models).

c) Analyse each of the 48 building models, using all the major nonlinear static (pushover) analysis procedures.

d) Reanalyse the above frames using nonlinear time history analysis procedure, considering 15 ground motion records each.

e) Perform a comparative study and rate the different pushover analysis procedures for their applicability to setback building frames.

f) Explore possible improvements in existing pushover analysis procedure (load vector and target displacement estimation) for its applicability to setback buildings.

1.5 ORGANISATION OF THE THESIS

This introductory chapter has presented the background, objective, scope and methodology of the present study. Chapter 2 starts with a description of the previous work done on setback moment-resisting frames by other researchers. Later in the chapter, a description of traditional pushover analysis procedures as per FEMA 356 and ATC 40 are presented and the major limitations of this procedure discussed. Finally, this chapter discusses selected alternative methods reported in literature to overcome the existing limitations.

Chapter 3 describes the analytical modelling used in the present study for representing the actual behaviour of different structural components in the building frame. It also describes in detail the modelling of point plastic hinges used in the present study, algorithm for generating hinge properties and the assumptions considered. This Chapter then presents the different geometries of setback building considered in the study.

Finally, this chapter presents the input ground motion and other parameters used for nonlinear time-history analysis.

Chapter 4 begins with a presentation of general behaviour of setback buildings under earthquake ground motion. It explains the proposed spatial distribution of lateral load for pushover analysis of setback buildings and pushover curves for the buildings by this proposed load pattern. This chapter also explains non-linear time history analysis for the buildings. Finally, this chapter presents the proposed improvement of displacement coefficient method for the estimation of target displacement of setback building.

Finally, Chapter 5 presents a summary including salient features, significant conclusions from this study and the future scope of research in this area.

CHAPTER 2

LITERATURE REVIEW

2.1 INTRODUCTION

The literature review is conducted in two major areas. These are: (i) Performances of setback buildings under seismic loading and (ii) Performance based seismic engineering that uses pushover analysis tools. The first half of this chapter is devoted to a review of published literature to setback building frames. This part describes a number of experimental and analytical works on setback buildings.

The second half of this chapter is devoted to a review of published literature related to performance based seismic engineering and pushover analysis methods. The nonlinear static analysis methods published in the ATC 40 (1996) report together with the FEMA 273/274 (1997) documents and the subsequent FEMA 356 (2000) report are described. A description of traditional pushover analysis procedures as per FEMA 356 and ATC 40 is presented. Pushover analysis, as explained in these guidelines, is not free from limitations and these are mostly in terms of the applicability of pushover analysis for the structure with significant higher modes. Also, the current procedure of pushover analysis does not consider the change in modal properties due to progressive yielding of the building component. There have been a number of efforts published in recent literature to extend pushover analysis to take higher mode effects into account (Paret *et. al*., 1996; Sasaki *et. al*., 1998; Moghadam and Tso, 2002; Chopra and Goel, 2001; Chopra and Goel, 2002). Recent trends also include consideration of progressive structural yielding using adaptive procedures with updated force distributions that take into

account the current state of strength and stiffness of the building frame at each step (Bracci *et. al*., 1997; Gupta and Kunnath, 2000; Requena and Ayala, 2000; Antoniou *et. al.,* 2002; Aydinoglu, 2003). At the end, this chapter discusses the major limitations of the current pushover analysis procedure and some selected alternative pushover analysis procedures reported in literature.

2.2 RESEARCH ON SETBACK BUILDING

Analytical and experimental investigations by a number of researchers have identified differences in the dynamic response of regular and setback buildings. The studies focus on the displacement response and ductility demands at the tower-base junction location.

Karavasilis *et. al*. (2008) carried out a study on the inelastic seismic response of plane steel moment resisting frames with setbacks. A family of 120 such frames, designed according to the European seismic and structural codes, is subjected to an ensemble of 30 ordinary earthquake ground motions scaled to different intensities in order to drive the structures to different limit states. The author concluded that the level of inelastic deformation and geometrical configuration play an important role on the height wise distribution of deformation demands. The maximum deformation demands are concentrated in the "tower" for tower like structures and in the neighborhood of the setbacks for other geometrical configurations.

Athanassiadou (2008) addressed seismic performance of multi-storey reinforced concrete (R/C) frame buildings irregular in elevation. Two ten-storey two-dimensional plane frames with two and four large setbacks in the upper floors respectively, as well as a third one, regular in elevation, have been designed to the provisions of the 2004 Eurocode 8 (EC8). All frames have been subjected to both inelastic static pushover analysis and inelastic dynamic time-history

analysis for selected input motions. It is concluded that the effect of ductility class on the cost of building is negligible. Seismic performance of irregular frames are equally satisfactory (and not inferior) to that of the regular ones even for motions twice as strong as the design earthquake. Also conventional pushover analysis seems to be underestimating the response quantities in the upper floors of the irregular frames. This conclusion is based on the multi-mode elastic analysis and evaluates the seismic design provisions of Eurocode EC-8 according to which the design provision given in the European standard for setback building are not inferior to that for regular buildings. As per this reference the setback building and regular building designed as per EC-8 performs equally good when subjected to seismic loadings.

Shahrooz and Moehle (1990) studied the effects of setbacks on the earthquake response of multi-storeyed buildings. In an effort to improve design methods for setback structures, an experimental and analytical study was undertaken. In the experimental study, a six-storey moment-resisting reinforced concrete space frame with 50% setback in one direction at mid-height was selected. The analytical study focused on the test structure. The displacement profiles were relatively smooth over the height. Relatively large inter-storey drifts at the tower-base junction were accompanied by a moderate increase in damage at that level. Overall, the predominance of the fundamental mode on the global translational response in the direction parallel to the setback was clear from the displacement and inertia force profiles. The distribution of lateral forces was almost always similar to the distribution specified by the UBC code; no significant peculiarities in dynamic response were detected. To investigate further, an analytical study was also carried out on six generic reinforced concrete setback frames.

Soni and Mistry (2006) reviewed the studies on the seismic behavior of vertically irregular structures along with their findings in the building codes and available literatures and

summarized the knowledge in the seismic response of vertically irregular building frames. The building codes provide criteria to classify the vertical irregular structures and suggest dynamic analysis to arrive at design lateral forces. He observed most of the studies agree on the increase in drift demand in the tower portion of setback structures and on the increase in seismic demand for buildings with discontinuous distribution in mass, stiffness and strength. The largest seismic demand is found for the combined stiffness and strength irregularity.

Wong and Tso (1994) studied the validity of design code requirements for buildings with setbacks that require a dynamic analysis with the base shear calibrated by the static base shear obtained using the code's equivalent static load procedure. The paper discusses two major issues: (i) whether the code static base shear is applicable for buildings with setbacks and (ii) whether the higher mode period should be used in computing the base shear when the modal weight of a higher mode is larger than that of the fundamental mode. With regard to the first issue, modification factors were derived for adjusting the code period formula so that it can provide a more reasonable estimate for the period of a building with a setback. With regard to the second issue, it was demonstrated that for cases where the modal weight of a higher mode is larger than that of the fundamental mode, using the higher mode period for base shear calculation will result in unnecessarily conservative design.

2.3 RESEARCH ON PERFORMANCE BASED SEISMIC ENGINEERING AND PUSHOVER ANALYSIS

Naeim *et. al*. (2001) described the seismic performance of buildings and performance objectives to define the state of the building following a design earthquake. They also outlined the promises and limitations of performance based seismic engineering. They introduced and discussed the methodologies and techniques embodied in the two leading guidelines of this subject i.e. ATC-

40 and FEMA-273/274. They provided some numerical examples to illustrate the practical applications of the methods used.

Chandler and Mendis (2000) reviewed the force based seismic design method and also the displacement based seismic assessment approach. They also presented a case study for reinforced concrete moment resisting frames designed and detailed according to European and Australian code provisions having low, medium and high ductility capacity. They used Elcentro NS earthquake ground motion as the seismic input to get the performance characteristics of these frames. The author concluded the displacement based approach predicts accurately the overall displacement demands for the frames.

Ghobarah (2001) reviewed the reliability of performance based design in earthquake engineering, need of multiple performances, and hazard levels for future seismic design practice. He also reviewed the advantage of performance based seismic engineering. He concluded that the advantage of performance based design is the possibility of achieving predictable seismic performance with uniform risk and there are several challenges to be addressed and much research and development remain to be done before procedures for performance-based design can be widely accepted and implemented.

Goel and Chopra (1997) evaluated the formulas specified in present U.S. codes using the available data on the fundamental period of buildings measured from their motions recorded during eight California earthquakes from 1971 San Fernando earthquake to 1994 Northridge earthquake. They developed improved formulas for estimating the fundamental periods of reinforced concrete and steel moment resisting frame buildings by regression analysis of the

measured period data. Also, the paper recommended factors to limit the period calculated by a rational analysis.

2.4 PUSHOVER ANALYSIS – AN OVERVIEW

The use of the nonlinear static analysis (pushover analysis) came in to practice in 1970's but the potential of the pushover analysis has been recognized for last 10-15 years. This procedure is mainly used to estimate the strength and drift capacity of existing structure and the seismic demand for this structure subjected to selected earthquake. This procedure can be used for checking the adequacy of new structural design as well. The effectiveness of pushover analysis and its computational simplicity brought this procedure in to several seismic guidelines (ATC 40 and FEMA 356) and design codes (Eurocode 8 and PCM 3274) in last few years.

Pushover analysis is defined as an analysis wherein a mathematical model directly incorporating the nonlinear load-deformation characteristics of individual components and elements of the building shall be subjected to monotonically increasing lateral loads representing inertia forces in an earthquake until a 'target displacement' is exceeded. Target displacement is the maximum displacement (elastic plus inelastic) of the building at roof expected under selected earthquake ground motion. Pushover analysis assesses the structural performance by estimating the force and deformation capacity and seismic demand using a nonlinear static analysis algorithm. The seismic demand parameters are global displacements (at roof or any other reference point), storey drifts, storey forces, component deformation and component forces. The analysis accounts for geometrical nonlinearity, material inelasticity and the redistribution of internal forces. Response characteristics that can be obtained from the pushover analysis are summarised as follows:

a) Estimates of force and displacement capacities of the structure. Sequence of the member yielding and the progress of the overall capacity curve.

b) Estimates of force (axial, shear and moment) demands on potentially brittle elements and deformation demands on ductile elements.

c) Estimates of global displacement demand, corresponding inter-storey drifts and damages on structural and non-structural elements expected under the earthquake ground motion considered.

d) Sequences of the failure of elements and the consequent effect on the overall structural stability.

e) Identification of the critical regions, where the inelastic deformations are expected to be high and identification of strength irregularities (in plan or in elevation) of the building.

Pushover analysis delivers all these benefits for an additional computational effort (modelling nonlinearity and change in analysis algorithm) over the linear static analysis. Step by step procedure of pushover analysis is discussed next.

2.4.1 Pushover Analysis Procedure

Pushover analysis is a static nonlinear procedure in which the magnitude of the lateral load is increased monotonically maintaining a predefined distribution pattern along the height of the building (Fig. 2.1a). Building is displaced till the 'control node' reaches 'target displacement' or building collapses. The sequence of cracking, plastic hinging and failure of the structural

components throughout the procedure is observed. The relation between base shear and control node displacement is plotted for all the pushover analysis (Fig. 2.1b). Generation of base shear – control node displacement curve is single most important part of pushover analysis. This curve is conventionally called as pushover curve or capacity curve. The capacity curve is the basis of 'target displacement' estimation as explained in Section 2.4.3. So the pushover analysis may be carried out twice: (a) first time till the collapse of the building to estimate target displacement and (b) next time till the target displacement to estimate the seismic demand. The seismic demands for the selected earthquake (storey drifts, storey forces, and component deformation and forces) are calculated at the target displacement level. The seismic demand is then compared with the corresponding structural capacity or predefined performance limit state to know what performance the structure will exhibit. Independent analysis along each of the two orthogonal principal axes of the building is permitted unless concurrent evaluation of bi-directional effects is required.

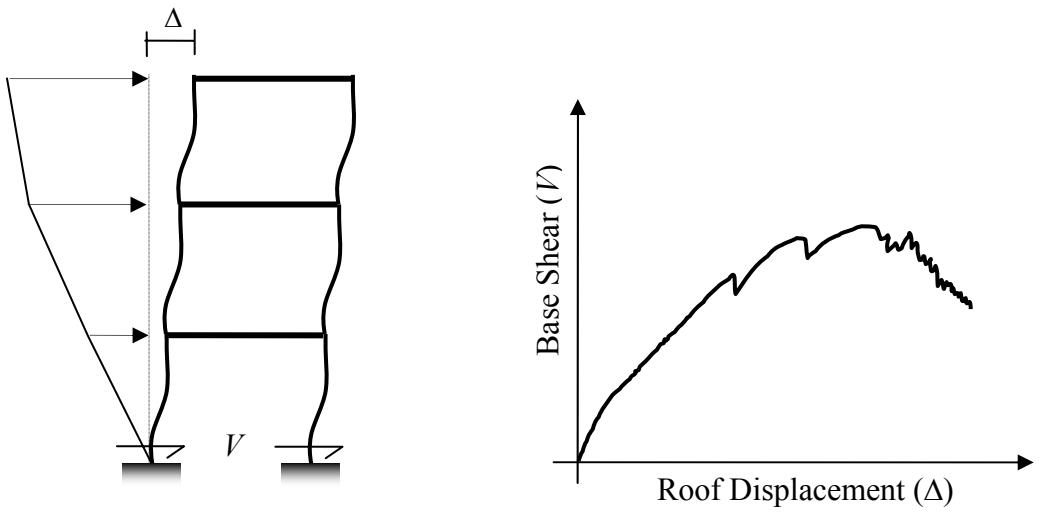

a) Building model b) Pushover curve

Fig. 2.1: Schematic representation of pushover analysis procedure

The analysis results are sensitive to the selection of the control node and selection of lateral load pattern. In general, the centre of mass location at the roof of the building is considered as control node. For selecting lateral load pattern in pushover analysis, a set of guidelines as per FEMA 356 is explained in Section 2.4.2. The lateral load generally applied in both positive and negative directions in combination with gravity load (dead load and a portion of live load) to study the actual behaviour.

2.4.2 Lateral Load Profile

In pushover analysis the building is pushed with a specific load distribution pattern along the height of the building. The magnitude of the total force is increased but the pattern of the loading remains same till the end of the process. Pushover analysis results (*i.e.*, pushover curve, sequence of member yielding, building capacity and seismic demand) are very sensitive to the load pattern. The lateral load patterns should approximate the inertial forces expected in the building during an earthquake. The distribution of lateral inertial forces determines relative

magnitudes of shears, moments, and deformations within the structure. The distribution of these forces will vary continuously during earthquake response as the members yield and stiffness characteristics change. It also depends on the type and magnitude of earthquake ground motion. Although the inertia force distributions vary with the severity of the earthquake and with time, FEMA 356 recommends primarily invariant load pattern for pushover analysis of framed buildings.

Several investigations (Mwafy and Elnashai, 2000; Gupta and Kunnath, 2000) have found that a triangular or trapezoidal shape of lateral load provide a better fit to dynamic analysis results at the elastic range but at large deformations the dynamic envelopes are closer to the uniformly distributed force pattern. Since the constant distribution methods are incapable of capturing such variations in characteristics of the structural behaviour under earthquake loading, FEMA 356 suggests the use of at least two different patterns for all pushover analysis. Use of two lateral load patterns is intended to bind the range that may occur during actual dynamic response. FEMA 356 recommends selecting one load pattern from each of the following two groups:

1. Group – I:

i) Code-based vertical distribution of lateral forces used in equivalent static analysis (permitted only when more than 75% of the total mass participates in the fundamental mode in the direction under consideration).

ii) A vertical distribution proportional to the shape of the fundamental mode in the direction under consideration (permitted only when more than 75% of the total mass participates in this mode).

iii) A vertical distribution proportional to the story shear distribution calculated by combining modal responses from a response spectrum analysis of the building (sufficient number of modes to capture at least 90% of the total building mass required to be considered). This distribution shall be used when the period of the fundamental mode exceeds 1.0 second.

2. Group – II:

i) A uniform distribution consisting of lateral forces at each level proportional to the total mass at each level.

ii) An adaptive load distribution that changes as the structure is displaced. The adaptive load distribution shall be modified from the original load distribution using a procedure that considers the properties of the yielded structure.

Instead of using the uniform distribution to bind the solution, FEMA 356 also allows adaptive lateral load patterns to be used but it does not elaborate the procedure. Although adaptive procedure may yield results that are more consistent with the characteristics of the building under consideration it requires considerably more analysis effort. Fig. 2.2 shows the common lateral load pattern used in pushover analysis.

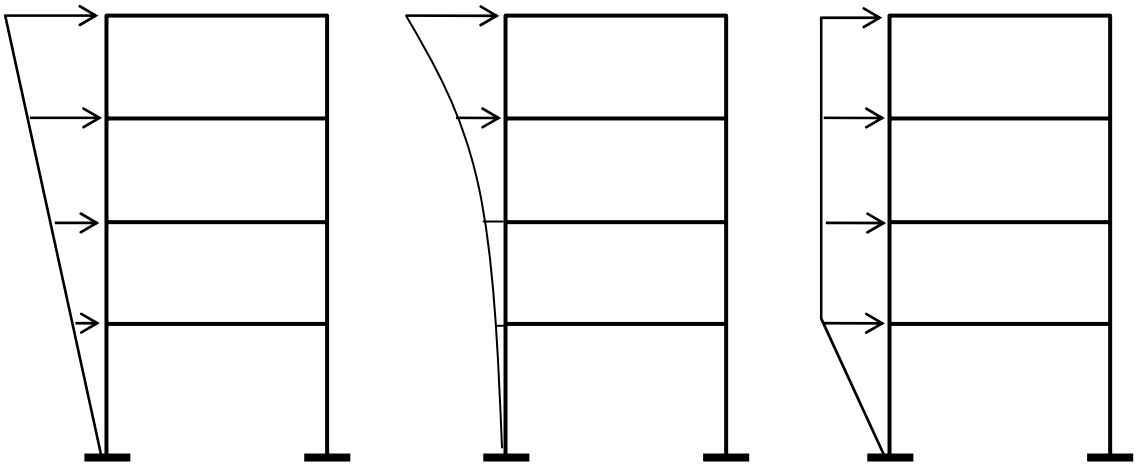

(a) Triangular (b) IS Code Based (c) Uniform

Fig. 2.2: Lateral load pattern for pushover analysis as per FEMA 356 (considering uniform mass distribution)

2.4.3 Target Displacement

Target displacement is the displacement demand for the building at the control node subjected to the ground motion under consideration. This is a very important parameter in pushover analysis because the global and component responses (forces and displacement) of the building at the target displacement are compared with the desired performance limit state to know the building performance. So the success of a pushover analysis largely depends on the accuracy of target displacement. There are two approaches to calculate target displacement:

(a) Displacement Coefficient Method (DCM) of FEMA 356 and

(b) Capacity Spectrum Method (CSM) of ATC 40.

Both of these approaches use pushover curve to calculate global displacement demand on the building from the response of an equivalent single-degree-of-freedom (SDOF) system. The only difference in these two methods is the technique used.

Displacement Coefficient Method (FEMA 356)

This method primarily estimates the elastic displacement of an equivalent SDOF system assuming initial linear properties and damping for the ground motion excitation under consideration. Then it estimates the total maximum inelastic displacement response for the building at roof by multiplying with a set of displacement coefficients.

The process begins with the base shear versus roof displacement curve (pushover curve) as shown in Fig. 2.3a. An equivalent period (T_{eq}) is generated from initial period (T_i) by graphical procedure. This equivalent period represents the linear stiffness of the equivalent SDOF system. The peak elastic spectral displacement corresponding to this period is calculated directly from the response spectrum representing the seismic ground motion under consideration (Fig. 2.3b).

$$S_d = \frac{T_{eq}^2}{4\pi^2} S_a \tag{2.1}$$

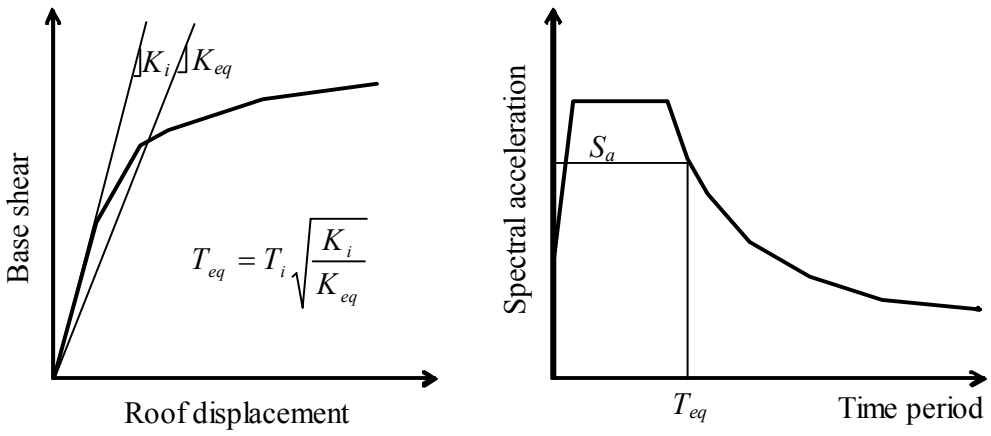

(a) Pushover Curve (b) Elastic Response Spectrum

Fig. 2.3: Schematic representation of Displacement Coefficient Method (FEMA 356)

Now, the expected maximum roof displacement of the building (target displacement) under the selected seismic ground motion can be expressed as:

$$\delta_t = C_0 C_1 C_2 C_3 S_d = C_0 C_1 C_2 C_3 \frac{T_{eq}^2}{4\pi^2} S_a \tag{2.2}$$

C_0 = a shape factor (often taken as the first mode participation factor) to convert the spectral displacement of equivalent SDOF system to the displacement at the roof of the building.

C_1 = the ratio of expected displacement (elastic plus inelastic) for an inelastic system to the displacement of a linear system.

C_2 = a factor that accounts for the effect of pinching in load deformation relationship due to strength and stiffness degradation

C_3 = a factor to adjust geometric nonlinearity (P-Δ) effects

These coefficients are derived empirically from statistical studies of the nonlinear response history analyses of SDOF systems of varying periods and strengths and given in FEMA 356.

From the above definitions of the coefficients, it is clear that the change in building geometry will affect C_0 significantly whereas it is likely to have very little influence on the other factors. As per FEMA 356, the values of C_0 factor for shear buildings depend only on the number of storeys and the lateral load pattern used in the pushover analysis. Table 2.1 presents the values of C_0 provided by the FEMA 356 for shear buildings. In practice, Setback buildings have 5 or more storeys and the C_0 factor, as per FEMA 356, is constant for buildings with 5 or more storeys (Table 2.1).

Table 2.1: Values of C_0 factor for shear building as per FEMA 356

Number of storeys	Triangular Load Pattern	Uniform Load Pattern
1	1.0	1.00
2	1.2	1.15
3	1.2	1.20
5	1.3	1.20
10+	1.3	1.20

Capacity Spectrum Method (ATC 40)

The basic assumption in Capacity Spectrum Method is also the same as the previous one. That is, the maximum inelastic deformation of a nonlinear SDOF system can be approximated from the maximum deformation of a linear elastic SDOF system with an equivalent period and damping. This procedure uses the estimates of ductility to calculate effective period and damping. This procedure uses the pushover curve in an acceleration-displacement response spectrum (ADRS) format. This can be obtained through simple conversion using the dynamic properties of the system. The pushover curve in an ADRS format is termed a 'capacity spectrum' for the structure. The seismic ground motion is represented by a response spectrum in the same ADRS format and it is termed as demand spectrum (Fig. 2.4).

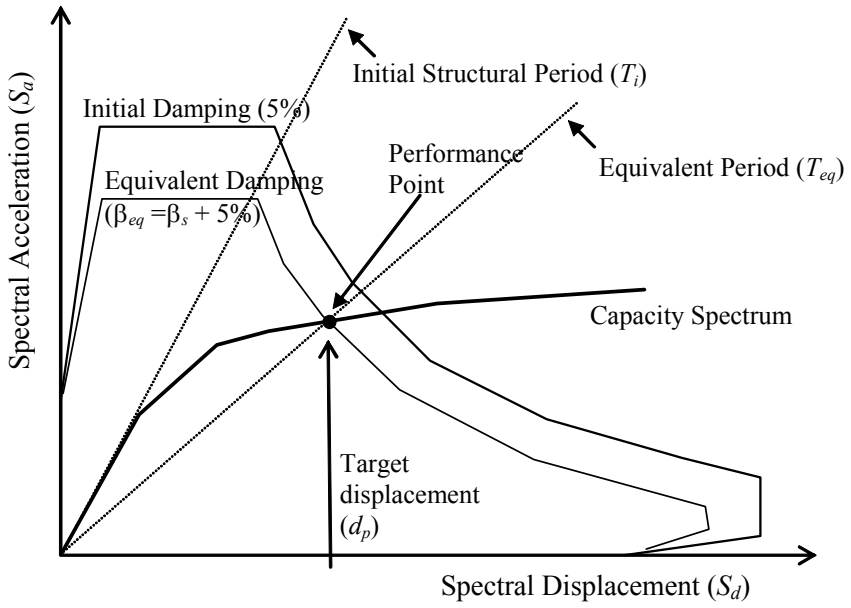

Fig. 2.4: Schematic representation of Capacity Spectrum Method (ATC 40)

The equivalent period (T_{eq}) is computed from the initial period of vibration (T_i) of the nonlinear system and displacement ductility ratio (μ). Similarly, the equivalent damping ratio (β_{eq}) is computed from initial damping ratio (ATC 40 suggests an initial elastic viscous damping ratio of 0.05 for reinforced concrete building) and the displacement ductility ratio (μ). ATC 40 provides the following equations to calculate equivalent time period (T_{eq}) and equivalent damping (β_{eq}).

$$T_{eq} = T_i \sqrt{\frac{\mu}{1 + \alpha\mu - \alpha}} \tag{2.3}$$

$$\beta_{eq} = \beta_i + \kappa \frac{2}{\pi} \frac{(\mu - 1)(1 - \alpha)}{\mu(1 + \alpha\mu - \alpha)} = 0.05 + \kappa \frac{2}{\pi} \frac{(\mu - 1)(1 - \alpha)}{\mu(1 + \alpha\mu - \alpha)} \tag{2.4}$$

where α is the post-yield stiffness ratio and κ is an adjustment factor to approximately account for changes in hysteretic behaviour in reinforced concrete structures.

ATC 40 relates effective damping to the hysteresis curve (Fig. 2.5) and proposes three hysteretic behaviour types that alter the equivalent damping level. Type A hysteretic behaviour is meant for new structures with reasonably full hysteretic loops, and the corresponding equivalent damping ratios take the maximum values. Type C hysteretic behaviour represents severely degraded hysteretic loops, resulting in the smallest equivalent damping ratios. Type B hysteretic behaviour is an intermediate hysteretic behaviour between types A and C. The value of κ decreases for degrading systems (hysteretic behaviour types B and C).

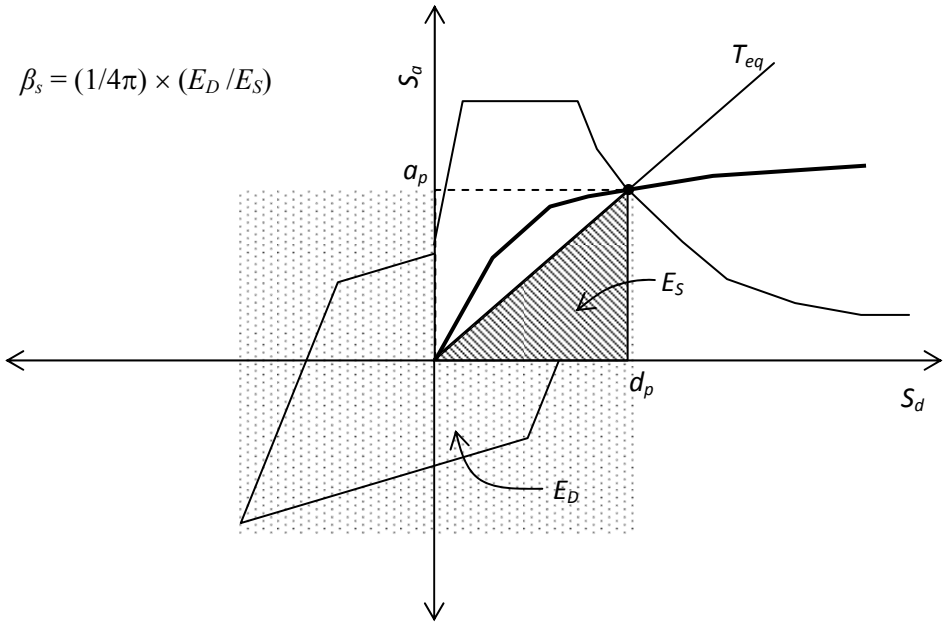

Fig. 2.5: Effective damping in Capacity Spectrum Method (ATC 40)

The equivalent period in Eq. 2.3 is based on a lateral stiffness of the equivalent system that is equal to the secant stiffness at the target displacement. This equation does not depend on the degrading characteristics of the hysteretic behaviour of the system. It only depends on the displacement ductility ratio (μ) and the post-yield stiffness ratio (α) of the inelastic system.

ATC 40 provides reduction factors to reduce spectral ordinates in the constant acceleration region and constant velocity region as a function of the effective damping ratio. The spectral reduction factors are given by:

$$SR_A = \frac{3.21 - 0.68\ln(100\beta_{eq})}{2.12} \tag{2.5}$$

$$SR_V = \frac{2.31 - 0.41\ln(100\beta_{eq})}{1.65} \tag{2.6}$$

where β_{eq} is the equivalent damping ratio, SR_A is the spectral reduction factor to be applied to the constant acceleration region, and SR_V is the spectral reduction factor to be applied to the constant velocity region (descending branch) in the linear elastic spectrum.

Since the equivalent period and equivalent damping are both functions of the displacement ductility ratio (Eq. 2.3 and Eq. 2.4), it is required to have prior knowledge of displacement ductility ratio. However, this is not known at the time of evaluating a structure. Therefore, iteration is required to determine target displacement. ATC 40 describes three iterative procedures with different merits and demerits to reach the solution.

2.4.4 Pushover Analysis of Buildings with Non-orthogonal Frames

Structural response of the building in one orthogonal horizontal direction under the earthquake ground motion in the other orthogonal horizontal direction is particularly important when the building has plan irregularity or non-orthogonal framing system, causing the structure to twist. Bi-directional seismic effect needs to be considered concurrently for pushover analysis of such buildings.

FEMA 356 recommends that the building response should be calculated for (a) forces and deformations associated with 100% of the design displacement in the X-direction plus the forces (not deformations) associated with 30% of the design displacements in the perpendicular horizontal Y-direction, and for (b) forces and deformations associated with 100% of the design displacements in the Y-direction plus the forces (not deformations) associated with 30% of the design displacements in the X-direction. FEMA 356 also allows other combination rules that are verified by experiment and analysis.

2.5 SHORTCOMINGS OF THE PUSHOVER ANALYSIS

Pushover analysis is a very effective alternative to nonlinear dynamic analysis, but it is an approximate method. Major approximations lie in the choice of the lateral load pattern and in the calculation of target displacement. FEMA 356 guideline for load pattern does not cover all possible cases. It is applicable only to those cases where the fundamental mode participation is predominant. Both the methods to calculate target displacement (given in FEMA 356 and ATC 40) do not consider the higher mode participation. Also, it has been assumed that the response of a MDOF system is directly proportional to that of a SDOF system. This approximation is likely to yield adequate predictions of the element deformation demands for low to medium-rise buildings, where the behaviour is dominated by a single mode. However, pushover analysis can be grossly inaccurate for buildings with irregularity, where the contributions from higher modes are significant. Many publications (Aschheim, *et. al*., 1998; Chopra and Chintanapakdee, 2001; Chopra and Goel, 1999; Chopra and Goel, 2000; Chopra, *et. al*., 2003; Dinh and Ichinose, 2005; Fajfar, 2000; Goel and Chopra, 2004; Gupta and Krawinkler, 2000; Kalkan and Kunnath, 2007; Moghadam and Hajirasouliha, 2006; Mwafy and Elnashai, 2000; Mwafy and Elnashai, 2001; Krawinkler and Seneviratna, 1998) have

demonstrated that traditional pushover analysis can be an extremely useful tool, if used with caution and acute engineering judgment, but it also exhibits significant shortcomings and limitations, which are summarized below:

a) One important assumption behind pushover analysis is that the response of a MDOF structure is directly related to an equivalent SDOF system. Although in several cases the response is dominated by the fundamental mode, this cannot be generalised. Moreover, the shape of the fundamental mode itself may vary significantly in nonlinear structures depending on the level of inelasticity and the location of damages.

b) Target displacement estimated from pushover analysis may be inaccurate for structures where higher mode effects are significant. The method, as prescribed in FEMA 356, ignores the contribution of the higher modes to the total response.

c) It is difficult to model three-dimensional and torsional effects. Pushover analysis is very well established and has been extensively used with 2-D models. However, little work has been carried out for problems that apply specifically to asymmetric 3-D systems, with stiffness or mass irregularities. It is not clear how to derive the load distributions and how to calculate the target displacement for the different frames of an asymmetric building. Moreover, there is no consensus regarding the application of the lateral force in one or both horizontal directions for such buildings.

d) The progressive stiffness degradation that occurs during the cyclic nonlinear earthquake loading of the structure is not considered in the present procedure. This degradation leads to changes in the periods and the modal characteristics of the

structure that affect the loading attracted during earthquake ground motion.

e) Only horizontal earthquake load is considered in the current procedure. The vertical component of the earthquake loading is ignored; this can be of importance in some cases. There is no clear idea on how to combine pushover analysis with actions at every nonlinear step that account for the vertical ground motion.

f) Structural capacity and seismic demand are considered independent in the current method. This is incorrect, as the inelastic structural response is load-path dependent and the structural capacity is always associated with the seismic demand.

2.6 ALTERNATE PUSHOVER ANALYSIS PROCEDURES

As discussed in the previous Section, pushover analysis lacks many important features of nonlinear dynamic analysis and it will never be a substitute for nonlinear dynamic analysis as the most accurate tool for structural analysis and assessment. Nevertheless, several possible developments can considerably improve the efficiency of the method. There are several attempts available in the literature to overcome the limitations of this analysis. These include the use of alternative lateral load patterns, use of higher mode properties and use of adaptive procedures. This Section presents some selected alternative procedures of pushover analysis.

2.6.1 Modal Pushover Analysis

Modal Pushover Analysis (MPA), developed by Chopra and Goel (2002), is an improved procedure to calculate target displacement. This procedure is developed based on the differential equations governing the response of a multi-story building subjected to an earthquake ground motion with acceleration, $\ddot{u}_g(t)$:

$$[m]\{\ddot{u}\}+[c]\{\dot{u}\}+[k]\{u\}=-[m]\{1\}\ddot{u}_g(t) \tag{2.7}$$

where $\{u\}$ is the floor displacements relative to the ground, $[m]$, $[c]$, and $[k]$ are the mass, classical damping, and lateral stiffness matrices of the system.

The right side of Eq. 2.7 can be interpreted as the effective earthquake force vector:

$$\{P_{eff}(t)\}=-[m]\{1\}\ddot{u}_g(t) \tag{2.8}$$

Thus, the height-wise distribution of these forces can be defined by $\{s\}=[m]\{1\}$ and their time variation by $\ddot{u}_g(t)$. This force distribution can be expanded as a combination of modal contributions $\{s_n\}$:

$$\{s\}=\sum_{n=1}^{N}\{s_n\}=\sum_{n=1}^{N}\Gamma_n[m]\{\phi_n\} \tag{2.9}$$

where $\{\phi_n\}$ is the n^{th} mode of the structure and N is the number of modes to be considered. The modal pushover analysis method recommends to carryout pushover analysis separately for first few modes (satisfying response spectrum analysis rule) using the load pattern as given in Eq. 2.9.

By utilizing the orthogonality property and decoupling of modes the solution of the differential equation (Eq. 2.7) can be written as:

$$\{u_n(t)\}=\{\phi_n\}q_n(t)=\Gamma_n\{\phi_n\}D_n(t) \tag{2.10}$$

where $q_n(t)$ is the modal coordinate, Γ_n is modal participation factor of the n^{th} mode and $D_n(t)$ is governed by the equation of motion for a SDOF system, with n^{th} mode natural frequency ω_n and damping ratio ξ_n, subjected to $\ddot{u}_g(t)$:

$$\ddot{D}_n + 2\xi_n\omega_n\dot{D}_n + \omega_n^2 D_n = -\ddot{u}_g(t) \tag{2.11}$$

Now, the displacement at the roof due to n^{th} mode can be expressed as:

$$u_{n,roof}(t) = \Gamma_n\phi_{n,roof}D_n(t) \tag{2.12}$$

where $\phi_{n,roof}$ is the value of the n^{th} mode shape at roof level.

The peak value of the roof displacement due to n^{th} mode can be expressed as:

$$u_{no,roof} = \Gamma_n\phi_{n,roof}D_n \tag{2.13}$$

where D_n, the peak value of $D_n(t)$, can be determined by solving Eq. 2.11 or from the inelastic response spectrum. $u_{no,roof}$ is the target displacement of the building at roof due to n^{th} mode. The peak modal responses from all the modes considered are combined according to appropriate modal combination rule (such as SRSS, CQC, etc.). This application of modal combination rules to inelastic systems obviously lacks a theoretical basis. However, it seems reasonable because it provides results for elastic buildings that are identical to the well-known RSA procedure. The lateral force distribution (Eq. 2.9) and the target displacement (Eq. 2.13) suggested for modal pushover analysis possesses two properties: (1) it keeps the invariant distribution of forces and (2) it provides the exact modal response for elastic systems. The steps in the MPA procedure to estimate target displacement of a multi-storeyed building are summarised below.

i. Compute the natural frequencies (ω_n) and modes shapes $\{\phi_n\}$ for linear elastic vibration of the building.

ii. For the n^{th} mode, develop the base shear versus roof displacement curve (pushover curve) for force distribution, $\Gamma_n[m]\{\phi_n\}$ or just $[m]\{\phi_n\}$.

iii. Idealise the pushover curve as a bilinear curve (Fig. 2.6). Convert the idealised base shear versus roof displacement curve of the multi-storeyed building to force-displacement relation for n^{th} mode inelastic equivalent SDOF system using the following relations:

$$F_{sn}/L_n = V_{Bn}/M_n^* \text{ and } D_n = u_{n,roof}/\Gamma_n\phi_{n,roof}$$

where F_{sn} and D_n are the force and displacement for equivalent SDOF system corresponding to n^{th} mode. V_{Bn} and $u_{n,roof}$ are base shear and roof displacement obtained from pushover analysis with n^{th} mode shape as lateral load pattern. The purpose of this step is to obtain the properties of n^{th} mode equivalent inelastic SDOF system.

iv. Compute the peak deformation (D_n) of n^{th} mode inelastic equivalent SDOF system defined in the previous step, either from inelastic design spectrum or from the empirical equations.

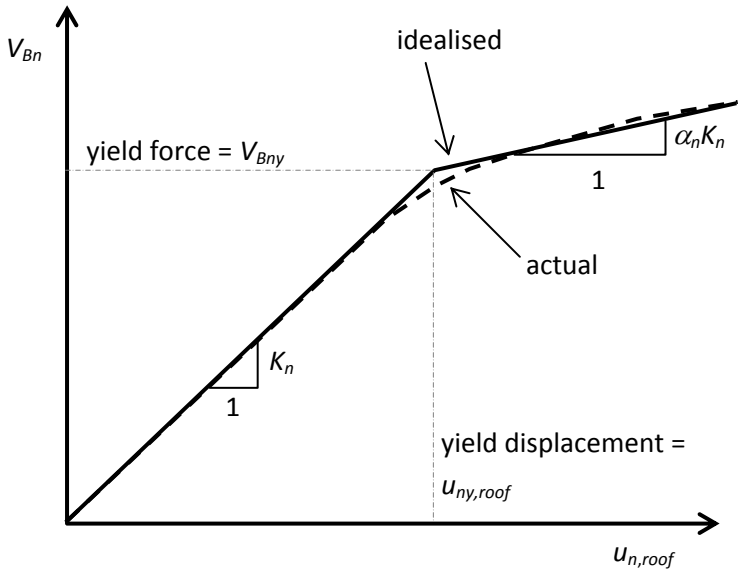

(a) Idealised pushover curve

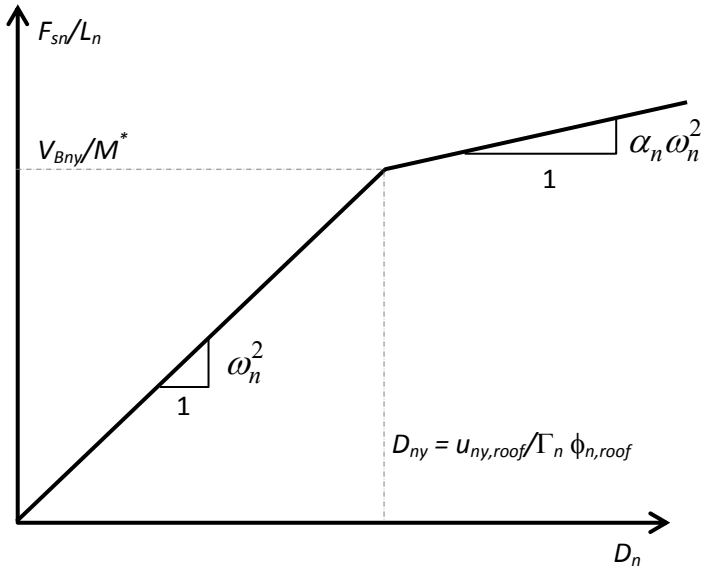

(b) $F_{sn}/L_n - D_n$ *relationship*

Fig. 2.6: Properties of the n^{th}-mode inelastic SDOF system from the pushover curve.

v. Calculate the peak roof displacement associated with n^{th} mode using the relation $u_{no,roof} = \Gamma_n \phi_{n,roof} D_n$.

vi. Repeat the process for as many modes required for sufficient accuracy.

vii. Determine the total response by combining the peak modal responses using SRSS combination rule.

Recent research shows that this procedure is capable of analysing buildings with plan asymmetry (Chopra and Goel, 2004) and some forms of vertical irregularity (Chintanapakdee and Chopra, 2004). However, a recent paper (Tjhin *et. al.*, 2006) concludes that the scope of the applicability of multimode pushover analysis is not very wide and should be used with caution when analysing a particular category of buildings. Park *et. al.* (2007) presents a new modal combination rule (factored modal combination) to estimate the load profile for pushover analysis. This combination is found to work for frames with vertical irregularities (soft ground story and vertical mass irregularity)

2.6.2 Modified Modal Pushover Analysis

Although the Modal Pushover Analysis (MPA) procedure explained in the previous section estimates seismic demands more accurately than current pushover procedures used in structural engineering practice (Goel and Chopra 2004, Chopra and Chintanapakdee 2004), it requires multiple runs to arrive at the solution. Modified Modal Pushover Analysis, proposed by Chopra and Goel (2002), reduces the computational effort in MPA by simplifying the computation of the response contributions of higher modes by assuming the building to be linearly elastic.

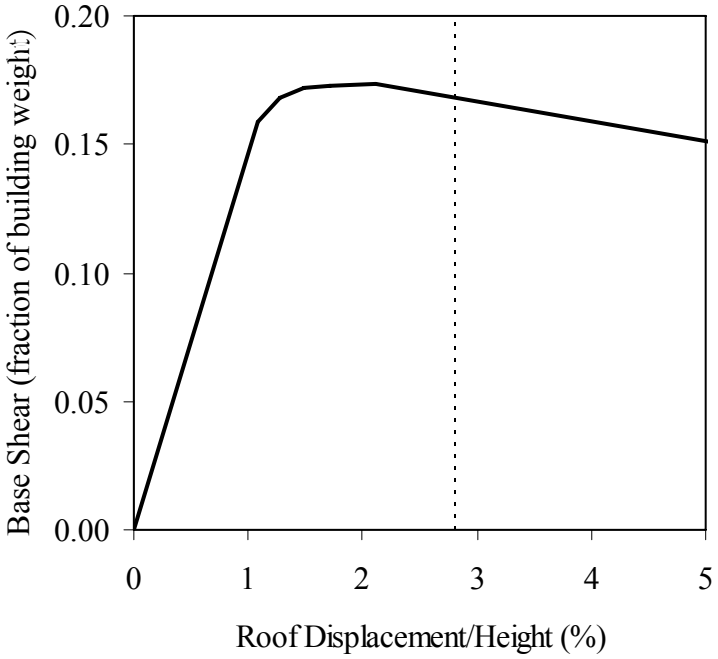

(a) First Mode

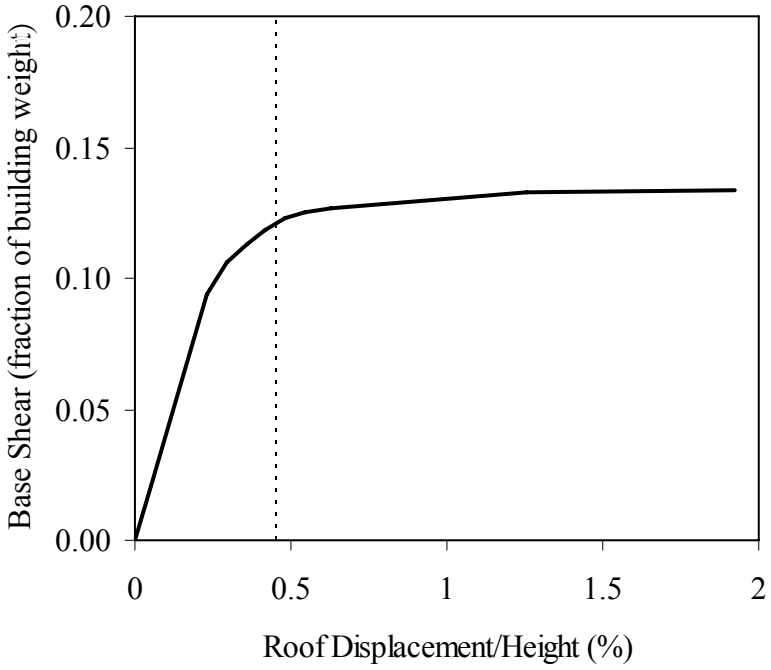

(b) Second Mode

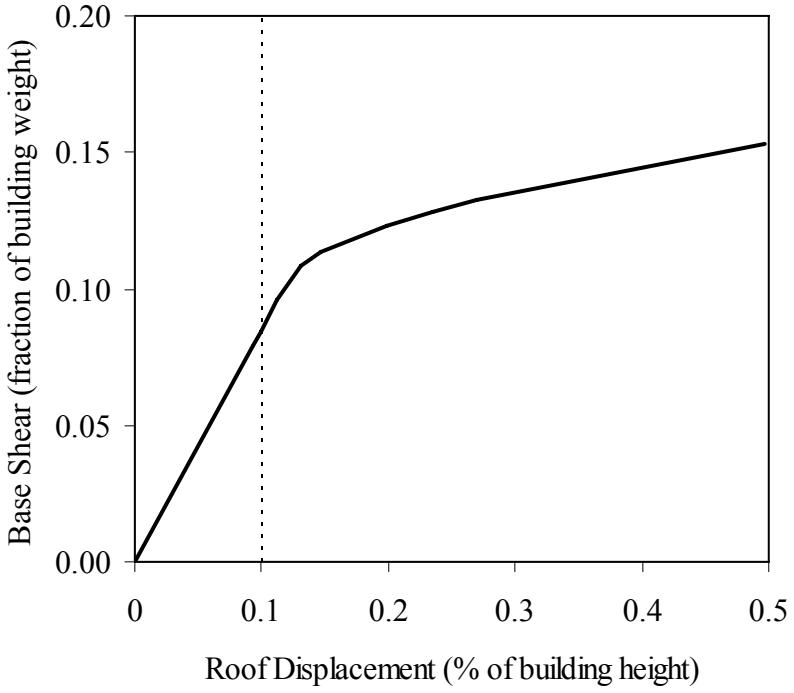

(c) Third Mode

Fig. 2.7: First-, second- and third- mode pushover curves for a typical building and corresponding target roof displacement (Chopra and Goel, 2004)

Figs 2.7(a) to 2.7(c) explain the fact that the contribution of the higher mode can be estimated from the elastic behaviour with considerable accuracy. These figures show pushover curves for a regular building frame under first, second and third mode load patterns respectively. The mean value of the modal roof displacements for the building due to 20 earthquake ground motions determined by the MPA procedure are presented in these figures.

These results suggest that for buildings subjected to intense excitation, consideration of inelastic behaviour of the structure is essential, mainly in the first mode pushover analysis, but may not be as important for the higher modes. This is the basis of Modified Modal Pushover Analysis (MMPA). The errors introduced in higher mode demands are expected to be less in estimating the total demand when we ignore the nonlinearity in the higher mode.

Thus, it may be possible to obtain sufficiently accurate estimates of target displacement by MMPA procedure that differs from MPA only in one sense: the seismic demands due to higher modes are computed under the assumption that the system is elastic. This part of the analysis then becomes identical to linear modal analysis and pushover analysis for higher modes is not needed. But this procedure again assumes that the higher mode contribution in the structural response is not significant and for that it suits only buildings with the plan symmetric about two orthogonal axes to earthquake ground motion along an axis of symmetry. Summarized below are a series of steps in the MMPA procedure to estimate the target displacement of a multi-storey building:

i. Follow the steps 1-5 of MPA for the first mode (or fundamental mode) alone and get the peak inelastic roof displacement associated with this mode.

ii. Compute the dynamic response due to higher modes (higher than the fundamental mode) under the assumption that the system remains elastic. This part of the analysis is identical to classical modal analysis of a linear MDOF system. The deformation response (D_n) of the linear *n*'th-mode SDOF system can be computed from elastic design spectrum. Repeat this analysis for as many modes as required for sufficient accuracy. Note that pushover analysis for higher modes is not needed in this Step, thus reducing the computational effort.

iii. Determine the total response by combining the peak modal responses using the SRSS rule.

2.6.3 Upper-Bound Pushover Analysis

To include the higher mode effects, this procedure suggests (Jan *et. al*., 2004) a new load pattern to carryout pushover analysis. This is based on an upper-bound (absolute sum) modal combination rule. This can be explained from the fundamental structural dynamics theory.

If we look at the solution of the differential equation (Eq. 2.7) governing the response of a MDOF system to an earthquake ground motion:

$$\{u(t)\} = \sum_{n=1}^{N} \{\phi_n\} q_n(t) \tag{2.14}$$

Now, the equivalent static forces can be expressed as:

$$\{f_s(t)\} = [k]\{u(t)\} = \sum_{n=1}^{N} [k]\{\phi_n\} q_n(t) = \sum_{n=1}^{N} \omega_n^2 [m]\{\phi_n\} q_n(t) \tag{2.15}$$

At any instant of time *t,* these forces $\{f_s(t)\}$ are the external forces that produce the displacements $\{u(t)\}$ at the same time *t* and the roof displacement at time *t* due to the forces $\{f_s(t)\}$, $u_{roof}(t)$ can be expressed in the following form:

$$u_{roof}(t) = \sum_{n=1}^{N} \phi_{n,roof} q_n(t) = u_{1,roof}(t)\left[1 + \sum_{n=2}^{N} \frac{\phi_{n,roof} q_n(t)}{\phi_{1,roof} q_1(t)}\right] \tag{2.16}$$

where $u_{1,roof}(t) = \phi_{1,roof} q_1(t)$, representing the roof displacement due to the first mode. If $\{\phi_n\}$ is normalized such that its value at the roof $\phi_{n,roof}$ = 1, then Eq. 2.16 can be simplified as

$$u_{roof}(t) = u_{1,roof}(t)\left[1 + \sum_{n=2}^{N} \frac{q_n(t)}{q_1(t)}\right] \tag{2.17}$$

where $\sum_{n=2}^{N} \frac{q_n(t)}{q_1(t)} = \sum_{n=2}^{N} \frac{\Gamma_n D_n(t)}{\Gamma_1 D_1(t)}$, which is a combination of the displacement–response contribution ratio of all higher modes to that of the fundamental mode.

With this background, Jan *et. al*. (2004) explained that the first two modes alone provide a reasonably accurate prediction for the structural response to earthquakes, and the third or higher mode can be ignored. Thus, the authors assumed that the displacement response is mainly controlled by the first two modes, and choose the absolute sum (ABSSUM) modal combination rule to determine peak response, Eq. 2.15 and Eq. 2.17 can be reduced to

$$\{f_s\} = \omega_1^2[m]\{\phi_1\}q_1 + \omega_2^2[m]\{\phi_2\}q_2 = q_1\left[\omega_1^2[m]\{\phi_1\} + \omega_2^2[m]\{\phi_2\}\frac{q_2}{q_1}\right] \tag{2.18}$$

$$u_{roof}(t) = u_{1,roof}\left[1 + \frac{\Gamma_2 D_2}{\Gamma_1 D_1}\right] \tag{2.19}$$

Since $\{f_s\}$ is a spatial vector and increases monotonically from zero, Eq. 2.18 can be simply expressed as

$$\{f_s\} = \omega_1^2[m]\{\phi_1\} + \omega_2^2[m]\{\phi_2\}\frac{q_2}{q_1} \tag{2.20}$$

In Eq. 2.19, $u_{1,roof}$ is the roof displacement contributed by only the 1st mode which can be approximately taken as the target displacement as defined by FEMA 356 for simplicity.

$$u_{roof}(t) = \delta_t \left[1 + \frac{\Gamma_2 D_2}{\Gamma_1 D_1} \right] \tag{2.21}$$

where δ_t is the target displacement calculated as per FEMA 356 (Eq. 2.2)

The principle steps of upper-bound pushover analysis procedure are as follows:

i. Perform an eigenvalue analysis and find out the natural periods and mode shapes of the structure. Normalize the mode shape $\{\phi_n\}$ such that its value at the roof, $\phi_{n,roof} = 1$ for all the modes.

ii. Use the elastic response spectrum of the selected earthquake to determine the upper-bound of the 2nd mode contribution ratio, $(q_2/q_1)_{UB}$, as given by the following expression:

$$\left(\frac{q_2}{q_1} \right)_{UB} = \left| \frac{\Gamma_2 D_2}{\Gamma_1 D_1} \right|$$

where Γ_n (n = 1, 2) is the modal participation factor and D_n (n = 1, 2) is the displacement obtained from the elastic displacement response spectrum for n'th mode.

iii. Determine the lateral load distribution (height-wise) for pushover analysis using the following formula:

$$\{f_{s,UB}\} = \omega_1^2 [m]\{\phi_1\} + \omega_2^2 [m]\{\phi_2\} \left(\frac{q_2}{q_1} \right)_{UB}$$

where ω_n (n = 1, 2) is the natural frequency for the nth-mode.

iv. Determine the target roof displacement $u_{roof,UB}$ as given by the following relationship:

$$u_{roof,UB} = \delta_t \left[1 + (q_2/q_1)_{UB}\right]$$

where δ_t is the target displacement predicted by the pushover analysis as per FEMA 356.

v. The seismic demands of a given structure are determined by pushover analysis with a lateral load profile $\{f_{s,UB}\}$, and the forces are monotonically increased until the target displacement $u_{roof,UB}$ is reached or a collapse mechanism developed.

2.6.4 Adaptive Pushover Analysis

Adaptive pushover analysis takes into account the current level of local resistance and updates the forcing function accordingly. According to this approach, the lateral load pattern is not kept constant during the analysis but it is continuously updated, based on a combination of the instantaneous mode shapes and spectral amplifications corresponding to the inelastic periods of the structure (Fig. 2.8). Bracci *et. al.* (1997) first developed adaptive pushover analysis procedure using the inelastic forces of the previous equilibrated load step to update the lateral load pattern. The story force distribution is obtained either by adding an increment of the new force vector to that existing from a previous step or by a new set of forces accounting for the current state of resistance distribution.

A displacement based adaptive pushover analysis (Papanikolaou *et. al.*, 2005) was developed where displacement or deformation was used for pushover analysis instead of the forcing function. Considering earthquake loading as a set of imposed energy input, applying displacements rather than force patterns in the pushover procedures appears to be more

appropriate and theoretically correct (Priestley, 1993). The applied displacements at every step would be determined by modal analysis or any other method that explicitly accounts for the structural characteristics at the current level of inelasticity, in a way that approximates the expected dynamic deformations. Although such procedures are theoretically more rigorous, they match the new trends for displacement-based design and assessment. Also, they expose the structural weaknesses that cannot be achievable with fixed-load and displacement patterns. However, this procedure is not popular in practice because of its computational difficulties.

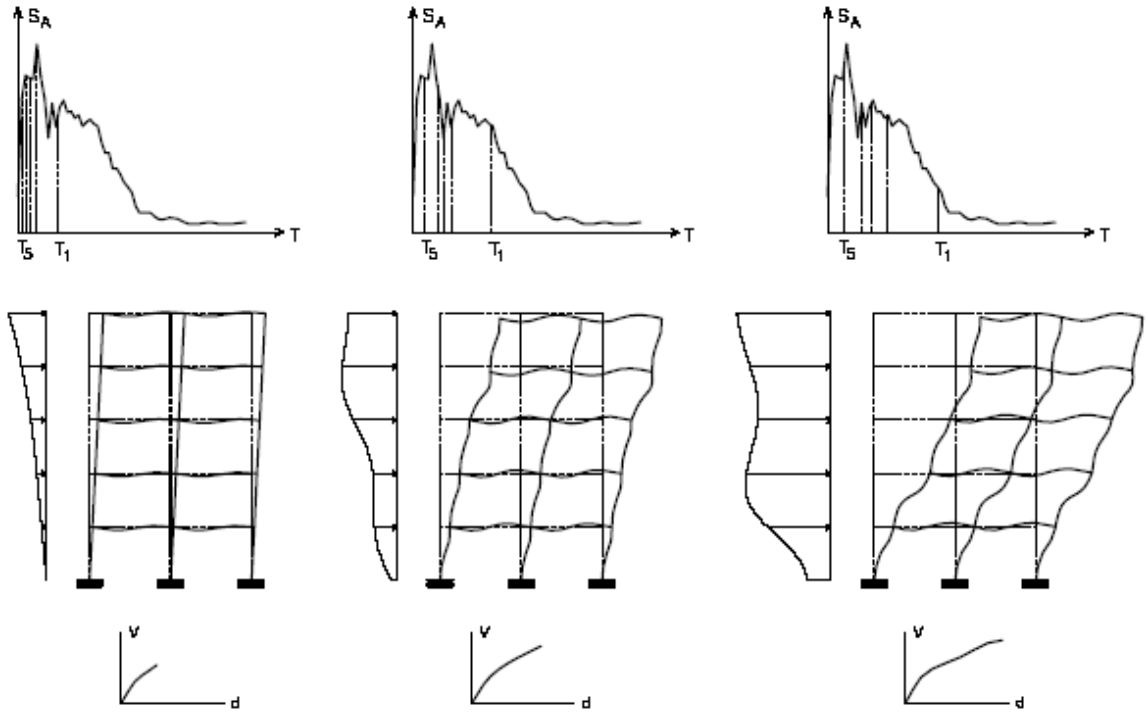

Fig. 2.8: Adaptive pushover analysis (Papanikolaou *et*. *al*., 2005)

2.7 IMPROVEMENT OVER CONVENTIONAL PUSHOVER ANALYSIS

The popularity of the traditional pushover analysis method among the practising engineers over other alternative approaches led FEMA to update the conventional pushover analysis method. Capacity spectrum method (CSM) and Displacement coefficient method (DCM) have been recently updated by the project ATC 55 that is principally aimed to improve the accuracy of the peak SDOF displacement estimations. The principal product of the ATC 55 project is the FEMA 440 (2005) report that presents the improved versions of the DCM and CSM. The empirical relations used in the improved DCM and CSM for estimating the expected peak inelastic SDOF displacements given in FEMA 440 is based on many research works (Ruiz-García and Miranda, 2003; Miranda, 1999; Miranda 2001; Miranda and Ruiz-García, 2002). This section discusses the modifications presented in the FEMA 440 for the peak SDOF displacement prediction.

The improved DCM modifies C_1 and C_2 coefficients (refer Eq. 2.2) to improve the expected elastoplastic oscillator deformation estimations from their elastic counterparts (C_1) and modify these estimations for cyclic degradation (C_2). This procedure suggests eliminating coefficient C_3 (used in the former version) that accounts for the amplification in deformations due to the P-Δ effects. Instead, it establishes a limit on the lateral strength to avoid dynamic instability. The recommended C_1 and C_2 expressions for the improved DCM are

$$C_1 = 1 + \frac{R-1}{aT_{eq}^2} \tag{2.22}$$

$$C_2 = 1 + \frac{1}{800}\left(\frac{R-1}{T_{eq}}\right)^2 \tag{2.23}$$

In Eq. 2.22 and 2.23, $R = F_e / F_y$ represents the normalized lateral strength ratio and defines the yield strength (F_y) capacity of the SDOF system relative to its elastic strength (F_e). The regression constant '*a*' is devised for the influence of different site classes. The coefficient C_2 is equal to 1 for periods greater than 0.7s in the improved DCM. This coefficient is taken as 1, since the differences in the peak roof and inter-story drifts computed from the bilinear and moderate stiffness-degradation hysteretic models are found as negligible in this study.

The improved CSM proposes new effective damping and period relationships for a wide variety of cyclic behaviour (bilinear, stiffness degrading, and in-cycle strength degrading) and post-yield stiffness to predict the nonlinear SDOF deformation demands through an equivalent linear system. The improved CSM determines the equivalent linear parameters (equivalent period, T_{eq} and equivalent damping, β_{eq}) through a statistical analysis that minimizes the extreme differences between the maximum response of an actual inelastic SDOF system and its equivalent linear counterpart (Guyader and Iwan, 2006). In the improved CSM, both T_{eq} and β_{eq} expressions are discontinuous at two distinct ductility values ($\mu = 4$ and $\mu = 6.5$), and they are suggested to be used for μ less than 10–12. The format of T_{eq} and β_{eq} expressions is given as follows:

For $\mu < 4$

$$\beta_{eq} = A(\mu - 1)^2 + B(\mu - 1)^3 + \beta_i \tag{2.24a}$$

$$T_{eq} = \left[G(\mu - 1)^2 + H(\mu - 1)^3 + 1 \right] T_i \tag{2.24b}$$

For $4 \leq \mu \leq 6.5$

$$\beta_{eq} = C + D(\mu - 1) + \beta_i \tag{2.25a}$$

$$T_{eq} = \left[I + J(\mu - 1) + 1 \right] T_i \tag{2.25b}$$

For $\mu > 6.5$

$$\beta_{eq} = E\left[\frac{F(\mu - 1) - 1}{F(\mu - 1)^2} \right] \left(\frac{T_{eq}}{T_0} \right) + \beta_i \tag{2.26a}$$

$$T_{eq} = \left[K\left(\sqrt{\frac{(\mu - 1)}{1 + L(\mu - 2)}} - 1 \right) + 1 \right] T_i \tag{2.26b}$$

The parameters, T_i and β_i = initial period and viscous damping of the bilinear SDOF system are idealized from the pushover curves. The constants *A* through *K* vary for different α values and hysteretic models. The improved CSM also presents alternative values for these constants that can be used for any case regardless of α and hysteretic model.

Recent studies (Akkar and Metin, 2007; Akkar and Ozen, 2005) present the statistics on transforming the SDOF deformations to MDOF response. These statistics show that the use of first-mode elastic dynamic properties as per FEMA 440 would not adequately simulate inelastic deformation profile. However, another study (Akkar and Miranda, 2005) shows that this method works considerably well when the fundamental period is more than one second. Tjhin *et. al*. (2005) also shows that the estimation of target displacement using FEMA 440 works well for regular and weak storey moment resisting frames.

2.8 SUMMARY

This chapter presents a detailed literature review of seismic performance of setback buildings. The chapter also presents the pushover analysis procedure, its limitations and recent improvements to this procedure. The research papers on setback buildings conclude that the displacement demand is dependent on the geometrical configuration of frame and concentrated in the neighbourhood of the setbacks for setback structures. The higher modes significantly contribute to the response quantities of structure. Also conventional pushover analysis seems to be underestimating the response quantities in the upper floors of the irregular frames.

Pushover analysis as explained in the FEMA 356 is primarily meant for regular buildings with dominant fundamental mod participation. There are many alternative approaches of pushover analysis reported in the literature to make it applicable for different categories of irregular buildings. These comprise (i) *modal pushover analysis* (chopra and goel, 2001), (ii) *modified modal pushover analysis* (Chopra et. al., 2004), *upper bound pushover analysis* (Jan *et. al*., 2004) and (iv) *adaptive pushover analysis*, etc. There is an effort by project ATC 55 to improve the current displacement coefficient method and capacity spectrum method. However, none of these alternative methods and the improved displacement coefficient and capacity spectrum method has been tested for setback buildings.

From the above conclusions, it is clear that the evaluation of seismic demands for setback buildings is necessary to assess the seismic performance of setback buildings.

CHAPTER 3

STRUCTURAL MODELLING

3.1 INTRODUCTION

The study in this thesis is based on nonlinear analysis of a family of structural models representing vertically irregular multi-storeyed setback buildings. The first part of this chapter presents a summary of various parameters defining the computational models, the basic assumptions and the building geometries considered for this study.

Accurate modelling of the nonlinear properties of various structural elements is very important in nonlinear analysis. In the present study, frame elements were modelled with inelastic flexural hinges using point plasticity model. The second part of this chapter presents the properties of the point plastic hinges, the procedure to generate these hinge properties and the assumptions made.

Finally, this chapter presents the important parameters used for nonlinear time-history analysis and details of the input ground motion considered in the analysis.

3.2 COMPUTATIONAL MODEL

Modelling a building involves the modelling and assemblage of its various load-carrying elements. The model must ideally represent the mass distribution, strength, stiffness and deformability. Modelling of the material properties and structural elements used in the present study is discussed below.

3.2.1 Material Properties

M-20 grade of concrete and Fe-415 grade of reinforcing steel are used for all the frame models used in this study. Elastic material properties of these materials are taken as per Indian Standard IS 456 (2000). The short-term modulus of elasticity (E_c) of concrete is taken as:

$$E_c = 5000\sqrt{f_{ck}} \text{ MPa} \tag{3.1}$$

Where f_{ck} ≡ characteristic compressive strength of concrete cube in MPa at 28-day (20 MPa in this case). For the steel rebar, yield stress (f_y) and modulus of elasticity (E_s) is taken as per IS 456 (2000).

3.2.2 Structural Elements

Beams and columns are modelled by 2D frame elements. The beam-column joints are modelled by giving end-offsets to the frame elements, to obtain the bending moments and forces at the beam and column faces. The beam-column joints are assumed to be rigid (Fig. 3.1). The column end at foundation was considered as fixed for all the models in this study. All the frame elements are modelled with nonlinear properties at the possible yield locations.

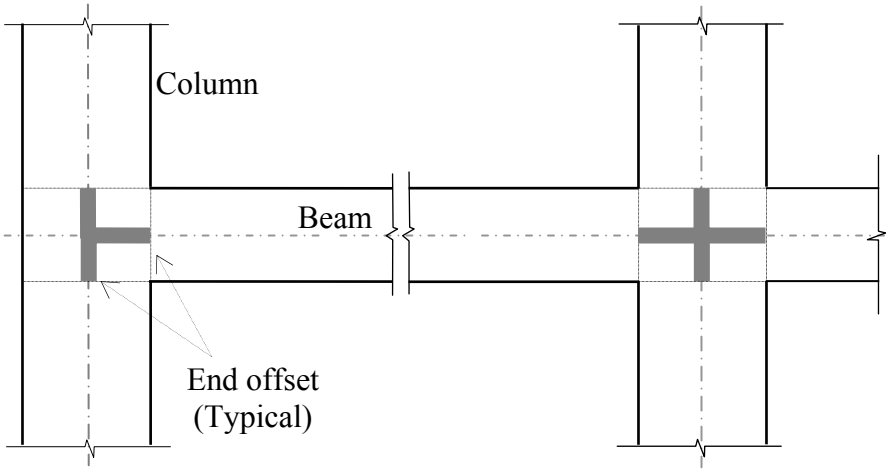

Fig. 3.1: Use of end offsets at beam-column joint

The structural effect of slabs due to their in-plane stiffness is taken into account by assigning 'diaphragm' action at each floor level. The mass/weight contribution of slab is modelled separately on the supporting beams.

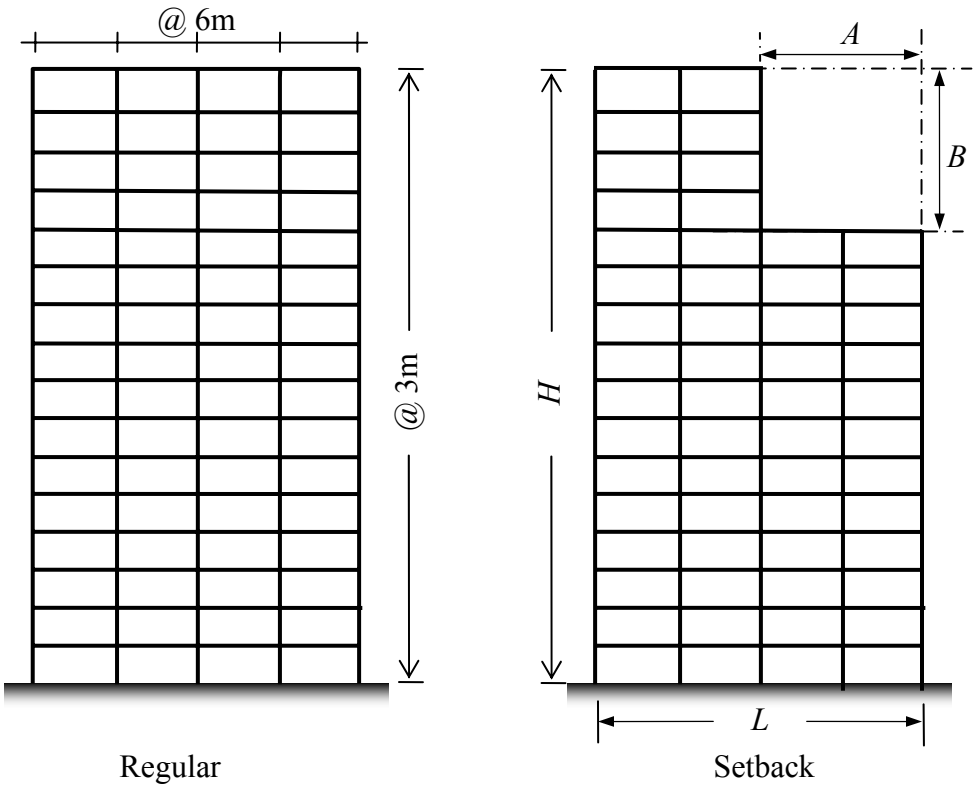

Fig. 3.2: Typical structural models used in the present study

3.3 BUILDING GEOMETRY

The study is based on frames which are plane and orthogonal with storey heights and bay widths. Different building geometries were taken for the study. These building geometries represent varying degree of irregularity or amount of setback. Three different width categories, ranging from 4 to 12 bays (in the direction of earthquake) with a uniform bay width of 6m were considered for this study. It should be noted that bay width of 4m – 6m is the usual case, especially in Indian and European practice. Similarly, four different height categories were considered for the study, ranging from 8

to 20 storeys, with a uniform storey height of 3m. Altogether 48 building frames with different amount of setback irregularities due to the successive reduction of 25% width and 25% height (S1), 50% width and 50% height (S2) and 75% width and 75% height (S3) were selected. The regular frame (R), without any setback, is also studied as shown in Fig. 3.2. The structures are modelled by using computer software SAP-2000 (v14). The gravity loads on the floor is assumed equal to 20.7 kN/m (dead and live loads). The earthquake ground motion is defined by the time history functions available in the software. The column sections defined for the frames satisfy both the requirements for strength and stiffness. All the selected models were designed with M-20 grade of concrete and Fe-415 grade of reinforcing steel as per Indian Standards. Fig. 3.2 shows the typical setback building model considered in the study and similar regular building.

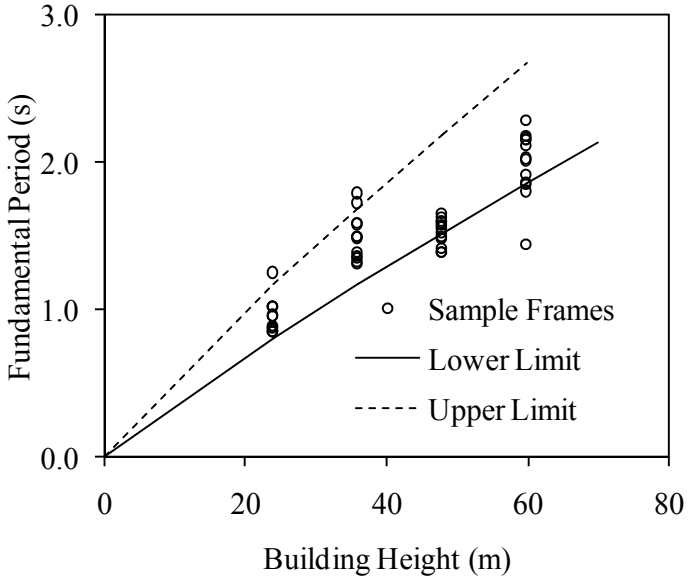

Fig. 3.3: Fundamental period versus overall height variation of all the selected frames

The name S1-X-Y represents that the building frame is of S1 type irregularity with X number of storeys and Y number of bays. It is found that the selected frames cover a wide

fundamental period range of 0.85s – 2.17s. It may also be noted that the fundamental period versus overall height variation of all the selected frames that are consistent with the empirical relationships presented by Goel and Chopra (1997) as shown in Fig. 3.3. This shows that the models selected for this study can be interpreted as being representative of general moment resisting RC frame behaviour for eight to twenty-storey levels, as established by Goel and Chopra (1997).

Table 3.1: The range of natural periods of the selected building models

Frame ID	Height (m)	Natural Period (s)
R-8-4	24	1.01873
S1-8-4	24	0.95978
S2-8-4	24	0.85052
S3-8-4	24	0.87247
R-8-8	24	1.01856
S1-8-8	24	0.95921
S2-8-8	24	0.85124
S3-8-8	24	0.87637
R-8-12	24	1.01859
S1-8-12	24	1.25123
S2-8-12	24	0.85577
S3-8-12	24	0.88815
R-12-4	36	1.58729
S1-12-4	36	1.495
S2-12-4	36	1.32296
S3-12-4	36	1.38455
R-12-8	36	1.57847
S1-12-8	36	1.48618
S2-12-8	36	1.49802

S3-12-8	36	1.34643
R-12-12	36	1.7896
S1-12-12	36	1.72412
S2-12-12	36	1.31372
S3-12-12	36	1.3598
R-16-4	48	1.62783
S1-16-4	48	1.5169
S2-16-4	48	1.41929
S3-16-4	48	1.65504
R-16-8	48	1.60203
S1-16-8	48	1.49111
S2-16-8	48	1.39134
S3-16-8	48	1.57634
R-16-12	48	1.59356
S1-16-12	48	1.48313
S2-16-12	48	1.38878
S3-16-12	48	1.55215
R-20-4	60	1.44035
S1-20-4	60	1.80156
S2-20-4	60	1.91469
S3-20-4	60	2.28232
R-20-8	60	2.17398
S1-20-8	60	2.02641
S2-20-8	60	1.86045
S3-20-8	60	2.15324
R-20-12	60	2.1593
S1-20-12	60	2.01256
S2-20-12	60	1.84872
S3-20-12	60	2.1116

3.4 MODELLING OF FLEXURAL PLASTIC HINGES

In the implementation of pushover analysis, the model must account for the nonlinear behaviour of the structural elements. In the present study, a point-plasticity approach is considered for modelling nonlinearity, wherein the plastic hinge is assumed to be concentrated at a specific point in the frame member under consideration. Beam and column elements in this study were modelled with flexure (M3 for beams and P-M2-M3 for columns) hinges at possible plastic regions under lateral load (*i.e.*, both ends of the beams and columns). Properties of flexure hinges must simulate the actual response of reinforced concrete components subjected to lateral load. In the present study the plastic hinge properties are calculated by SAP 2000 (v14). The analytical procedure used to model the flexural plastic hinges are explained below.

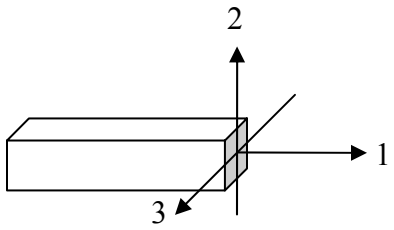

Fig. 3.4: The coordinate system used to define the flexural and shear hinges

Flexural hinges in this study are defined by moment-rotation curves calculated based on the cross-section and reinforcement details at the possible hinge locations. For calculating hinge properties it is required to carry out moment–curvature analysis of each element. Constitutive relations for concrete and reinforcing steel, plastic hinge length in structural element are required for this purpose. The flexural hinges in beams are modelled with uncoupled moment (M3) hinges whereas for column elements the flexural hinges are modelled with coupled P-M2-M3 properties that include the interaction of axial force and

bi-axial bending moments at the hinge location. Although the axial force interaction is considered for column flexural hinges the rotation values were considered only for axial force associated with gravity load.

3.4.1 Stress-Strain Characteristics for Concrete

The stress-strain curve of concrete in compression forms the basis for analysis of any reinforced concrete section. The characteristic and design stress-strain curves specified in most of design codes (IS 456: 2000, BS 8110) do not truly reflect the actual stress-strain behaviour in the post-peak region, as (for convenience in calculations) it assumes a constant stress in this region (strains between 0.002 and 0.0035). In reality, as evidenced by experimental testing, the post-peak behaviour is characterised by a descending branch, which is attributed to 'softening' and micro-cracking in the concrete. Also, models as per these codes do not account for strength enhancement and ductility due to confinement. However, the stress-strain relation specified in ACI 318M-02 consider some of the important features from actual behaviour. A previous study (Chugh, 2004) on stress-strain relation of reinforced concrete section concludes that the model proposed by Panagiotakos and Fardis (2001) represents the actual behaviour best for normal-strength concrete. Accordingly, this model has been selected in the present study for calculating the hinge properties. This model is a modified version of Mander's model (Mander *et. al.*, 1988) where a single equation can generate the stress f_c corresponding to any given strain ε_c:

$$f_c = \frac{f'_{cc}\, x\, r}{r - 1 + x^r} \tag{3.2}$$

where, $x = \frac{\varepsilon_c}{\varepsilon_{cc}}$; $r = \frac{E_c}{E_c - E_{sec}}$; $E_c = 5000\sqrt{f'_{co}}$; $E_{sec} = \frac{f'_{cc}}{\varepsilon_{cc}}$; and f'_{cc} is the peak strength expressed as follows:

$$f'_{cc} = f'_{co}\left[1 + 3.7\left(\frac{0.5k_e\rho_s f_{yh}}{f'_{co}}\right)^{0.85}\right] \tag{3.3}$$

The expressions for critical compressive strains (ref. Fig. 3.5) are expressed in this model as follows:

$$\varepsilon_{cu} = 0.004 + \frac{0.6\rho_s f_{yh}\varepsilon_{sm}}{f'_{cc}} \tag{3.4}$$

$$\varepsilon_{cc} = \varepsilon_{co}\left[1 + 5\left(\frac{f'_{cc}}{f'_{co}} - 1\right)\right] \tag{3.5}$$

where, f'_{co} is unconfined compressive strength = 0.75 f_{ck}, ρ_s = volumetric ratio of confining steel, f_{yh} = grade of the stirrup reinforcement, ε_{sm} = steel strain at maximum tensile stress and k_e is the "confinement effectiveness coefficient", having a typical value of 0.95 for circular sections and 0.75 for rectangular sections.

Fig. 3.5 shows a typical plot of stress-strain characteristics for M-20 grade of concrete as per Modified Mander's model (Panagiotakos and Fardis, 2001). The advantage of using this model can be summarized as follows:

- A single equation defines the stress-strain curve (both the ascending and descending branches) in this model.

- The same equation can be used for confined as well as unconfined concrete sections.
- The model can be applied to any shape of concrete member section confined by any kind of transverse reinforcement (spirals, cross ties, circular or rectangular hoops).
- The validation of this model is established in many literatures (*e.g.*, Pam and Ho, 2001).

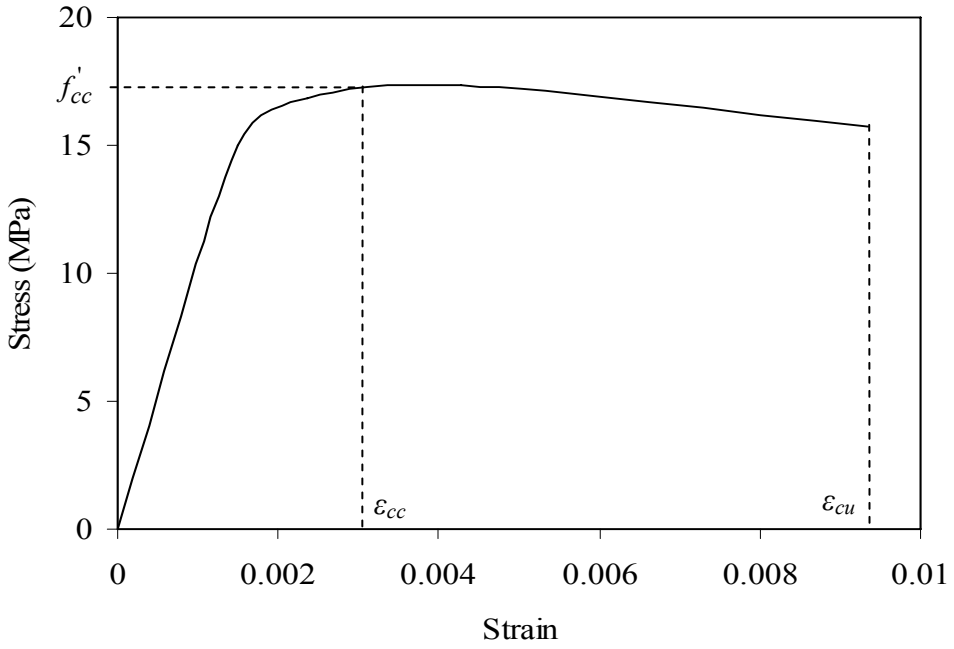

Fig. 3.5: Typical stress-strain curve for M-20 grade concrete (Panagiotakos and Fardis, 2001)

3.4.2 Stress-Strain Characteristics for Reinforcing Steel

The constitutive relation for reinforcing steel given in IS 456 (2000) is well accepted in literature and hence considered for the present study. The 'characteristic' and 'design' stress-strain curves specified by the Code for Fe-415 grade of reinforcing steel (in tension or compression) are shown in Fig. 3.6.

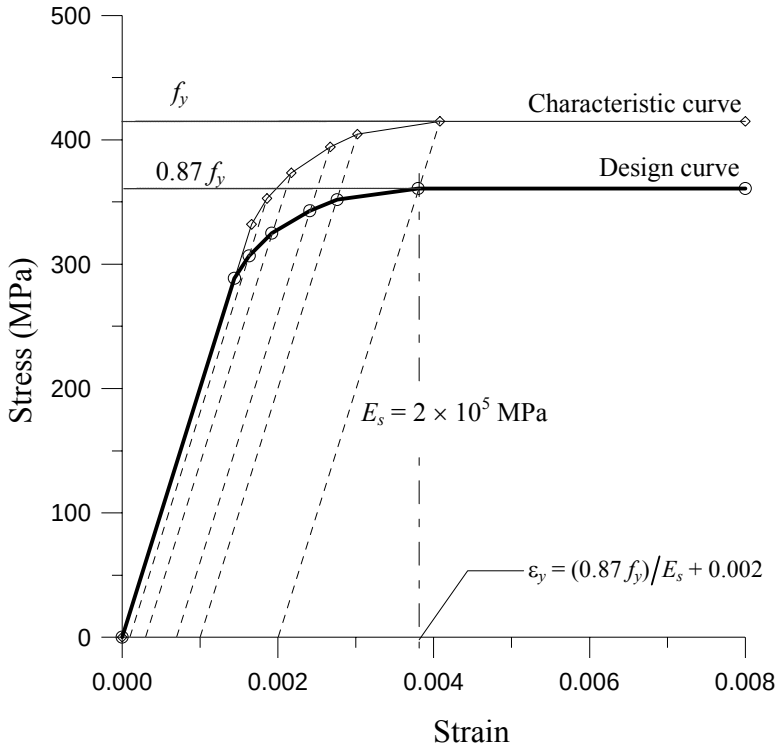

Fig. 3.6: Stress-strain relationship for reinforcement – IS 456 (2000)

3.4.3 Moment-Curvature Relationship

Moment-curvature relation is a basic tool in the calculation of deformations in flexural members. It has an important role to play in predicting the behaviour of reinforced concrete (RC) members under flexure. In nonlinear analysis, it is used to consider secondary effects and to model plastic hinge behaviour.

Curvature (φ) is defined as the reciprocal of the radius of curvature (R) at any point along a curved line. When an initial straight beam segment is subject to a uniform bending moment throughout its length, it is expected to bend into a segment of a circle with a curvature φ that increases in some manner with increase in the applied moment (M). Curvature φ may be alternatively defined as the angle change in the slope of the elastic

curve per unit length $\left(\varphi = 1/R = d\theta/ds\right)$. At any section, using the 'plane sections remain plane' hypothesis under pure bending, the curvature can be computed as the ratio of the normal strain at any point across the depth to the distance measured from the neutral axis at that section (Fig. 3.7).

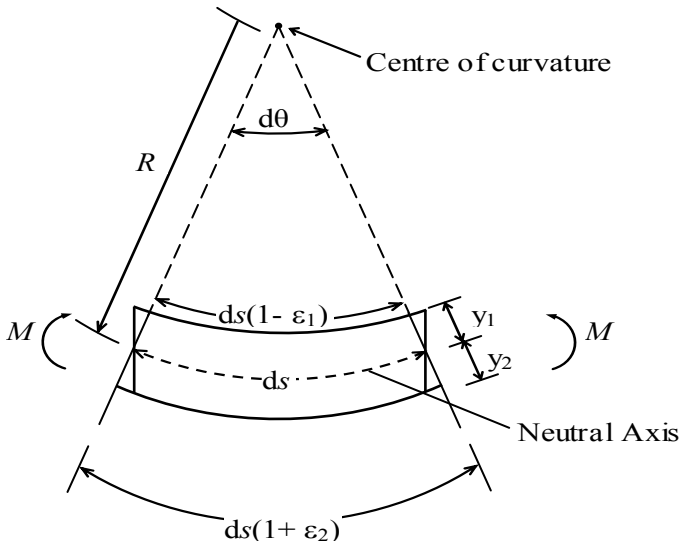

Fig. 3.7: Curvature in an initially straight beam section

If the bending produces extreme fibre strains of ε_1 and ε_2 at top and bottom at any section as shown in Fig. 3.7 (compression on top and tension at bottom assumed in this case), then, for small deformations, it can be shown that $\varphi = \left(\varepsilon_1 + \varepsilon_2\right)/D$, where D is the depth of the beam. If the beam behaviour is linear elastic, then the moment-curvature relationship is linear, and the curvature is obtained as

$$\varphi = \frac{M}{EI}$$

where EI is the flexural rigidity of the beam, obtained as a product of the modulus of elasticity E and the second moment of area of the section I.

When an RC flexural member is subjected to a gradually increasing moment, it's behaviour transits through various stages, starting from the initial un-cracked state to the ultimate limit state of collapse. The stresses in the tension steel and concrete go on increasing as the moment increases. The behaviour at the ultimate limit state depends on the percentage of steel provided, i.e., on whether the section is 'under-reinforced' or 'over-reinforced'. In the case of under-reinforced sections, failure is triggered by yielding of tension steel whereas in over-reinforced section the steel does not yield at the limit state of failure. In both cases, the failure eventually occurs due to crushing of concrete at the extreme compression fibre, when the ultimate strain in concrete reaches its limit. Under-reinforced beams are characterised by 'ductile' failure, accompanied by large deflections and significant flexural cracking. On the other hand, over-reinforced beams have practically no ductility, and the failure occurs suddenly, without the warning signs of wide cracking and large deflections.

In the case of a short column subject to uni-axial bending combined with axial compression, it is assumed that Eq 3.4 remains valid and that "plane sections before bending remain plane". However, the ultimate curvature (and hence, ductility) of the section is reduced as the compression strain in the concrete contributes to resisting axial compression in addition to flexural compression.

3.4.4 Modelling of Moment-Curvature in RC Sections

Using the Modified Mander model of stress-strain curves for concrete (Panagiotakos and Fardis, 2001) and Indian Standard IS 456 (2000) stress-strain curve for reinforcing steel, for a specific confining steel, moment curvature relations can be generated for beams and

columns (for different axial load levels). The assumptions and procedure used in generating the moment-curvature curves are outlined below.

Assumptions

i. The strain is linear across the depth of the section ('plane sections remain plane').

ii. The tensile strength of the concrete is ignored.

iii. The concrete spalls off at a strain of 0.0035.

iv. The initial tangent modulus of the concrete, E_c is adopted from IS 456 (2000), as $5000\sqrt{f_{ck}}$.

v. In determining the location of the neutral axis, convergence is assumed to be reached within an acceptable tolerance of 1%.

Algorithm for Generating Moment-Curvature Relation

i. Assign a value to the extreme concrete compressive fibre strain (normally starting with a very small value).

ii. Assume a value of neutral axis depth measured from the extreme concrete compressive fibre.

iii. Calculate the strain and the corresponding stress at the centroid of each longitudinal reinforcement bar.

iv. Determine the stress distribution in the concrete compressive region based on the Modified Mander stress-strain model for given volumetric ratio of confining steel. The resultant concrete compressive force is then obtained by numerical integration of the stress over the entire compressive region.

v. Calculate the axial force from the equilibrium and compare with the applied axial load (for beam element both of these will be zero). If the difference lies within the specified tolerance, the assumed neutral axis depth is adopted. The moment capacity and the corresponding curvature of the section are then calculated. Otherwise, a new neutral axis is determined from the iteration (using bisection method) and steps (iii) to (v) are repeated until it converges.

vi. Assign the next value, which is larger than the previous one, to the extreme concrete compressive strain and repeat steps (ii) to (v).

vii. Repeat the whole procedure until the complete moment-curvature is obtained.

3.4.5 Moment-Rotation Parameters for Beams

Moment-rotation parameters are the actual input for modelling the hinge properties and this can be calculated from the moment-curvature relation. This can be explained with a simple cantilever beam AB shown in Fig. 3.8(a) with a concentrated load applied at the free end B. To determine the rotation between the ends an idealized inelastic curvature distribution and a fully cracked section in the elastic region may be assumed. Figs 3.8(b) and 3.8(c) represent the bending moment diagram and probable distribution of curvature at the ultimate moment.

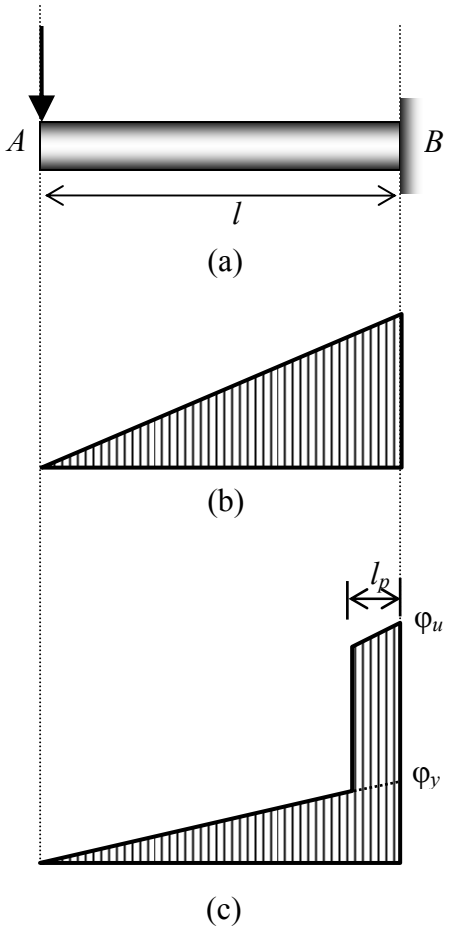

Fig. 3.8: (a) cantilever beam, (b) Bending moment distribution, and (c) Curvature distribution (Park and Paulay 1975)

The rotation between A and B is given by

$$\theta = \int_A^B \varphi \, dx \tag{3.6}$$

where φ is the curvature and dx is an element length of the member

$$\textit{i.e.}, \text{ ultimate rotation}, \theta_u = \varphi_y \frac{l}{2} + (\varphi_u - \varphi_y) l_p \tag{3.7}$$

$$\text{Where the yield rotation } \theta_y = \varphi_y \frac{l}{2} \tag{3.8}$$

$$\text{or, plastic rotation, } \theta_p = (\varphi_u - \varphi_y) l_p \tag{3.9}$$

where φ_u is the ultimate curvature, φ_y is the yield curvature, l is the length of the element and l_p is the equivalent length of plastic hinge over which plastic curvature is considered to be constant. The physical definition of the plastic hinge length, considering the ultimate flexural strength developing at the support, is the distance from the support over which the applied moment exceeds the yield moment. A good estimate of the effective plastic hinge length may be obtained from the following equation (Paulay and Priestley, 1992)

$$l_p = 0.08l + 0.15 d_b f_y \tag{3.10}$$

where, l_p is the length of plastic hinge, l is the length of the element, d_b is the diameter of the longitudinal bar and f_y is the yield strength of the longitudinal reinforcement (in 'ksi'). For typical beam and column proportions Eq. 3.10 results in following equation (FEMA-274; Paulay and Priestley, 1992) where D is the overall depth of the section.

$$l_p = 0.5D \tag{3.11}$$

The moment-rotation curve can be idealised as shown in Fig. 3.9, and can be derived from the moment-curvature relation. The main points in the moment-rotation curve shown in the figure can be defined as follows:

- The point 'A' corresponds to the unloaded condition.
- The point 'B' corresponds to the nominal yield strength and yield rotation θ_y.

- The point 'C' corresponds to the ultimate strength and ultimate rotation θ_u, following which failure takes place.

- The point 'D' corresponds to the residual strength, if any, in the member. It is usually limited to 20% of the yield strength, and ultimate rotation, θ_u can be taken with that.

- The point 'E' defines the maximum deformation capacity and is taken as $15\theta_y$ or θ_u, whichever is greater.

While applying Eq 3.7 and Eq 3.8 to determine the ultimate and yield rotations, care must be taken to adopt the correct value of the length *l*, applicable for cantilever action. In the case of a frame member in a multi-storey frame subject to lateral loads, it may be conveniently assumed that the points of contraflexure are located (approximately) at the mid-points of the beams and columns. In such cases, an approximate value of *l* is given by half the span of the member under consideration.

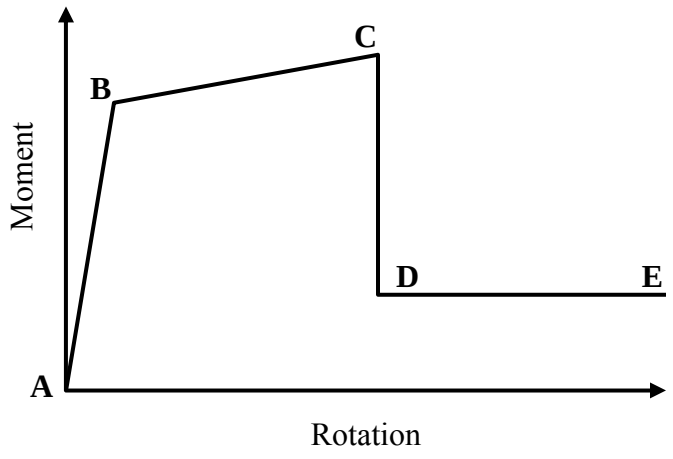

Fig. 3.9: Idealised moment-rotation curve of RC beam sections

3.4.6 Moment-Rotation Parameters for Columns (PMM Hinges)

For the PMM hinge, an interaction (yield) surface is specified in three-dimensional P-M2-M3 space that represents where yielding first occurs for different combinations of axial force P, minor moment M2, and major moment M3. The surface is specified as a set of P-M2-M3 curves, where P is the axial force, and M2 and M3 are the moments (Figure 3.10).

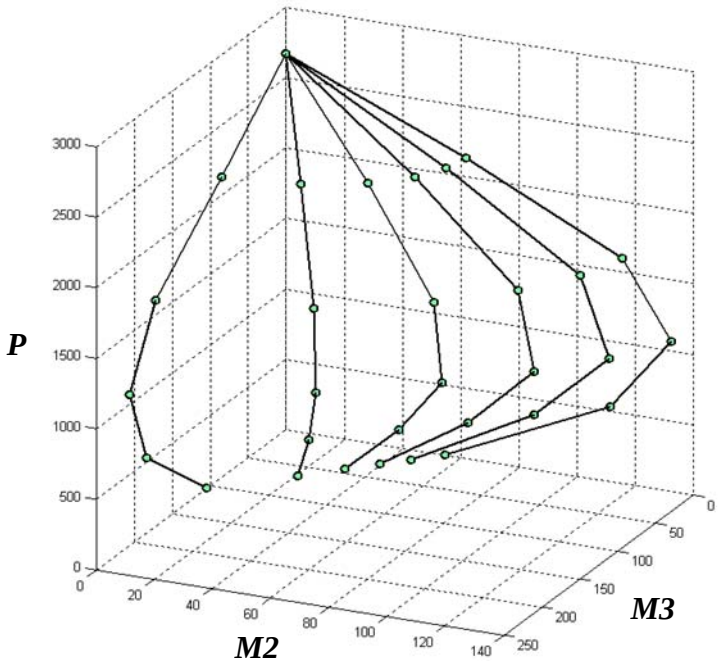

Fig. 3.10: PMM Interaction Surface

For PMM hinges it requires to specify multiple moment -rotation curves corresponding to different values of P. However, in the present thesis one moment-rotation curve is supplied where abscissa presents the absolute rotation values corresponding to the axial force due to gravity loading only and ordinate presents Moment values normalized with yield moment (Figure 3.11). Yield moment is calculated from the PMM interaction surface for the appropriate axial force.

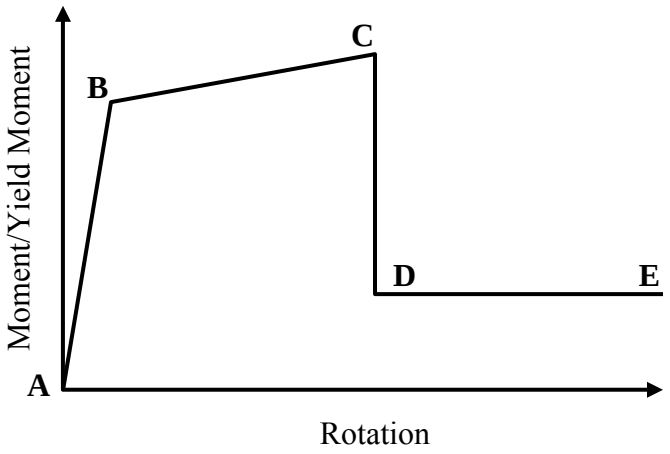

Fig. 3.11: Idealised moment-rotation curve of RC elements

3.5 MODELLING OF SHEAR HINGES FOR BEAMS AND COLUMNS

Flexural plastic hinges will develop, along with the predicted values of ultimate moment capacity, provided there is no prior failure in shear. In order to prevent this occurrence, design codes prescribe specifications (e.g. ductile detailing requirement of IS 13920: 1993) for adequate shear reinforcement, corresponding to the ultimate moment capacity level.

However, in practice, shear failure are commonly seen to occur in beams and columns in the event of a severe earthquake, owing to inadequate shear design. In non-linear analysis, this can be modelled by employing 'shear hinges'. These hinges should ideally be located at the same points as the flexural hinges near the beam column joints. If the shear hinge mechanism is triggered before the formation of flexural hinge, the moment demand gets automatically restricted and the full flexural hinge may not develop.

Shear force-deformation curves to assign shear hinges for beams and columns has been calculated based on IITM-SERC Manual (2005) and explained as follows. It is assumed

to be symmetric for positive and negative shear forces. A typical force-deformation curve is shown in Figure 3.12.

Yield shear strength (V_y) is calculated by adding strength of the shear reinforcement (V_{sy}) to the shear strength of the concrete section (V_c) in case of column. But for beam, when it is designed for medium and high ductility, shear strength contribution of concrete is completely ignored as in cracked section concrete does not provide any shear resistance. Shear resistance carried by shear reinforcement (V_{sy}) as per clause 40.4 of IS 456: 2000 is.

$$V_{sy} = 0.87 f_y A_{sv} \frac{d}{s_v} \tag{3.12}$$

Where, f_y ≡ yield stress of the transverse reinforcement

A_{sv} ≡ Total cross sectional area of one stirrup considering all the legs

d ≡ effective depth

S_v ≡ Spacing between two stirrup

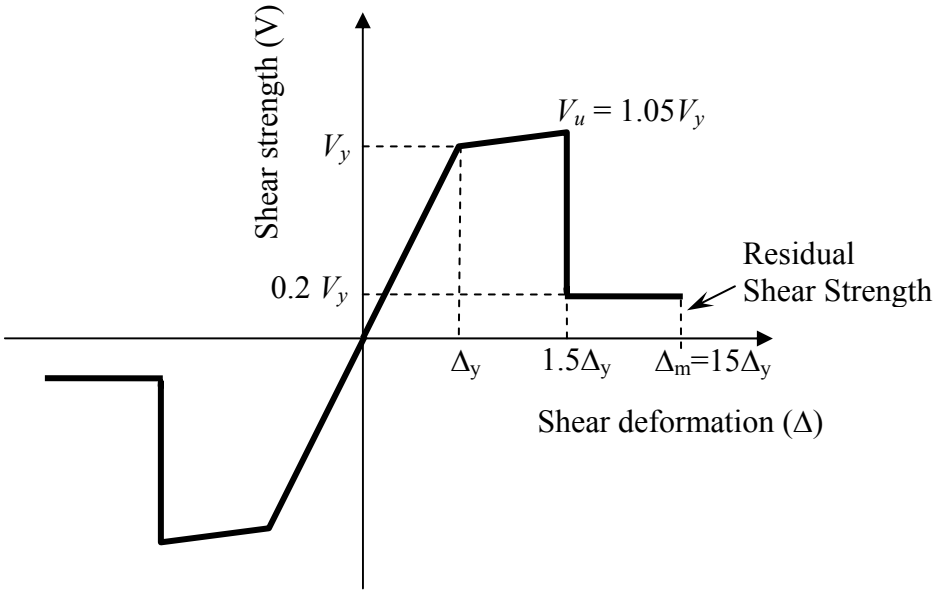

Fig. 3.12: Typical shear force-deformation curves to model shear hinges

For calculation of V_{sy}, above formula is used putting $1.00f_y$ instead of $0.87f_y$ for the actual strain hardened reinforcement.

$$V_{sy} = 1.0 f_y A_{sv} \frac{d}{s_v} \tag{3.13}$$

In case of column shear strength in existing construction is calculated by the following expression

$$V_y = V_c + V_{sy} \tag{3.14}$$

Shear resistance taken by the concrete (V_c) as given in the clause 40.2.2 of IS 456: 2000 is

$$V_c = \delta \tau_c b d$$

$$\text{where } \delta = 1 + \frac{3P_u}{A_g f_{ck}} \le 1.5 \text{ and } \tau_c = \frac{0.85\sqrt{0.8 f_{ck}}\,(\sqrt{1+5\beta}-1)}{6\beta} \tag{3.15}$$

$$\text{Here } \beta = \frac{0.116 f_{ck} b d}{100 A_{st}} \ge 1.0$$

For moderate and high ductility of the column section $\delta = 0 + \frac{3P_u}{A_g f_{ck}} \le 0.5$ is taken in calculation (ATC 40)

Shear deformation (Δ) is to be calculated using the following formula.

$$\Delta = \frac{\text{Yield shear strength}}{\text{Shear stiffness}} = \frac{R}{K_V} \tag{3.16}$$

Yield deformation should be calculated using shear stiffness of un-cracked member as shown in Equation C21

$$K_V = \frac{1}{f}\left(\frac{G \times b_W d}{l}\right) \tag{3.17}$$

Where G = Shear modulus of the reinforced concrete section

A_g = Gross area of the section

l = Length of member

f = Factor to account non-uniform distribution of shear stress. For rectangular section, f = 1.2 and for T and I section f = 1.0.

Ultimate shear deformation can be calculated using shear stiffness of the cracked member. Shear stiffness for the cracked member can be calculated using the procedure given in Park and Paulay (1975). The expression for shear stiffness of a rectangular section with 450 diagonal cracks and vertical stirrups is given in Equation 3.18

$$K_{v,45} = \frac{\rho_v}{1+4n\rho_v} E_s b_w d \tag{3.18}$$

Here, $\rho_v = \frac{A_{sv}}{s_v b_w}$; $n = \frac{E_s}{E_c}$ and $b_w = \text{web width}$

Similar expression is available for other inclination of cracking and stirrups in Park and Paulay (1975)

The ultimate shear strength (V_u) is taken as 5% more than yield shear strength (V_y) and residual shear strength is taken as 20% of the yield shear strength for modelling of the shear hinges as shown in Figure 3.10. Similarly maximum shear deformation is taken as 15 times the yield deformation. The values were taken as per FEMA recommendations.

3.6 NONLINEAR TIME HISTORY ANALYSIS

Time-history analysis is a step-by-step analysis of the dynamical response (in time domain) of a structure subjected to a specified ground motion. This section explains the nonlinear parameters, input ground motion, time integration and damping used in the present study. The dynamic input has been given as a ground acceleration time-history which was applied uniformly at all the points of the base of the structure; only one horizontal component of the ground motion has been considered. Fifteen natural ground acceleration time histories were employed for the dynamic analysis of the study. Computer software SAP2000 was used for carrying out nonlinear time-history analysis.

To maintain the similarity between the dynamic analysis and the pushover analysis, standard hinges were used to model nonlinearity in the frame through nonlinear links. Limitation of using this model is that the buildings do not undergo hysteretic energy dissipation during nonlinear dynamic analysis. Accepting this limitation results obtained from nonlinear dynamic analysis can still give an insight into the seismic behaviour of setback building frames. Also, soil-structure interaction effect and P-Δ effects were neglected in both pushover and dynamic analysis.

The damping matrix was calculated as a linear combination of the stiffness matrix scaled by a coefficient, and the mass matrix scaled by a second coefficient. These coefficients were not specified directly, but were computed by specifying equivalent fractions of critical modal damping at two different periods.

'Hilber-Hughes-Taylor alpha' (HHT) method was used for performing direct-integration time-history analysis. The HHT method is an implicit method and is popular due to its intrinsic stability. The HHT method uses a single parameter (alpha) whose value is bounded by 0 and -1/3.

Table 3.2: Characteristics of the selected ground motion

No.	Earthquake	Magnitude	Epicentre Distance (KM)	Duration (sec)	PGA (g)
1	Imperial Valley Earthquake May 18, 1940	6.9	16.9	12	0.32
2	Loma Prieta-Oakland October 17, 1989	7.1	3.5	40	0.28
3	Loma Prieta-Corralitos, October 17, 1989	7.1	7	40	0.63
4	Loma Prieta- Hollister, October 17, 1989	7.1	48	60	0.37
5	Loma Prieta- Lexington Dam October 17, 1989	7.1	6.3	40	0.44
6	Northridge-Santa Monica January 17, 1994	6.7	23	60	0.37
7	Northridge-Sylmar, January 17, 1994	6.7	16	60	0.84
8	Northridge-Century City, January 17, 1994	6.7	20	60	0.22
9	Northridge-Newhall, January 17, 1994	6.7	20	60	0.59
10	Landers-Yermo, June 28, 1992	7.3	84	80	0.15
11	Landers- Lucerne Valley June 28, 1992	7.3	42	48	0.68
12	Petrolia -Cape Mendocino April 25, 1992	7.1	8.5	60	0.59
13	Sierra Madre-Altadena, June 28, 1991	5.6	12.6	40	0.44
14	Imperial Valley Earthquake-El Centro, October 15,1979	6.6	13.2	40	0.37
15	Morgan Hill-Gilroy 4, April 24, 1984	6.2	37.4	60	0.18

3.6.1 Natural Record of Earthquake Ground Motion

Fifteen natural ground acceleration time histories have been used for the dynamic analysis of the structural models. All these acceleration data were collected from Strong Motion Database available in the website of Center for Engineering Strong Motion Data, USA (http://www.strongmotioncenter.org/) and were scaled to have various peak ground accelerations ranging from 0.36g to 0.72g. The main characteristics of the input motion used are summarized in Table 3.1.

3.6 SUMMARY

This chapter presents details of the basic modelling technique for the linear and nonlinear analyses of RC framed structures. It also describes the selected building geometries used in the present study. The remaining sections of this chapter deal with plastic hinge (flexure and shear) modelling used for the present study. Finally, the important parameters for nonlinear time-history analysis and the input ground motion used in the present study are described.

CHAPTER 4

RESULTS AND DISCUSSIONS

4.1 INTRODUCTION

All the 48 building models with different possible setback irregularities presented in Chapter 3 are analyzed for linear/nonlinear static/dynamic behaviour using SAP2000 (v14). This chapter presents the results obtained from the above analyses. The results presented here are focussed on following two broad categories: (i) Lateral load pattern suitable for carrying out nonlinear static analyses and (ii) Estimation of target displacement.

The first half of this chapter is devoted on choosing a correct load pattern for nonlinear static analyses of setback buildings. Only invariant load patterns are considered for convenience and simplicity. The next half of this chapter presents the study on C_0 factor to improve the displacement coefficient method as outlined in FEMA 356: 2000 for the setback buildings. The chapter shows that nonlinear static analyses carried out as per the proposed load pattern and target displacement estimation procedure consistently predicting the results close to that of nonlinear dynamic analyses.

4.2 STUDY ON INVARIANT LOAD PATTERNS

The pattern of lateral load over the height of the building has great influence on the result of pushover analysis. FEMA 356: 2000 uses invariant distribution of load pattern as lateral inertial forces to determine relative magnitudes of shears, moments and deformations within the structure during earthquake. FEMA 356 also recommends using more than one lateral load pattern to bind the range of design actions that may occur during actual dynamic response. It will

be appropriate to consider adaptive load pattern in pushover analysis in order to include the effect of progressive structural yielding. However, for the present study only invariant load distribution shapes are planned to be utilise in pushover analysis, in order to keep the procedure computationally simple and attractive for design office environment. In the present study nonlinear static analysis or pushover analysis is ran by five different load patterns to justify which load pattern is good to determine the relative magnitudes of shears, moments and deformations within the structure during actual earthquake ground motion. The five different load patterns used in the analysis are listed below:

1. Mass Proportional Uniform load pattern (UNIFORM)
2. Mass Proportional Triangular Load Pattern (TLP)
3. Load Pattern similar to the First Mode Shape of the building (Mode Shape 1st)
4. Load Pattern similar to the IS 1893: 2002 static load distribution shape (IS-1893)
5. Upper bound pushover analysis as described by the Jan *et. al*. 2004 (UBPA)

There are many other procedures for carrying out pushover analysis available in literature where more than one load patterns are used. Those procedures are not considered as the focus of the present study is to use single load pattern.

4.2.1 Comparison of the Shape of available Load Patterns

Shape of all the five load patterns listed above are calculated for all 48 building models selected for this study and presented in Figures 4.1 to 4.48.

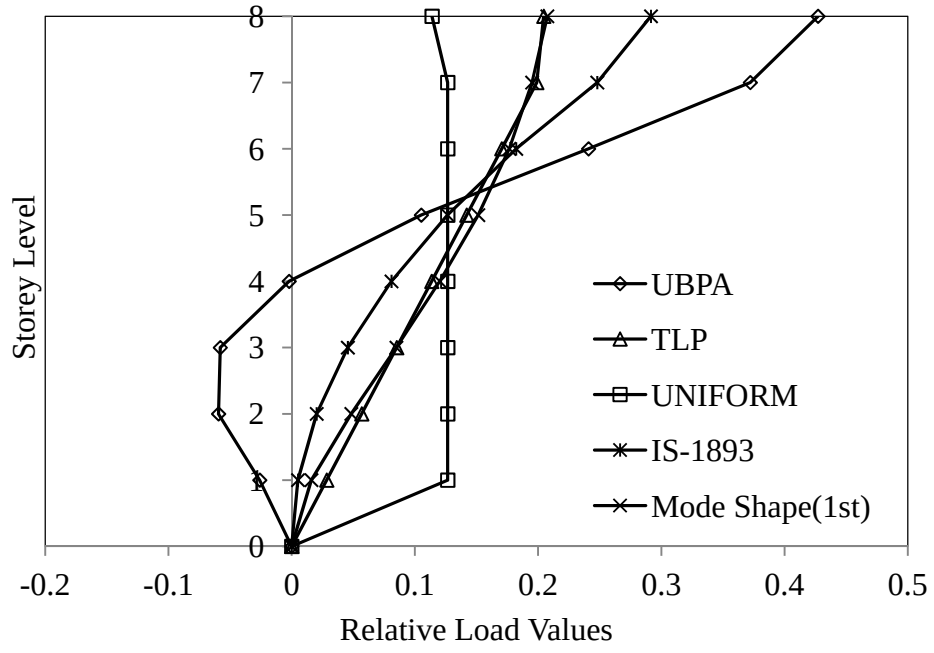

Fig. 4.1: Lateral load patterns for R-8-4 building frame

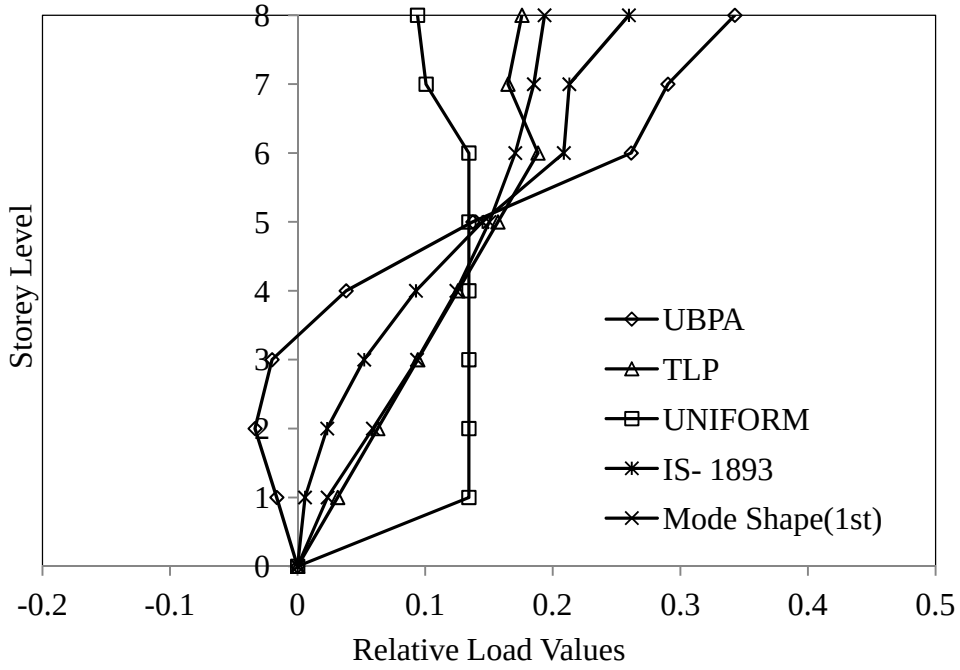

Fig. 4.2: Lateral load pattern for S1-8-4 building frame

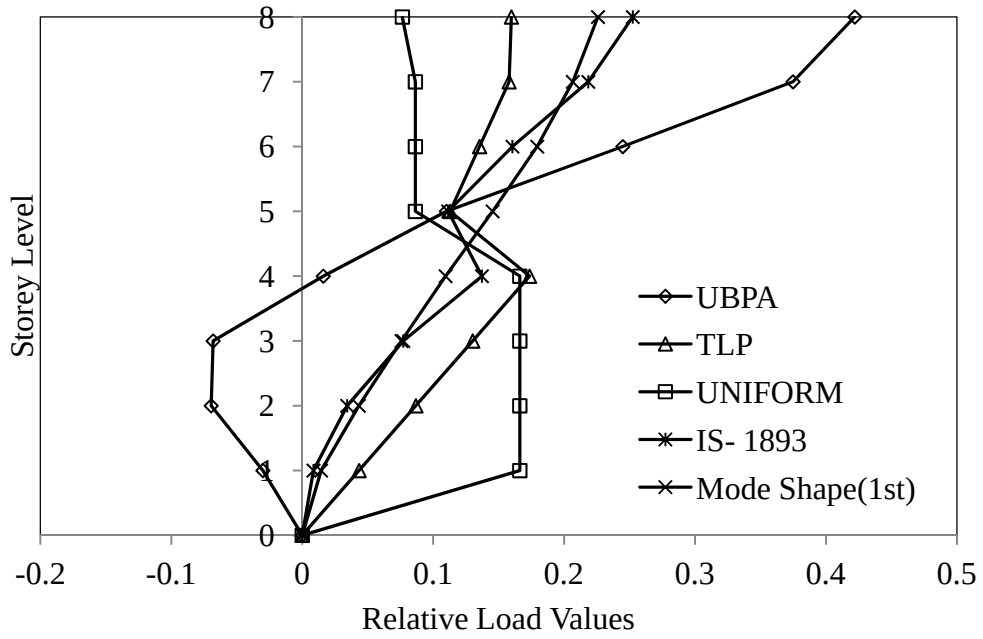

Fig. 4.3: Lateral load pattern for S2-8-4 building frame

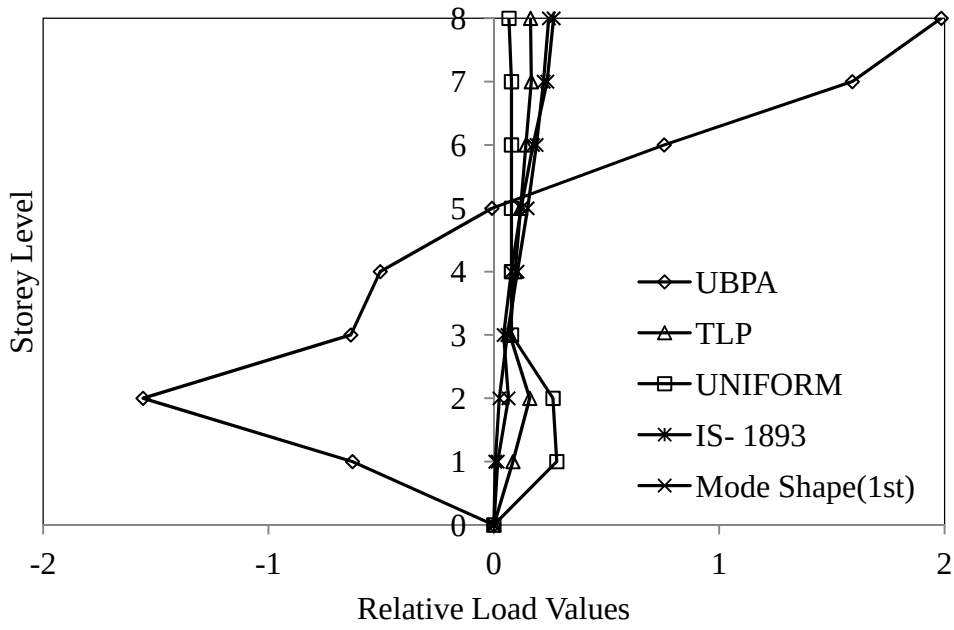

Fig. 4.4: Lateral load pattern for S3-8-4 building frame

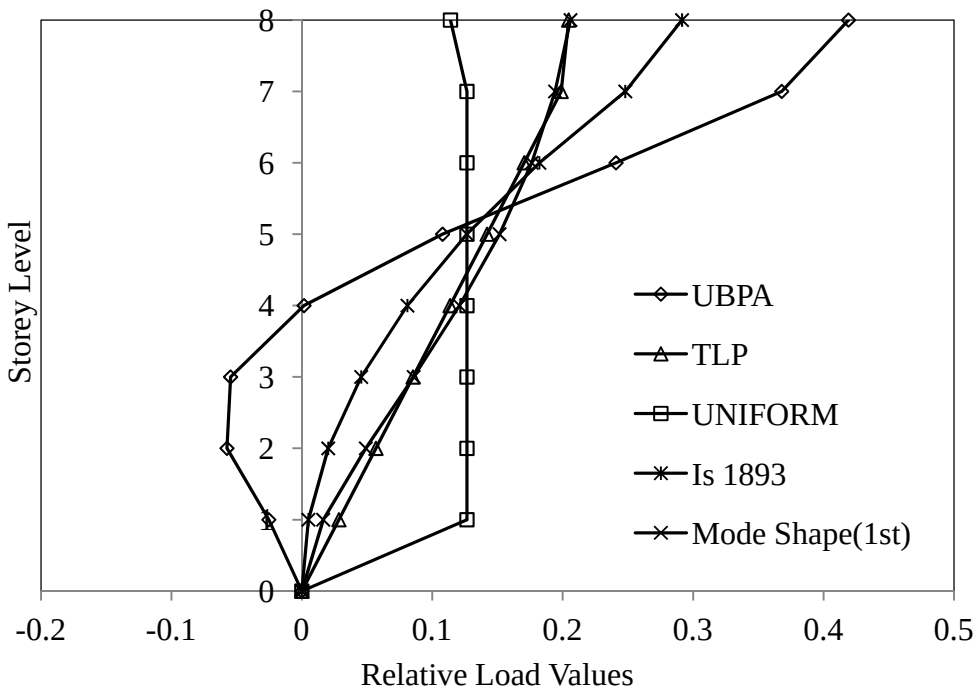

Fig. 4.5: Lateral load pattern for R-8-8 building frame

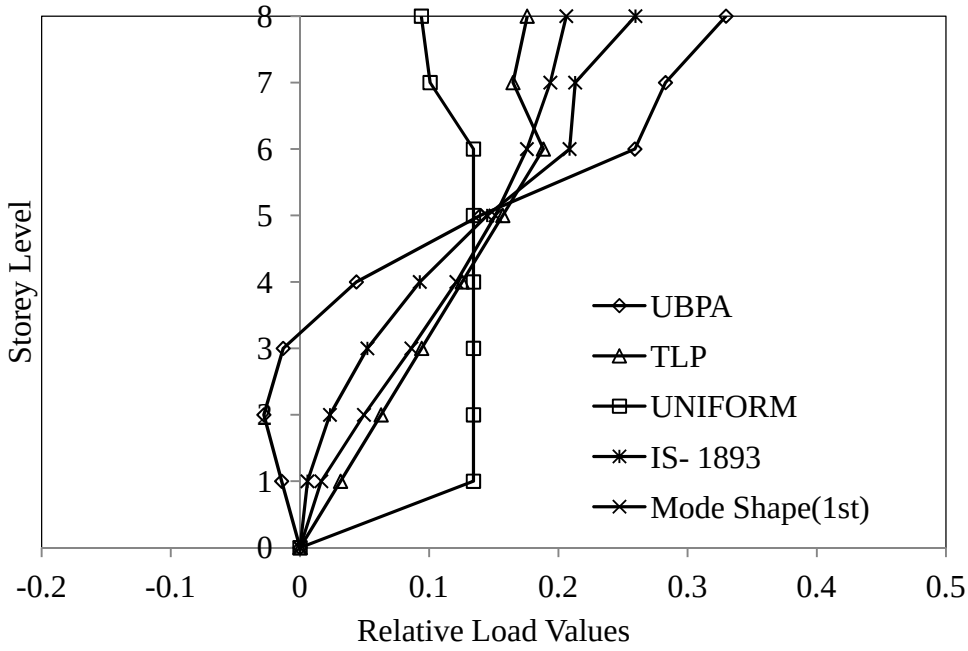

Fig. 4.6: Lateral load pattern for S1-8-8 building frame

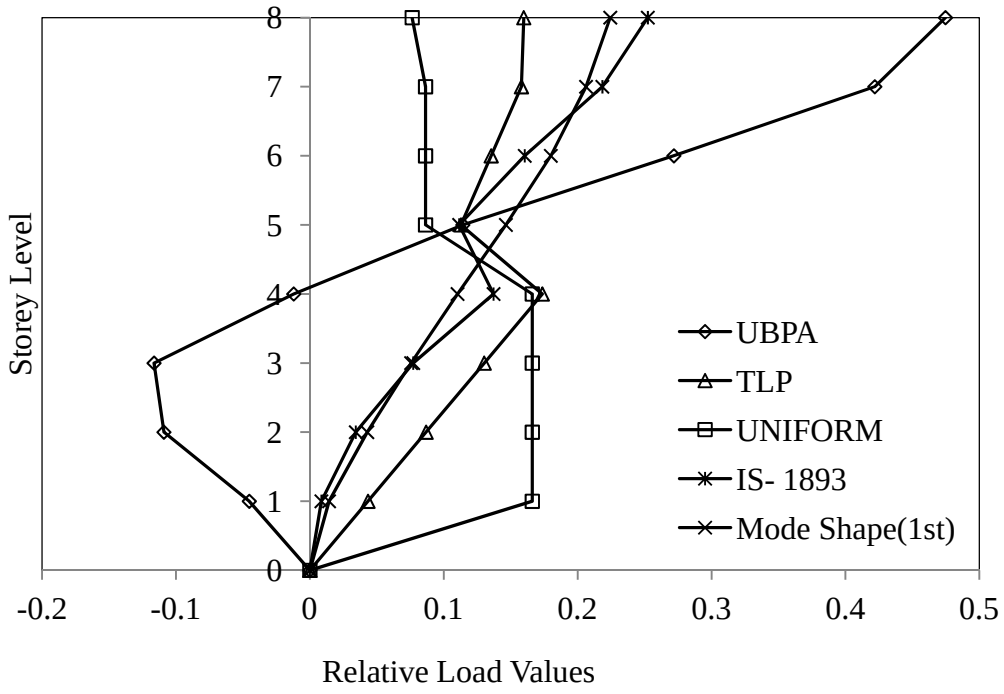

Fig. 4.7: Lateral load pattern for S2-8-8 building frame

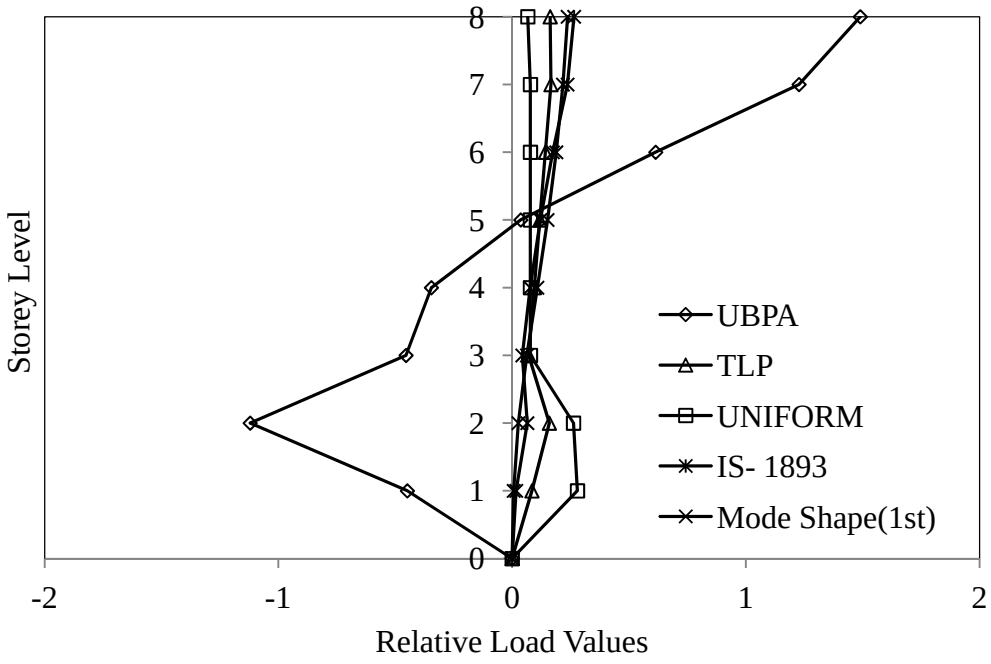

Fig. 4.8: Lateral load pattern for S3-8-8 building frame

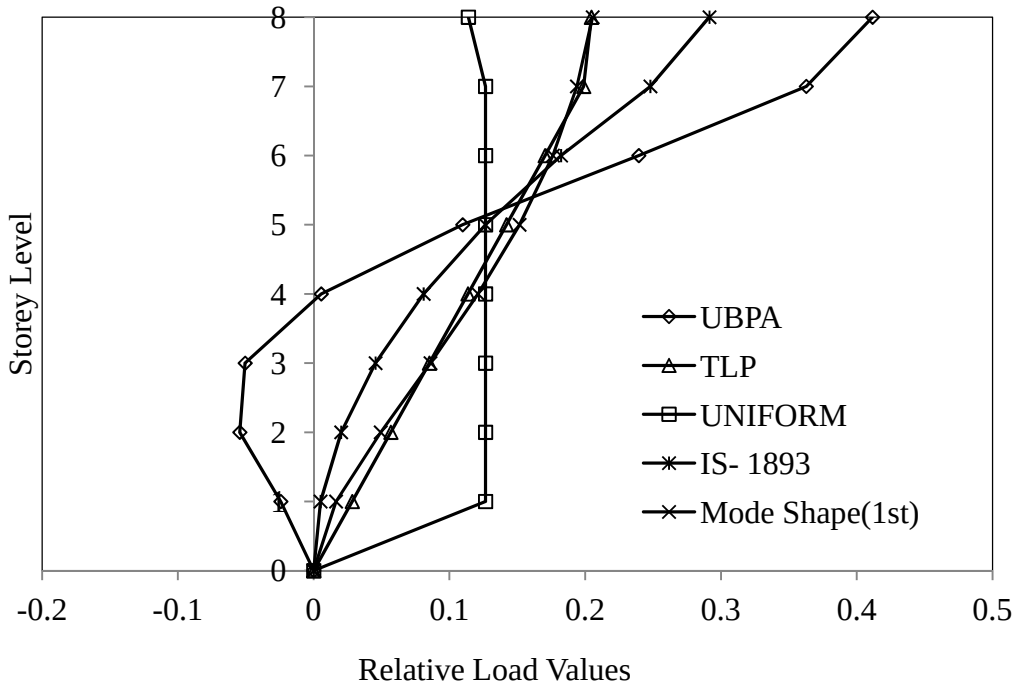

Fig. 4.9: Lateral load pattern for R-8-12 building frame

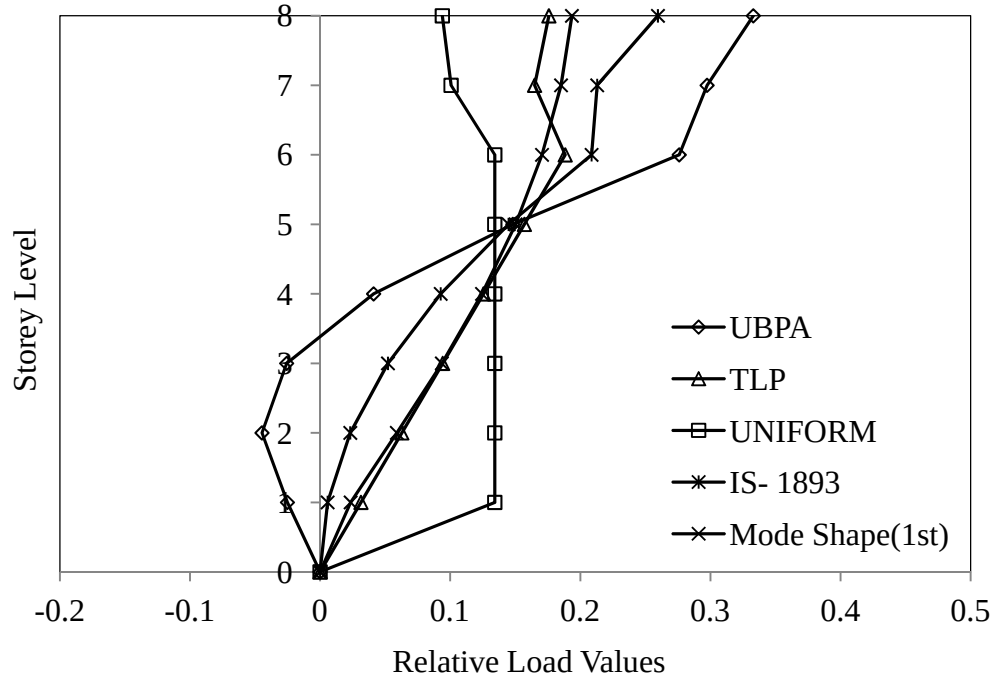

Fig. 4.10: Lateral load pattern for S1-8-12 building frame

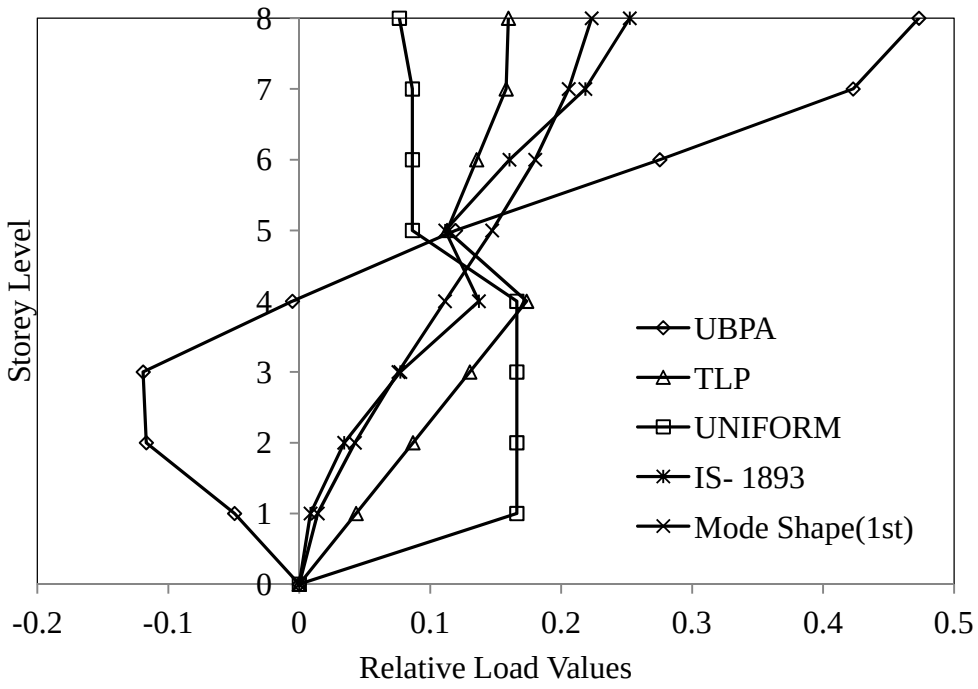

Fig. 4.11: Lateral load pattern for S2-8-12 building frame

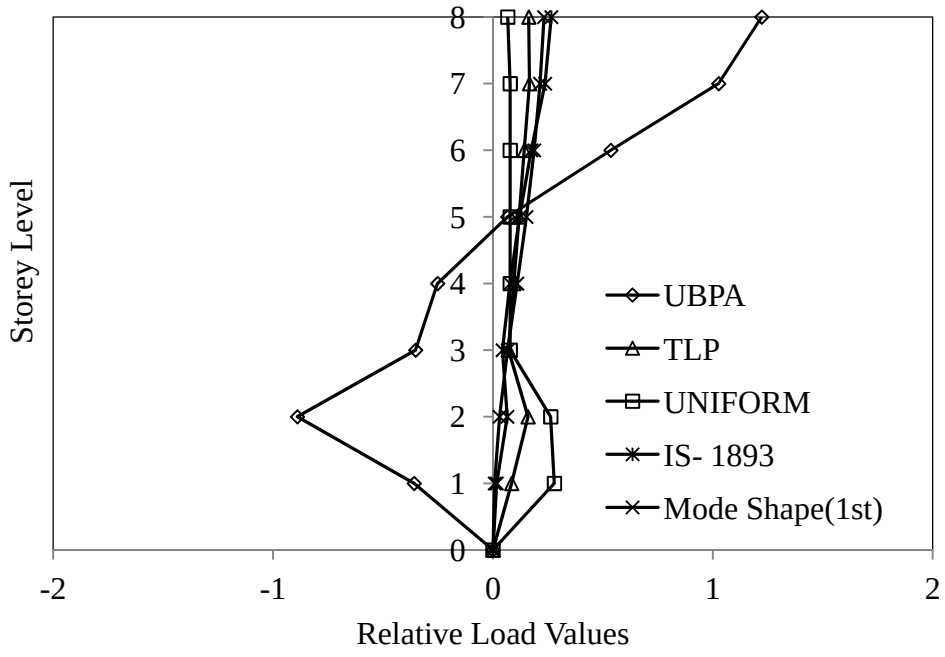

Fig. 4.12: Lateral load pattern for S3-8-12 building frame

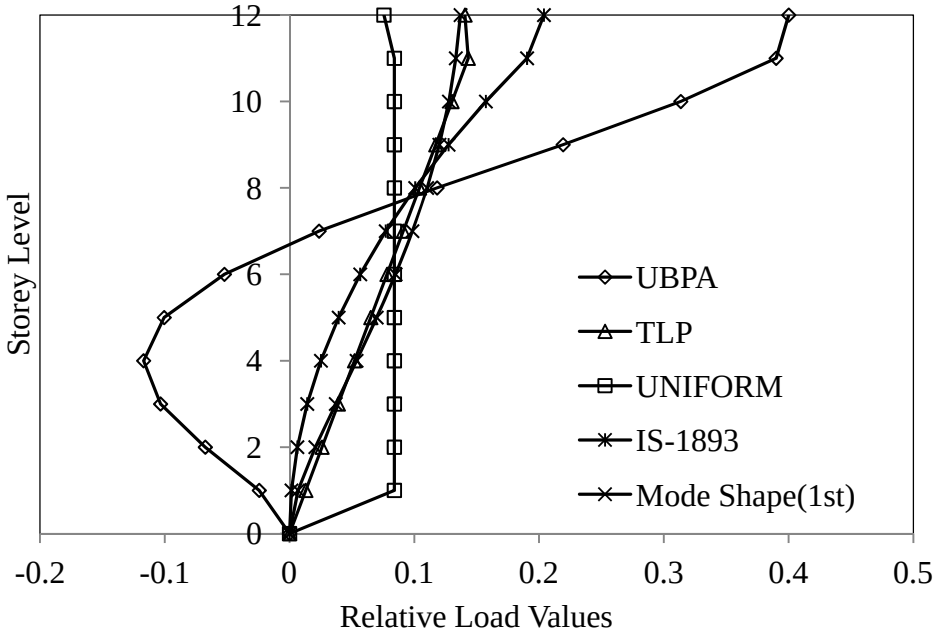

Fig. 4.13: Lateral load pattern for R-12-4 building frame

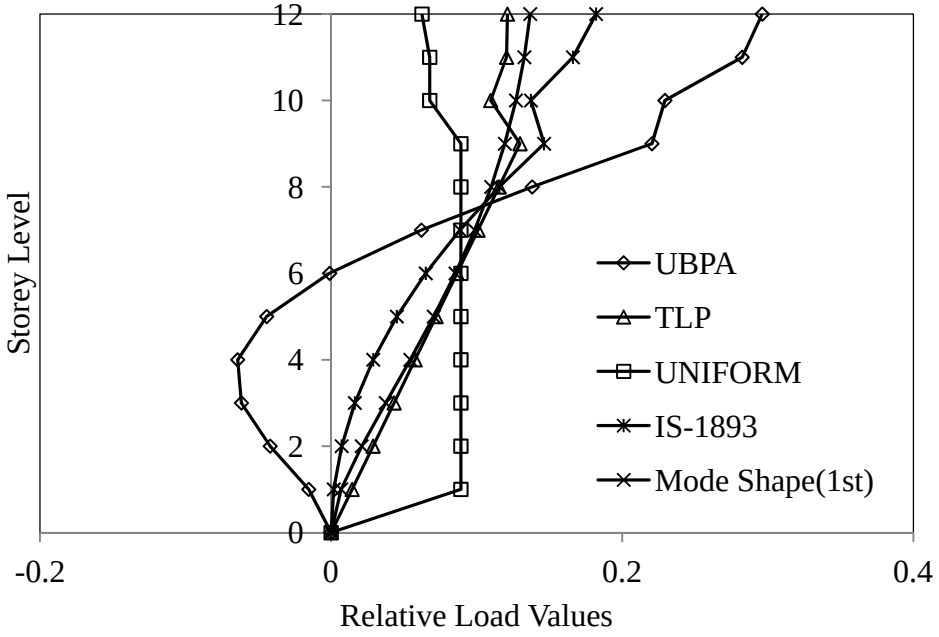

Fig. 4.14: Lateral load pattern for S1-12-4 building frame

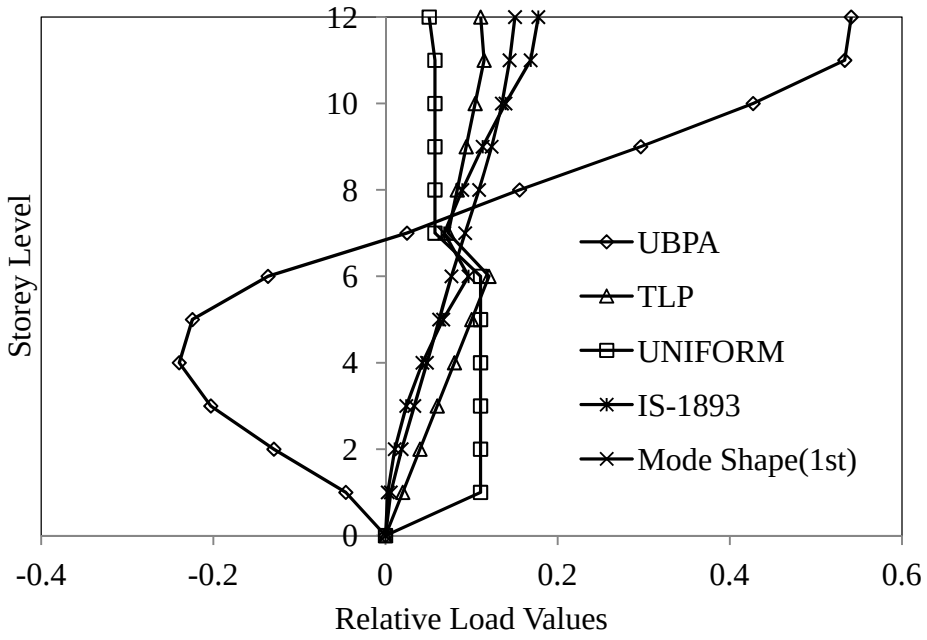

Fig. 4.15: Lateral load pattern for S2-12-4 building frame

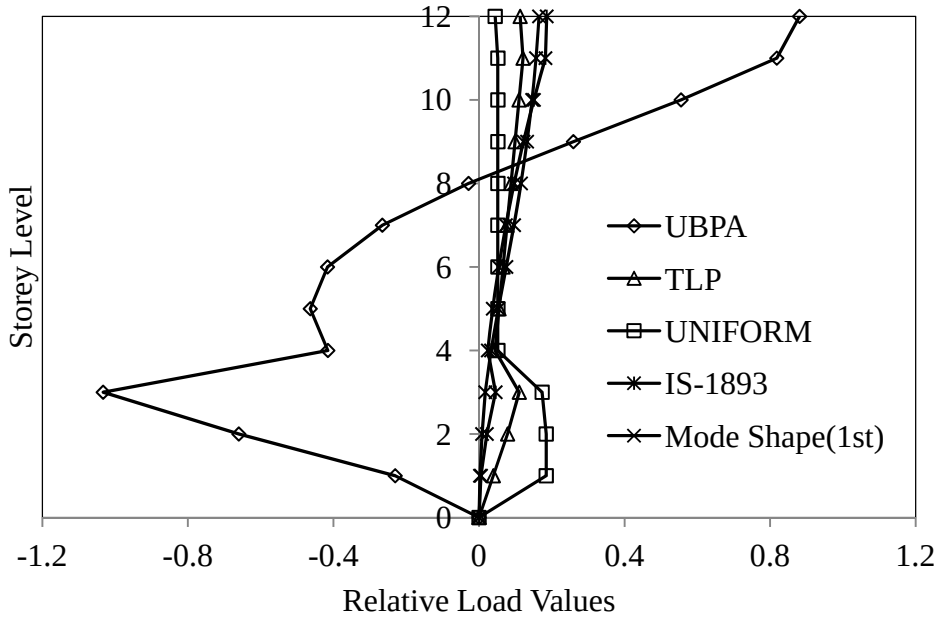

Fig. 4.16: Lateral load pattern for S3-12-4 building frame

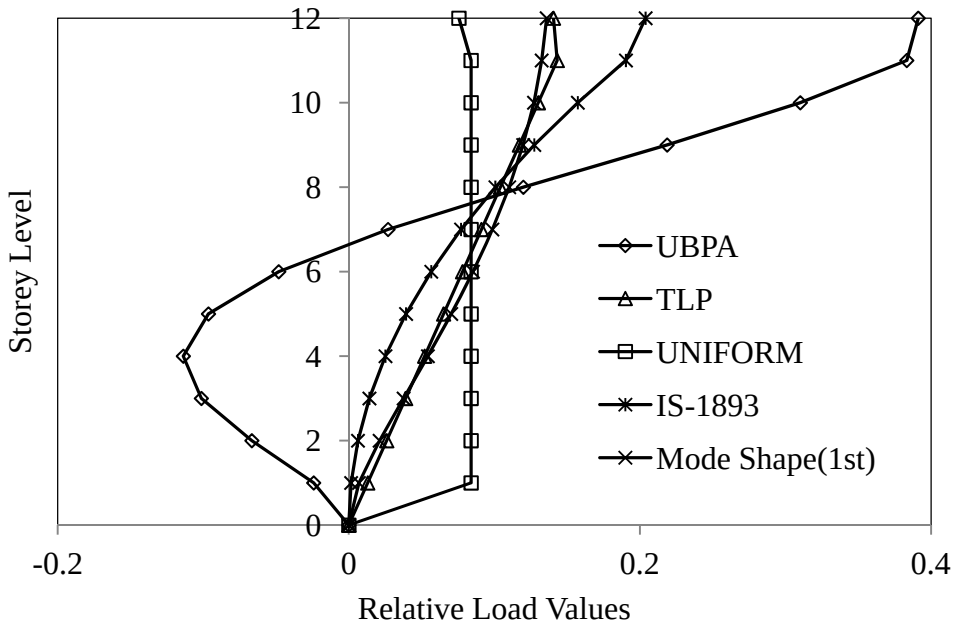

Fig. 4.17: Lateral load pattern for R-12-8 building frame

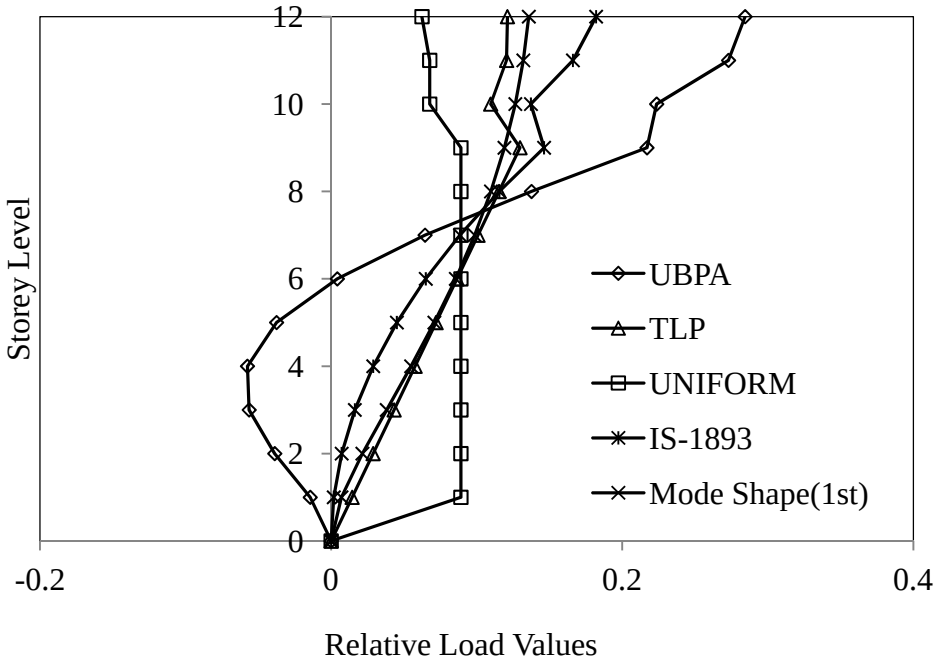

Fig. 4.18: Lateral load pattern for S1-12-8 building frame

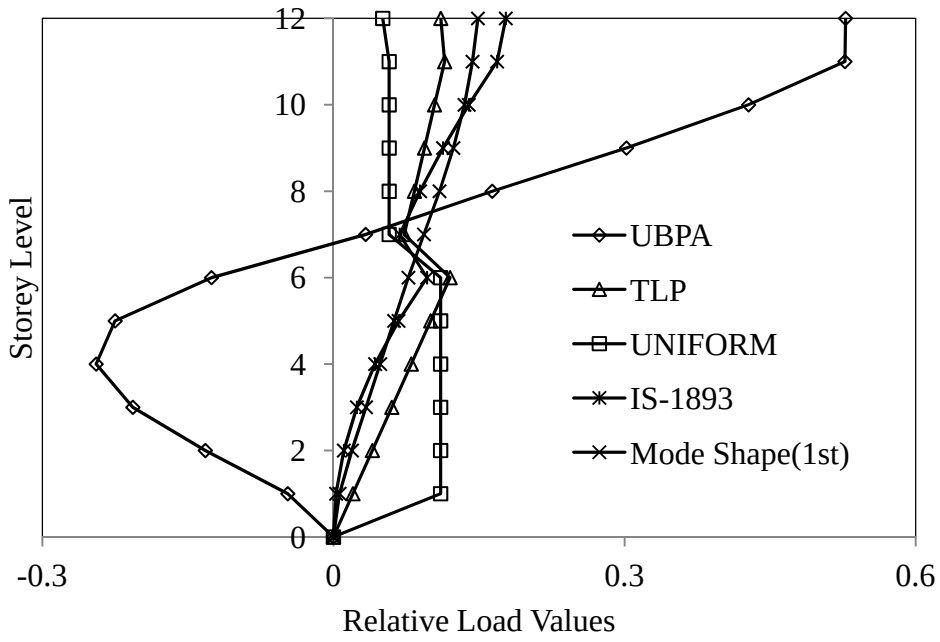

Fig. 4.19: Lateral load pattern for S2-12-8 building frame

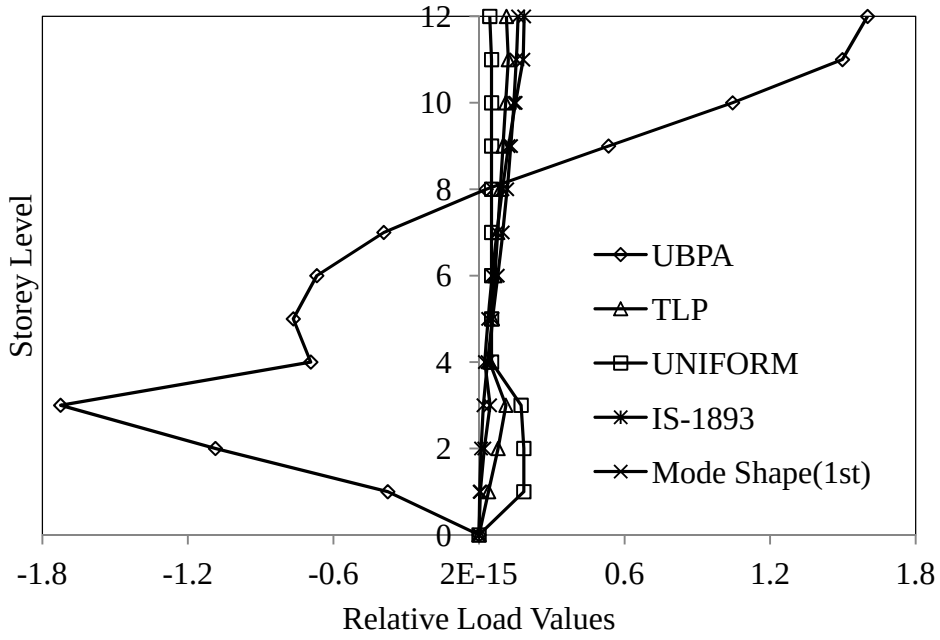

Fig. 4.20: Lateral load pattern for S3-12-8 building frame

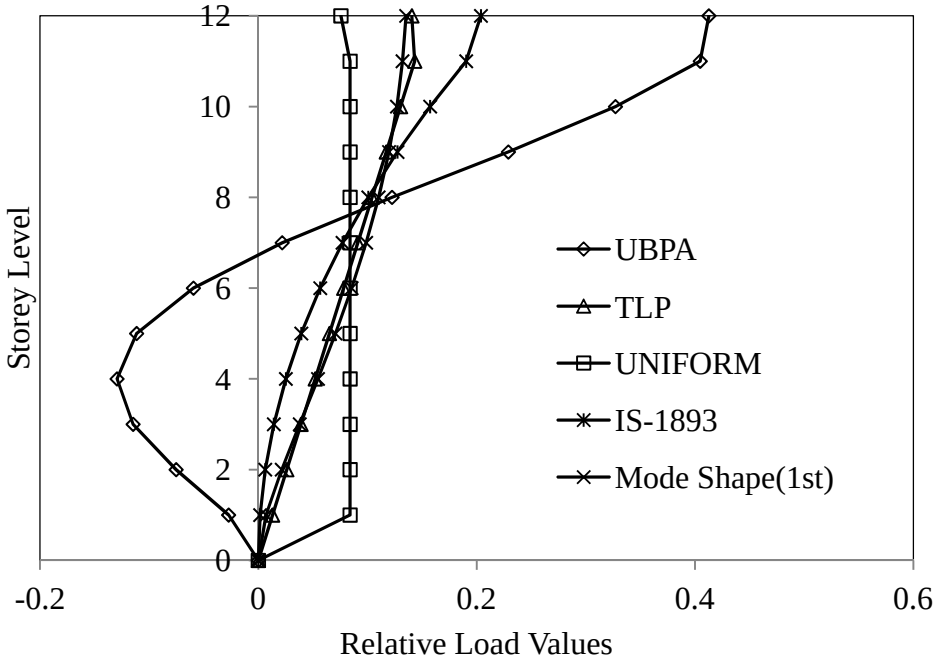

Fig. 4.21: Lateral load pattern for R-12-12 building frame

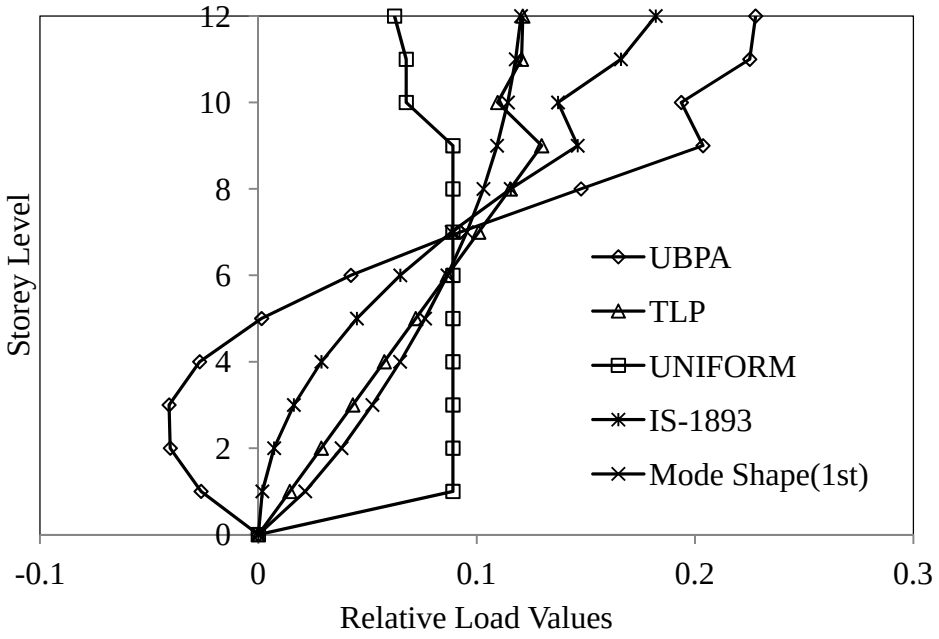

Fig. 4.22: Lateral load pattern for S1-12-12 building frame

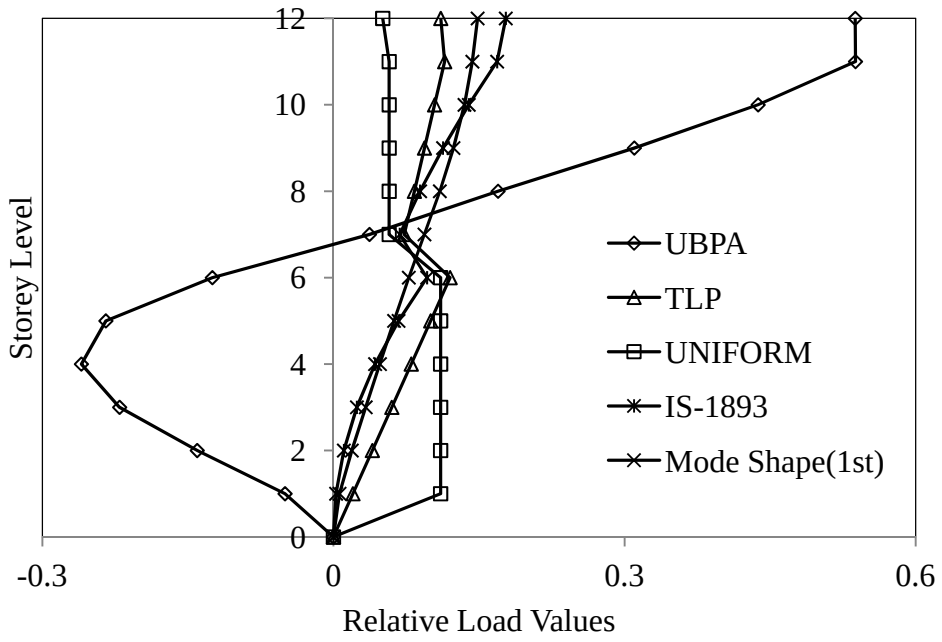

Fig. 4.23: Lateral load pattern for S2-12-12 building frame

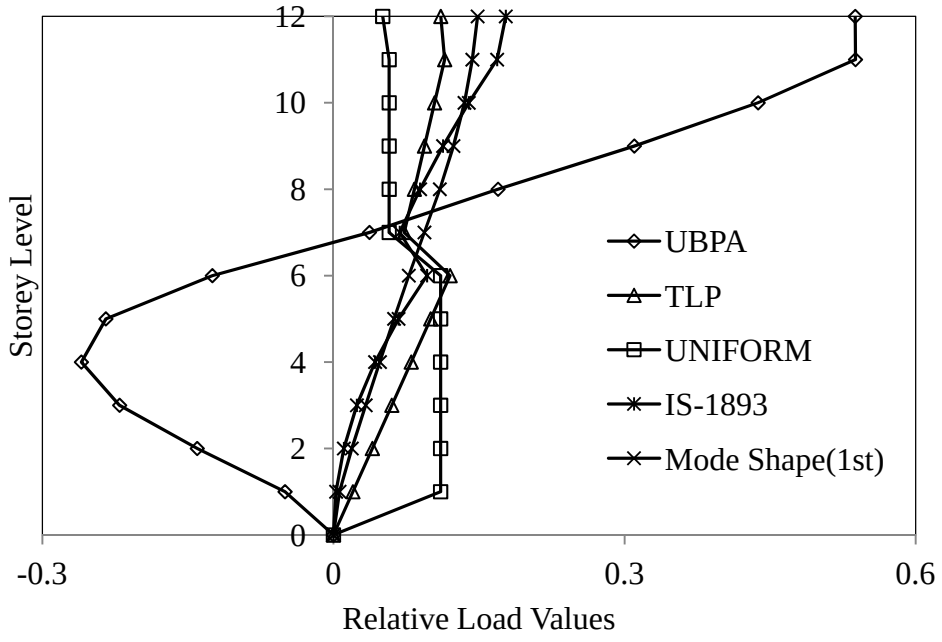

Fig. 4.24: Lateral load pattern for S3-12-12 building frame

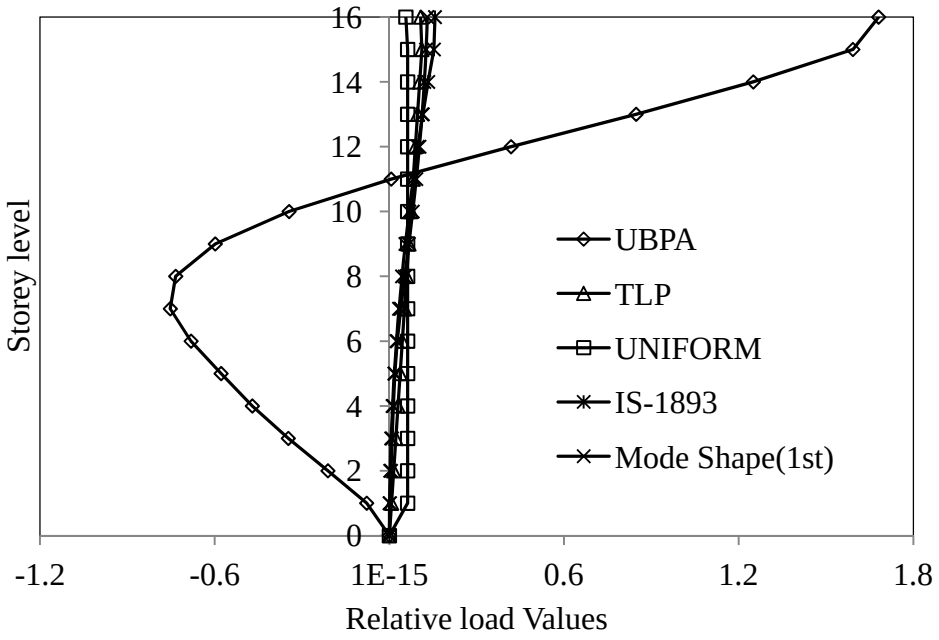

Fig. 4.25: Lateral load pattern for R-16-4 building frame

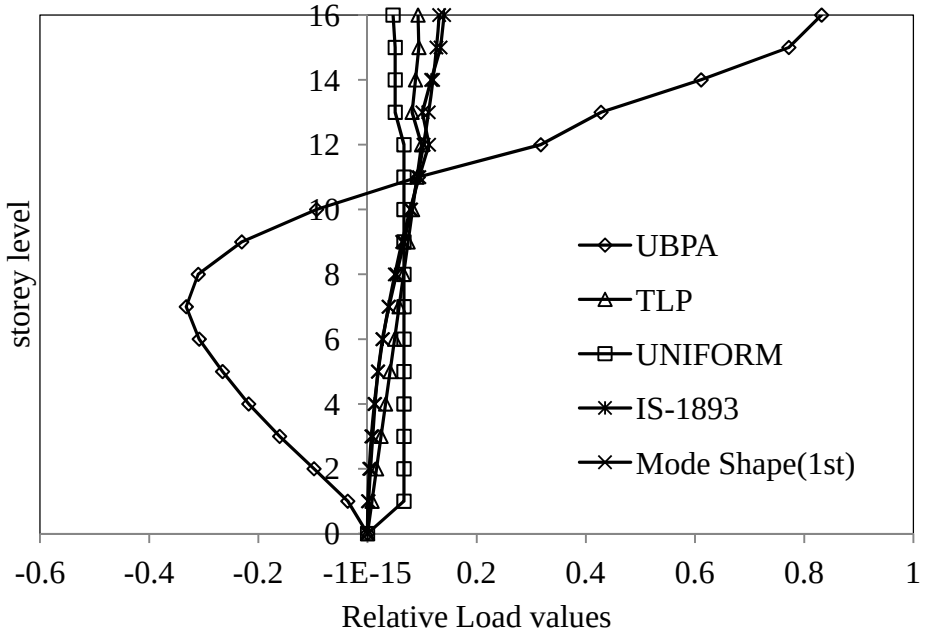

Fig. 4.26: Lateral load pattern for S1-16-4 building frame

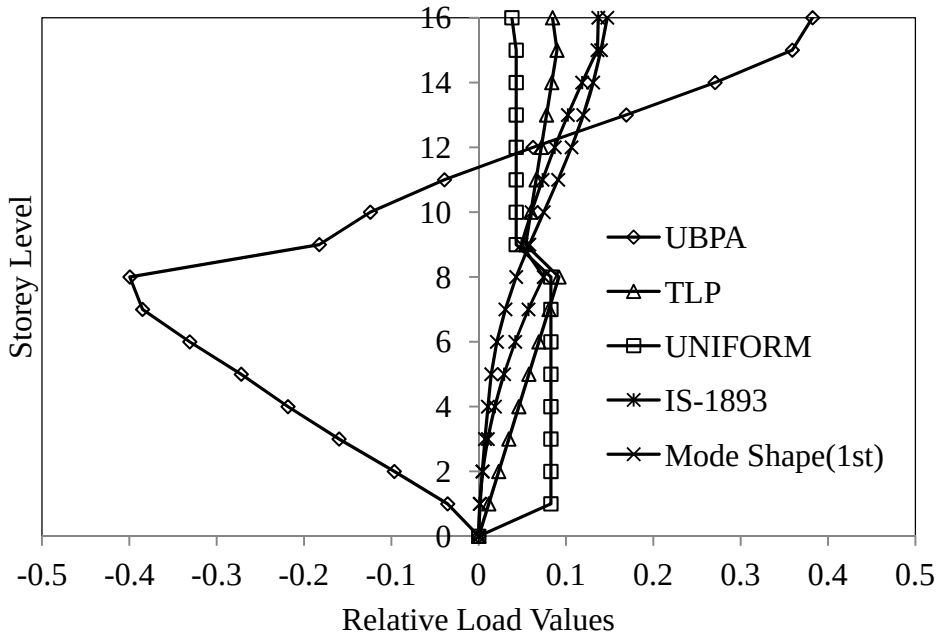

Fig. 4.27: Lateral load pattern for S2-16-4 building frame

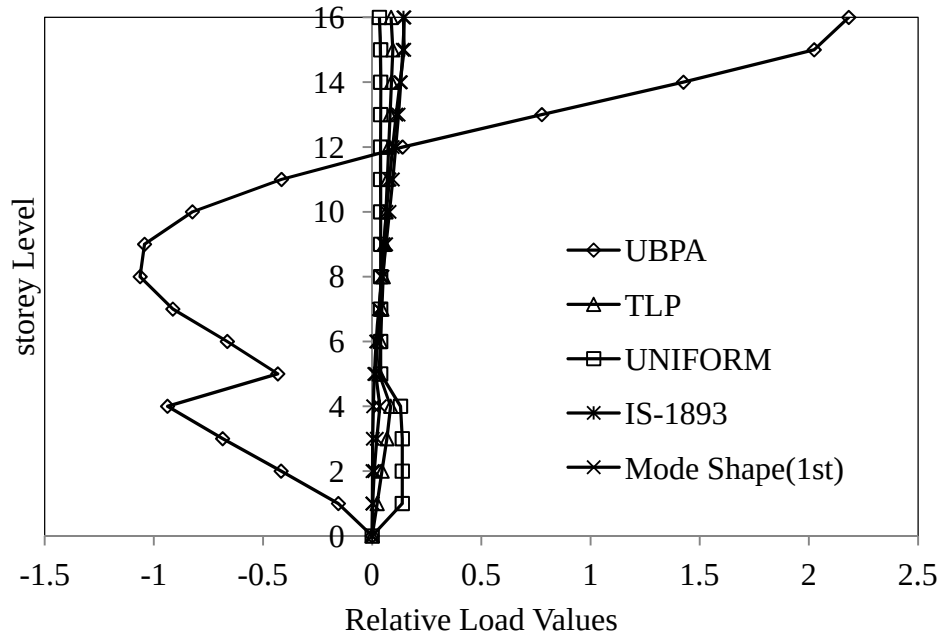

Fig. 4.28: Lateral load pattern for S3-16-4 building frame

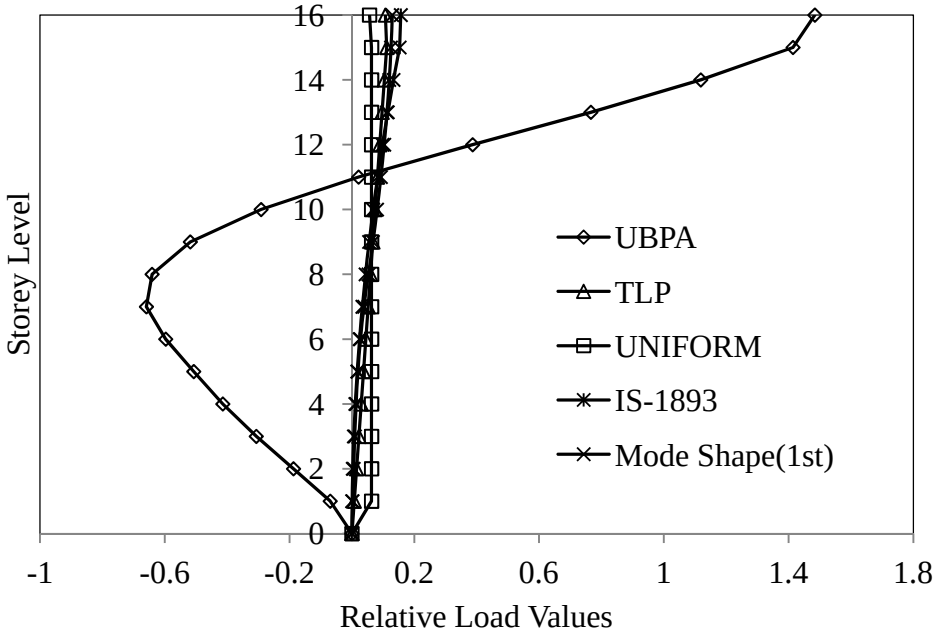

Fig. 4.29: Lateral load pattern for R-16-8 building frame

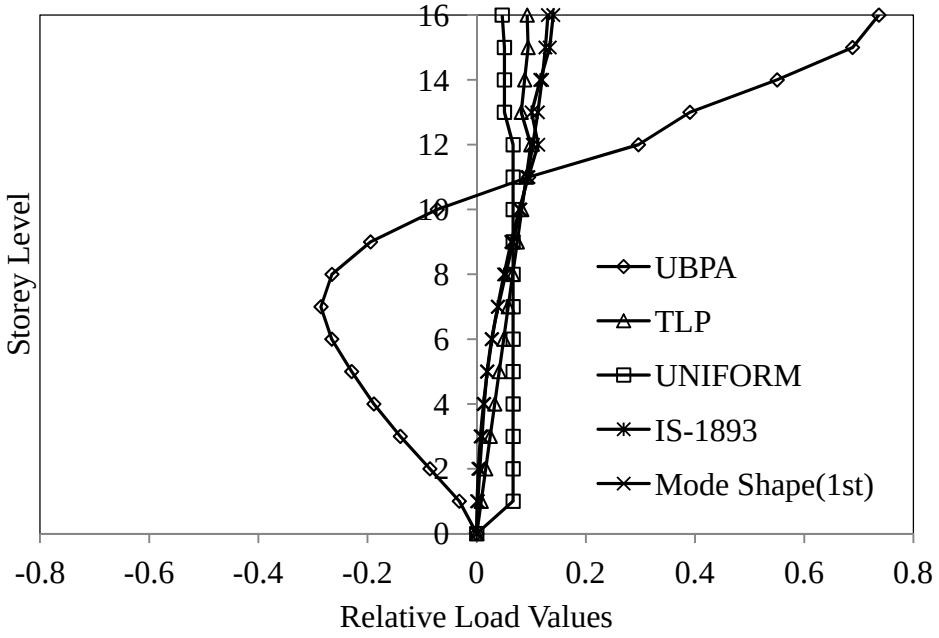

Fig. 4.30: Lateral load pattern for S1-16-8 building frame

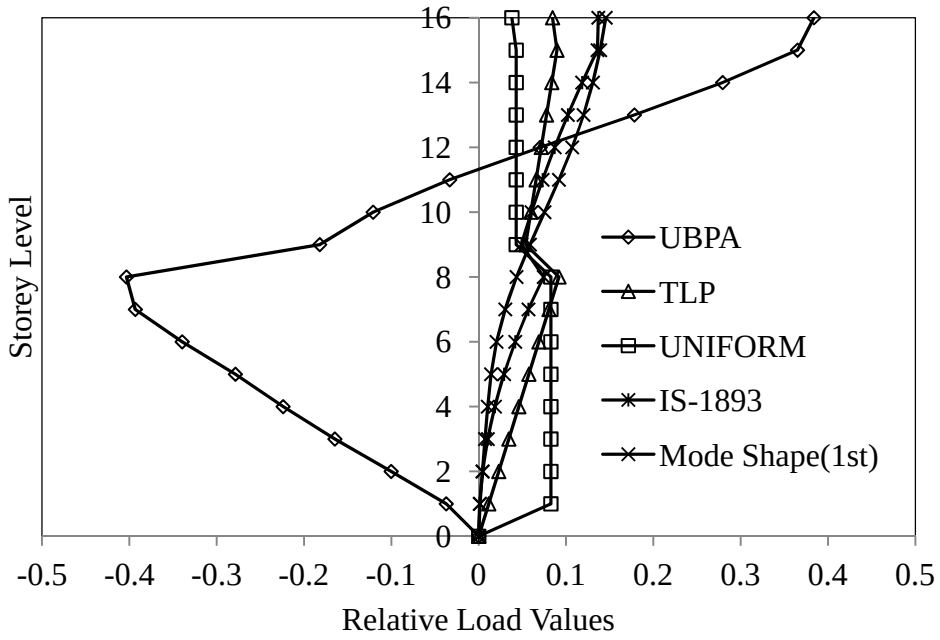

Fig. 4.31: Lateral load pattern for S2-16-8 building frame

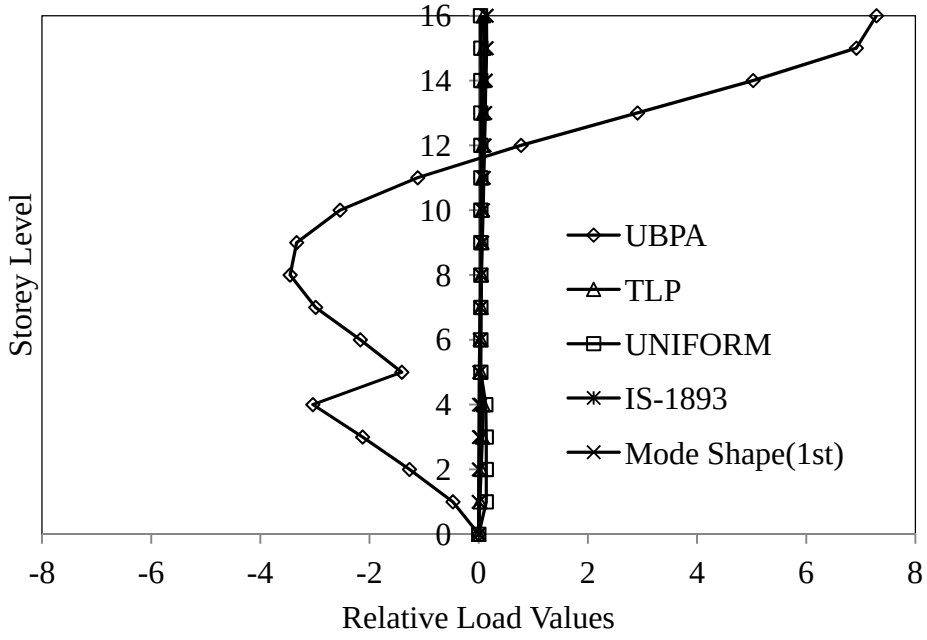

Fig. 4.32: Lateral load pattern for S3-16-8 building frame

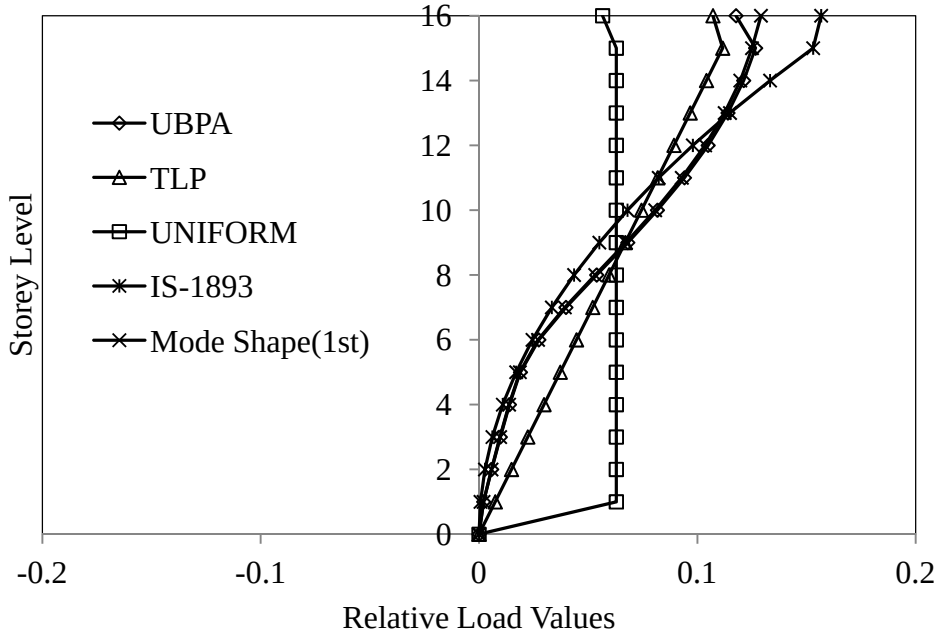

Fig. 4.33: Lateral load pattern for R-16-12 building frame

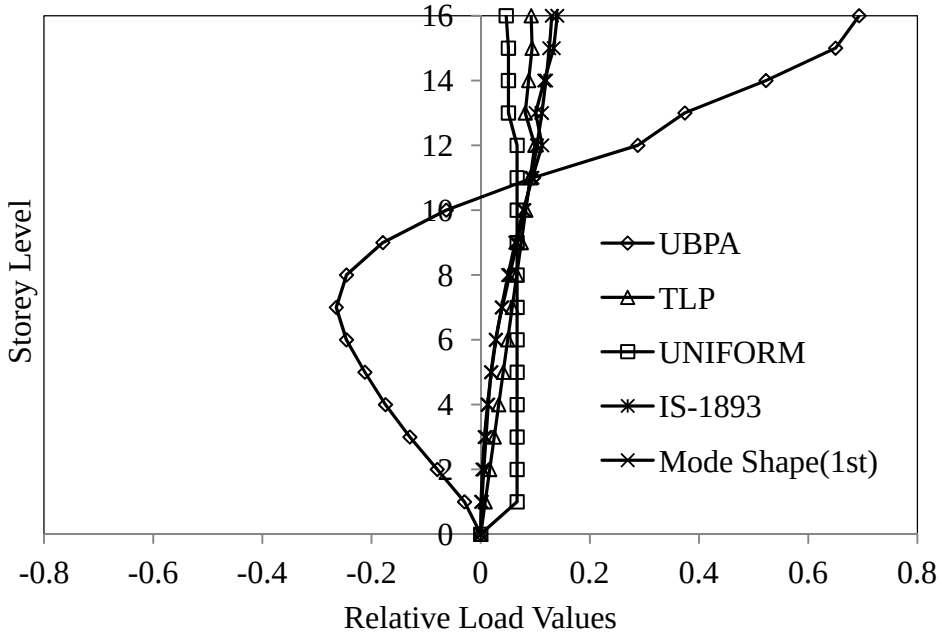

Fig. 4.34: Lateral load pattern for S1-16-12 building frame

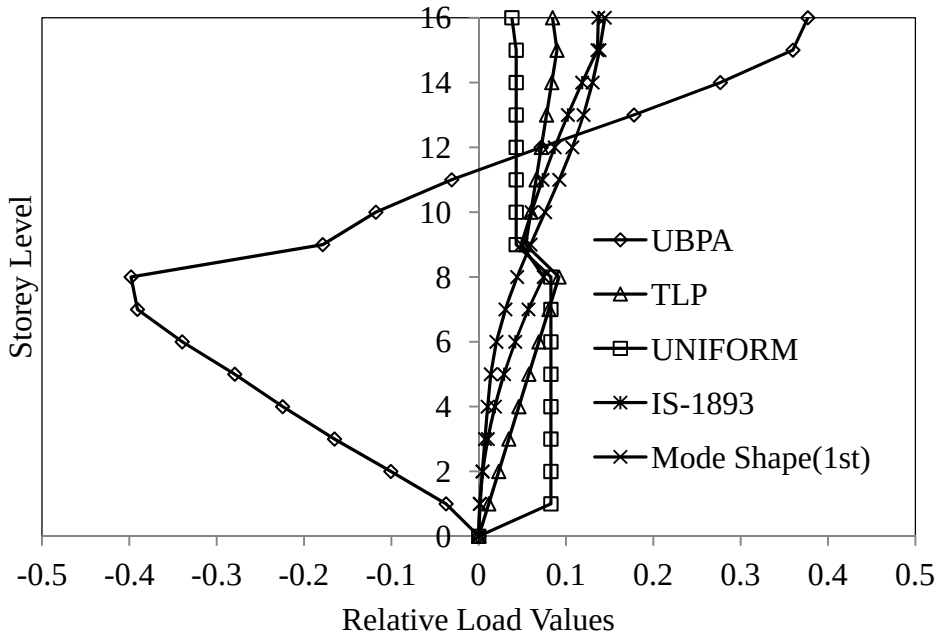

Fig. 4.35: Lateral load pattern for S2-16-12 building frame

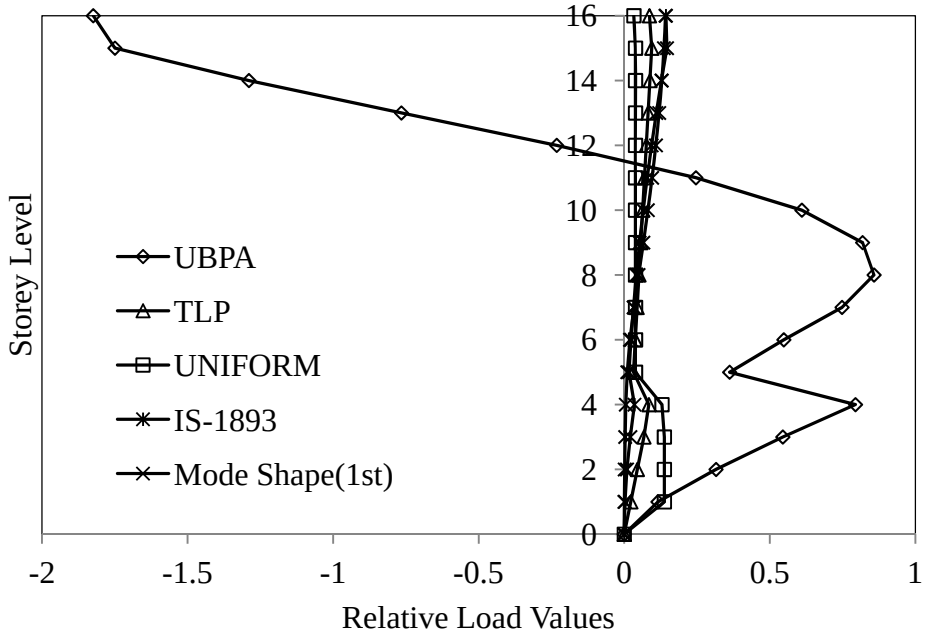

Fig. 4.36: Lateral load pattern for S3-16-12 building frame

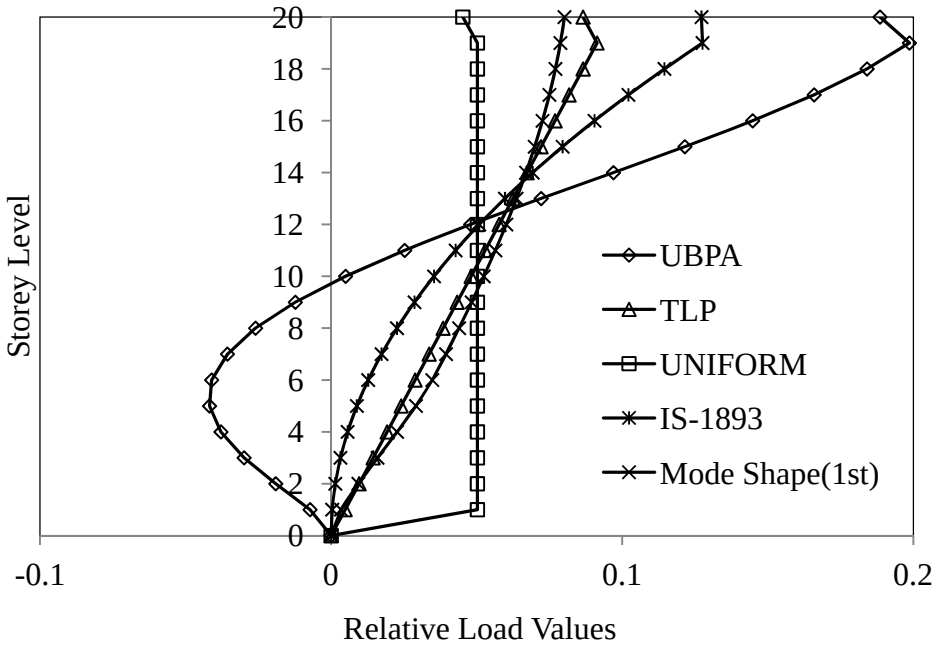

Fig. 4.37: Lateral load pattern for R-20-4 building frame

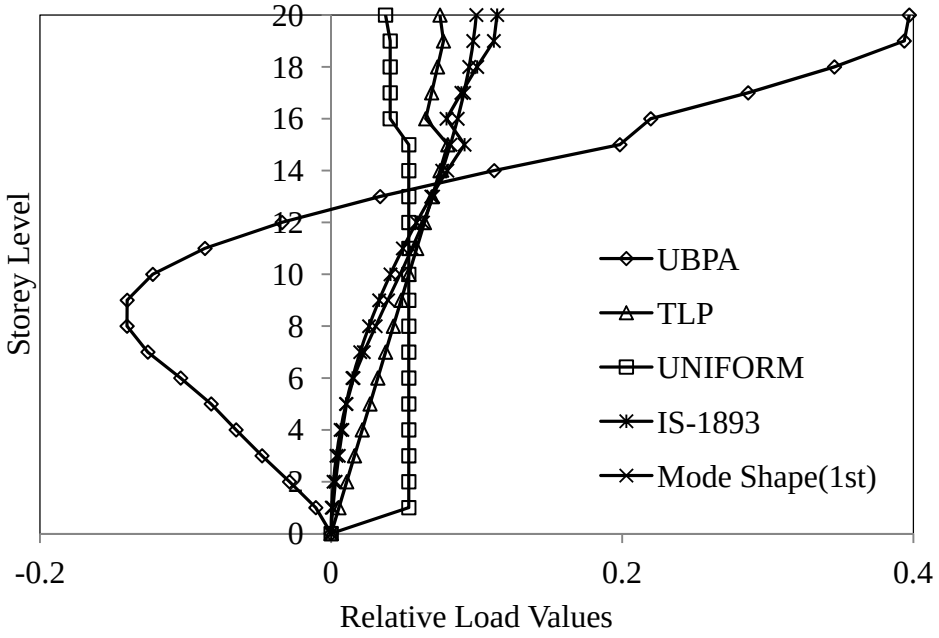

Fig. 4.38: Lateral load pattern for S1-20-4 building frame

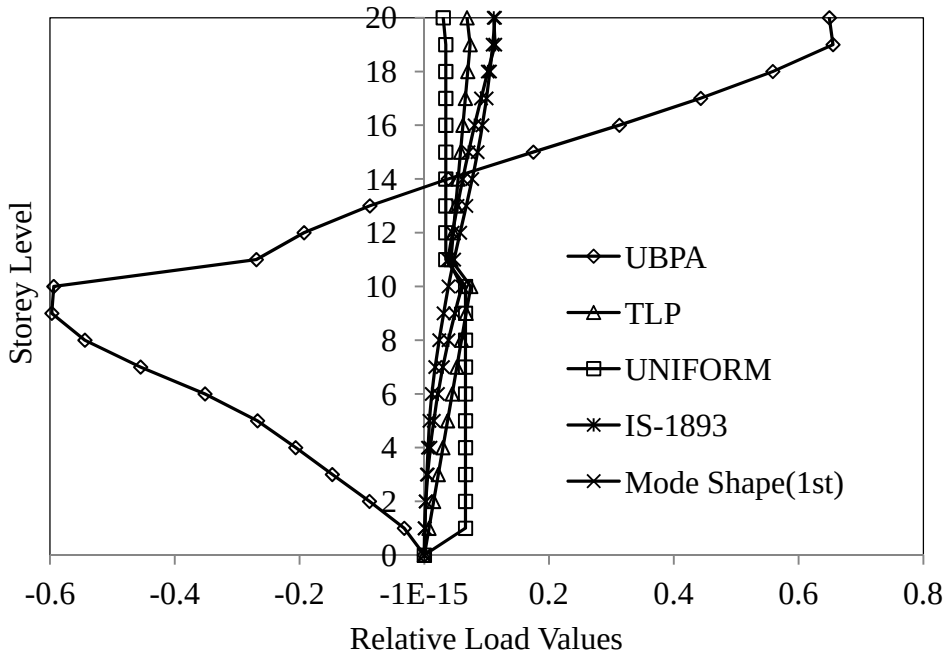

Fig. 4.39: Lateral load pattern for S2-20-4 building frame

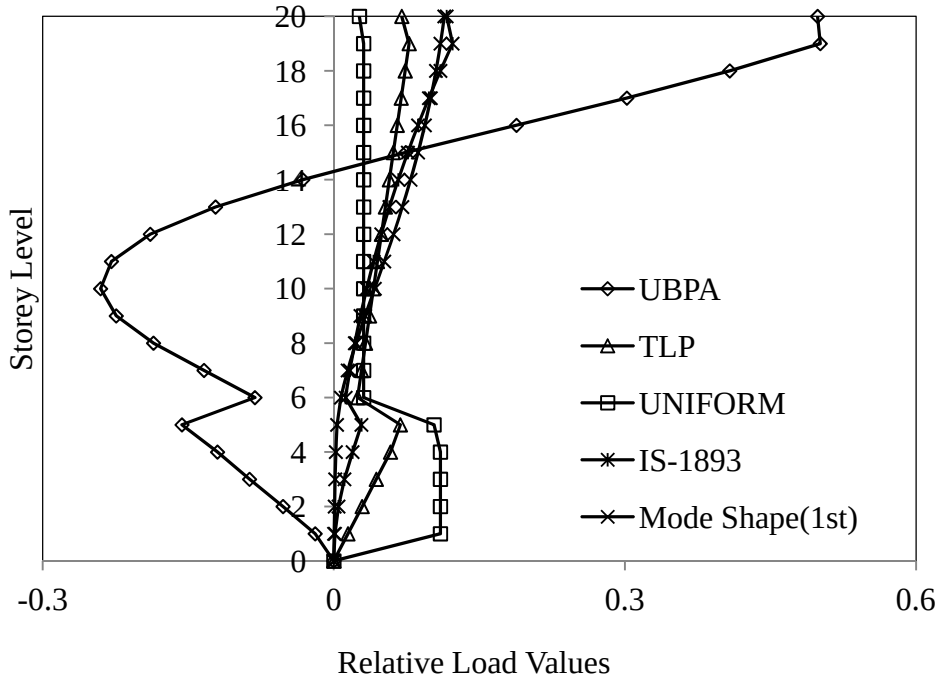

Fig. 4.40: Lateral load pattern for S3-20-4 building frame

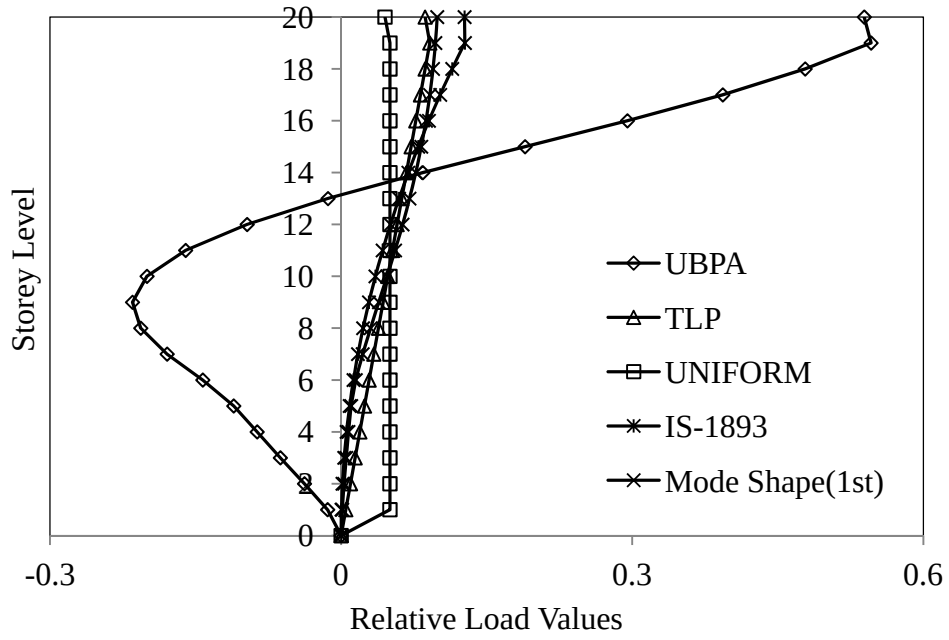

Fig. 4.41: Lateral load pattern for R-20-8 building frame

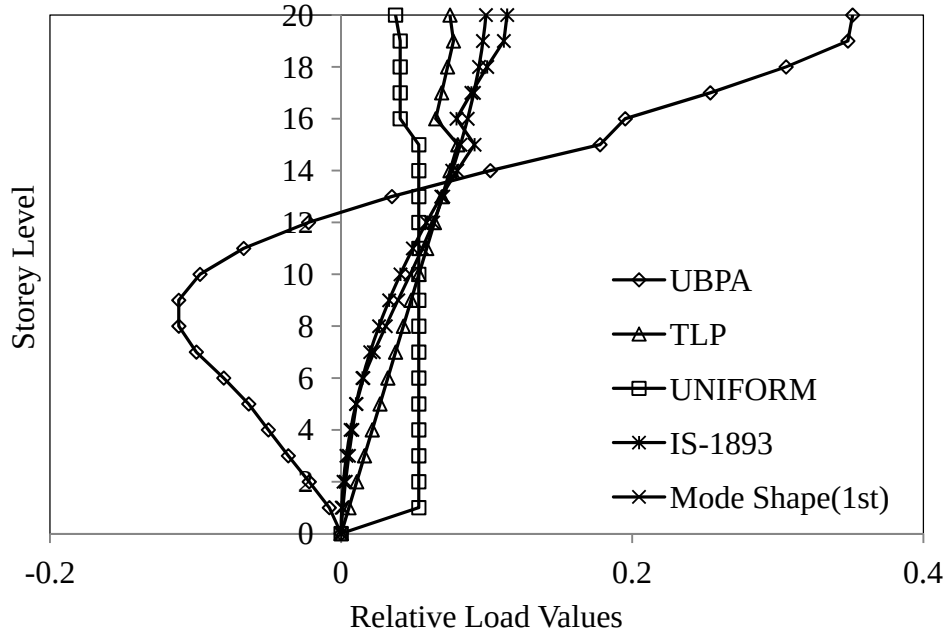

Fig. 4.42: Lateral load pattern for S1-20-8 building frame

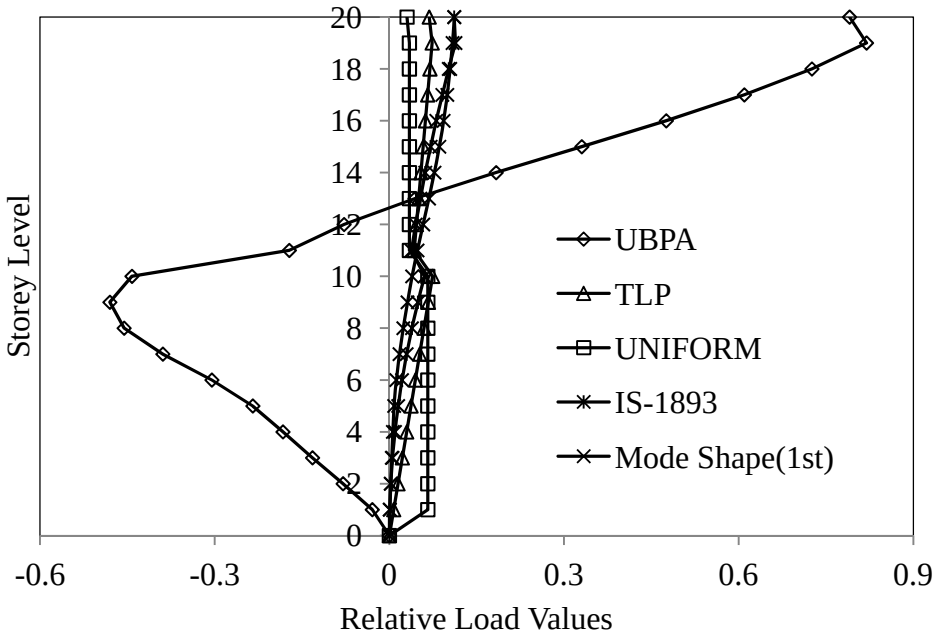

Fig. 4.43: Lateral load pattern for S2-20-8 building frame

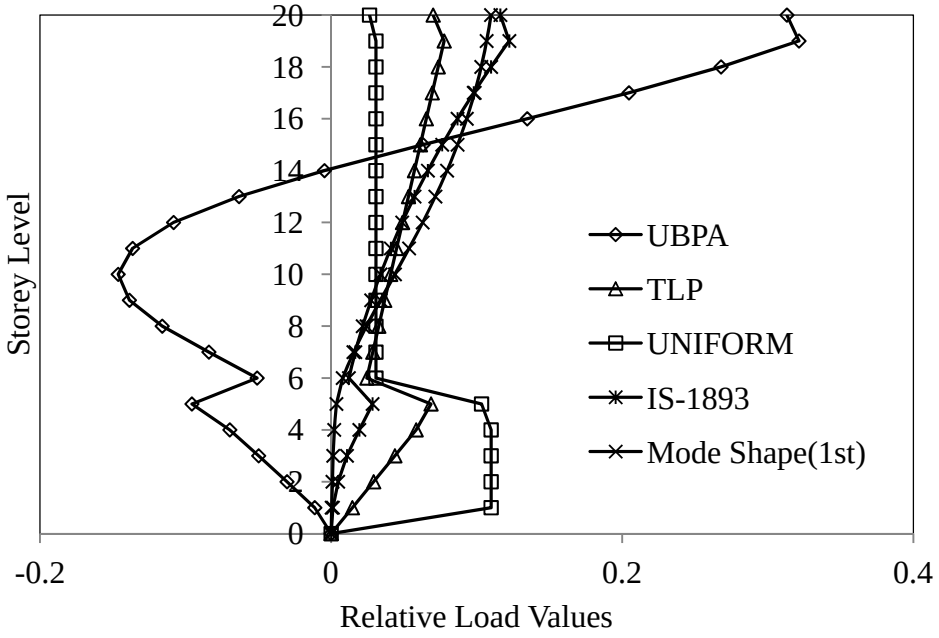

Fig. 4.44: Lateral load pattern for S3-20-8 building frame

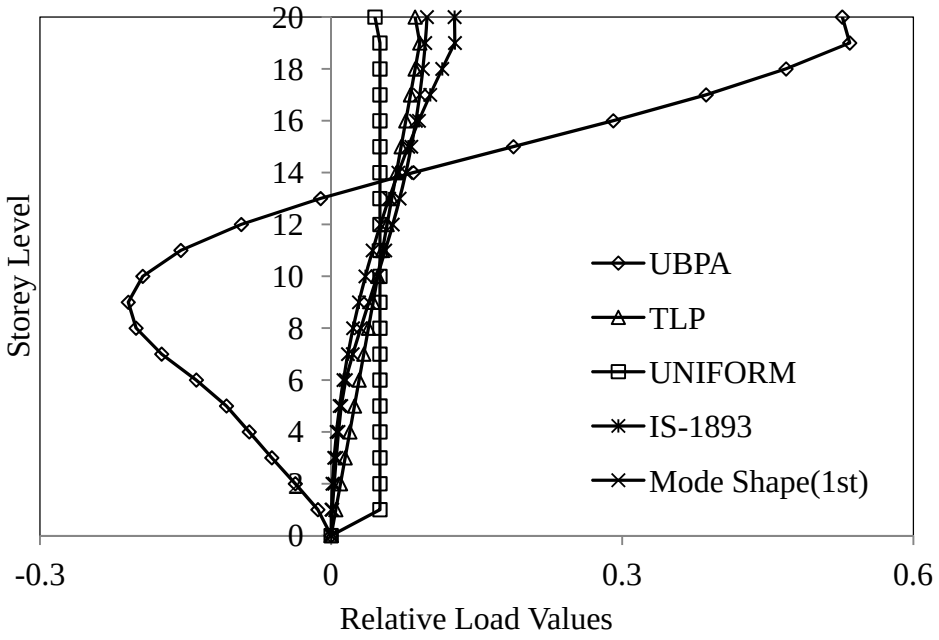

Fig. 4.45: Lateral load pattern for R-20-12 building frame

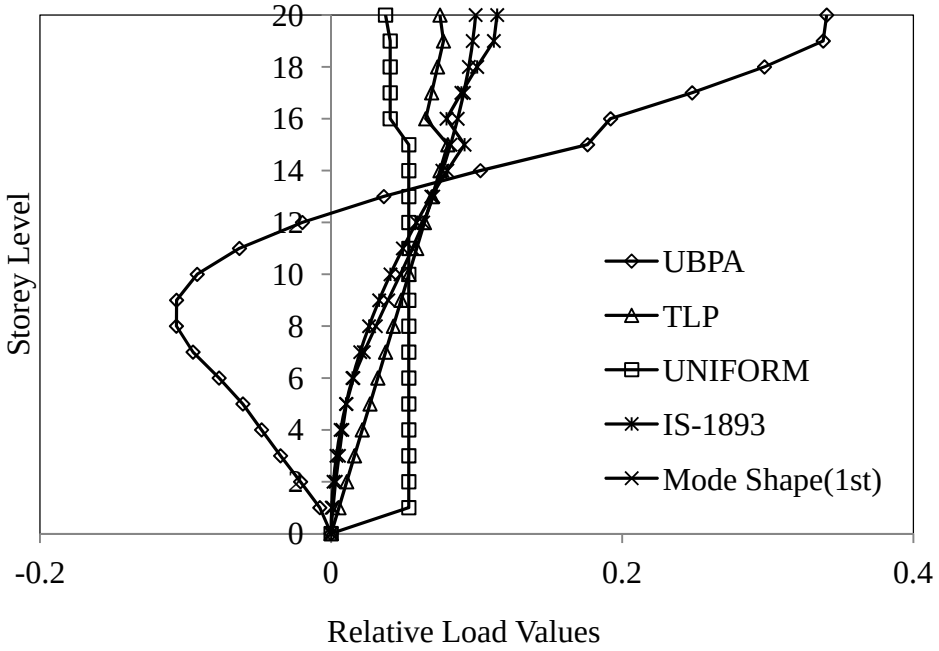

Fig. 4.46: Lateral load pattern for S1-20-12 building frame

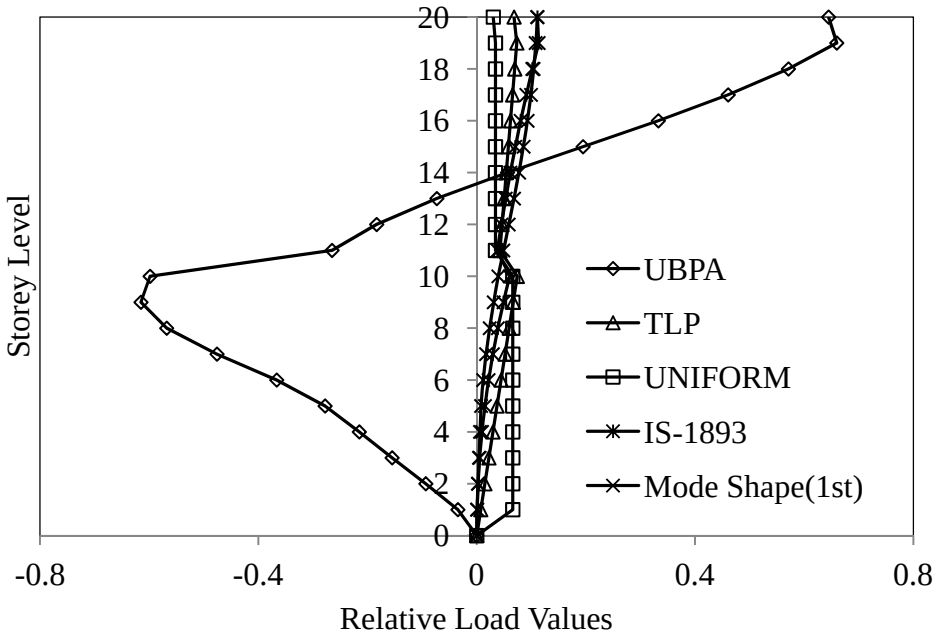

Fig. 4.47: Lateral load pattern for S2-20-12 building frame

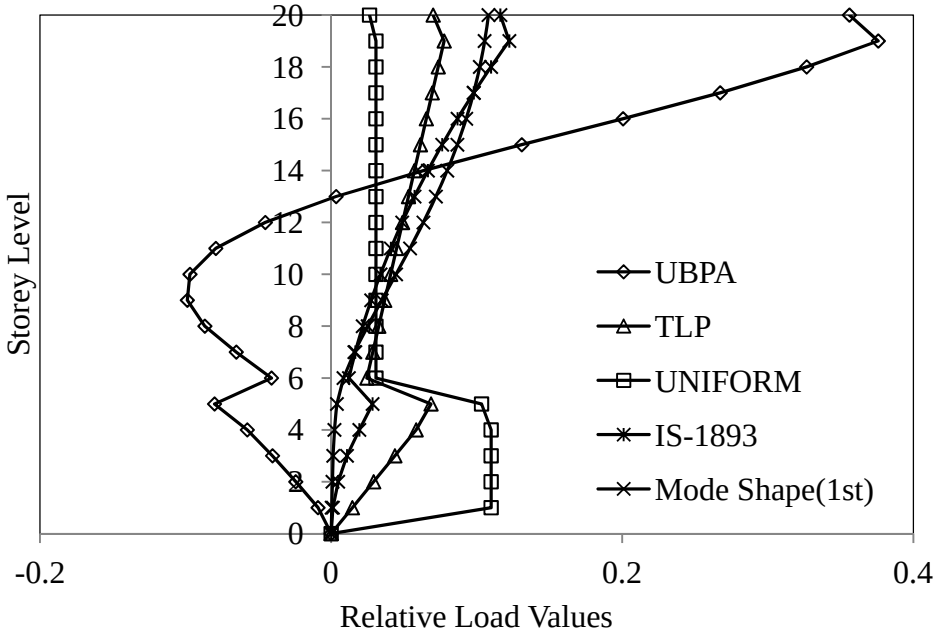

Fig. 4.48: Lateral load pattern for S3-20-12 building frame

Following observations are made from the Figures 4.1 to 4.48:

i) Shape of UBPA load pattern has two curvatures for all the building models. Load has to be applied both from positive and negative directions as per this model. Lower half of the building should be loaded in the negative direction whereas the upper half should be loaded in positive direction.

ii) Shape of mass proportional triangular load pattern (TLP) and the first mode shape are almost matching for mid-rise regular buildings (up to twelve storey buildings). However, there are differences between these two load patterns for mid-rise setback buildings and high-rise buildings.

iii) The distribution of load in mass proportional uniform load pattern (UNIFORM) is quite different from that of other load patterns. Unlike other load patterns, uniform load pattern apply more loads in the lower storeys of the buildings as compared to the upper storeys of the buildings.

4.2.2 Comparison of the Load Patterns for their Applicability to Setback Buildings

Pushover analyses are carried out for all the selected 48 buildings using five selected load patterns. Also nonlinear dynamic analyses for the above buildings are carried out for fifteen natural earthquake ground motions. Selected ground motions were normalised to peak ground acceleration (PGA) of 0.36g. The details of the ground motions considered and other parameters for carrying out nonlinear dynamic analyses are described in Section 3.5. Modelling of the buildings for nonlinear analyses is presented in Section 3.4.

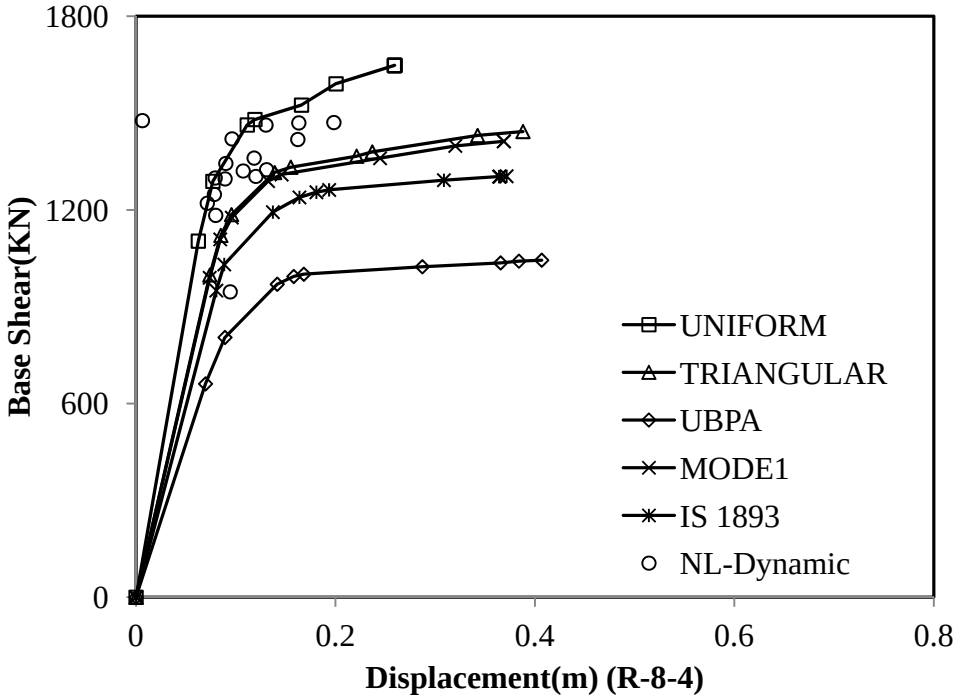

Fig. 4.49: Pushover curve for different load patterns for R-8-4 building category

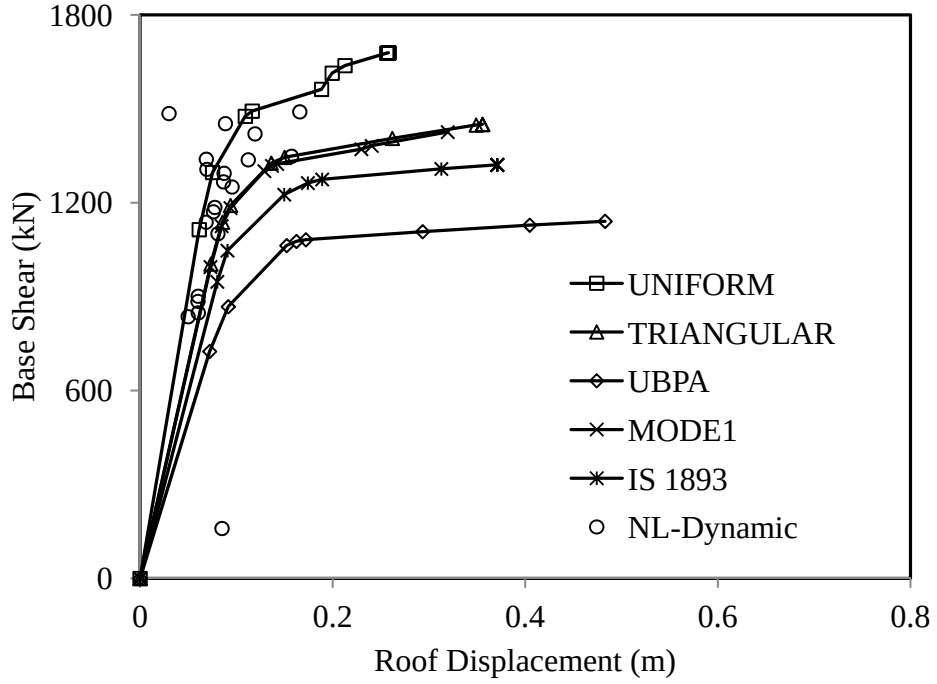

Fig. 4.50: Pushover curve for different load patterns for S1-8-4 building category

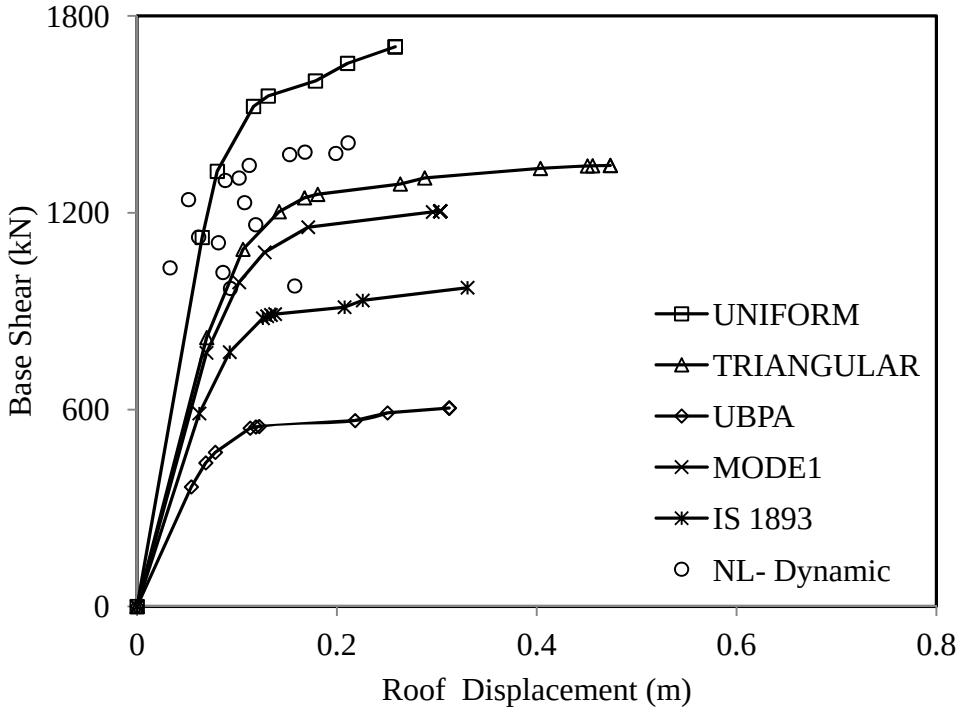

Fig. 4.51: Pushover curve for different load patterns for S2-8-4 building category

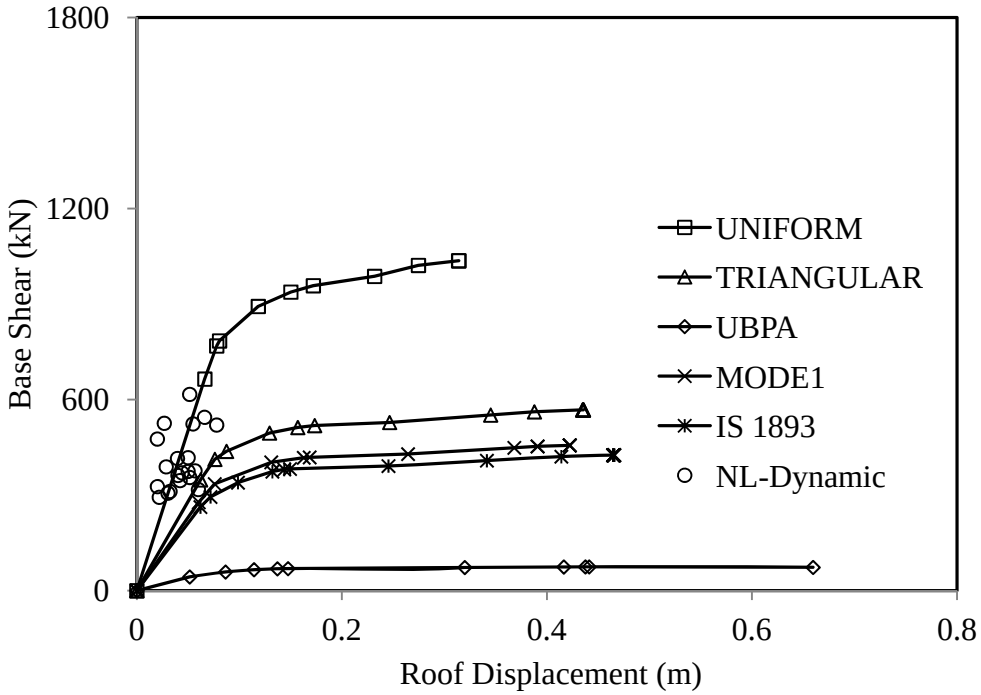

Fig. 4.52: Pushover curve for different load patterns for S3-8-4 building category

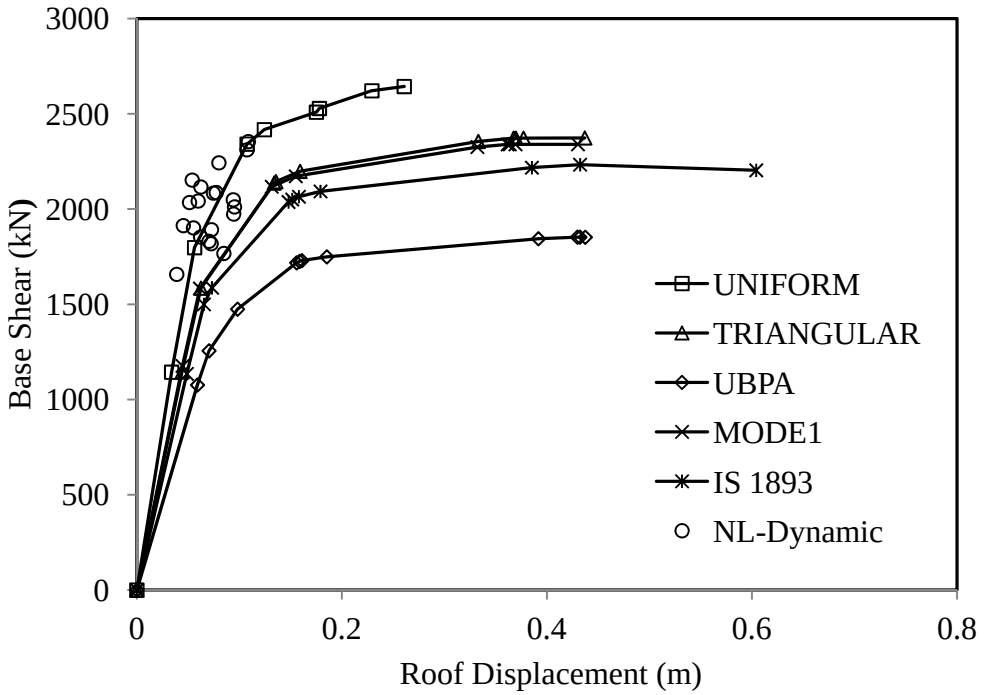

Fig. 4.53: Pushover curve for different load patterns for R-8-8 building category

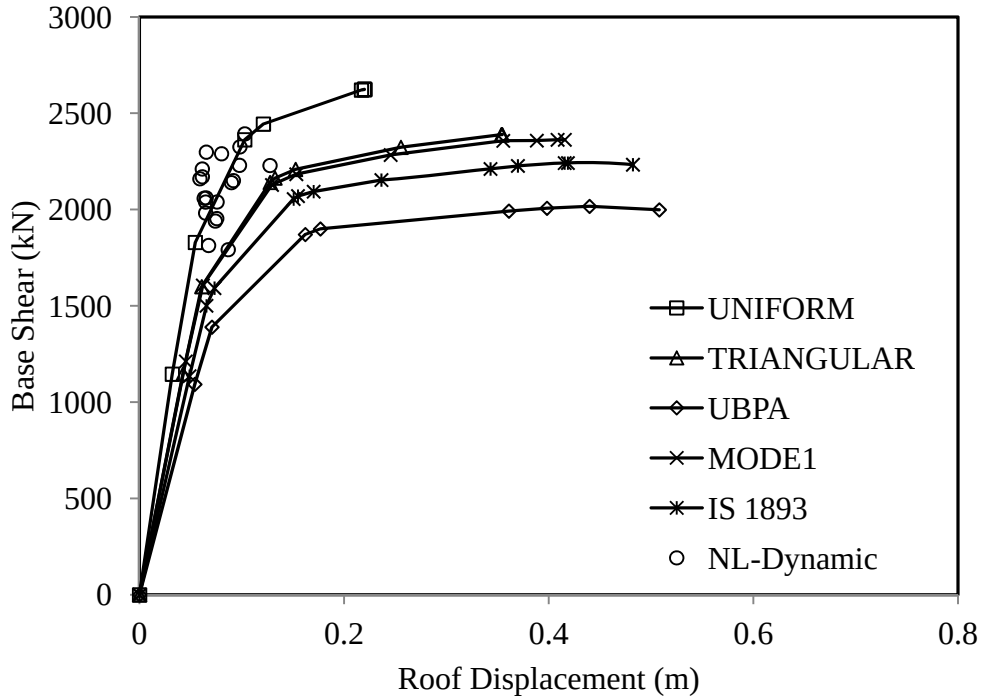

Fig. 4.54: Pushover curve for different load patterns for S1-8-8 building category

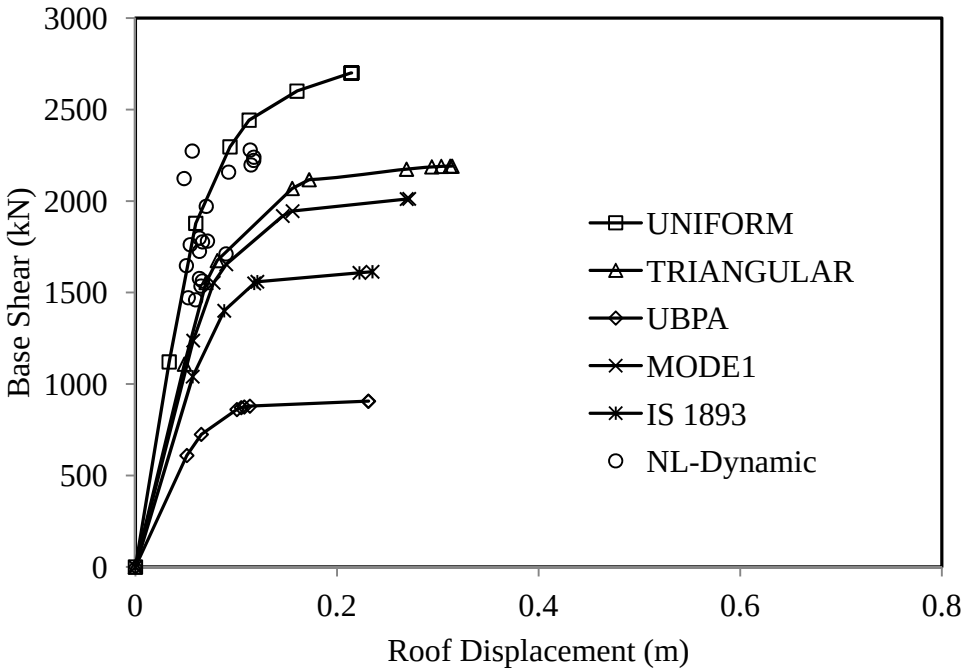

Fig. 4.55: Pushover curve for different load patterns for S2-8-8 building category

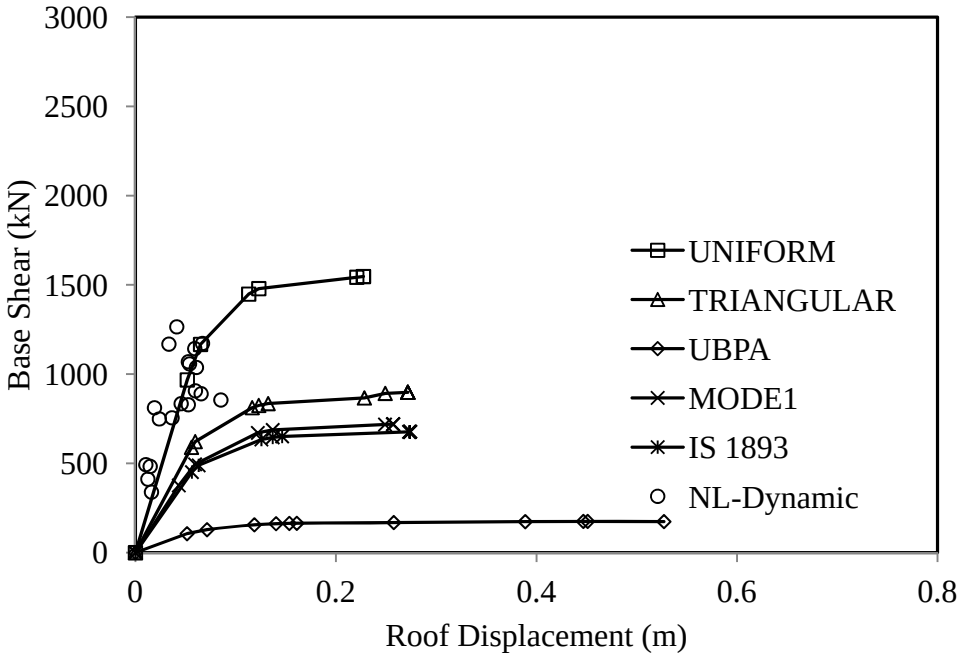

Fig. 4.56: Pushover curve for different load patterns for S3-8-8 building category

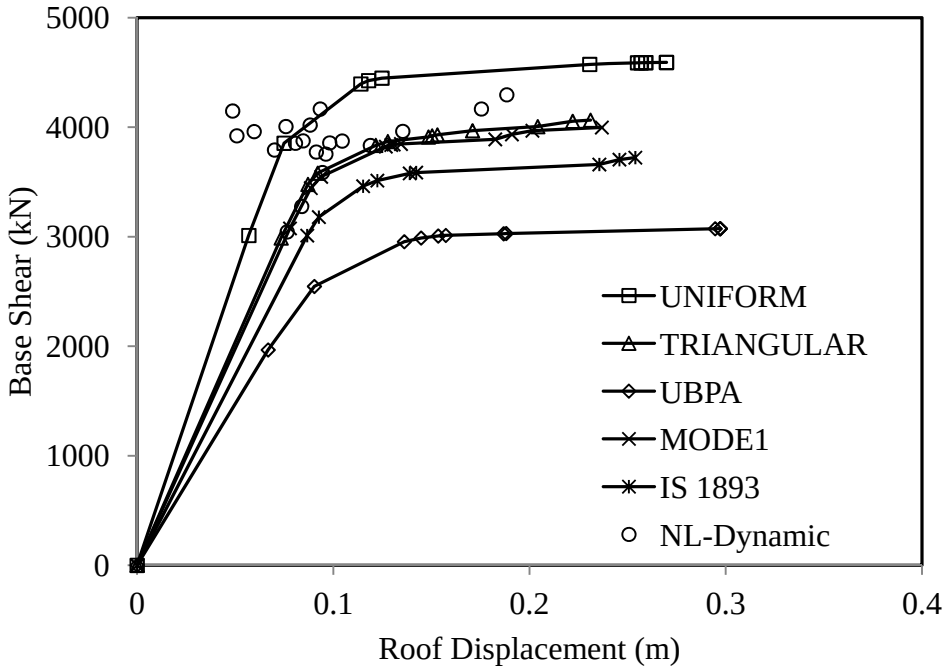

Fig. 4.57: Pushover curve for different load patterns for R-8-12 building category

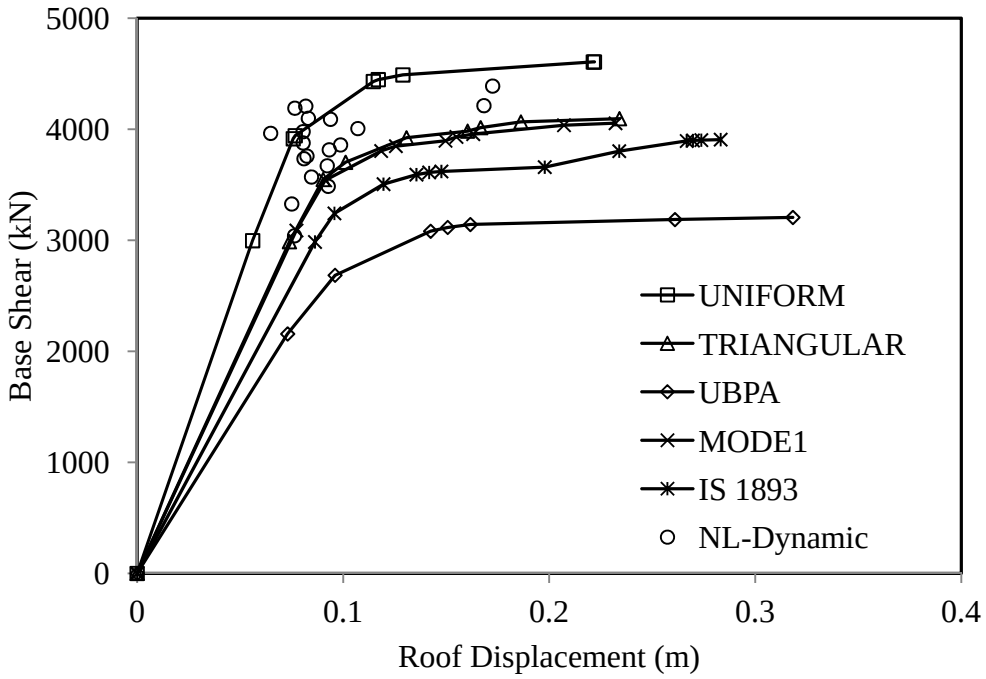

Fig. 4.58: Pushover curve for different load patterns for S1-8-12 building category

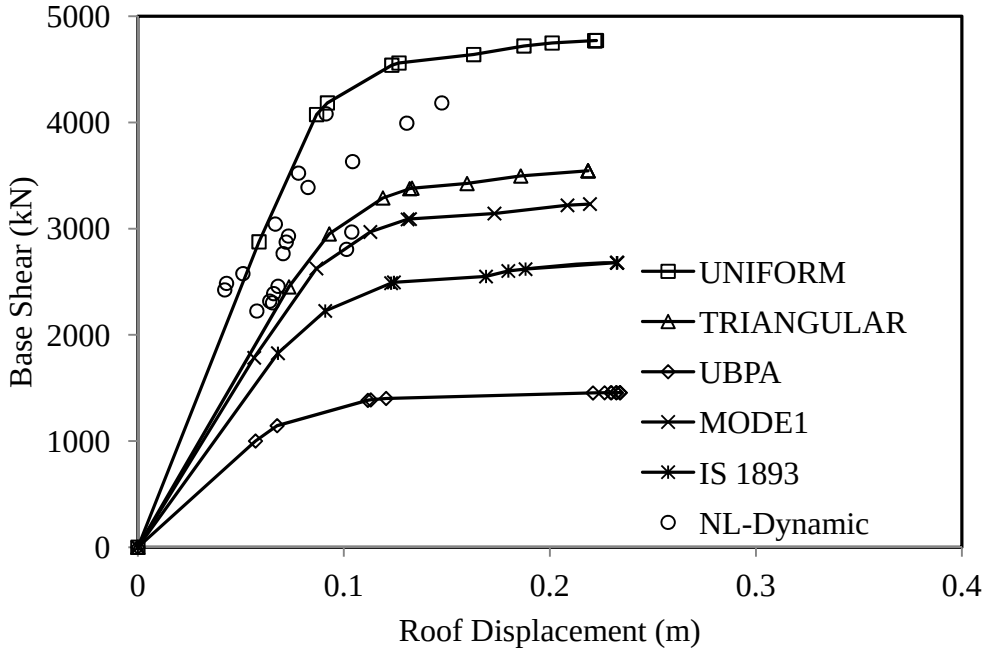

Fig. 4.59: Pushover curve for different load patterns for S2-8-12 building category

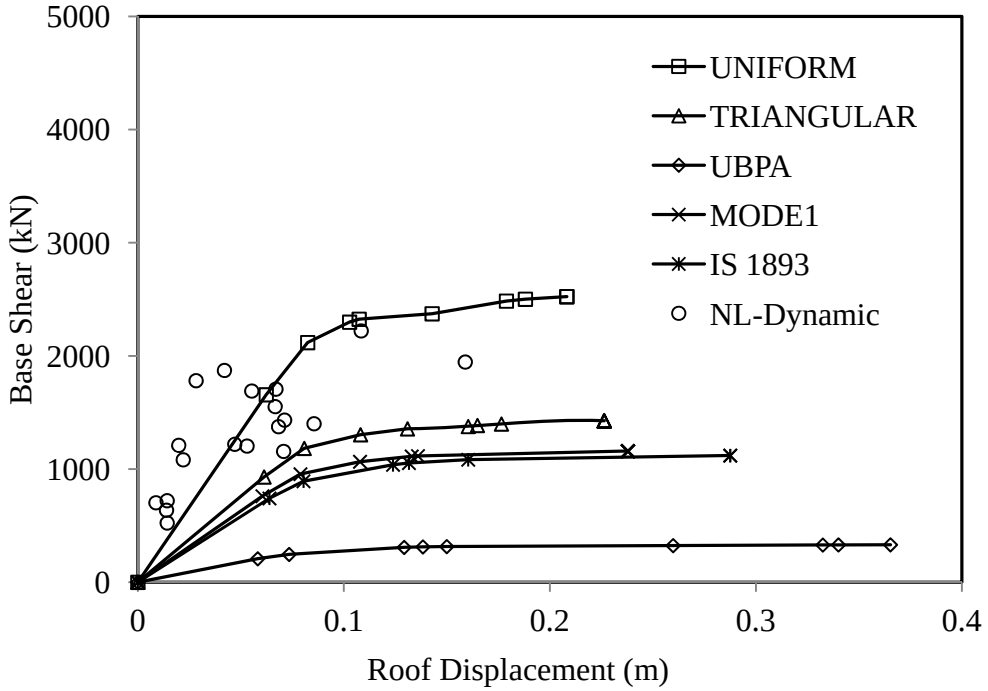

Fig. 4.60: Pushover curve for different load patterns for S3-8-12 building category

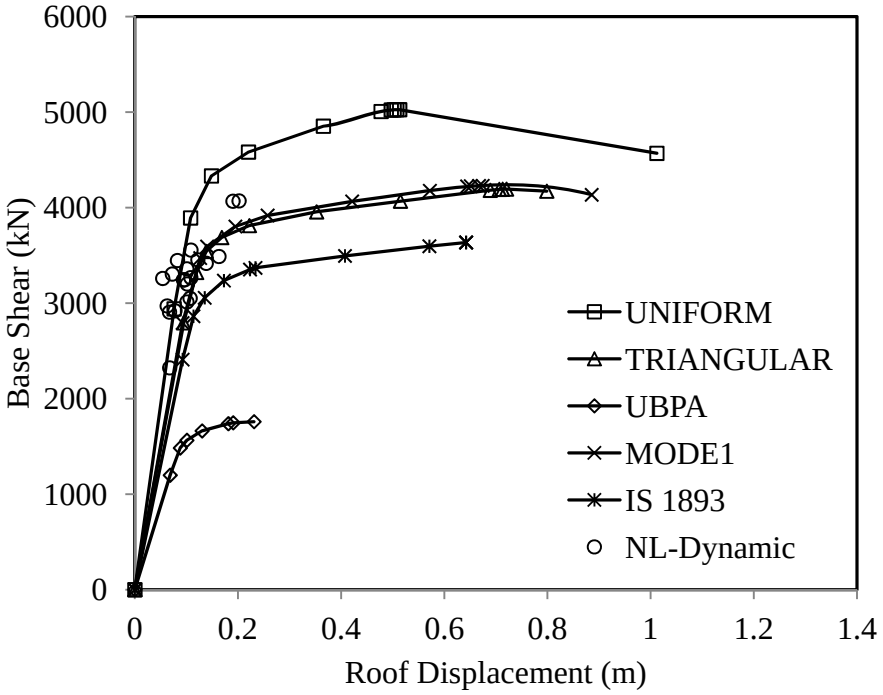

Fig. 4.61: Pushover curve for different load patterns for R-12-4 building category

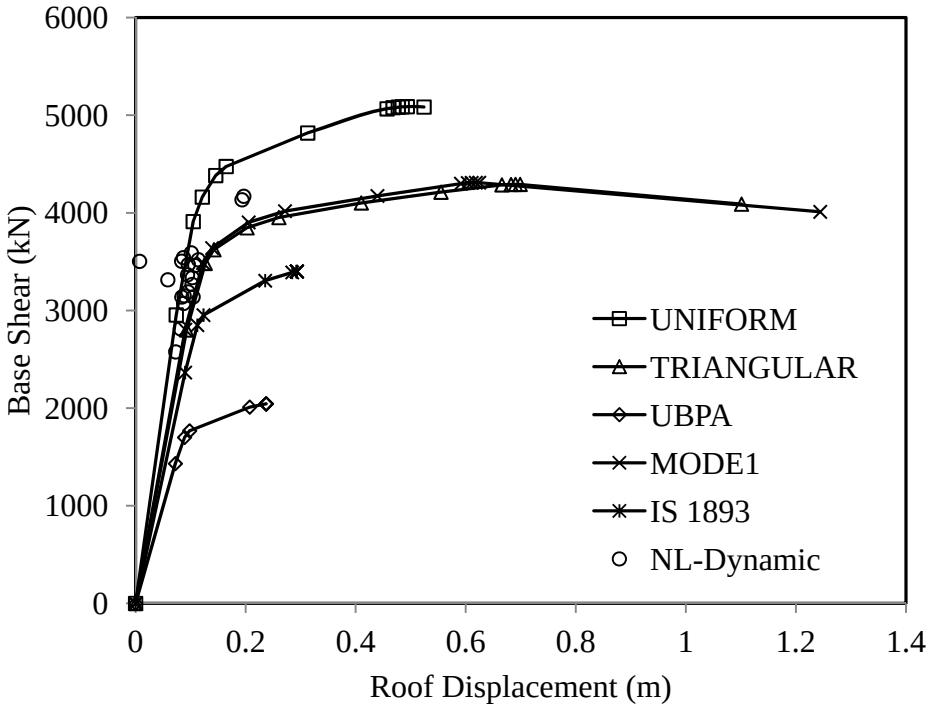

Fig. 4.62: Pushover curve for different load patterns for S1-12-4 building category

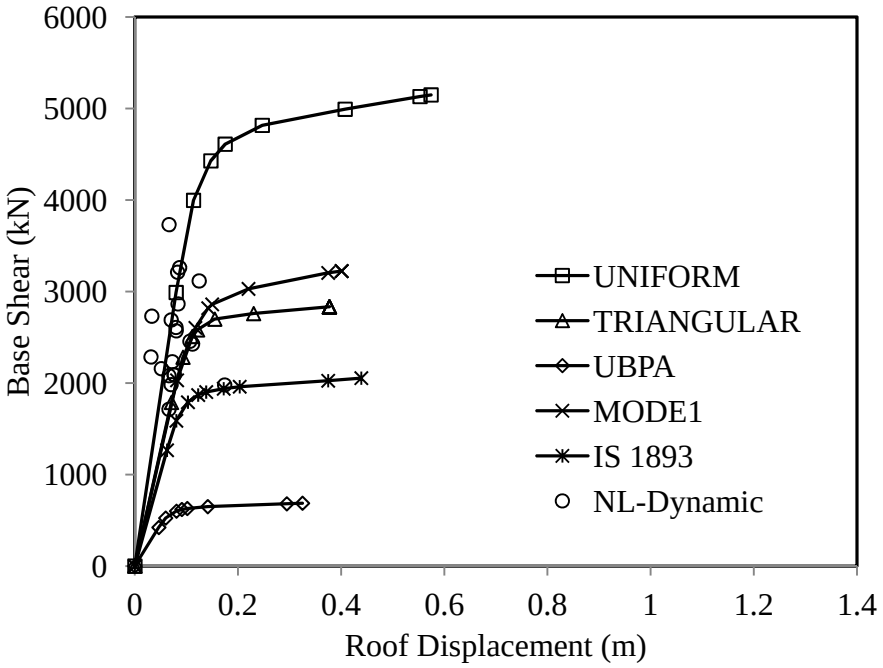

Fig. 4.63: Pushover curve for different load patterns for S2-12-4 building category

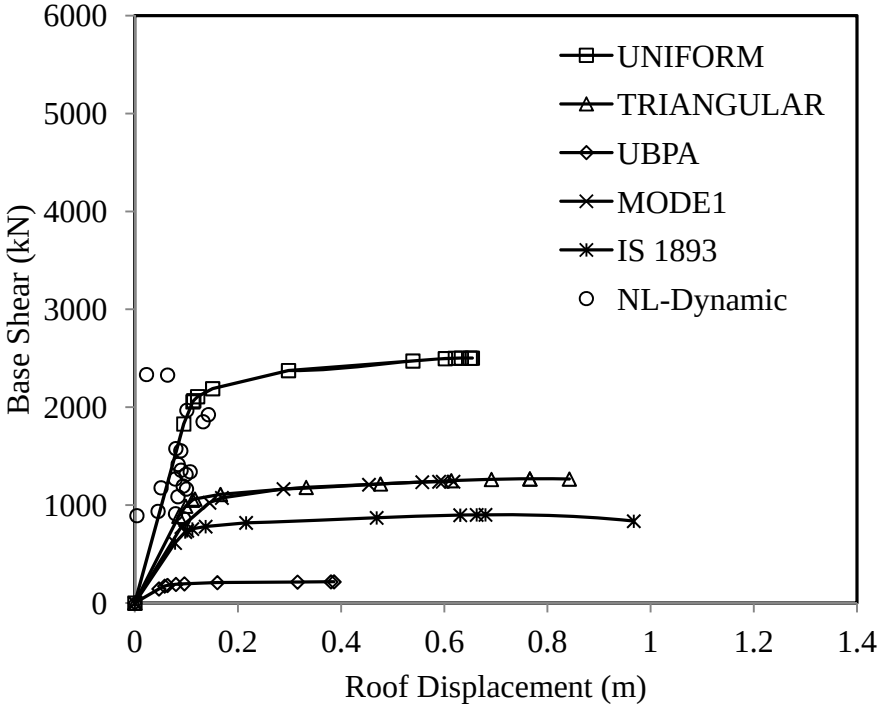

Fig. 4.64: Pushover curve for different load patterns for S3-12-4 building category

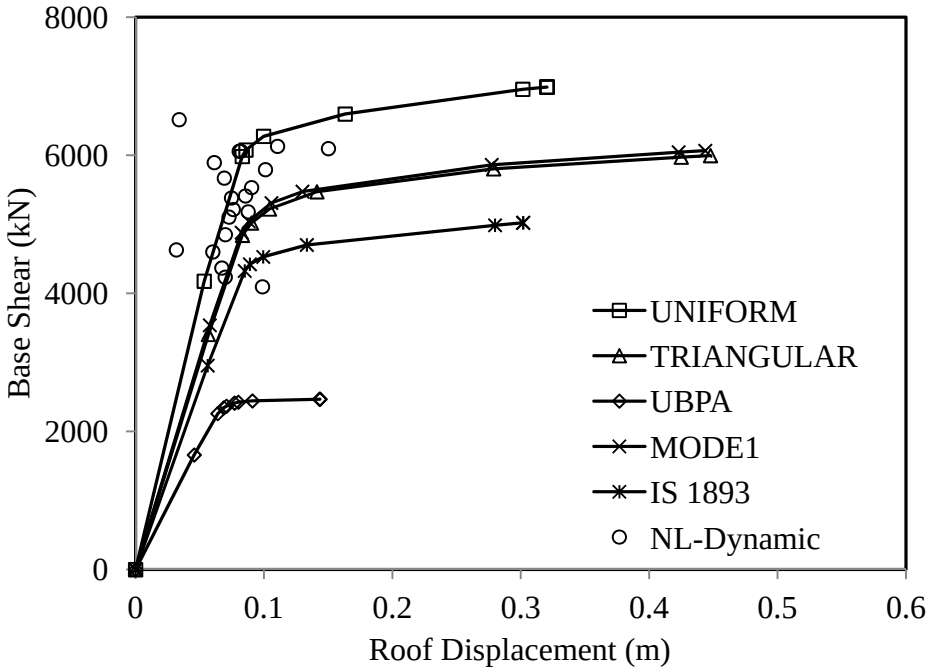

Fig. 4.65: Pushover curve for different load patterns for R-12-8 building category

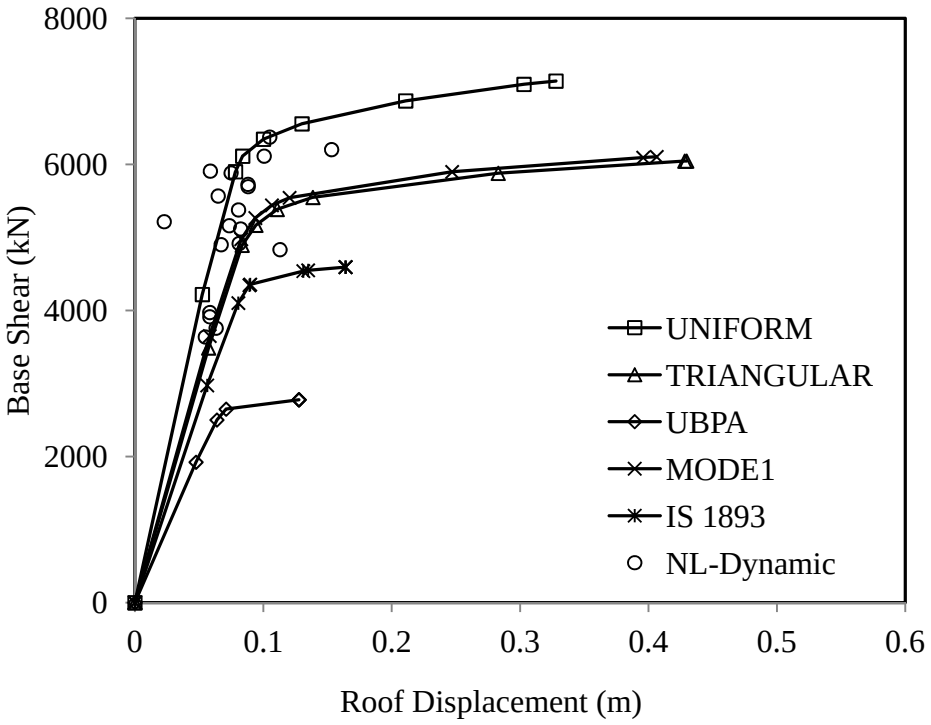

Fig. 4.66: Pushover curve for different load patterns for S1-12-8 building category

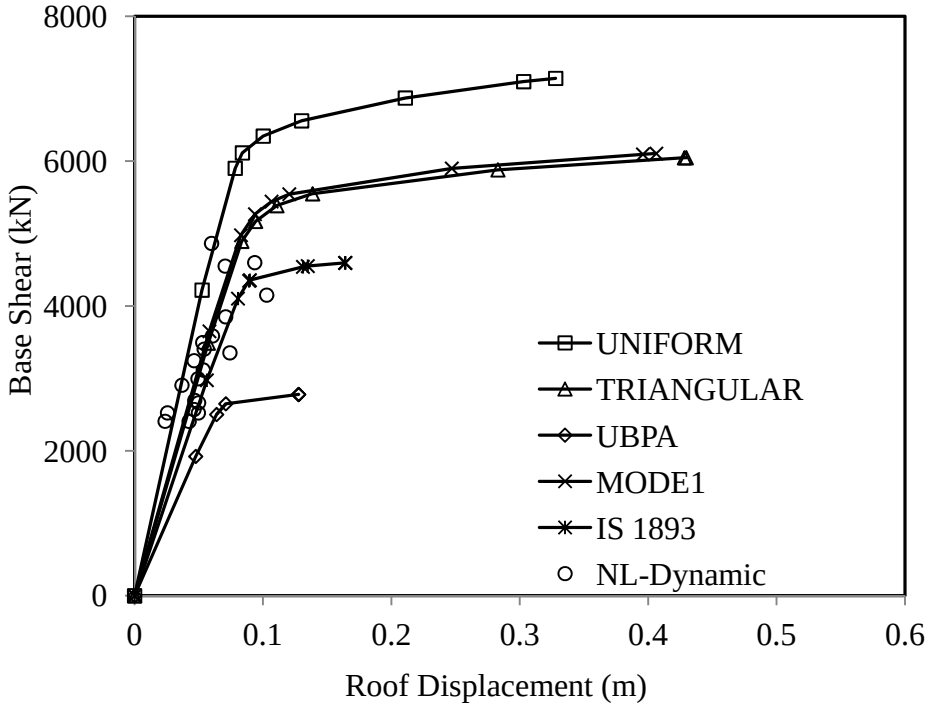

Fig. 4.67: Pushover curve for different load patterns for S2-12-8 building category

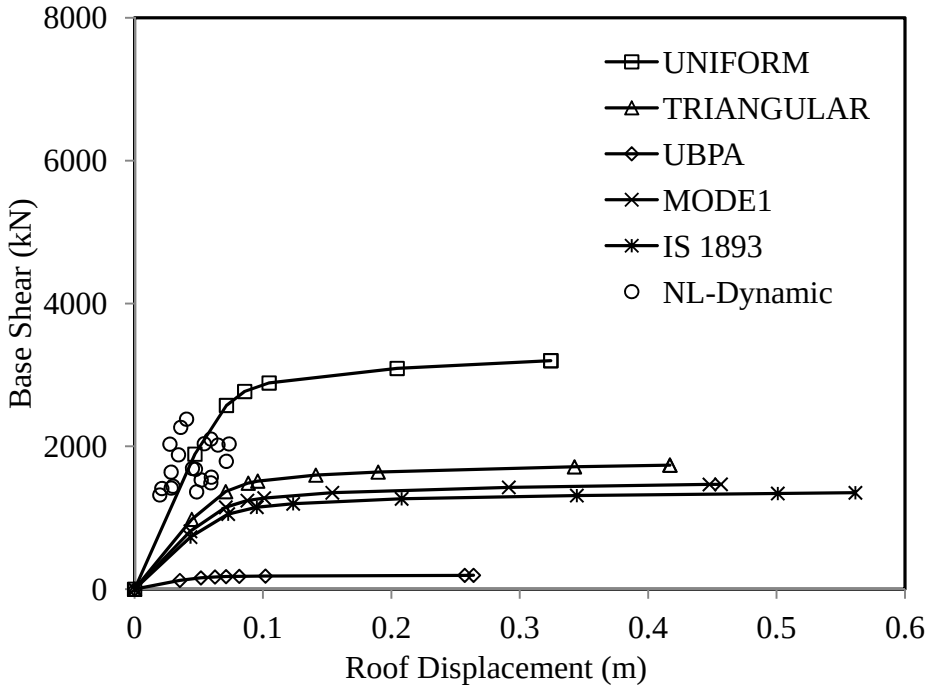

Fig. 4.68: Pushover curve for different load patterns for S3-12-8 building category

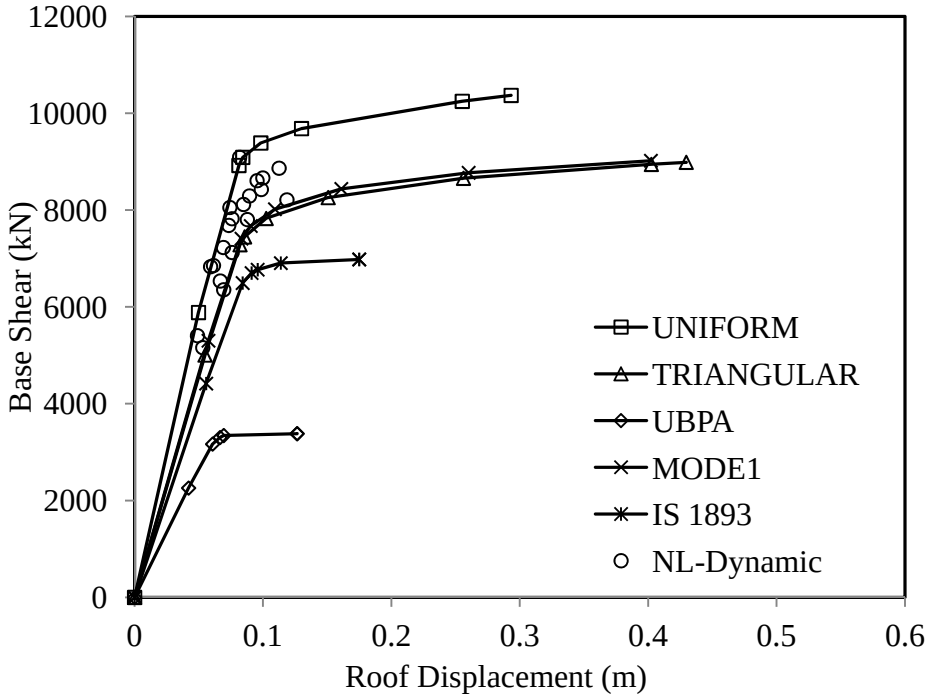

Fig. 4.69: Pushover curve for different load patterns for R-12-12 building category

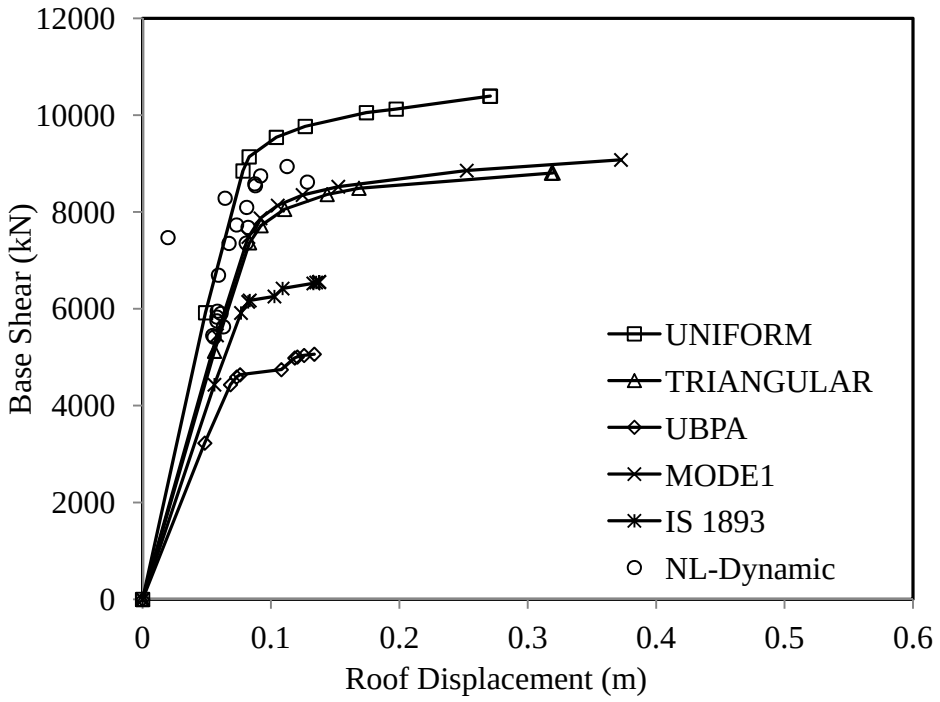

Fig. 4.70: Pushover curve for different load patterns for S1-12-12 building category

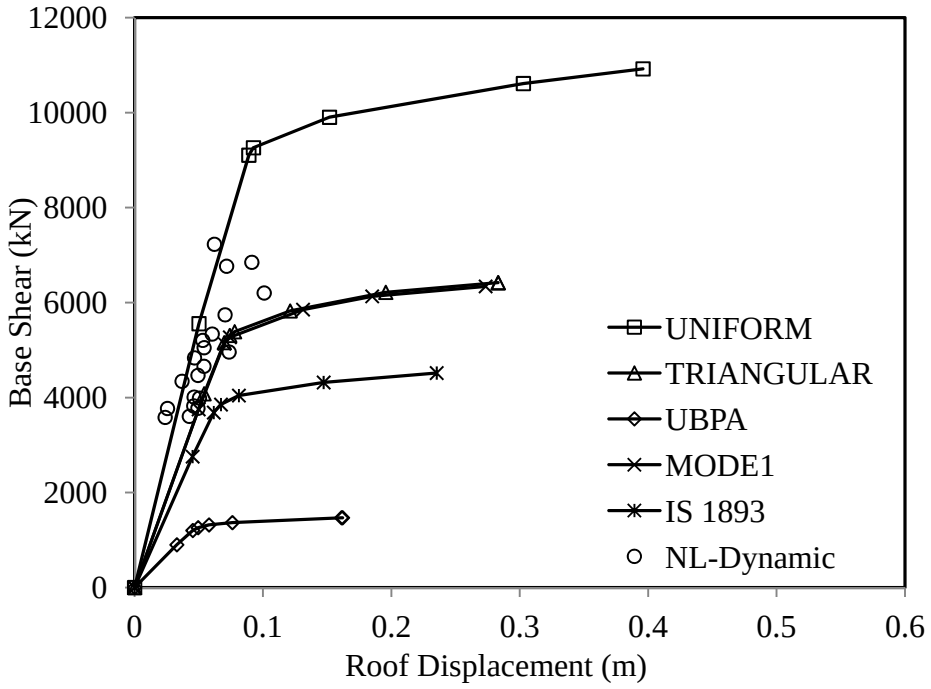

Fig. 4.71: Pushover curve for different load patterns for S2-12-12 building category

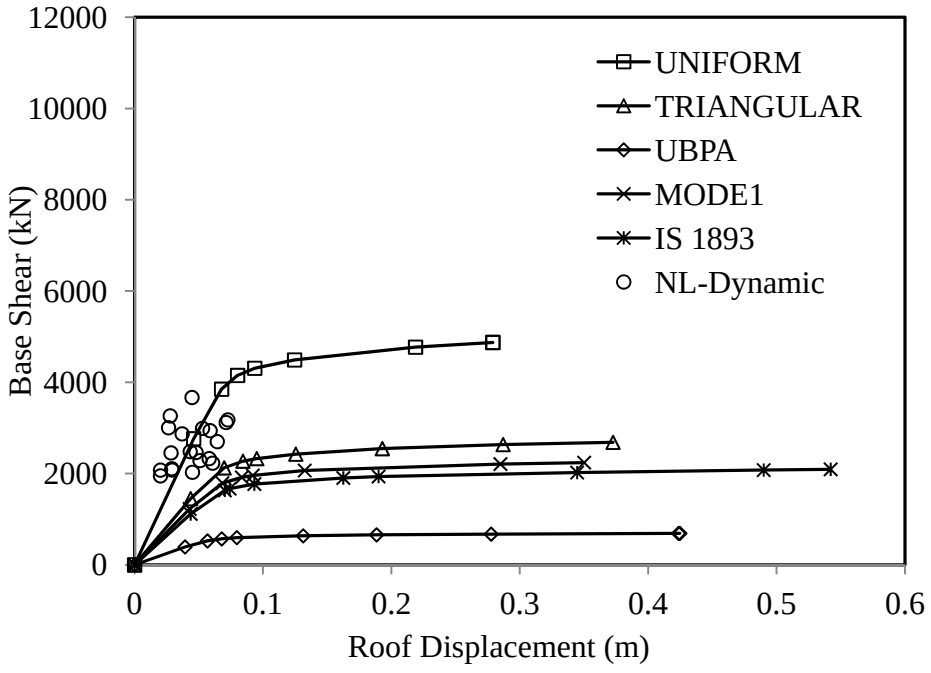

Fig. 4.72: Pushover curve for different load patterns for S3-12-12 building category

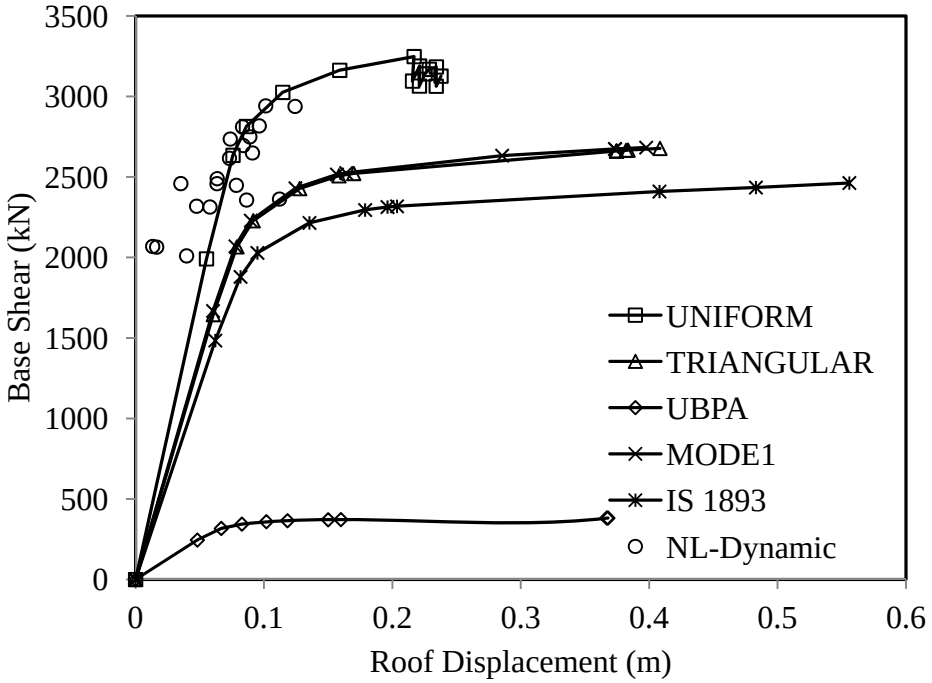

Fig. 4.73: Pushover curve for different load patterns for R-16-4 building category

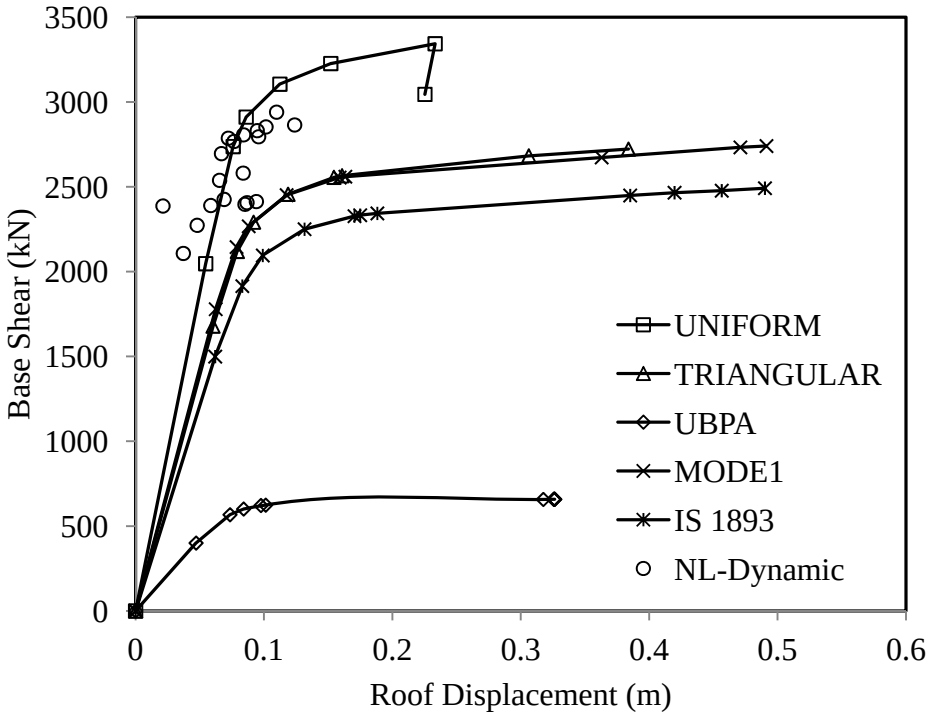

Fig. 4.74: Pushover curve for different load patterns for S1-16-4 building category

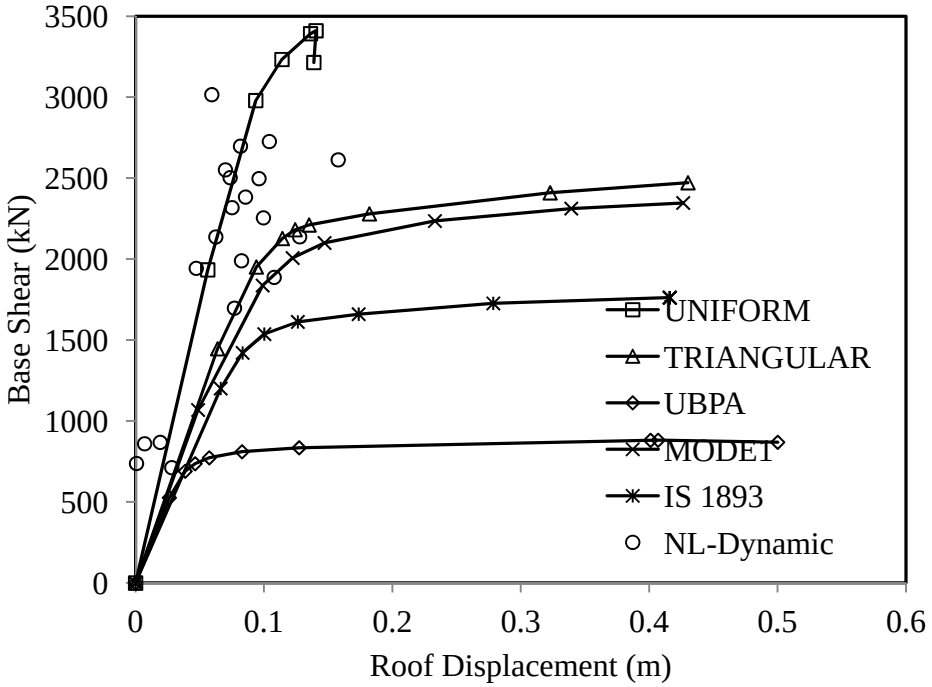

Fig. 4.75: Pushover curve for different load patterns for S2-16-4 building category

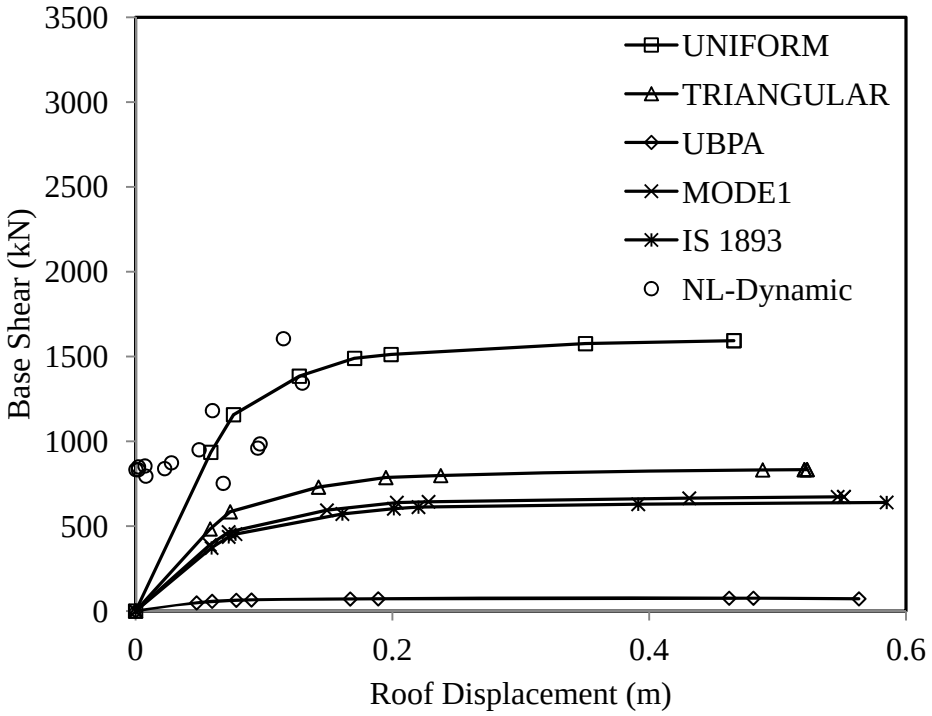

Fig. 4.76: Pushover curve for different load patterns for S3-16-4 building category

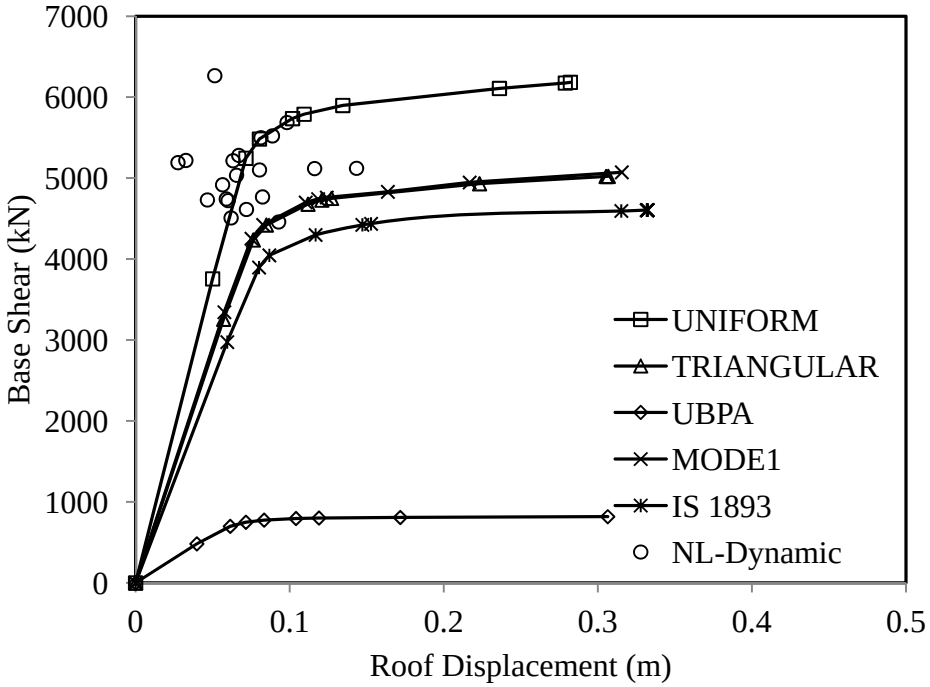

Fig. 4.77: Pushover curve for different load patterns for R-16-8 building category

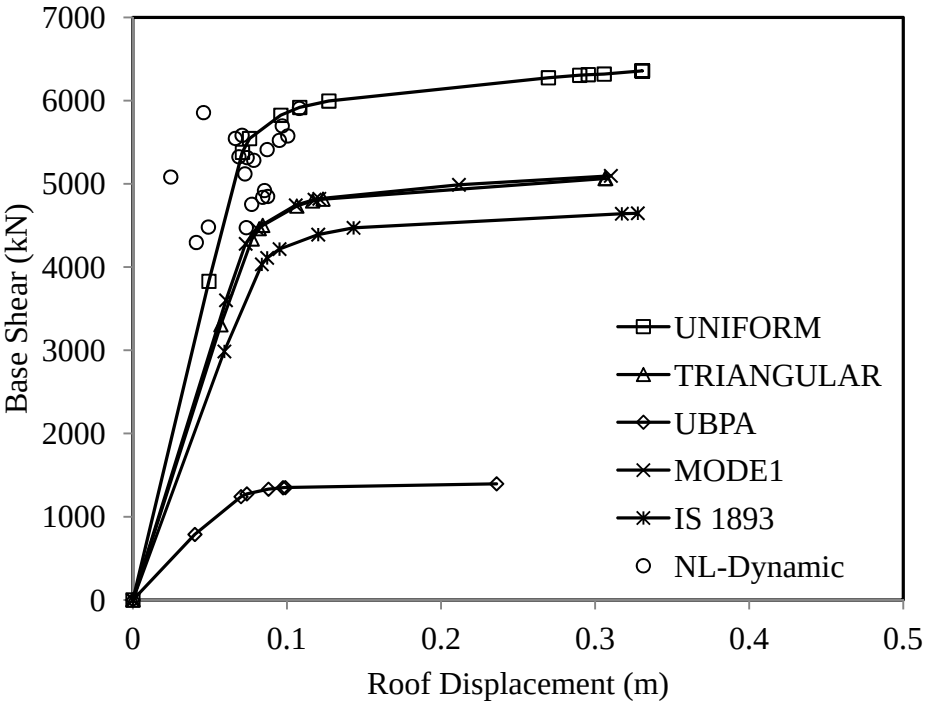

Fig. 4.78: Pushover curve for different load patterns for S1-16-8 building category

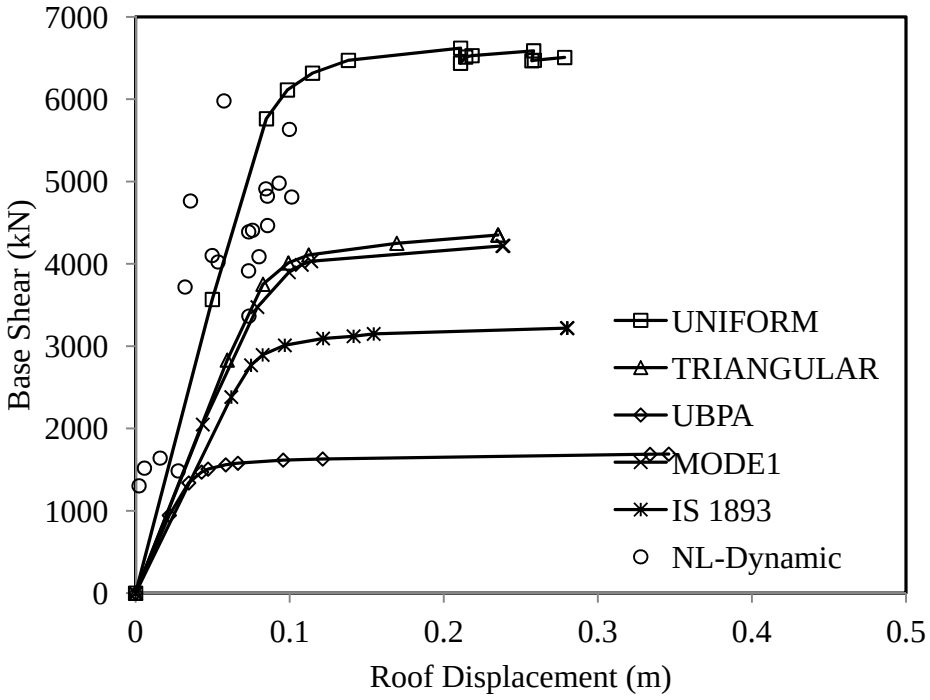

Fig. 4.79: Pushover curve for different load patterns for S2-16-8 building category

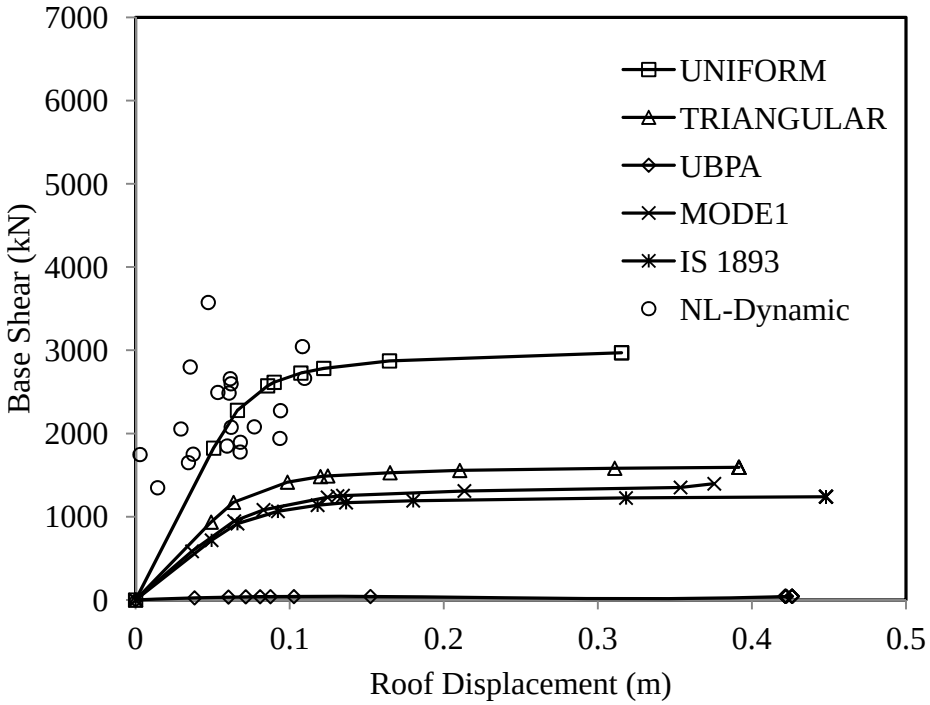

Fig. 4.80: Pushover curve for different load patterns for S3-16-8 building category

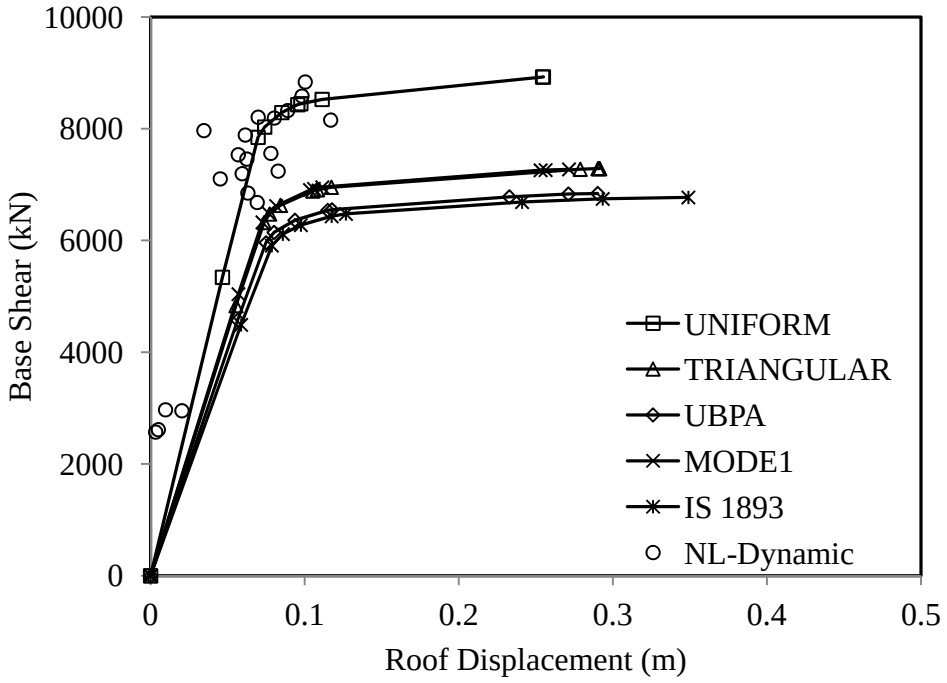

Fig. 4.81: Pushover curve for different load patterns for R-16-12 building category

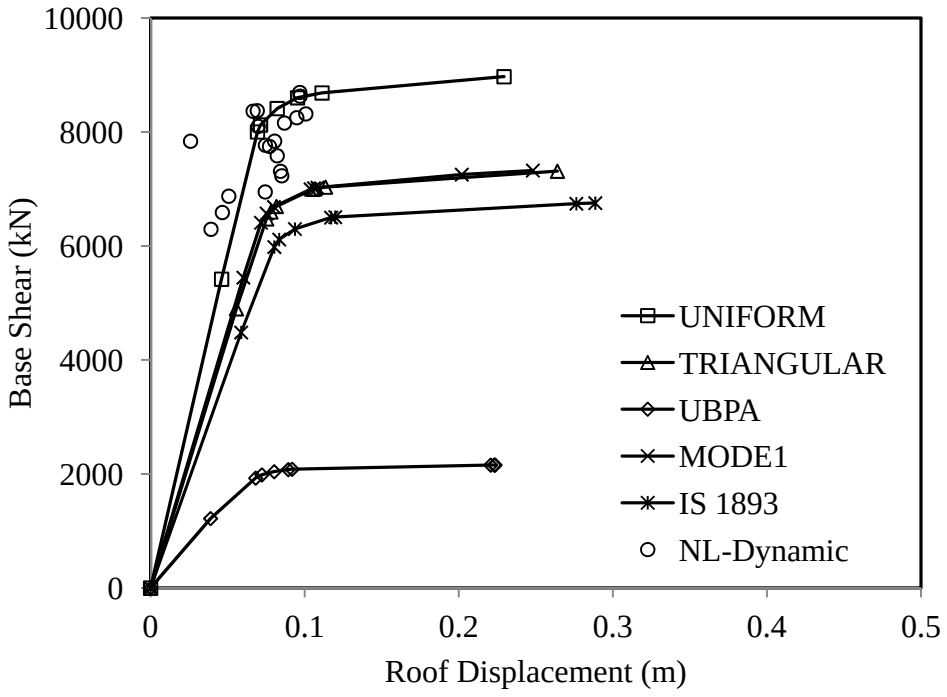

Fig. 4.82: Pushover curve for different load patterns for S1-16-12 building category

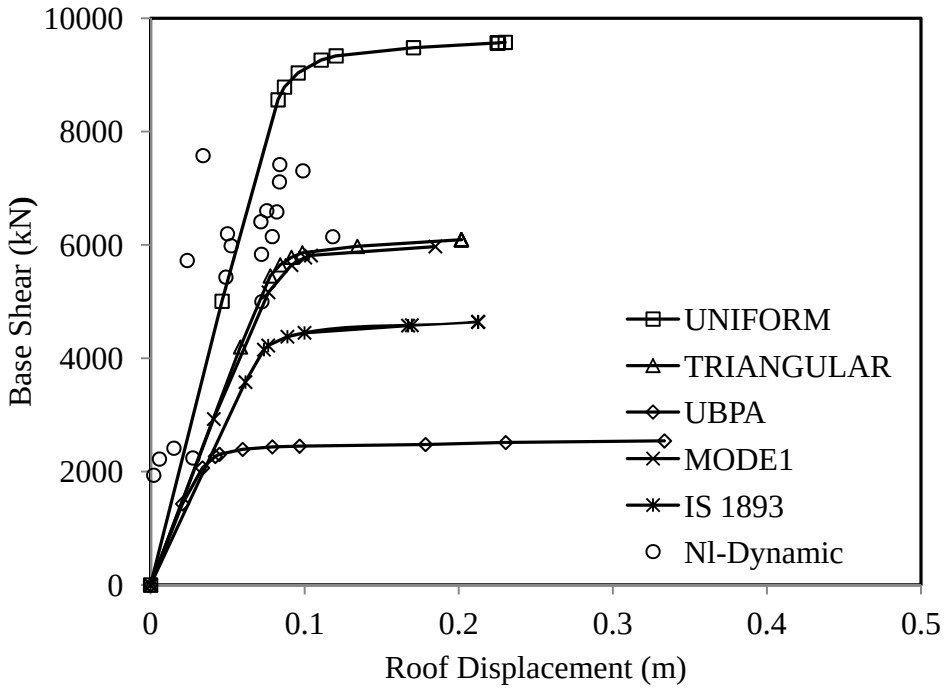

Fig. 4.83: Pushover curve for different load patterns for S2-16-12 building category

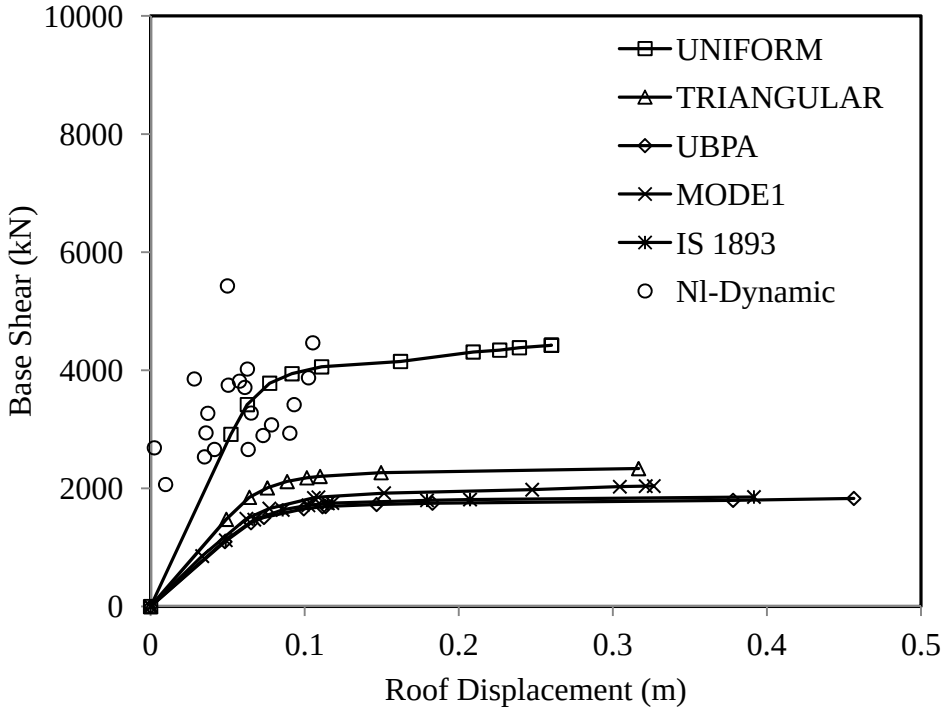

Fig. 4.84: Pushover curve for different load patterns for S3-16-12 building category

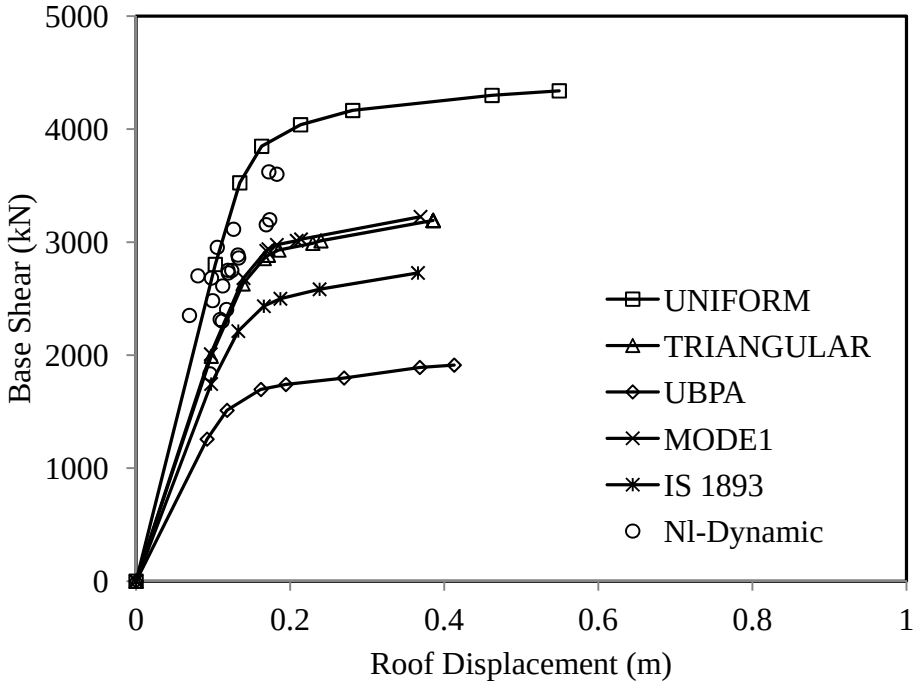

Fig. 4.85: Pushover curve for different load patterns for R-20-4 building category

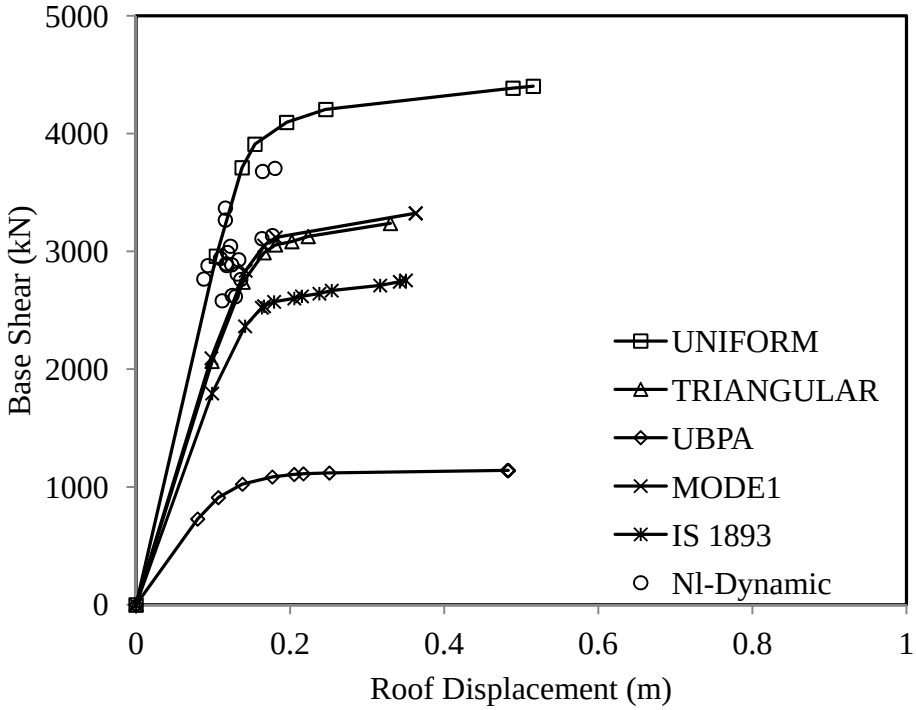

Fig. 4.86: Pushover curve for different load patterns for S1-20-4 building category

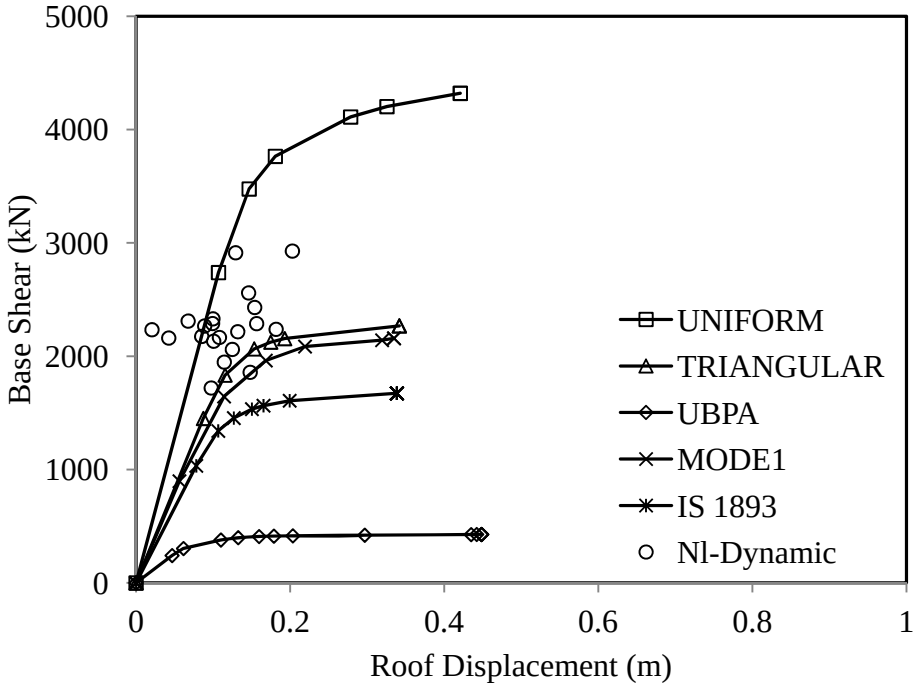

Fig. 4.87: Pushover curve for different load patterns for S2-20-4 building category

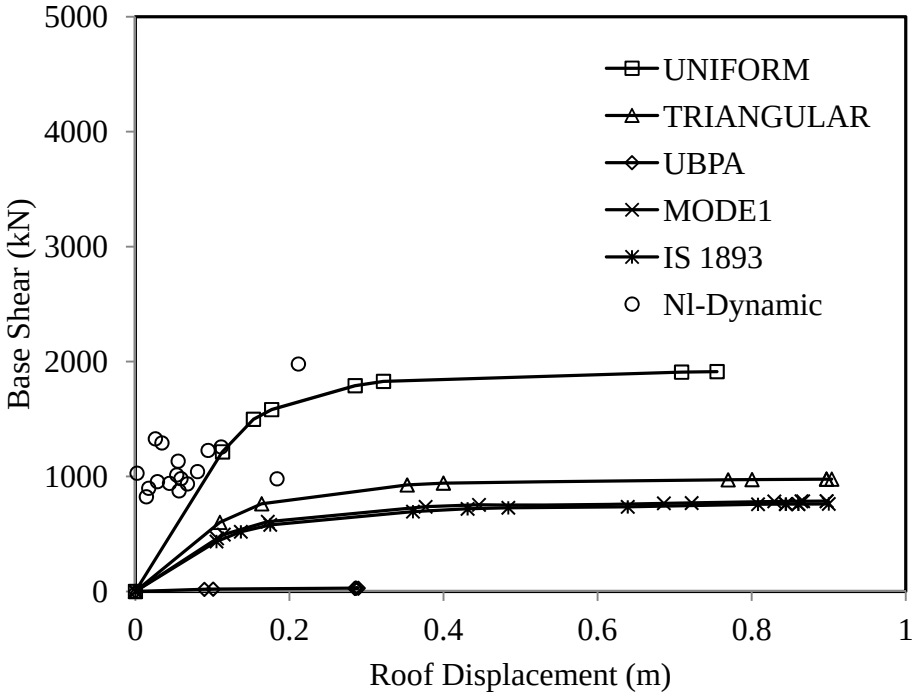

Fig. 4.88: Pushover curve for different load patterns for S3-20-4 building category

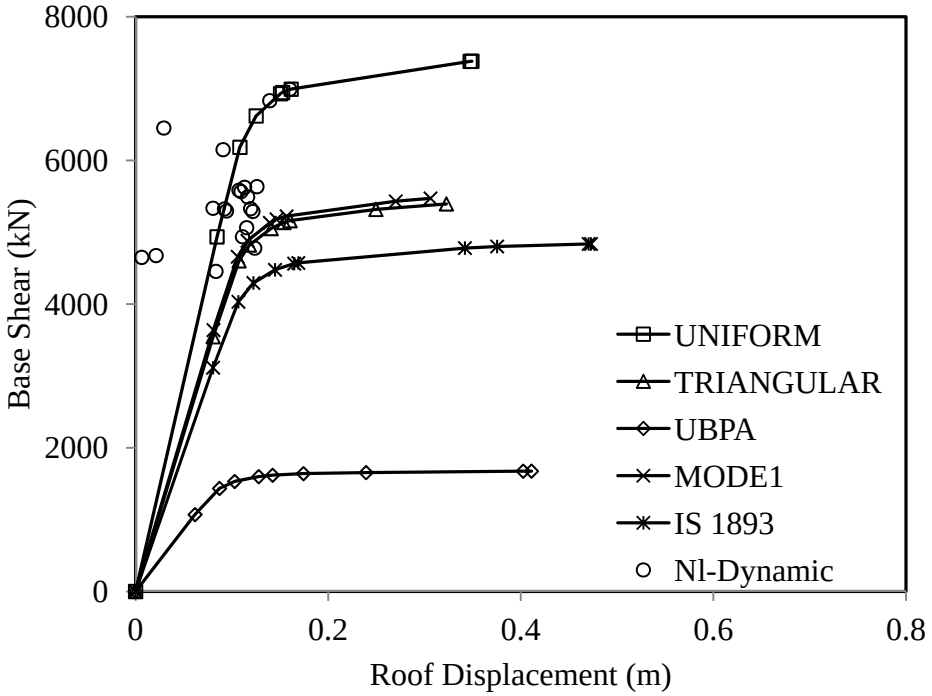

Fig. 4.89: Pushover curve for different load patterns for R-20-8 building category

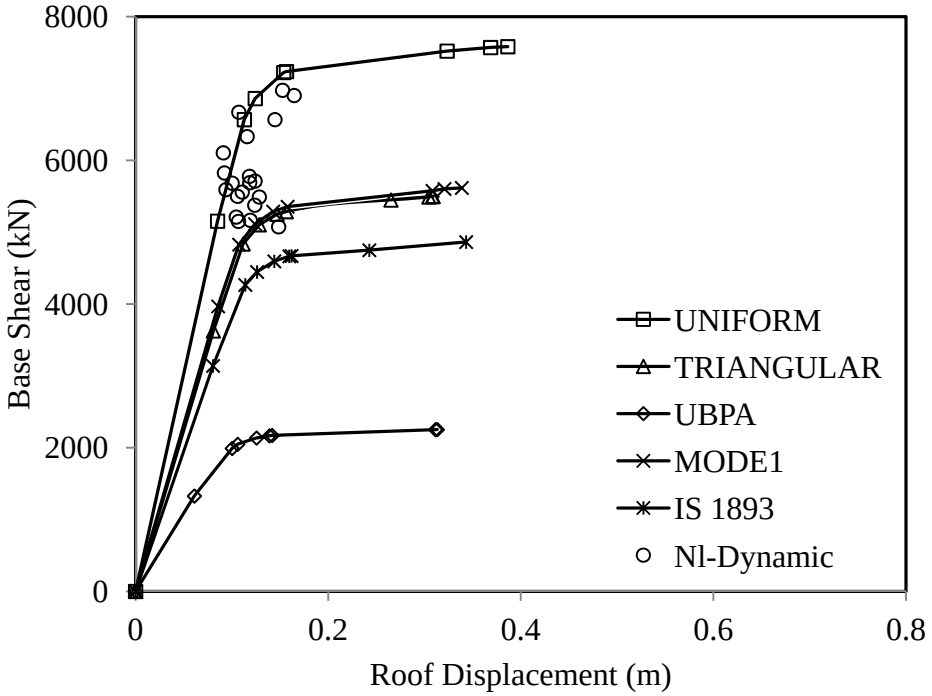

Fig. 4.90: Pushover curve for different load patterns for S1-20-8 building category

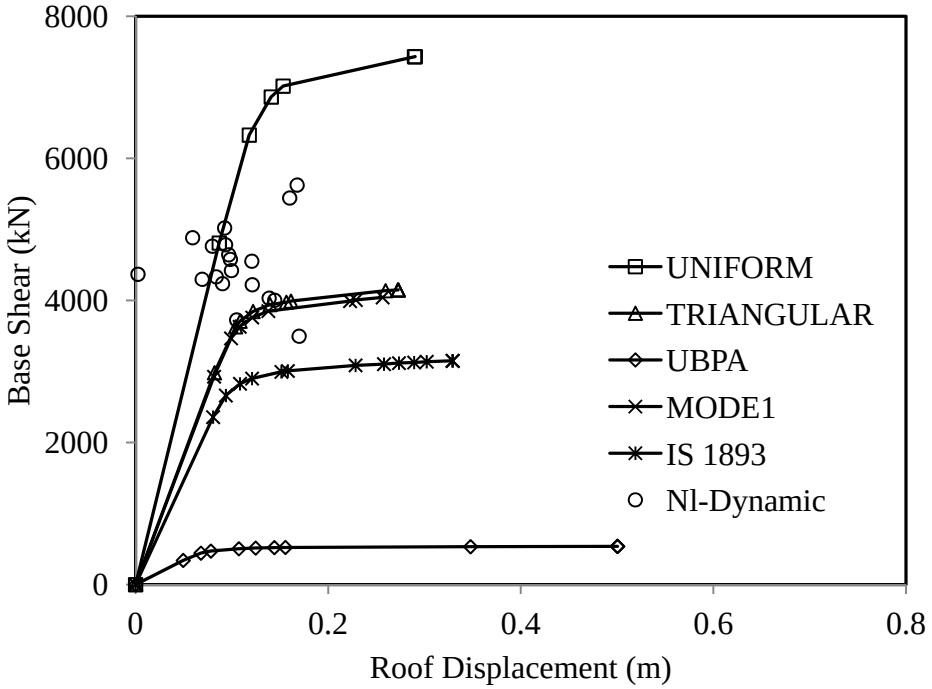

Fig. 4.91: Pushover curve for different load patterns for S2-20-8 building category

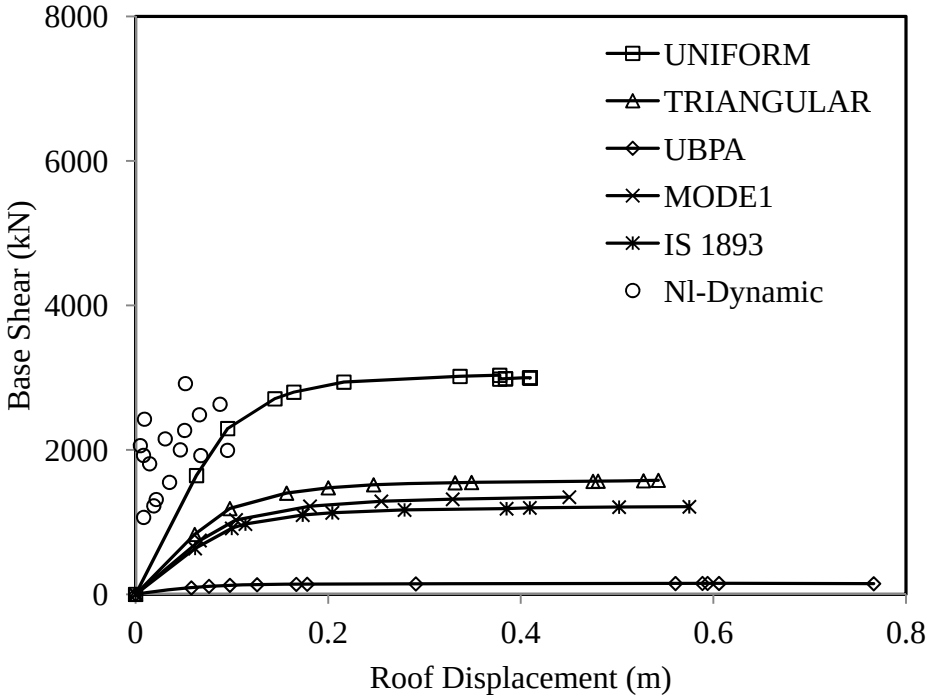

Fig. 4.92: Pushover curve for different load patterns for S3-20-8 building category

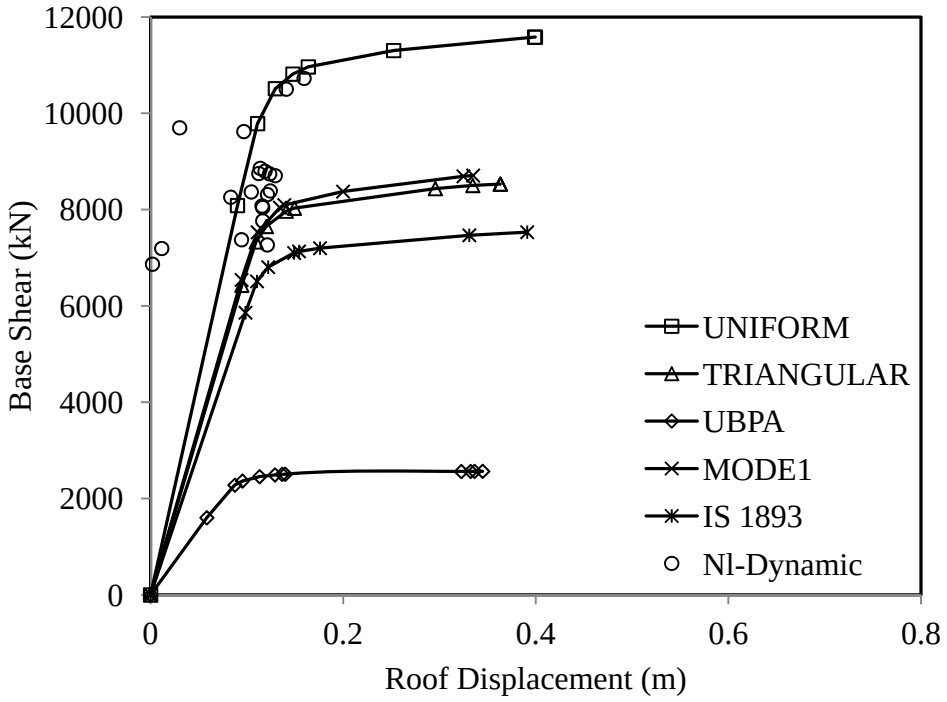

Fig. 4.93: Pushover curve for different load patterns for R-20-12 building category

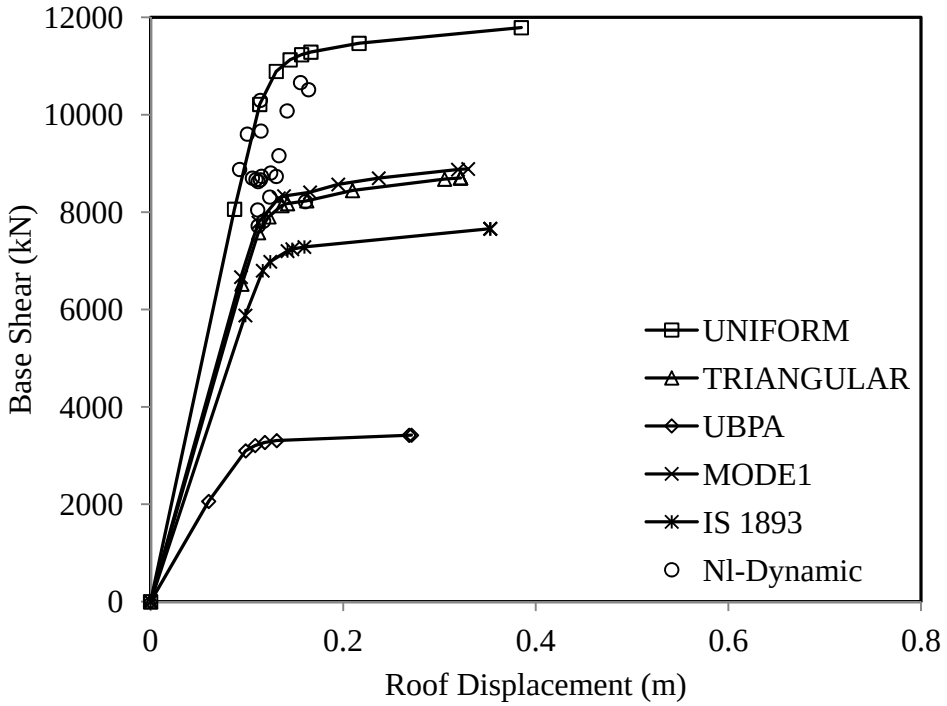

Fig. 4.94: Pushover curve for different load patterns for S1-20-12 building category

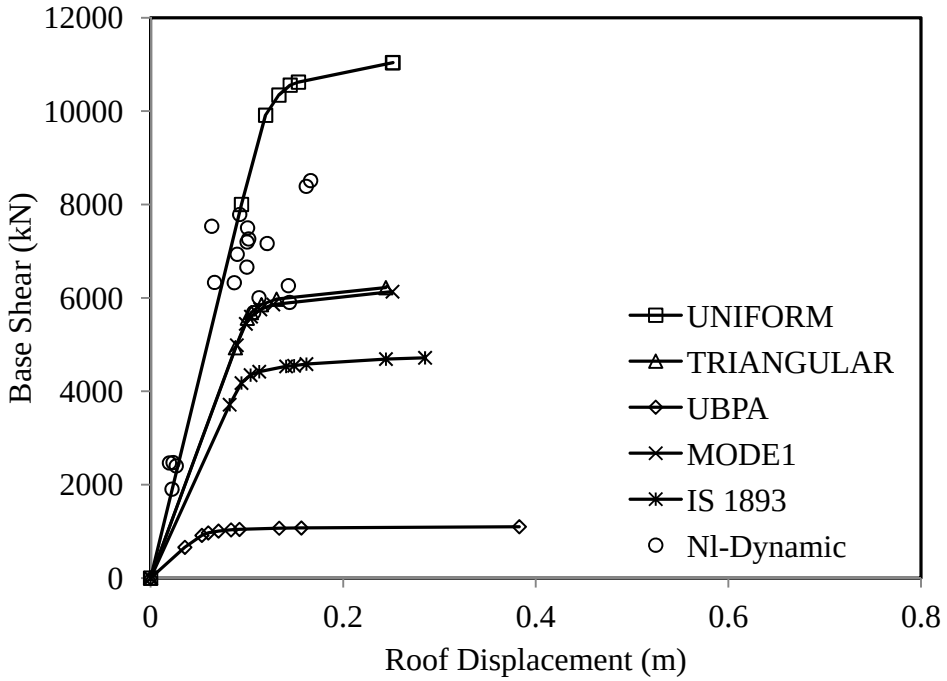

Fig. 4.95: Pushover curve for different load patterns for S2-20-12 building category

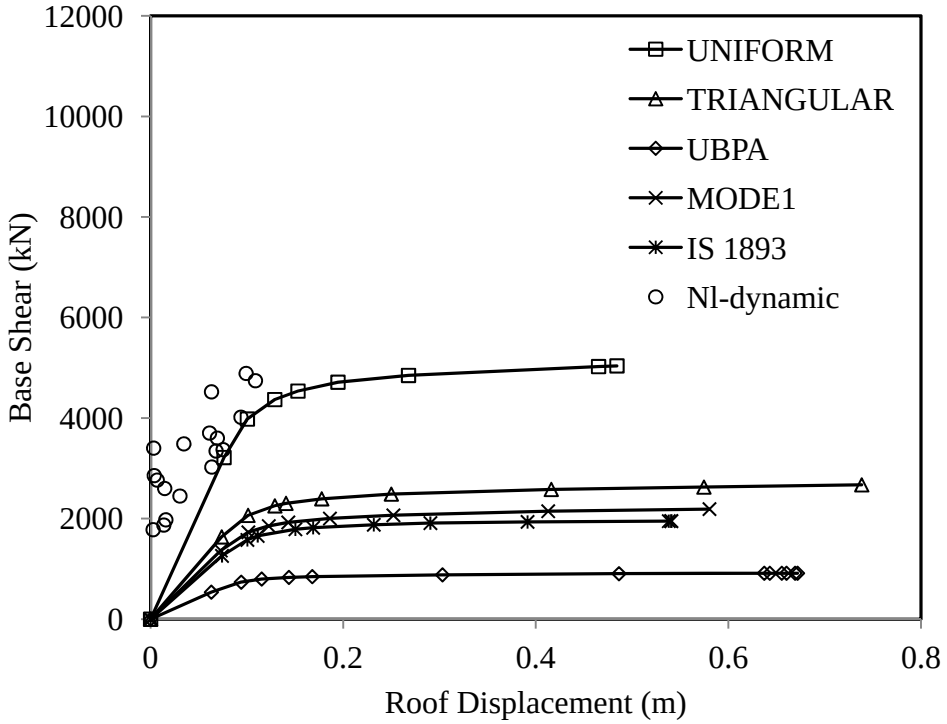

Fig. 4.96: Pushover curve for different load patterns for S3-20-12 building category

From these figures it can be concluded that the base shear capacities increases with increase in storey and bay numbers for all the load pattern considered here. This is because seismic weight of building increases with the increase of number of storeys as well as number of bays. Upper bound pushover analysis severely underestimates base shear capacities.

Maximum roof displacement capacity also increases with the increase of storey number for all the load pattern considered here except IS 1893 and UBPA load pattern. Maximum roof displacement capacity estimated with IS 1893 load pattern fall within a specific range for a specific height category and this variation of displacement demand with increase in storey height is not clear. Maximum roof displacement capacity decreases with the increase in bay number for all the load patterns considered in the study but the trend of variation is not clear. Upper bound pushover analysis procedure yields more ductile structures compared to other load pattern.

In uniform load pattern the base shear values approximately remains same in 8-storey buildings for regular frames, S-1 type setback frames, S-2 type setback frames but suddenly decreases for S-3 type setback frames for the same height and same bay building frame. For 12-storey, 16-storey and 20-storey height category frames also the base shear values approximately remains same for regular frame, S-1 type setback frames and S-2 type setback frames but suddenly decreases to half of this value for S-3 type setback frame. The pushover curves resulting from triangular load patterns and first mode shape load pattern estimates same base shear for the regular frame and S-1 type setback frame. So the pushover curves of triangular load pattern and first mode shape load pattern merge each other for regular and S-1 type setback frames but the pushover curves of these two load patterns do not merge for S-2 and S-3 types of setback frames and the base shear capacities decreases successively for S-2 and S-3 types of setback frames. This is because the first mode shape for regular and less irregular (S1-type) frame is very close to

inverted triangular shape. For the pushover curves resulting from IS 1893 load pattern and upper bound pushover analysis also the base shear demand remains same for regular and S1- type setback frames and decreases successively for S-2 and S-3 type setback frames. It is studied that the displacement capacity remains approximately same for all the pushover curves resulting from each load pattern for a specific height category and bay number and it is not affected by increase in setbacks.

The figures show that nonlinear time history envelopes follow the pushover curve of uniform load pattern closely for all the frames. For all the pushover curves the time history envelopes lie between uniform load pattern pushover curve and triangular load pattern pushover curve for regular and S-1 type setback frame as expected in FEMA 356:2000 and the time history envelopes scatter more as the setback irregularity increases. The uniform load pattern pushover curve seems to be more un-conservative for regular and S-1 type setback frames as compared to other two setbacks, S-2 and S-3 as the time history envelopes fall beyond the yielding capacity of pushover curve for regular and S-1 type setback frames.

Following observations can be drawn from the above figures:

i) As the shape of the triangular load pattern and first mode shape are similar for mid-rise regular buildings and close for other buildings, the resulting pushover curves are also found to be similar for almost all the building studied here.

ii) Mass proportional uniform load pattern always predicts highest base shear capacity amongst the five load patterns considered here.

iii) UBPA load pattern severely underestimates the base shear capacity for all the buildings studied here. These figures presented above clearly shows that the performance of UBPA load patterns is poorest for setback buildings.

iv) FEMA 356 suggests that pushover analyses with uniform and triangular load pattern will bind all the solutions related to base shear versus roof displacement of regular buildings. Results presented in Figures 4.49-4.96 support this statement for regular buildings. However, this is not true for setback buildings especially for high-rise buildings with higher irregularity (S3-type).

v) From this study it is clear that mass proportional uniform load pattern predicts base shear capacity of setback buildings with higher irregularity (S2 and S3 type) those are close to the nonlinear dynamic analyses results consistently. However, this load pattern overestimates the base shear capacity for regular and setback buildings with lesser irregularity (R and S1 type) slightly.

4.3 STUDY ON TARGET DISPLACEMENT

There are many methods available for estimating target displacements as discussed in Section 2.4.3. Among them displacement coefficient method as given in FEMA 356:2000 is most popular in design office because of its inherent simplicity. An effort has been made in the present study to modify this procedure to make it useful for estimating target displacement of Setback Buildings. The details of the displacement coefficient method as per FEMA 356:2000 is discussed in Section 2.4.3. Following sections presents the proposed modification to the displacement coefficient method and its justification.

4.3.1 Proposed Procedure of Target Displacements Estimation for Setback Buildings

The displacement coefficient method as outlined in the FEMA 356:2000 reveals that the building geometry affects C_0 factor significantly where as it has a little influence on the other factors, *i.e*. on C_1, C_2, and C_3. So to assess the applicability of the values of C_0 factor given in FEMA 356, linear time history analysis of 48 setback frames has been carried out. Each frame is subjected to 15 earthquake ground motions, scaled for PGA = 0.36g. The mean value of the maximum roof displacement of each frame and the mean value of spectral displacement of corresponding equivalent SDOF system for all the 15 earthquakes are calculated. The natural period of the equivalent SDOF system is calculated based on FEMA356. The results of the 48 (frames) * 15 (ground motions) = 720 linear time history analysis were done to get a set of response databank. The equivalent period (T_{eq}) can be generated from the base shear versus roof displacement curve or pushover curve by a graphical procedure as per 356:2000. The elastic spectral displacement corresponding to this period is calculated directly from the response spectrum representing the seismic ground motion under consideration for a specified damping ratio 5%. The ratio of maximum roof displacement of each frame to the corresponding elastic spectral displacement for equivalent period is calculated and compared with the C_0 values given in FEMA 356. Also the effect of bay and storey numbers on the value of C_0 factor is studied.

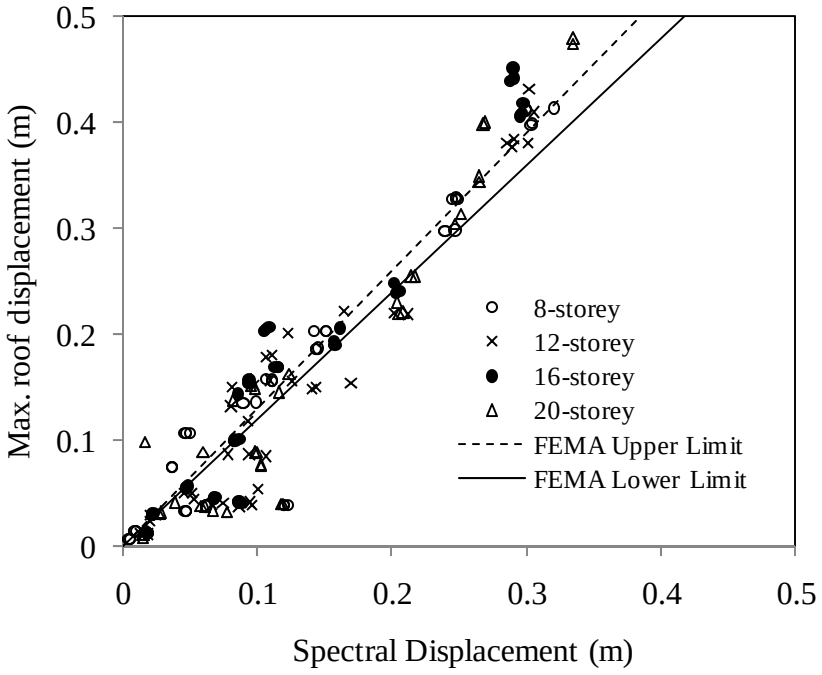

Fig. 4.97: Correlation between maximum roof displacements of regular frames to the spectral displacement for corresponding equivalent SDOF system

Figs 4.97, 4.98, 4.99 and 4.100 presents mean value of the maximum roof displacement of each frame versus the mean value of spectral displacement of corresponding equivalent SDOF system obtained for regular frame, S1-type setback frame, S2 type setback frame and S3 type setback frames respectively. Results for four height categories in each of these types of frames are shown here. These figures also show two lines representing the C_0 values given by FEMA 356 for triangular load pattern (C_0 =1.3) and uniform load pattern (C_0 =1.2). From these figures it is clear that, for most of the cases, C_0 does not match with the FEMA prescribed limits. For regular frame (R), the deviation is less but for setback frames the deviation tends to increase. Also, for the lower storey frames the deviation from the FEMA values is less compared to the higher storey frames. This indicates that the deviation in the ratio of elastic roof displacement for an

exact MDOF frame to the elastic spectral displacement for equivalent SDOF system increases with the increase in the number of storeys (building height) and with increase in irregularity.

FEMA-356 recommends a range of values for C_0 factors to estimate inelastic displacement demand of regular buildings. The results obtained from this study shows that the actual values of C_0 factors for setback buildings do not match within the FEMA limits. It can also be noted that FEMA limits failed to predict actual values of C_0 for high rise regular buildings also.

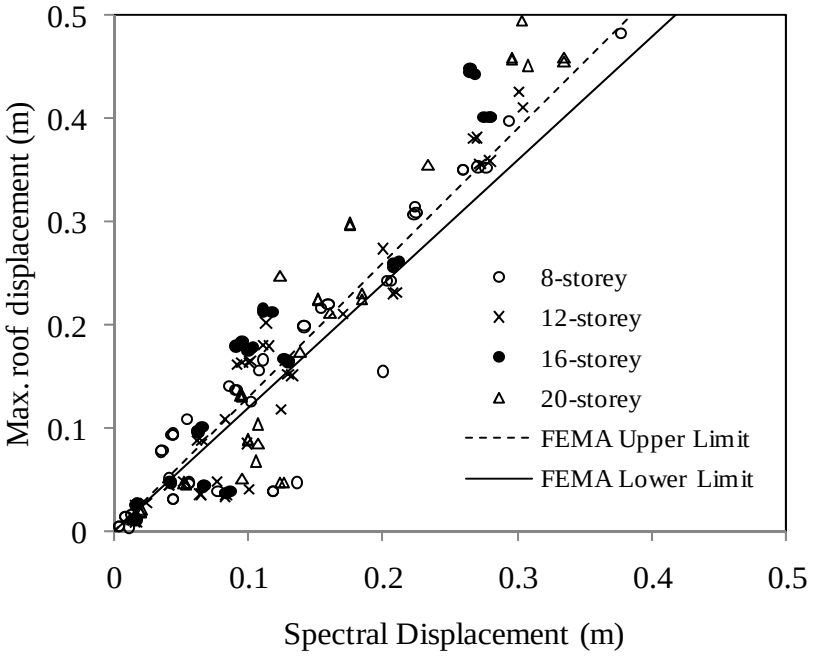

Fig. 4.98: Correlation between maximum roof displacements of setback frames (S1) to the spectral displacement for corresponding equivalent SDOF system

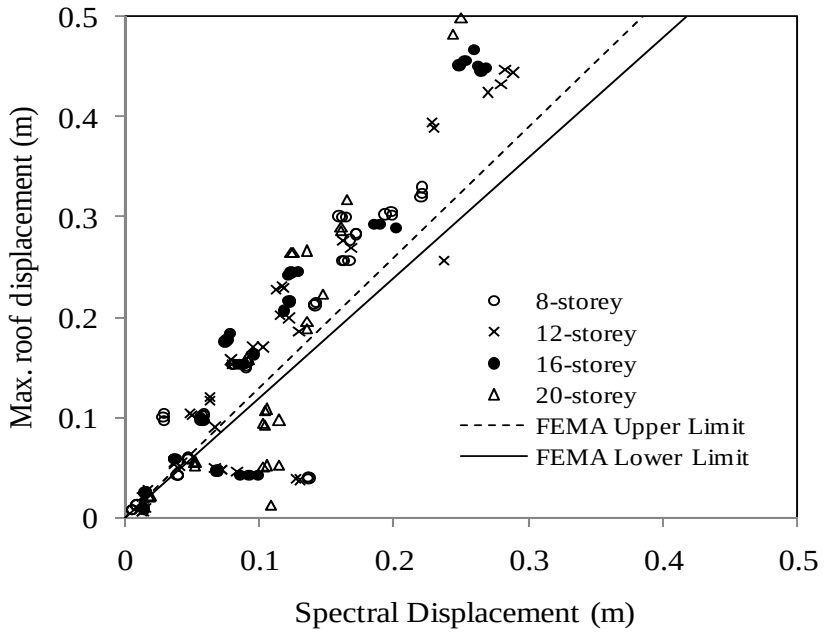

Fig. 4.99: Correlation between maximum roof displacements of setback frames (S2) to the spectral displacement for corresponding equivalent SDOF system

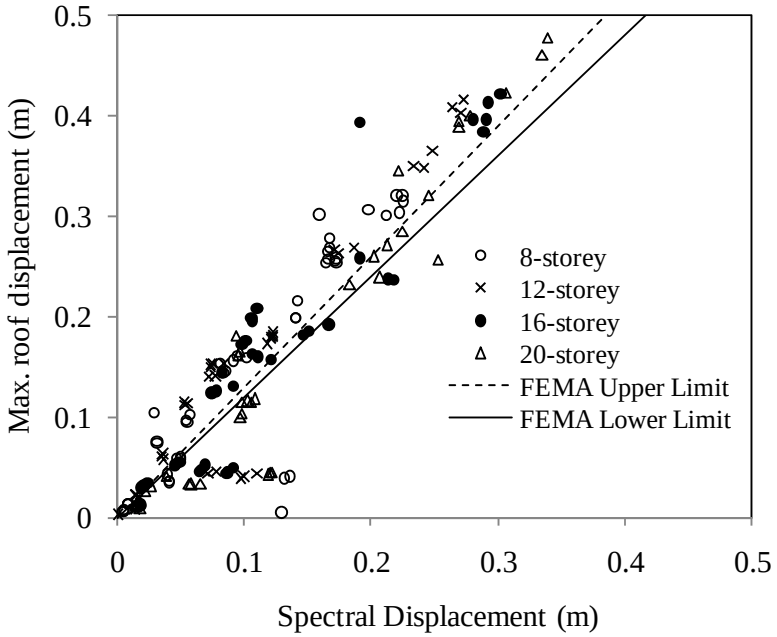

Fig. 4.100: Correlation between maximum roof displacements of setback frames (S3) to the spectral displacement for corresponding equivalent SDOF system

A study was taken up to check the effect of number of bays on the C_0 value. Figs. 4.101, 4.102, 4.103 and 4.104 present the variation of C_0 value with respect to number of bays when height and regularity index is constant. These four figures show that C_0 factor has hardly any dependence on the bay numbers for mid-rise building. However, for very tall building C0 factor is sensitive to the number of bays (Fig. 104).

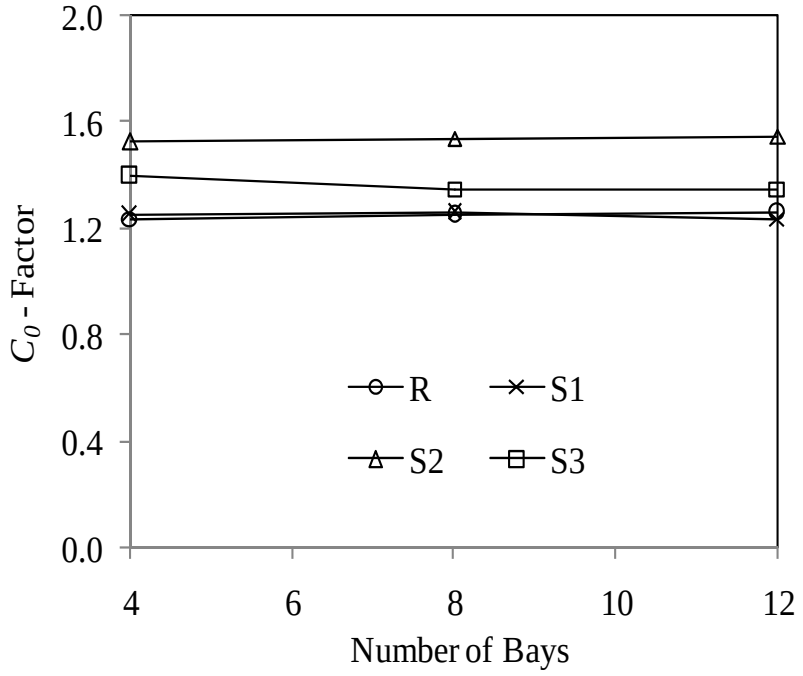

Fig. 4.101: Variation of C_0-Factor with bay numbers for 8-storey building variants

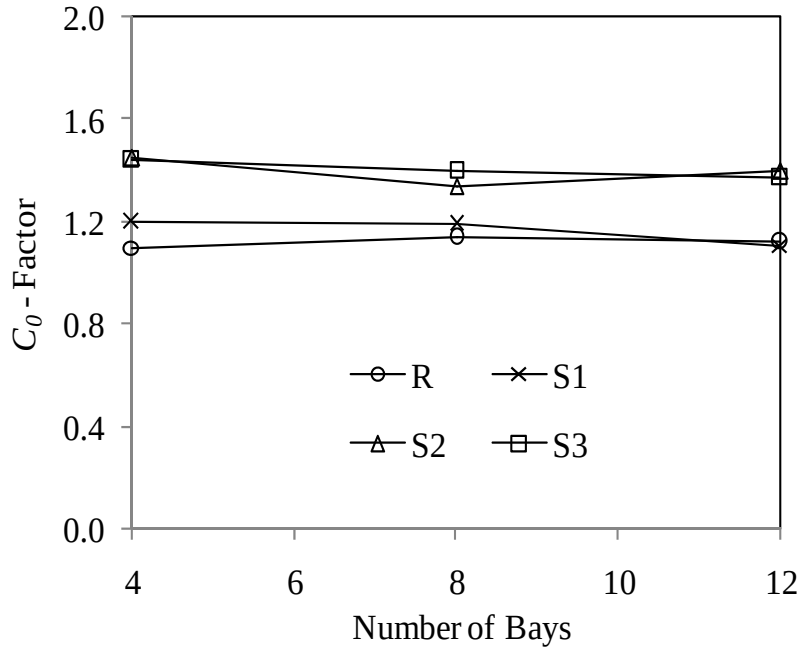

Fig. 4.102: Variation of C_0-Factor with bay numbers for 12-storey building variants

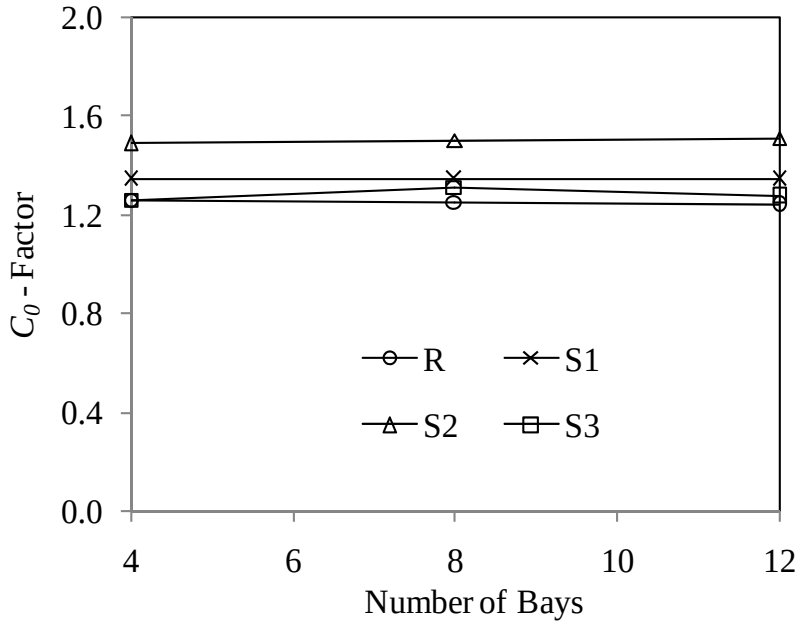

Fig. 4.103: Variation of C_0-Factor with bay numbers for 16-storey building variants

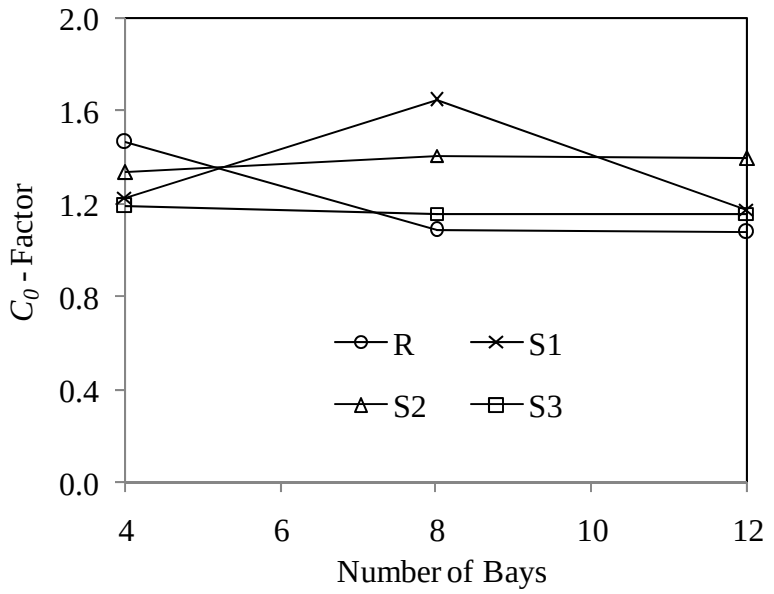

Fig. 4.104: Variation of C_0-Factor with bay numbers for 20-storey building variants

Figs. 4.105 to 4.107 present the variation of C_0 factor with overall building height for constant number of bays. These figures show that the building height affects the value of C_0 factor although the range of variation is low.

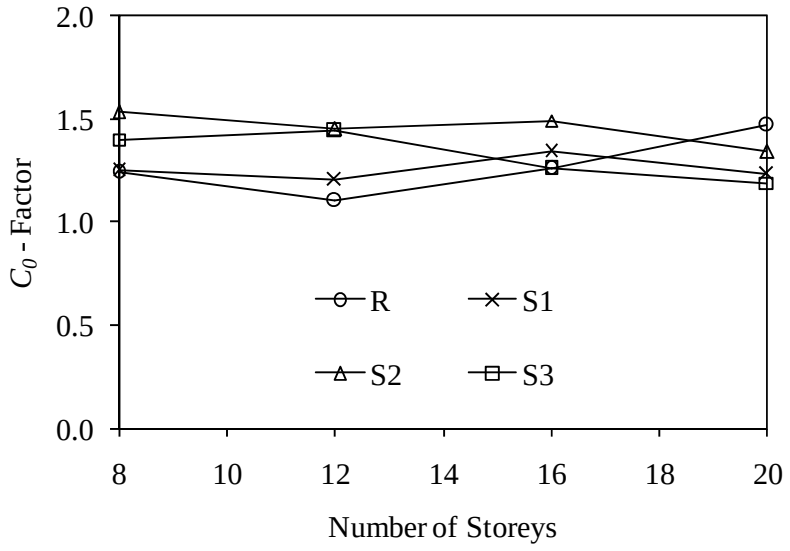

Fig. 4.105: Variation of C_0-Factor with storey numbers for 4-bay building variants

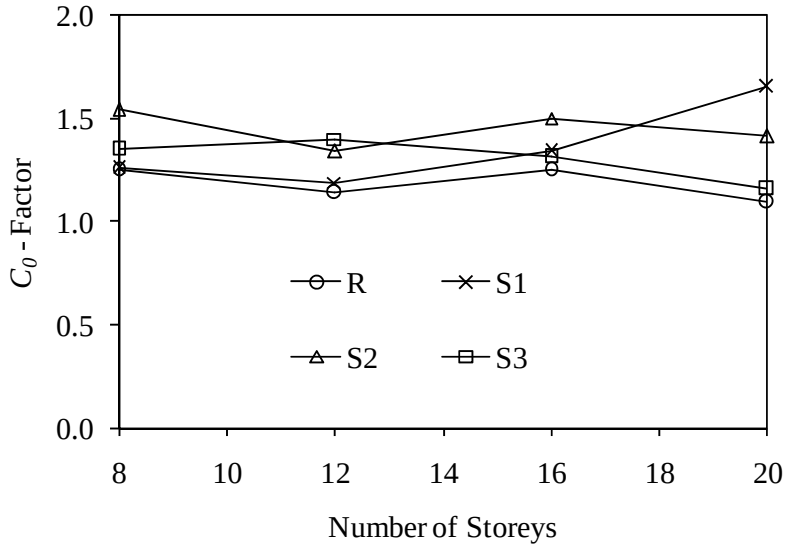

Fig. 4.106: Variation of C_0-Factor with storey numbers for 8-bay building variants

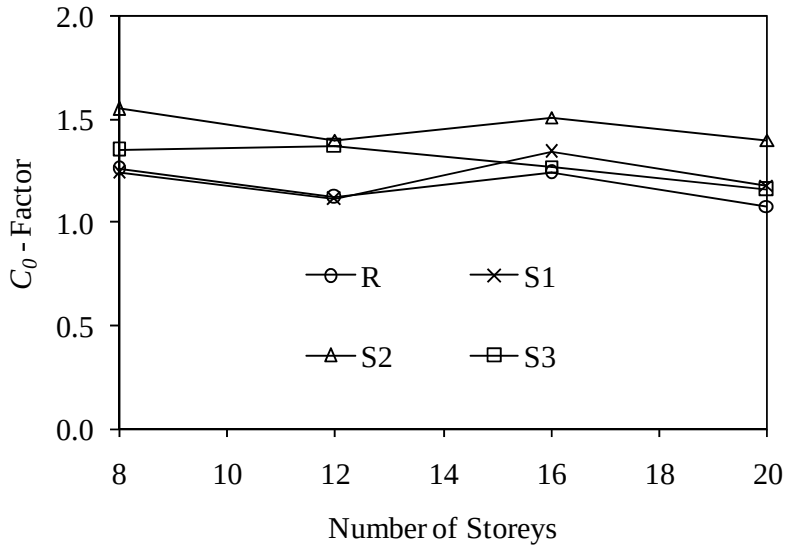

Fig. 4.107: Variation of C_0-Factor with storey numbers for 12-bay building variants

Figs. 4.108 to 4.111 present the variation of C_0 factor with percentage setback present in a building frame. These figures show that the setback irregularity has an important role in the value of C_0 factor.

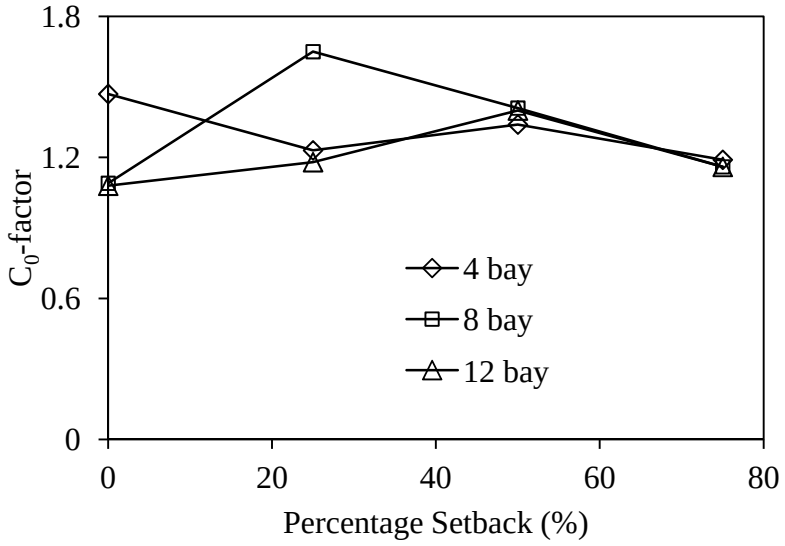

Fig. 4.108: Variation of C_0-Factor with percentage setback for 20-storey building variants

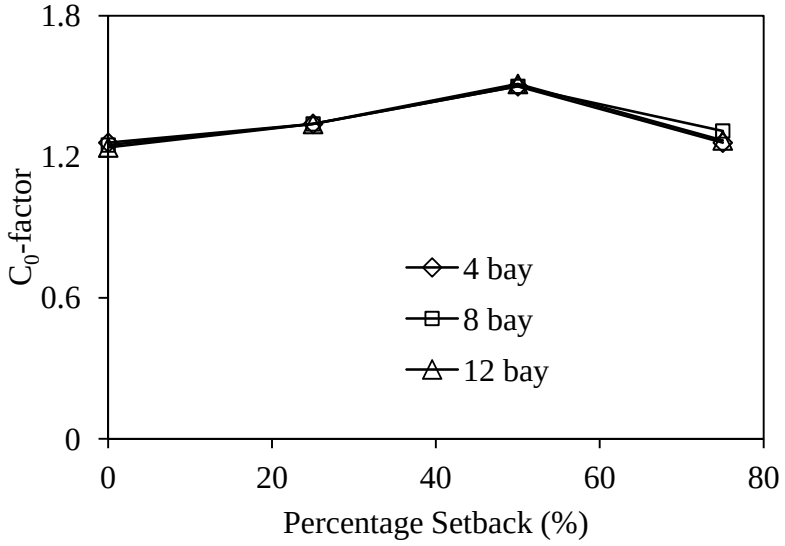

Fig. 4.109: Variation of C_0-Factor with percentage setback for 16-storey building variants

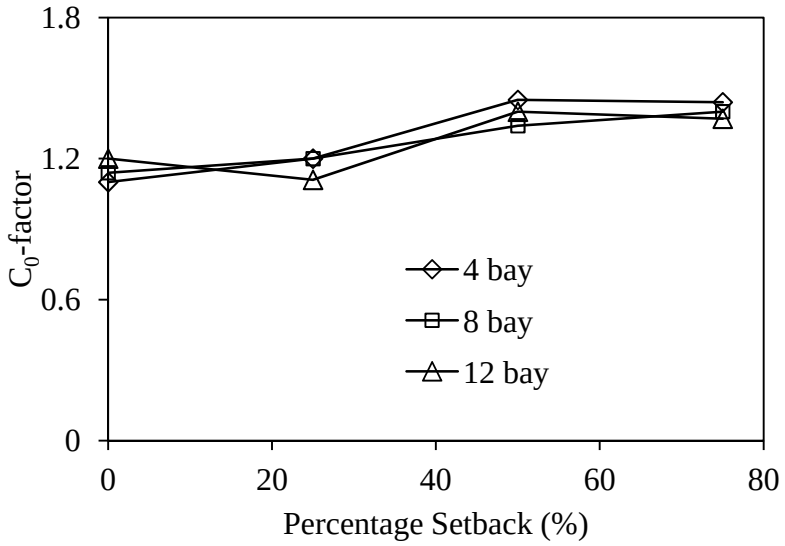

Fig. 4.110: Variation of C_0-Factor with percentage setback for 12-storey building variants

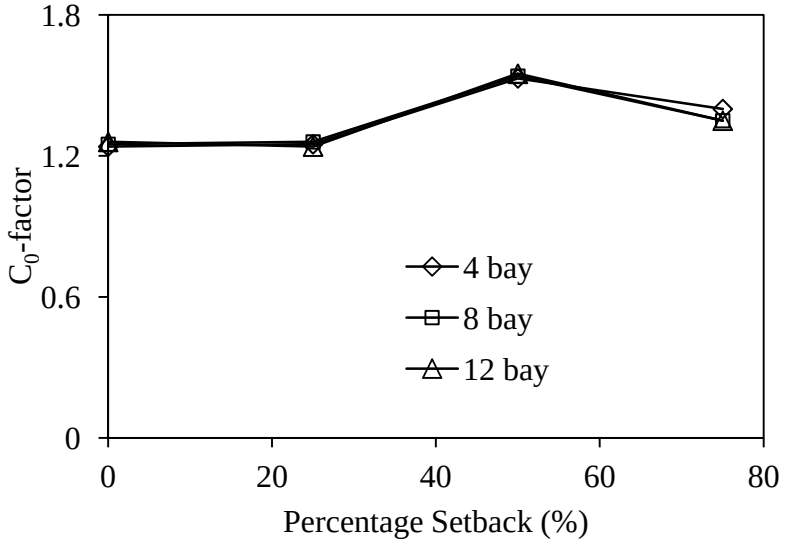

Fig. 4.111: Variation of C_0-Factor with percentage setback for 8-storey building variants

The results indicate that the C_0 factor is a function of bay width, building height and extent of irregularity (% Setback) present in the building. However considering the small range of variation (especially for mid-rise building) it can be assumed that the C_0 factor is independent of building width and building height. A regression analysis is carried out considering the C_0 factor is a function of irregularity (% Setback) presents in the building only and the following equation is derived to calculate C_0 factor:

$$C_0 = 0.7 + \frac{(1-x)(1+9x^2)}{2} \tag{4.1}$$

Where x = percentage setback ($0 < x < 1.0$).

Fig. 4.112 presents the comparison of C_0 factor obtained from mean time-history results and the proposed function.

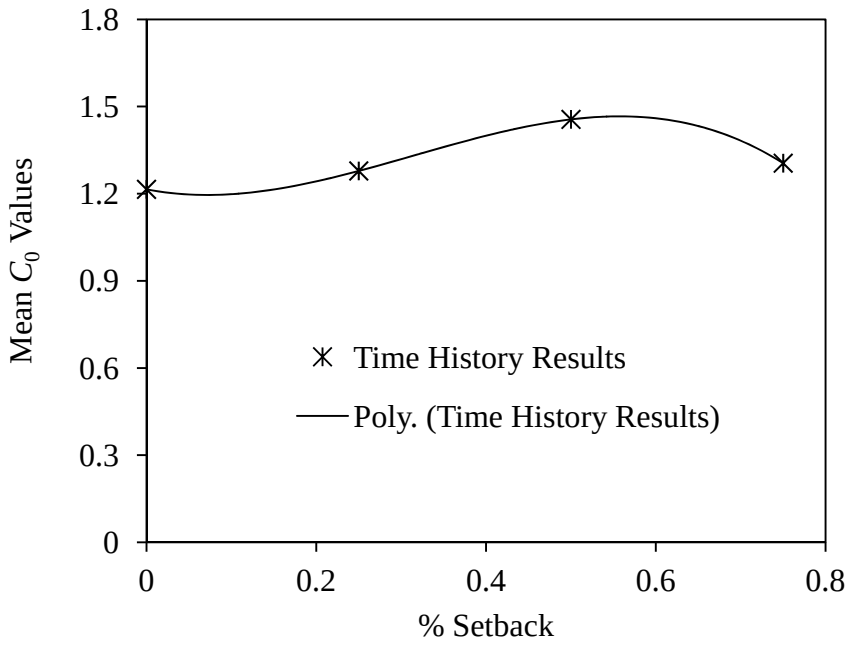

Fig. 4.112: Comparison of mean time-history results and the proposed function.

4.4 PERFORMANCE OF PROPOSED PUSHOVER ANALYSIS

Pushover analyses of all the selected building frames are carried out using the mass proportional uniform load pattern and the proposed modification in target displacement estimation procedure. The target displacement results obtained from these analyses are presented in the Table 4.1. From this table it can be observed that capacity spectrum method (CSM) of ATC-40 always underestimate the target displacement for a setback building whereas Upper bound pushover analysis (UBPA) overestimates the target displacement for regular and for setback buildings also.

Table 4.1 shows that the estimated target displacement by proposed procedure is consistently matching with the target displacement obtained from dynamic analysis procedure unlike the target displacement obtained from other existing pushover analysis procedures available.

The standard error of the pushover results with respect to the dynamic analysis results are calculated as per following equation (Menjivar, 2004) and presented in Table 4.1:

$$Error(\%) = 100\sqrt{\frac{1}{n}\sum_{i=1}^{n}\left|\frac{\Delta_{iD} - \Delta_{iP}}{\Delta_{iD}}\right|} \qquad (2)$$

Where Δ_{iD} = Target displacement estimated by dynamic analysis procedure

Δ_{iP} = Target displacement estimated by pushover analysis procedure

n = Number of buildings considered for error calculation

It can be seen from Table 4.1 that error associated with the proposed procedure is less compared to the other existing pushover analysis procedures when setback buildings are considered.

Table 4.1: Comparison of estimated target displacement using different procedures

Sl No.	Building Frame	Proposed Procedure	DCM of FEMA-356	CSM of ATC-40	UBPA	Dynamic Analysis
1	R-8-4	0.17	0.14	0.08	0.15	0.20
2	R-8-8	0.11	0.15	0.09	0.15	0.11
3	R-8-12	0.18	0.15	0.09	0.15	0.19
4	R-12-4	0.20	0.16	0.10	0.18	0.20
5	R-12-8	0.17	0.14	0.08	0.16	0.15
6	R-12-12	0.12	0.18	0.08	0.20	0.12
7	R-16-4	0.13	0.15	0.10	0.18	0.12
8	R-16-8	0.14	0.15	0.09	0.17	0.14
9	R-16-12	0.13	0.15	0.09	0.18	0.12
10	R-20-4	0.24	0.11	0.14	0.12	0.18
11	R-20-8	0.25	0.33	0.13	0.37	0.16
12	R-20-12	0.25	0.32	0.13	0.37	0.16
13	S1-8-4	0.18	0.14	0.08	0.15	0.17
14	S1-8-8	0.15	0.26	0.09	0.28	0.13
15	S1-8-12	0.18	0.11	0.09	0.12	0.17
16	S1-12-4	0.27	0.12	0.10	0.14	0.20
17	S1-12-8	0.16	0.12	0.08	0.13	0.15
18	S1-12-12	0.13	0.17	0.08	0.19	0.13
19	S1-16-4	0.12	0.12	0.10	0.15	0.12
20	S1-16-8	0.11	0.12	0.09	0.15	0.11
21	S1-16-12	0.11	0.12	0.09	0.14	0.10
22	S1-20-4	0.18	0.18	0.13	0.21	0.18
23	S1-20-8	0.16	0.24	0.12	0.28	0.16
24	S1-20-12	0.16	0.24	0.12	0.28	0.16
25	S2-8-4	0.21	0.12	0.08	0.13	0.21

26	S2-8-8	0.12	0.12	0.08	0.13	0.12
27	S2-8-12	0.14	0.12	0.09	0.13	0.15
28	S2-12-4	0.18	0.10	0.10	0.12	0.17
29	S2-12-8	0.10	0.12	0.08	0.15	0.10
30	S2-12-12	0.11	0.10	0.08	0.13	0.10
31	S2-16-4	0.18	0.10	0.10	0.13	0.16
32	S2-16-8	0.10	0.10	0.09	0.13	0.10
33	S2-16-12	0.11	0.10	0.09	0.13	0.12
34	S2-20-4	0.20	0.19	0.13	0.24	0.20
35	S2-20-8	0.16	0.18	0.12	0.20	0.17
36	S2-20-12	0.16	0.18	0.12	0.22	0.17
37	S3-8-4	0.08	0.12	0.07	0.14	0.08
38	S3-8-8	0.08	0.13	0.07	0.15	0.09
39	S3-8-12	0.20	0.12	0.08	0.13	0.16
40	S3-12-4	0.14	0.10	0.09	0.12	0.14
41	S3-12-8	0.08	0.10	0.07	0.12	0.07
42	S3-12-12	0.08	0.10	0.07	0.10	0.07
43	S3-16-4	0.16	0.16	0.09	0.18	0.15
44	S3-16-8	0.12	0.15	0.08	0.17	0.11
45	S3-16-12	0.11	0.14	0.08	0.16	0.11
46	S3-20-4	0.32	0.40	0.13	0.46	0.21
47	S3-20-8	0.17	0.32	0.11	0.37	0.14
48	S3-20-12	0.14	0.29	0.11	0.32	0.11
Standard Error (%)		**32.6**	**59.9**	**54.8**	**68.8**	-

4.5 SUMMARY

All the selected building models with different setback irregularities are analyzed for linear/nonlinear static/dynamic behaviour. An effort has been made to choose a correct load pattern for nonlinear static analyses of setback buildings. A number of invariant load patterns available in literature are tested and it is found that pushover analysis with mass proportional uniform load pattern predicts the base shear and roof displacement capacity closer to that of nonlinear dynamic analysis. Also an improved procedure for estimating target displacement of setback buildings is proposed. This proposal is a simple modification of the displacement coefficient method as outlined in FEMA 356: 2000. The chapter shows that nonlinear static analyses carried out as per the proposed load pattern and target displacement estimation procedure consistently predicting the results close to that of nonlinear dynamic analyses.

CHAPTER 5

SUMMARY AND CONCLUSIONS

5.1 SUMMARY

The behaviour of a multi-storey framed building during strong earthquake motions depends on the distribution of mass, stiffness, and strength in both the horizontal and vertical planes of a building. In multi-storeyed framed buildings, damage from earthquake ground motion generally initiates at locations of structural weaknesses present in the lateral load resisting frames. Further, these weaknesses tend to accentuate and concentrate the structural damage through plastification that eventually leads to complete collapse. In some cases, these weaknesses may be created by discontinuities in stiffness, strength or mass between adjacent storeys. Such discontinuities between storeys are often associated with sudden variations in the frame geometry along the height. There are many examples of failure of buildings in past earthquakes due to such vertical discontinuities. Structural engineers have developed confidence in the design of buildings in which the distributions of mass, stiffness and strength are more or less uniform. But there is a less confidence about the design of structures having irregular geometrical configurations.

A common type of vertical geometrical irregularity in building structures arises is the presence of setbacks, *i.e*. the presence of abrupt reduction of the lateral dimension of the building at specific levels of the elevation. This building category is known as ‘setback building’. This building form is becoming increasingly popular in modern multi-storey

building construction mainly because of its functional and aesthetic architecture. In particular, such a setback form provides for adequate daylight and ventilation for the lower storeys in an urban locality with closely spaced tall buildings. This type of building form also provides for compliance with building bye-law restrictions related to 'floor area ratio' (practice in India). Setback buildings are characterised by staggered abrupt reductions in floor area along the height of the building, with consequent drops in mass, strength and stiffness.

Height-wise changes in stiffness and mass render the dynamic characteristics of these buildings different from the 'regular' building. It has been reported in the literature that higher mode participation is significant in these buildings. Also, the inter-storey drifts for setback building are expected to be more in the upper floors and less in the lower floors, compared to regular buildings without setback.

Many investigations have been performed to understand the behaviour of irregular structures as well as setback structures and to ascertain method of improving their performance.

It may not be possible to evaluate the seismic performance of setback building accurately using conventional nonlinear static (pushover) analysis outlined in FEMA 356 (2000) and ATC 40 (1996), because of its limitations for the irregular structures with significant higher modes effects. There have been a number of efforts reported in literature to extend the pushover analysis procedure to include different irregular building categories. However, so far, setback buildings have not been addressed in this regard. It is instructive to study the performance of conventional pushover analysis methodology as well as other alternative pushover methodologies for

setback buildings and to suggest improvements suitable for setback buildings. This is the primary motivation underlying the present study.

To get a clear idea about the dynamic performance of setback buildings a detailed literature review is carried out in two major areas. These are: (i) Performances of setback buildings under seismic loading and (ii) Performance based seismic engineering that uses pushover analysis tools. The research papers on setback buildings conclude that the displacement demand is dependent on the geometrical configuration of frame and concentrated in the neighbourhood of the setbacks for setback structures. The higher modes significantly contribute to the response quantities of structure. Also conventional pushover analysis seems to be underestimating the response quantities in the upper floors of the irregular frames. So it is necessary to evaluate the seismic demands for setback buildings to assess the seismic performance of setback buildings.

To achieve the objective of the study altogether 48 building frames were selected for the study which are plane and orthogonal with storey heights and bay widths. Different building geometries were taken for the study. These building geometries represent varying degree of irregularity or amount of setback. Three different width categories, ranging from 4 to 12 bays (in the direction of earthquake) with a uniform bay width of 6m were considered for this study. It should be noted that bay width of 4m – 6m is the usual case, especially in Indian and European practice. Similarly, four different height categories were considered for the study, ranging from 8 to 20 storeys, with a uniform storey height of 3m. The selected building models have different amount of setback irregularities due to the successive reduction of 25% width and 25% height (S1), 50% width and 50% height (S2) and 75% width and 75% height (S3). The regular frame (R),

without any setback, is also studied. All the selected models were designed with M-20 grade of concrete and Fe-415 grade of reinforcing steel as per Indian Standards.

In the present study, a point-plasticity approach is considered for modelling nonlinearity, wherein the plastic hinge is assumed to be concentrated at a specific point in the frame member under consideration. Beam and column elements in this study were modelled with flexure (M3 for beams and P-M2-M3 for columns) hinges at possible plastic regions under lateral load (*i.e*., both ends of the beams and columns). Properties of flexure hinges must simulate the actual response of reinforced concrete components subjected to lateral load. Flexural hinges in this study are defined by moment-rotation curves calculated based on the cross-section and reinforcement details at the possible hinge locations.

All the 48 building models with different setback are analyzed for linear/nonlinear static/dynamic behaviour using commercial software SAP2000 (v14). In the present study nonlinear static analysis or pushover analysis is ran by five different load patterns available in literatures to justify which load pattern is good to determine the relative magnitudes of shears, moments and deformations within the structure during actual earthquake ground motion. The five different load patterns used in the analysis are listed below:

1. Mass Proportional Uniform load pattern (UNIFORM)
2. Mass Proportional Triangular Load Pattern (TLP)
3. Load Pattern similar to the First Mode Shape of the building (Mode Shape 1st)
4. Load Pattern similar to the IS 1893: 2002 static load distribution shape (IS-1893)
5. Upper bound pushover analysis as described by the Jan *et. al*. 2004 (UBPA)

Non-linear time history analysis is carried out for all the selected 48 building models to get the dynamic response of the selected buildings. The dynamic input has been given as a ground acceleration time-history which was applied uniformly at all the points of the base of the structure; only one horizontal component of the ground motion has been considered. Fifteen natural input time histories were employed for the dynamic analysis of the study. All these acceleration data were collected from Strong Motion Database available in the website of Centre for Engineering Strong Motion Data, USA (http://www.strongmotioncenter.org/) and were scaled to have various peak ground accelerations ranging from 0.36g to 0.72g. To maintain the similarity between the dynamic analysis and the pushover analysis, standard hinges were used to model nonlinearity in the frame through nonlinear links.

Also an improved procedure for estimating target displacement of setback buildings is proposed. This proposal is a simple modification of the displacement coefficient method as outlined in FEMA 356: 2000. This study shows that nonlinear static analyses carried out as per the proposed load pattern and target displacement estimation procedure consistently predicting the results close to that of nonlinear dynamic analyses.

5.2 CONCLUSIONS

Based on the work presented in this thesis following point-wise conclusions can be drawn:

i) A detailed literature review on setback buildings conclude that the displacement demand is dependent on the geometrical configuration of frame and concentrated in the neighbourhood of the setbacks for setback structures.

The higher modes significantly contribute to the response quantities of setback structure. Also conventional pushover analysis seems to be underestimating the response quantities in the upper floors of the irregular frames.

ii) As the shape of the triangular load pattern and first mode shape are similar for mid-rise regular buildings and close for high-rise and setback buildings, the resulting pushover curves are found to be similar for almost all the building studied here.

iii) FEMA 356 suggests that pushover analyses with uniform and triangular load pattern will bind all the solutions related to base shear versus roof displacement of regular buildings. Results presented here support this statement for regular buildings. However, this is not true for setback buildings especially for high-rise buildings with higher irregularity (S3-type).

iv) Mass proportional uniform load pattern found to be suitable for carrying out pushover analysis of Setback buildings as the capacity curve obtained using this load pattern closely matches the response envelop obtained from nonlinear dynamic analyses.

v) Upper bound pushover analysis severely underestimates base shear capacities of setback as well as regular building frames.

vi) This study shows that C_0–factor, in most of the cases, does not lie within the FEMA-356 prescribed limits. For regular frame (R), the deviation is less but for setback frames the deviation tends to increase. Also, for the lower storey frames the deviation from the FEMA values is less compared to the higher storey frames.

vii) The study concludes that the C_0 factor is a function of bay width, building height and extent of irregularity (% Setback) presents in the building. However considering the small range of variation (especially for mid-rise building) it can be assumed that the C_0 factor is independent of building width and building height. However, this factor is found to be very sensitive to the setback irregularity (% Setback) present in the building.

viii) This study proposes a modification to the magnitude of FEMA-356 prescribed C_0 factor that estimates more accurate target displacements of setback building. Unlike FEMA-356 recommendation, this modified C_0 factor is a function of setback irregularity.

ix) Pushover analyses of setback buildings using the mass proportional uniform load pattern and the proposed modification in target displacement gives superior results compared to other available existing procedures.

5.3 SCOPE OF FUTURE STUDY

i) The present study is limited to reinforced concrete (RC) multi-storeyed building frames with setbacks only in one direction. There is a future scope of study on three dimensional building models having setbacks in both of the horizontal orthogonal directions.

ii) The plan asymmetry arising out of the vertical geometric irregularity strictly calls for three-dimensional analysis to account properly for torsion effects. This is also an important research area that needs attention.

iii) It will be appropriate to consider adaptive load pattern in pushover analysis in order to include the effect of progressive structural yielding.

iv) There is a scope of research on the behaviour of setback building considering soil flexibility.

APPENDIX A

RESPONSE SPECTRUM FOR THE SELECTED GROUND MOTIONS

Figs A.1 to A.15 present the elastic response spectrum (spectral acceleration vs. Natural period) of the fifteen selected ground motions for constant (5%) damping. These response spectrum curves are generated using computer software SAP 2000.

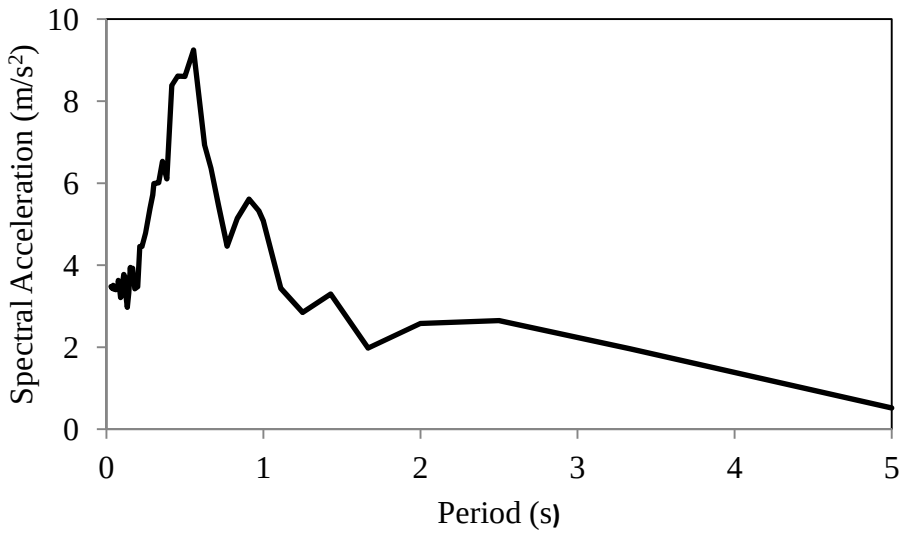

Fig. A.1: Elastic response spectrum (acceleration) of Imperial Valley Earthquake (1940)

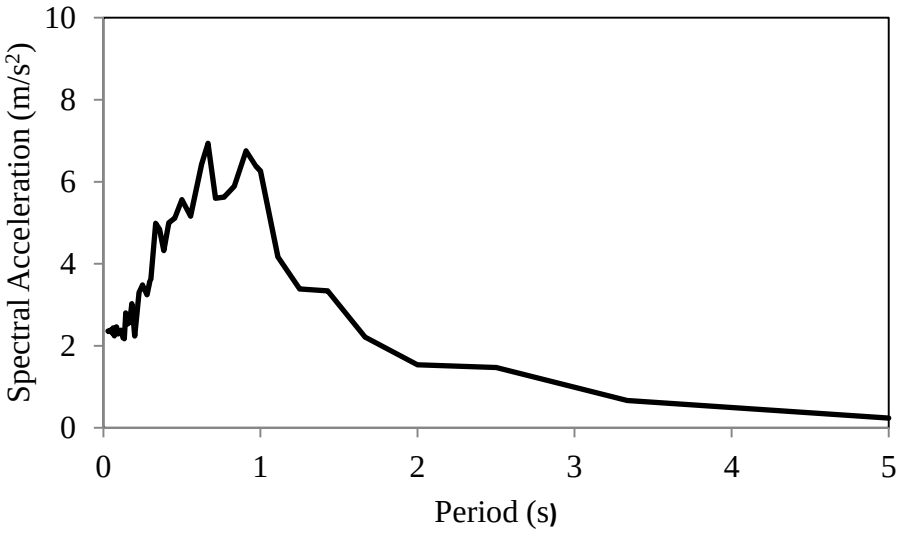

Fig. A.2: Elastic response spectrum (acceleration) of Loma Prieta- Oakland Earthquake (1989)

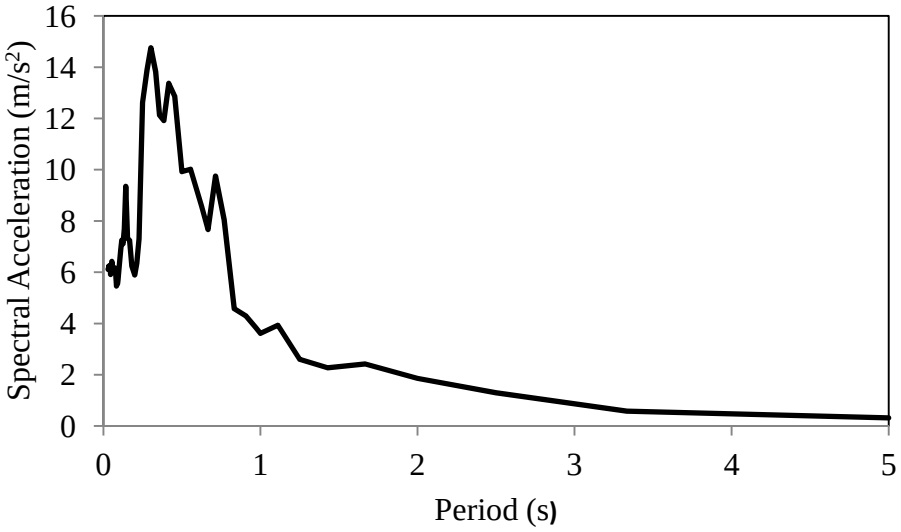

Fig. A.3: Elastic response spectrum (acceleration) of Loma Prieta- Corralitos Earthquake (1989)

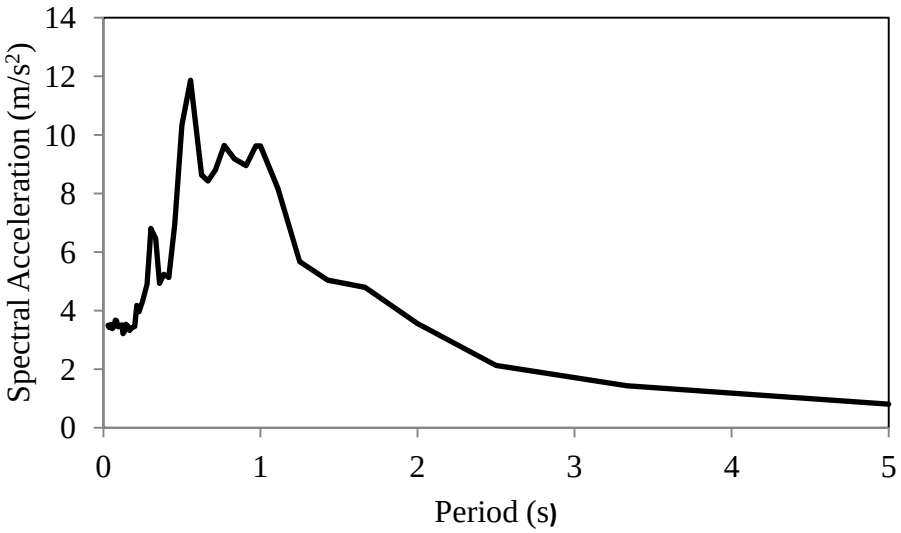

Fig. A.4: Elastic response spectrum (acceleration) of Loma Prieta- Hollister Earthquake (1989)

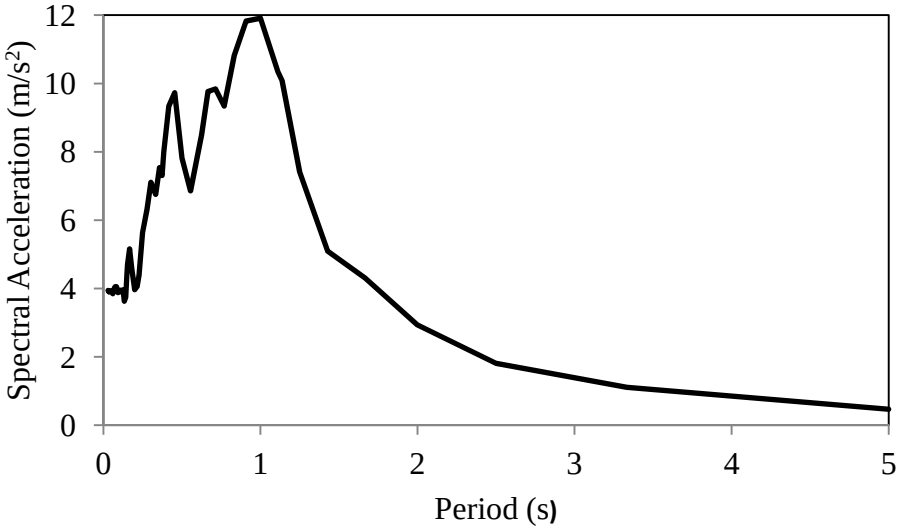

Fig. A.5: Elastic response spectrum (acceleration) of Loma Prieta- Lexington Dam Earthquake (1989)

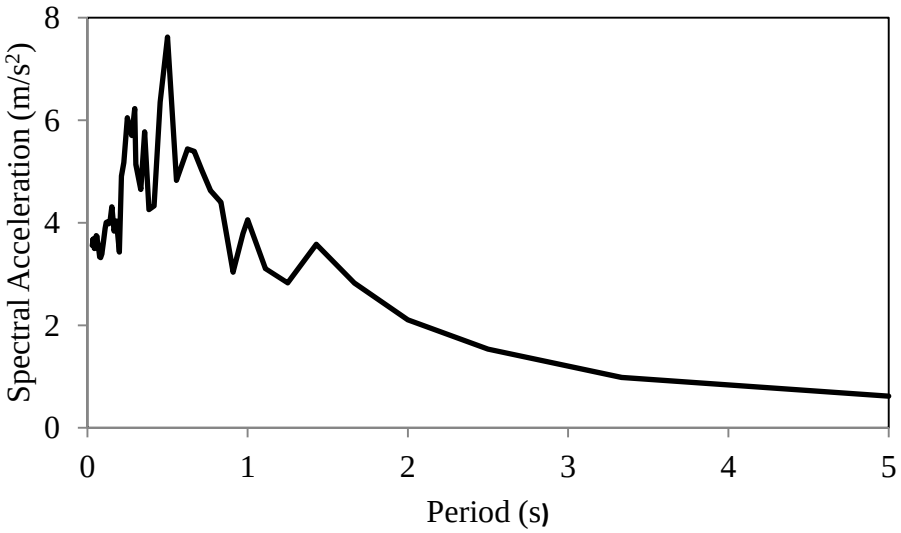

Fig. A.6: Elastic response spectrum (acceleration) of Northridge-Santa Monica Earthquake (1994)

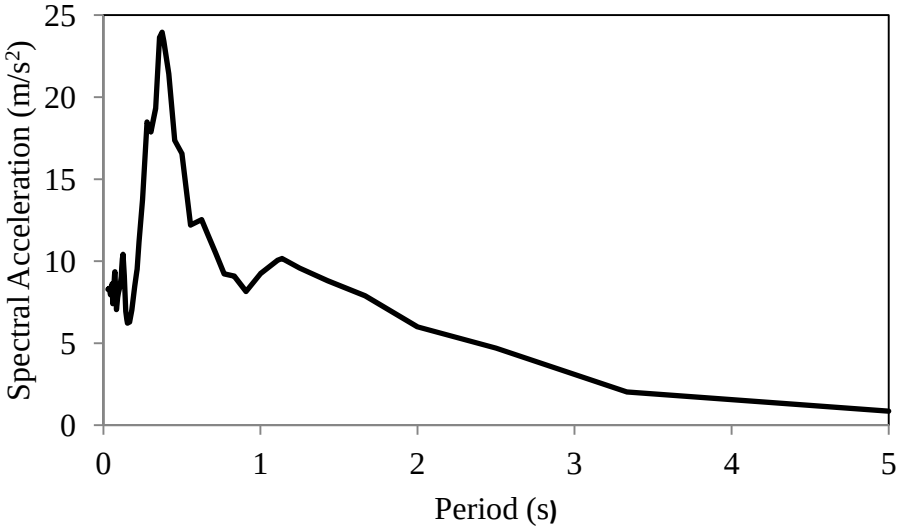

Fig. A.7: Elastic response spectrum (acceleration) of Northridge-Sylmar Earthquake (1994)

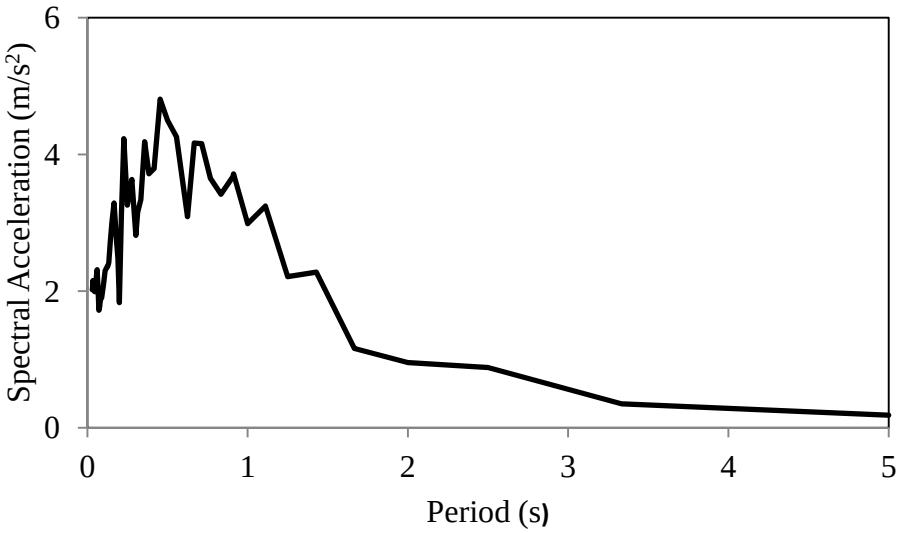

Fig. A.8: Elastic response spectrum (acceleration) of Northridge-Century City Earthquake (1994)

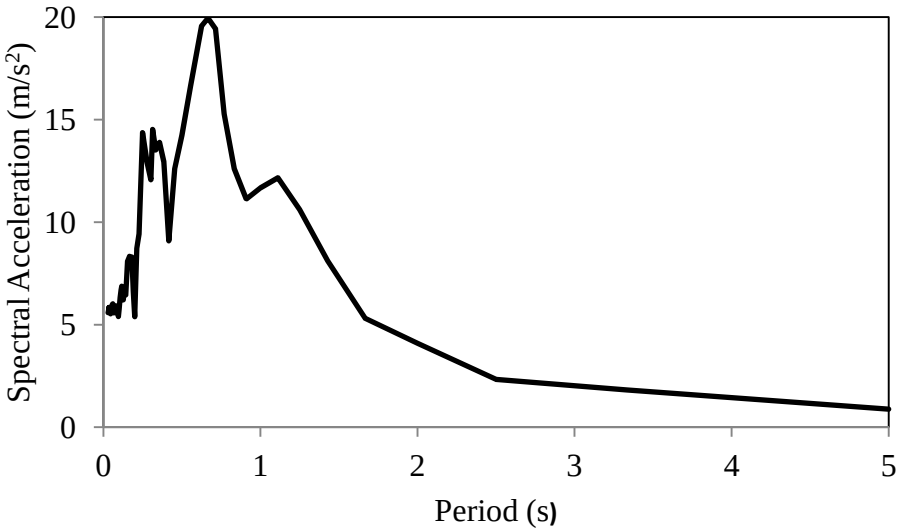

Fig. A.9: Elastic response spectrum (acceleration) of Northridge-Newhall Earthquake (1994)

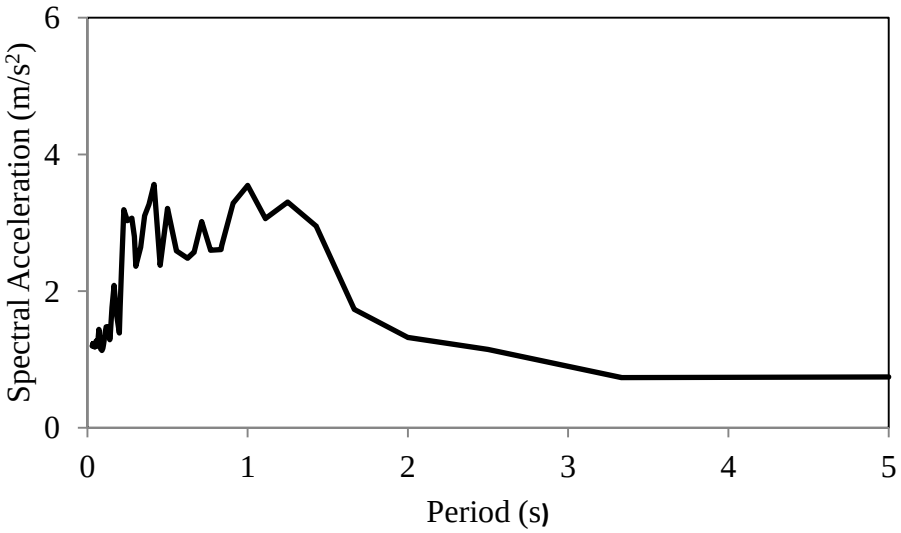

Fig. A.10: Elastic response spectrum (acceleration) of Landers- Yermo Earthquake (1992)

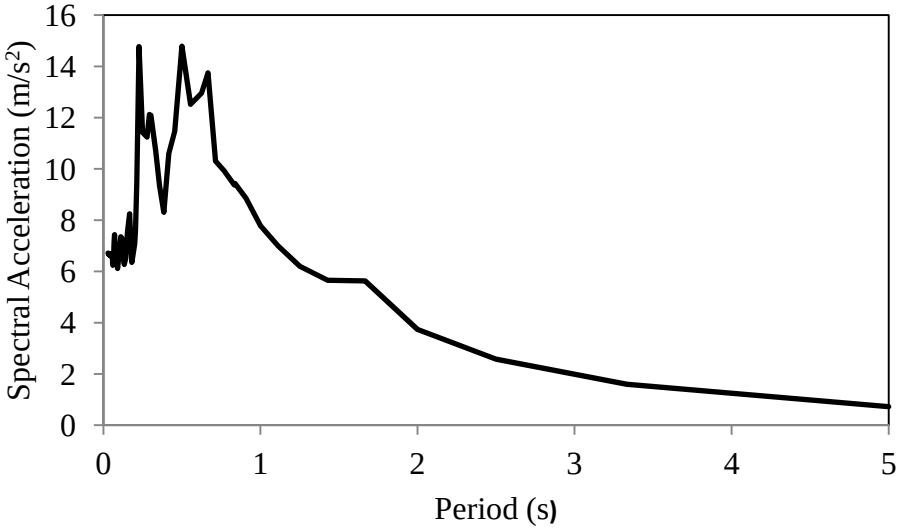

Fig. A.11: Elastic response spectrum (acceleration) of Landers- Lucerne Valley Earthquake (1992)

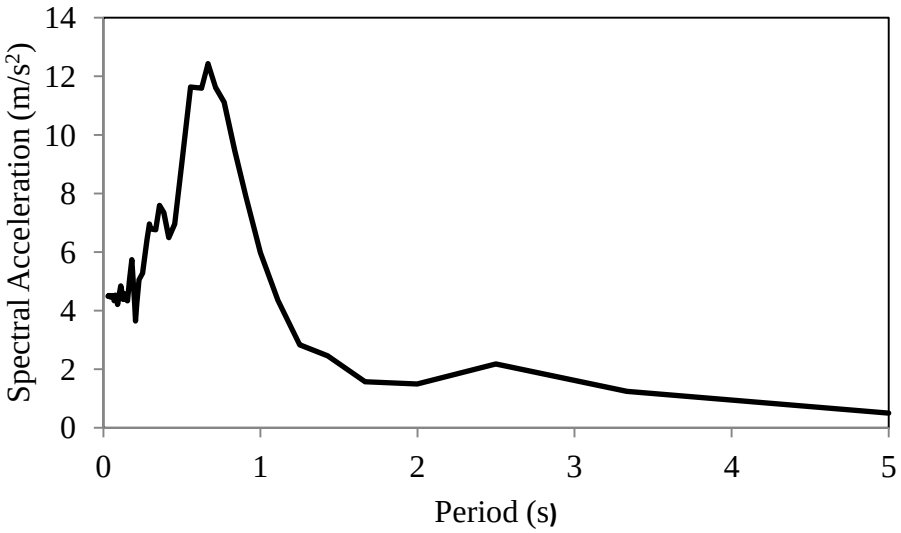

Fig. A.12: Elastic response spectrum (acceleration) of Petrolia-Cape Mendocino Earthquake (1992)

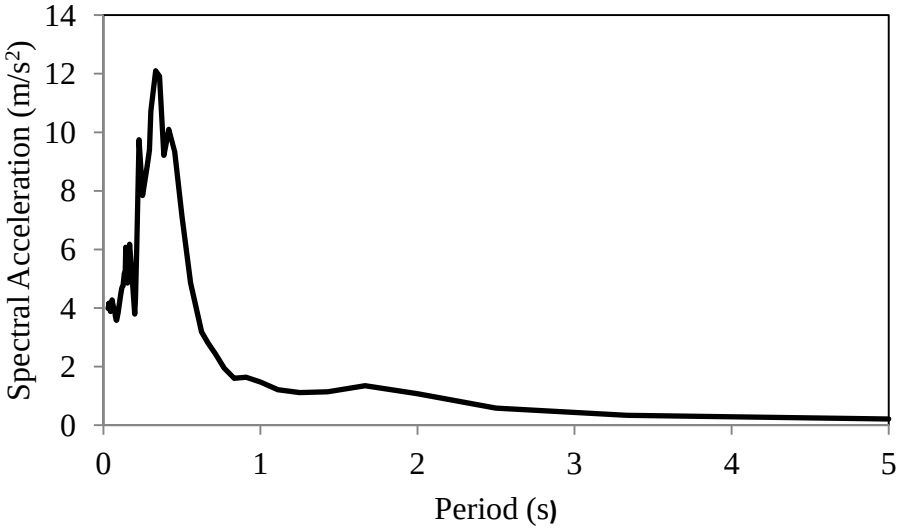

Fig. A.13: Elastic response spectrum (acceleration) of Sierra Madre- Altadena Earthquake (1991)

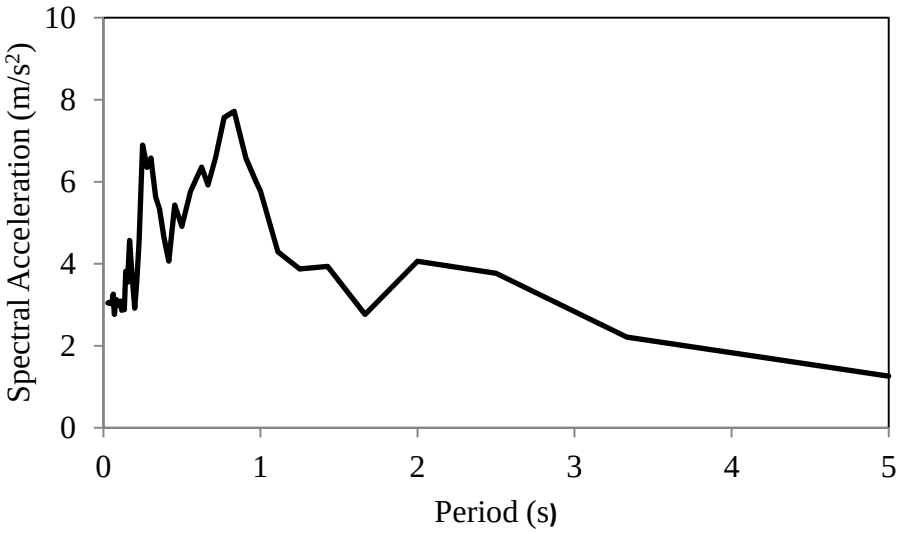

Fig. A.14: Elastic response spectrum (acceleration) of Imperial Valley Earthquake –El Centro (1979)

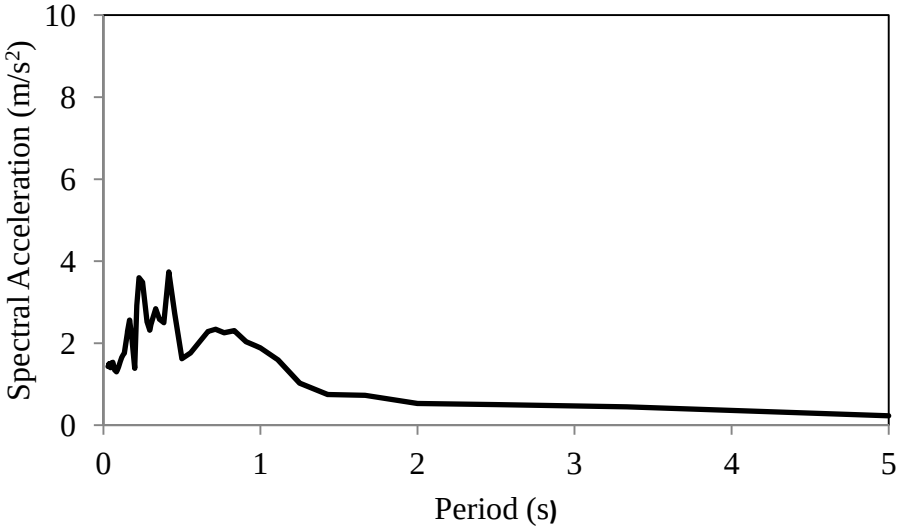

Fig. A.15: Elastic response spectrum (acceleration) of Morgan Hill-Gilroy 4 Earthquake (1984)

APPENDIX B

LINEAR AND NONLINEAR DYNAMIC ANALYSES RESULTS FOR 20-STOREY BUILDING VARIANTS

B.1 NATURAL MODE SHAPES OF 20-STOREY BUILDING VARIANTS

Figs B.1 to B.12 present the elastic mode shapes of the four 20-storey building models considered in the present study (namely R-20-4, S1-20-4, S2-20-4 and S3-20-4). All of these four building models have four bays. These mode shapes are obtained from modal analysis carried out using computer software SAP 2000.

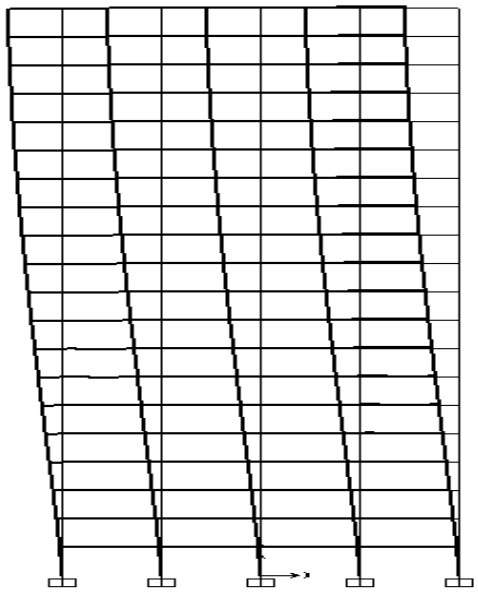

Fig. B.1: First mode shape of R-20-4 building model

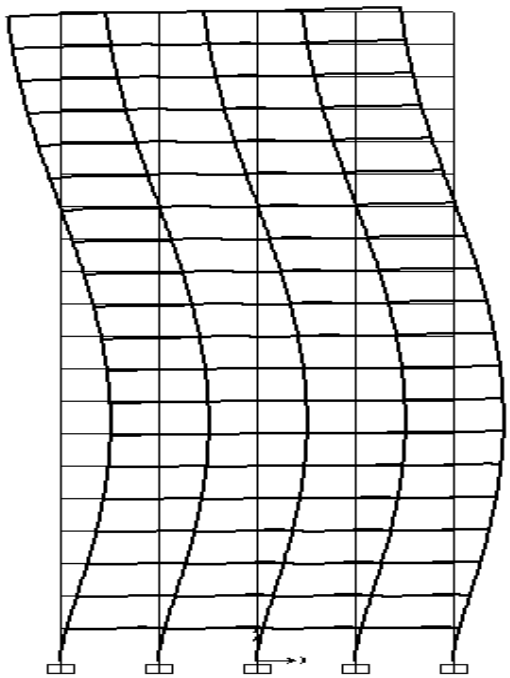

Fig. B.2: Second mode shape of R-20-4 building model

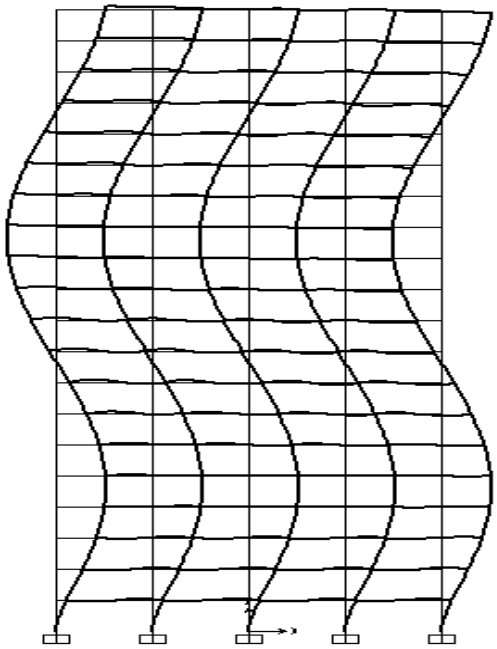

Fig. B.3: Third mode shape of R-20-4 building model

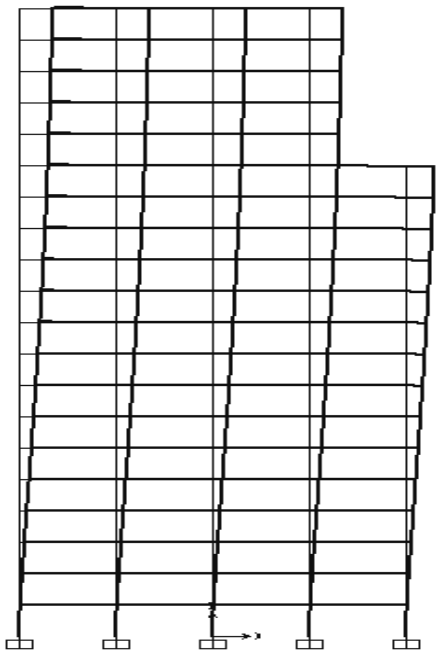

Fig. B.4: First mode shape of S1-20-4 building model

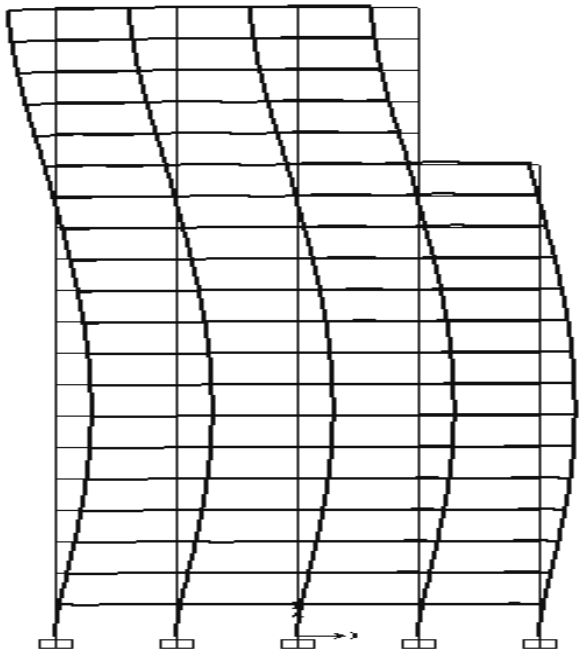

Fig. B.5: Second mode shape of S1-20-4 building model

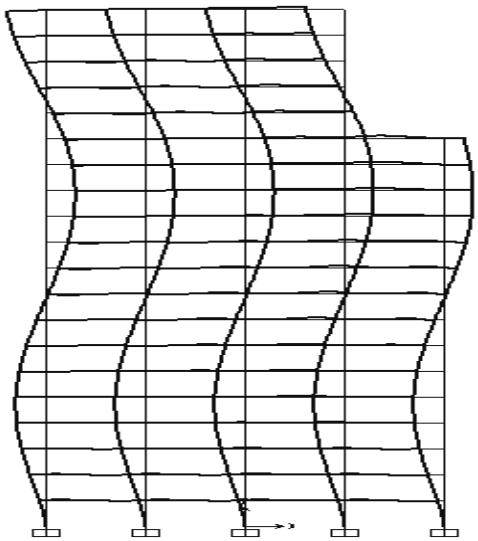

Fig. B.6: Third mode shape of S1-20-4 building model

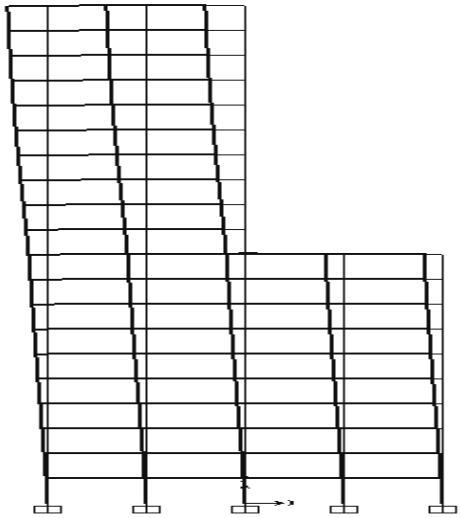

Fig. B.7: First mode shape of S2-20-4 building model

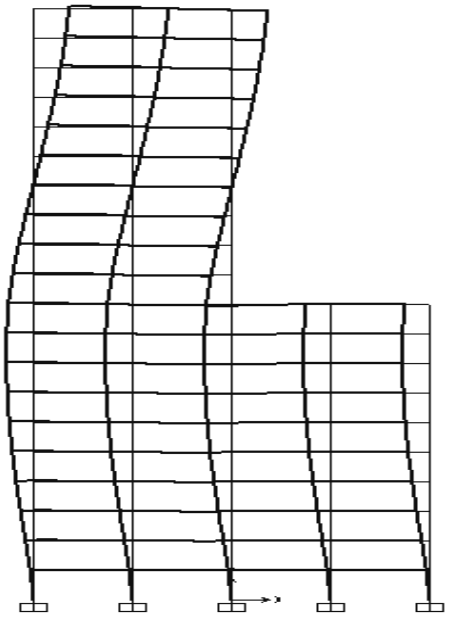

Fig. B.8: Second mode shape of S2-20-4 building model

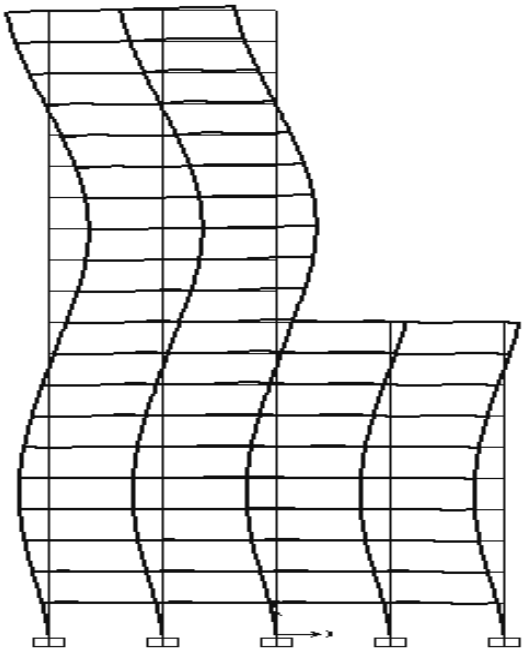

Fig. B.9: Third mode shape of S2-20-4 building model

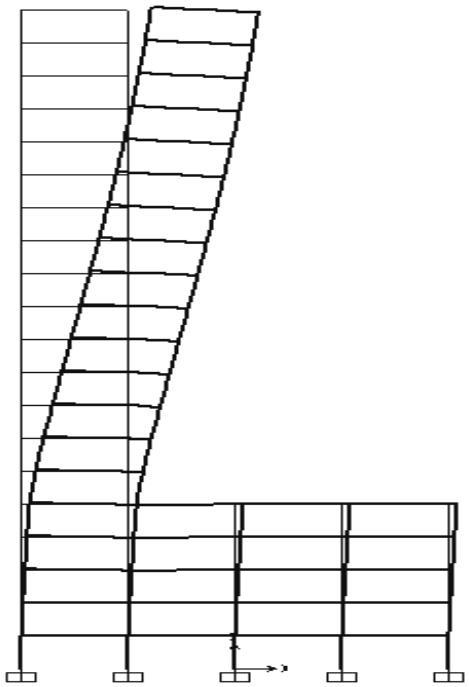

Fig. B.10: First mode shape of S3-20-4 building model

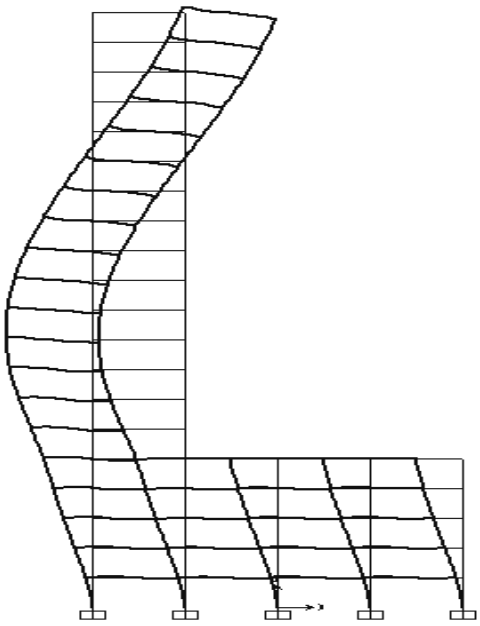

Fig. B.11: Second mode shape of S3-20-4 building model

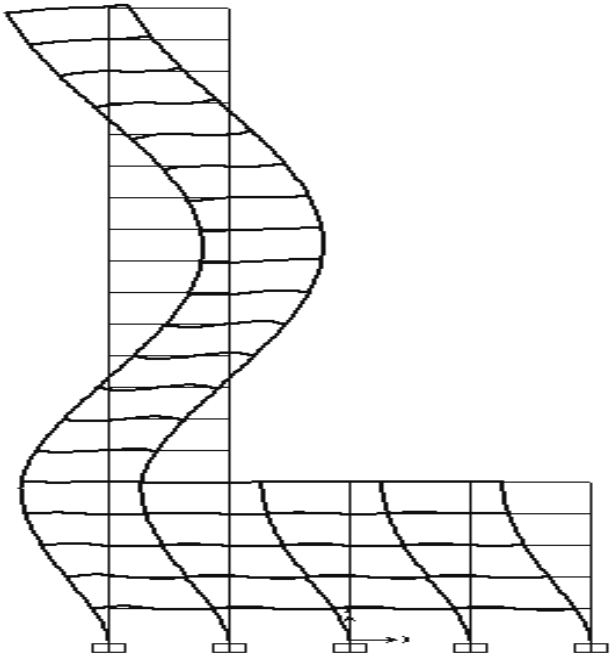

Fig. B.12: Third mode shape of S3-20-4 building model

Table B.1 presents the normalised modal participation factors for the four 20-storey buildings for first three modes. Modal participation factors defined as follows:

$$\Gamma_i = \frac{\{\phi_i\}^T [M] \{1\}}{\{\phi_i\}^T [M] \{\phi_i\}} \tag{b.1}$$

where ϕ_i is the mode shape of i^{th} mode. To calculate normalised modal participation factors these mode shape values are normalized, or scaled, with respect to the mass matrix such that:

$$\{\phi_i\}^T [M] \{\phi_i\} = 1 \tag{b.2}$$

Table B.1: Normalised Modal Participation Factors (kN-s^2) for the 20-storey buildings

Building ID	Mode-1	Mode-2	Mode-3
R-20-4	40.64	15.13	8.63
S1-20-4	39.31	14.37	8.56
S2-20-4	32.9	17.09	8.41
S3-20-4	20.27	16.2	12.99

B.2 DISTRIBUTION OF HINGES

Figs. B.13 to B.17 presents the distribution of hinges at collapse for an eight-storey four-bay setback building (S2-8-4) as obtained from pushover analysis using five different load patterns. It is found from these figures that distribution of hinges, and thereby collapse mechanism, of the building are identical for triangular and Mode-1 load pattern. This correlates the pushover curve of the building under these two load patterns (refer Fig.).

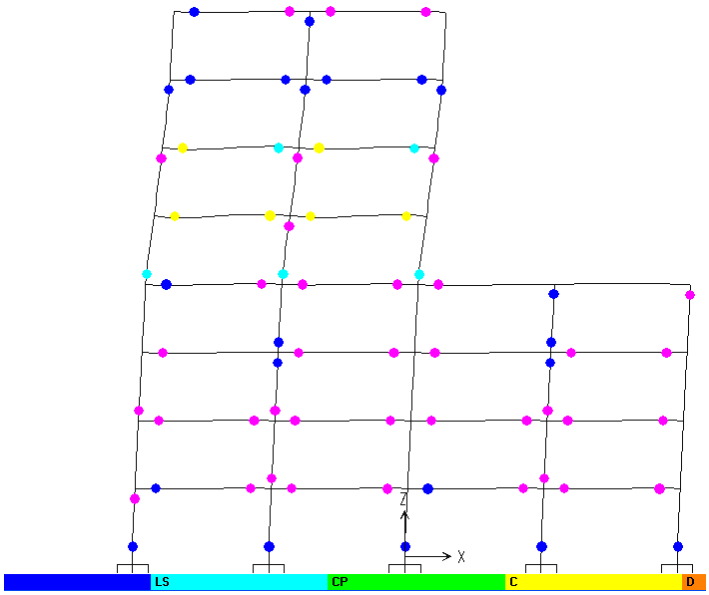

Fig. B.13: Distribution of hinges in S2-8-4 model by triangular load pattern

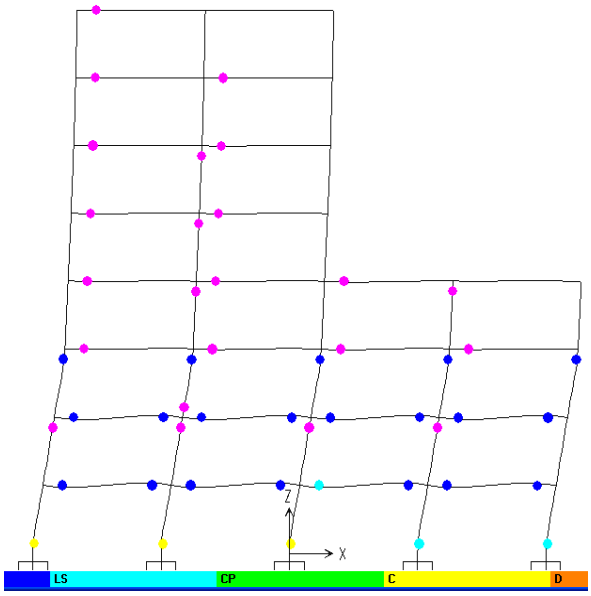

Fig. B.14: Distribution of hinges in S2-8-4 model by uniform load pattern

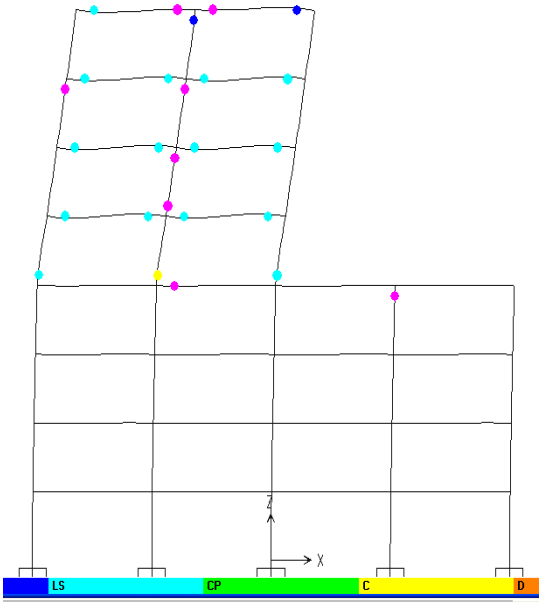

Fig. B.15: Distribution of hinges in S2-8-4 model by UBPA load pattern

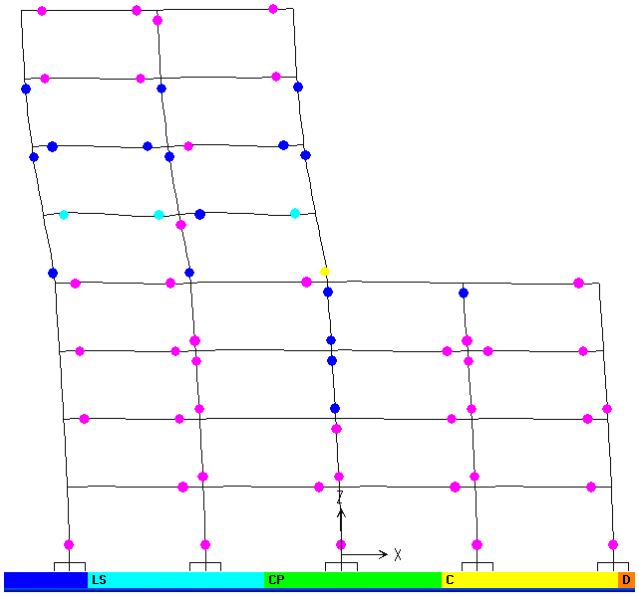

Fig. B.16: Distribution of hinges in S2-8-4 model by MODE-1 load pattern

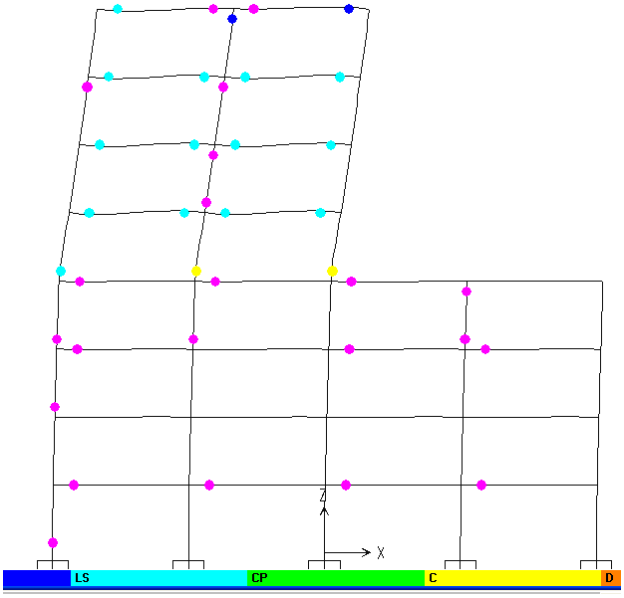

Fig. B.17: Distribution of hinges in S2-8-4 model by IS- 1893 load pattern

Figs. B.18 to B.21 present the distribution of hinges at collapse for four eight-storey four-bay regular and setback buildings as obtained from pushover analysis using triangular

load pattern. These figures show the change in collapse mechanism due to the change in setbacks in the building models for the same load pattern.

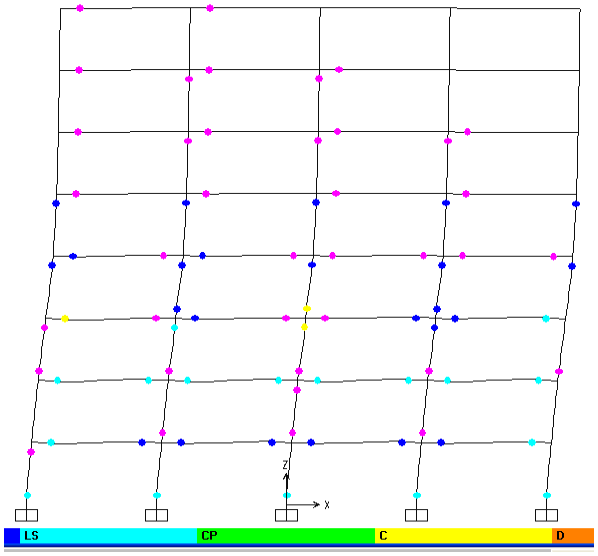

Fig. B.18: Distribution of hinges in R-8-4 model by triangular load pattern

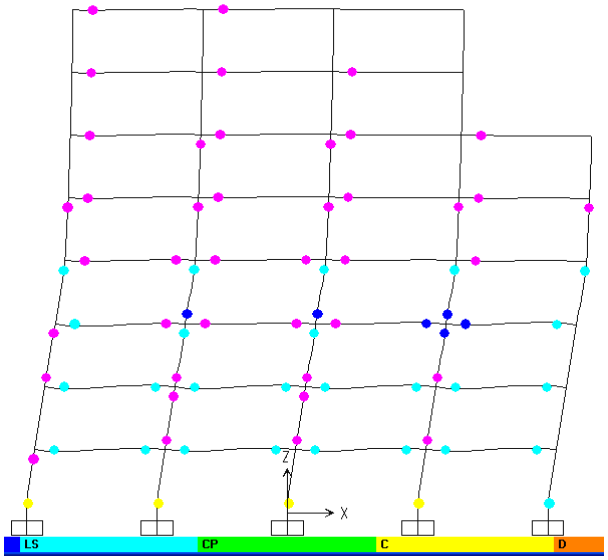

Fig. B.19: Distribution of hinges in S1-8-4 model by triangular load pattern

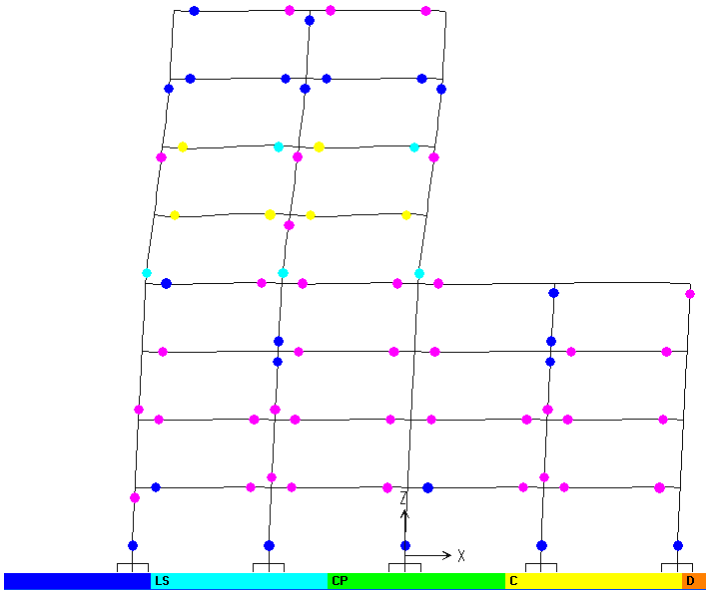

Fig. B.20: Distribution of hinges in S2-8-4 model by triangular load pattern

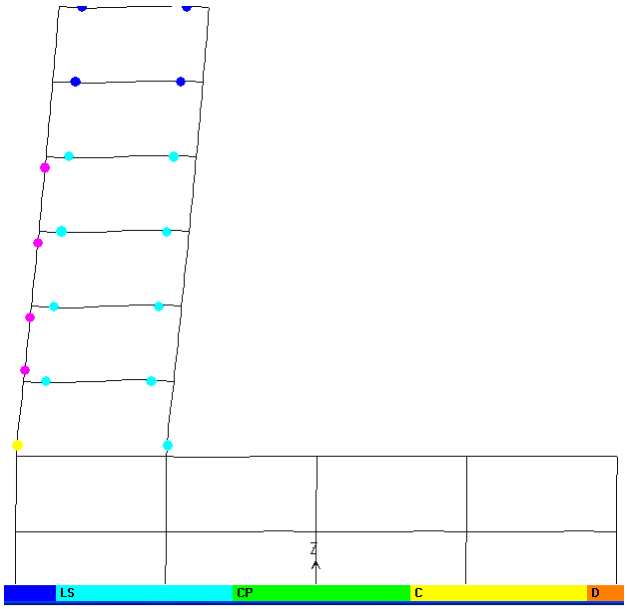

Fig. B.21: Distribution of hinges in S3-8-4 model by triangular load pattern

REFERENCES

1. **ACI 318** (2005). "Building code requirements for reinforced concrete and commentary" ACI 318-05/ACI 318R-05, American Concrete Institute.

2. **Akkar, S.D.** and **Metin, A.** (2007). Assessment of Improved Nonlinear Static Procedures in FEMA-440. *Journal of Structural Engineering* ASCE, **133**(9), 1237-1246.

3. **Akkar, S.D.**, and **Miranda, E.** (2005). Statistical evaluation of approximate methods for estimating maximum deformation demands on existing structures. *Journal of Structural Engineering,* ASCE, **131**(1), 160–172.

4. **Akkar, S.**, and **Özen, Ö** (2005). Effect of peak ground velocity on deformation demands for SDOF systems. *Earthquake Engineering and Structural Dynamics*, **34**, 1551–1571.

5. **Antoniou S.**, **Rovithakis A.** and **Pinho R.** (2002). Development and verification of a fully adaptive pushover procedure, *Proceedings Twelfth European Conference on Earthquake Engineering,* London, UK, Paper No. 822.

6. **Aschheim, M.A.**, **Maffei, J.**, and **Black, E.F.** (1998). Nonlinear static procedures and earthquake displacement demands. *Proceedings of 6th U.S. National Conference on Earthquake Engineering,* Seattle, Paper 167.

7. **ATC 40** (1996), Seismic Evaluation and Retrofit of Concrete Buildings: Vol. 1, Applied Technology Council, USA.

8. **Athanassiadou, C.J.** (2008) Seismic performance of R/C plane frames irregular in elevation. *Engineering structures*. **30**, 1250-1261.

9. **Aydinoğlu, M.N.** (2003). An incremental response spectrum analysis procedure based on inelastic spectral displacements for multi-mode seismic performance evaluation, *Bulletin of Earthquake Engineering,* No. 1, 3-36.

10. **Bracci, J.M.**, **Kunnath, S.K.** and **Reinhorn, A.M.** (1997). Seismic performance and retrofit evaluation of reinforced concrete structures. *Journal of Structural Engineering*, **123**(1), 3-10.

11. **BS 8110** Part 1 and 2 (1997) Structural Use of Concrete, Code of Practice for Design and Construction, British Standards Institute.

12. **Chintanapakdee, C.** and **Chopra, A.K.** (2004) Seismic response of vertically irregular frames: Response history and modal pushover analyses. *ASCE Journal of Structural Engineering*. **130**(8), 1177-1185.

13. **Chopra, A.K.**, and **Chintanapakdee, C.** (2001). Comparing response of SDF systems to near-fault and far-fault earthquake motions in the context of spectral regions. *Earthquake Engineering and Structural Dynamics,* **30**(10), 375–388.

14. **Chopra, A.** and **Chintanapakdee, C.** (2004). Inelastic deformation ratios for design and evaluation of structures: Single degree of freedom bilinear systems. *ASCE Journal of Structural Engineering.* **130**(9), 1309-1319.

15. **Chopra, A.K.**, and **Goel, R.K.** (1999). Capacity-demand-diagram methods for estimating seismic deformation of inelastic structures: SDF systems. Report No. PEER-1999/02, Pacific Earthquake Engineering Research Center, University of California, Berkeley, California.

16. **Chopra, A.K.**, and **Goel, R.K.** (2000). Evaluation of NSP to estimate seismic deformation: SDF systems. *Journal of Structural Engineering,* ASCE, **126**(4), 482–490.

17. **Chopra, A.K.**, and **Goel, R.K.** (2000b). Building period formulas for estimating seismic displacements. *Earthquake Spectra*, **16**(2), 533–536.

18. **Chopra, A.K.** and **Goel, R.K.** (2001). A modal pushover analysis procedure to estimate seismic demands for buildings: Theory and preliminary evaluation. PEER Report 2001/03, Pacific Earthquake Engineering Research Center, College of Engineering, University of California, Berkeley.

19. **Chopra, A.K.** and **Goel, R.K.** (2002). A modal pushover analysis procedure for estimating seismic demands for buildings. *Earthquake Engineering and Structural Dynamics*, **31**, 561-582.

20. **Chopra, A.K. and Goel, R.K.** (2004) A modal pushover analysis procedure to estimate seismic demands for unsymmetric-plan buildings. *Earthquake Engineering and Structural Dynamics.* **33**, 903-927.

21. **Chopra, A. K.**, **Goel, R. K.**, and **Chintanapakdee, C.** (2003). Statistics of Single-Degree-of-Freedom Estimate of Displacement for Pushover Analysis of Buildings. *Journal of Structural Engineering* ASCE, **129**(4), 449-469

22. **Chopra, A.K., Goel, R.K.** and **Chintanapakdee, C.** (2004). Evaluation of a modified MPA procedure assuming higher modes as elastic to estimate seismic demands. *Earthquake Spectra*. **20**(3), 757-778.

23. **Chugh, R.** (2004) "Studies on RC Beams, Columns and Joints for Earthquake Resistant Design", M. Tech. Project Report, Indian Institute of Technology Madras, Chennai, India.

24. **Dinh, T.V.** and **Ichinose, T.** (2005) Probabilistic estimation of seismic story drifts in reinforced concrete buildings. *ASCE Journal of Structural Engineering.* **131**(3), 416-427.

25. **Eurocode 8** (2004), Design of Structures for Earthquake Resistance, Part-1: General Rules, Seismic Actions and Rules for Buildings, European Committee for Standardization (CEN), Brussels.

26. **Fajfar, P.** (2000). A nonlinear analysis method for performance-based seismic design. *Earthquake Spectra*, **16**(3), 573–592.

27. **FEMA 273** (1997). NEHRP Guidelines for the seismic rehabilitation of buildings. *Federal Emergency Management Agency*, Applied Technology Council, Washington D.C., USA.

28. **FEMA 274** (1997). NEHRP Commentary on the Guidelines for the Seismic Rehabilitation of Buildings. *Federal Emergency Management Agency*, Applied Technology Council, Washington D.C., USA.

29. **FEMA 356** (2000), Prestandard and Commentary for the Seismic Rehabilitation of Buildings, American Society of Civil Engineers, USA.

30. **FEMA 440** (2005), Improvement of nonlinearstatic seismic analysis procedures, Applied Technology Council (ATC) Washington, D.C.

31. **Goel, R.K.** and **Chopra A.K.** (1997) Period formulas for moment resisting frame buildings. *ASCE Journal of Structural Engineering.* **123**(11), 1454-1461.

32. **Goel, R.K.** and **Chopra, A.K.** (2004) Evaluation of modal and FEMA pushover analyses: SAC buildings. *Earthquake Spectra*. **20**(1), 225-254.

33. **Gupta, A.**, and **Krawinkler, H.** (2000). Estimation of seismic drift demand for frame structures. *Earthquake Engineering and Structural Dynamics*, **29**(9), 1287–1305.

34. **Gupta, B.** and **Kunnath, S.K.** (2000). Adaptive spectra-based pushover procedure for seismic evaluation of structures. *Earthquake Spectra*, **16**(2), 367-391.

35. **IS 456** (2000). Indian Standard for Plain and Reinforced Concrete - Code of Practice, Bureau of Indian Standards, New Delhi.

36. **Jan, T.S.**; **Liu, M.W.** and **Kao, Y.C.** (2004), An upper-bond pushover analysis procedure for estimating the seismic demands of high-rise buildings. *Engineering structures*. 117-128.

37. **Kalkan, E.** and **Kunnath S.K.** (2007) Assessment of current nonlinear static procedures for seismic evaluation of buildings. *Engineering Structures*. **29**, 305-316.

38. **Karavasilis, T.L., Bazeos, N.** and **Beskos, D.E.** (2008) Seismic response of plane steel MRF with setbacks: Estimation of inelastic deformation demands. *Journal of Constructional Steel Research*. **64,** 644-654.

39. **Krawinkler, H.** and **Seneviratna, G.D.P.K** (1998). Pros and cons of a pushover analysis of seismic performance evaluation. Engineering Structures, **20**, 452-464.

40. **Menjivar, M.A.L.** (2004). A Review of Existing Pushover Methods for 2-D Reinforced Concrete Buildings. Ph.D. Thesis, ROSE School, Italy.

41. **Miranda, E.** (1999). Approximate seismic lateral deformation demands in multistory buildings. *Journal of Structural Engineering,* ASCE, **125**(4), 417–425.

42. **Miranda, E.** (2001). Estimation of inelastic deformation demands of SDOF systems. *Journal of Structural Engineering,* ASCE, **127**(9), 1005–1012.

43. **Miranda, E.**, and **Ruiz-García, J.** (2002). Evaluation of approximate methods to estimate maximum inelastic displacement demands. *Earthquake Engineering and Structural Dynamics,* **31**(3), 539–560.

44. **Moghadam, H.** and **Hajirasouliha, I.** (2006). An investigation on the accuracy of pushover analysis for estimating the seismic deformation of braced steel frames. *Journal of Constructional Steel Research.* **62**, 343-351.

45. **Moghadam, A.S.** and **Tso, W.K.** (2002). A pushover procedure for tall buildings. *Proceedings of the 12th European Conference on Earthquake Engineering*, Paper 395. Elsevier Science Ltd.

46. **Mwafy, A.M.** and **Elnashai, S.A.** (2000). Static pushover versus dynamic-to-collapse analysis of RC buildings. Engineering Seismology and Earthquake Engineering Section, Imperial College of Science, Technology and Medicine. Report No. 00/1.

47. **Mwafy, A.M.** and **Elnashai, A.S.** (2001) Static pushover versus dynamic collapse analysis of RC buildings. *Engineering structures*. **23,** 1-12.

48. **Papanikolaou, V.K.**; **Elnashai, A.S.** and **Pareja, J.F.** (2005). Limits of Applicability of Conventional and Adaptive Pushover Analysis for Seismic Response Assessment. Report, Mid-America Earthquake Center, University of Illinois at Urbana-Champaign.

49. **Pam, H.J.**, and **Ho, J.C.M.** (2001). Flexural Strength Enhancement of Confined Reinforced Concrete Columns, Structures and Buildings Journal, **146**(4), 363-370.

50. **Panagiotakos, T.B.** and **Fardis, M.N.** (2001). Deformation of Reinforced Concrete Members at Yielding and Ultimate, *ACI Structural Journal*, **98**(2), 135-148.

51. **Paret, T.F.**, **Sasaki, K.K.**, **Elibeck, D.H.** and **Freeman, S.A.** (1996). Approximate inelastic procedures to identify failure mechanism from higher mode effects. *Proceedings of the Eleventh World Conference on Earthquake Engineering*, Acapulco, México, Paper 966.

52. **Park, H.**; **Eom, T.** and **Lee, H.** (2007). Factored Modal Combination for Evaluation of Earthquake Load Profiles. *Journal of Structural Engineering* ASCE, **133**(7), 956-968.

53. **Park R**, and **Paulay T.** (1975). Reinforced concrete structures. John Wiley & Sons, New York.

54. **Paulay, T** and **Priestley, M.J.N.** (1992). Seismic design of reinforced concrete and masonry buildings, John Wiley and Sons, New York

55. **PCM 3274** (2003). Primi Elementi in Materia di Criteri Generali per la Classificazione Sismica del Territorio Nazionale e di Normative Tecniche per le Costruzioni in Zona Sismica (in Italian), Roma, Italy.

56. **Priestley, M.J.N.** (1993). Myths and fallacies in earthquake engineering-conflicts between design and reality, *Bulletin of New Zealand National Society for Earthquake Engineering*, **26**(3), 329-341.

57. **Requena, M.** and **Ayala, G.** (2000). Evaluation of a simplified method for the determination of the non-linear seismic response of RC frames. *Proceedings of the Twelfth World Conference on Earthquake Engineering*, Upper Hutt, New Zealand. Paper 2109.

58. **Ruiz-Garcia, J.** and **Miranda E.** (2003). Inelastic displacement ratios for evaluation of existing structures. *Earthquake Engineering and Structural Dynamics.* **32**, 1237-1258.

59. **SAP 2000** (2009). Integrated Software for Structural Analysis and Design, Version 14.0. Computers & Structures, Inc., Berkeley, California.

60. **Sasaki, K.K.**; **Freeman, S.A.** and **Paret, T.F.** (1998). Multi-mode pushover procedure (MMP) – a method to identify the effects of higher modes in a pushover analysis. *Proceedings of the Sixth U.S. National Conference on Earthquake Engineering*, Oakland, California.

61. **Sharooz, B.B.** and **Moehle, J.P.** (1990). Seismic Response and Design of Setback Buildings. Journal of Structural Division, ASCE, **116**(5), 2002-2014

62. **Tjhin, T., Aschheim, M.** and **Hernandez-Montes, E.** (2005) Estimates of peak roof displacement using "Equivalent" single degree of freedom systems. *ASCE Journal of Structural Engineering.* **131**(3), 517-522.

63. **Tjhin, T., Aschheim, M.** and **Hernandez-Montes, E.** (2006) Observations on reliability of alternative multiple mode pushover analysis methods. *ASCE Journal of Structural Engineering.* **132**(3), 471-477.

64. **Wong, C.M.** and **Tso, W.K.** (1994) Seismic loading for buildings with setbacks. *Canadian Journal of Civil Engineering*, **21**(5), 863-871.

65. Combined Strong-Motion Data. The Center for Engineering Strong Motion Data, < http://www.strongmotioncenter.org/> (Aug. 11, 2012)

66. **Ghobarah, A.** (2001). Performance-based Design in Earthquake engineering: State Of Development. *Engineering Structures*. **23**, 878-884.

67. **Chandler, A.M. and Mendis, P.A.** (2000). Performance of Reinforced Concrete Frames Using Force and displacement Based Seismic Assessment Methods. *Engineering Structures.* **22**, 352-363.

68. **Soni, D.P. and Mistry, B.B.** (2006) Qualitative review of seismic response of vertically irregular building frames. *ISET Journal of Earthquake Technology*, **43**, 121-132.

69. **Naeim, F., Bhatia, H., and Roy, M.L.** (2001) Performance Based Seismic Engineering, Chapter 15.

LIST OF PAPERS SUBMITTED ON THE BASIS OF THIS THESIS

REFEREED JOURNALS

1. **Tripathy, R. and Sarkar, P.** (2012). Pushover Analysis of R/C Setback Building Frames. *International Journal of Civil Engineering*, IASET, **1**, 70-92.

PRESENTATION IN CONFERENCES

2. **Tripathy, R.** and **Sarkar, P.** (2010) Improved displacement coefficients for target displacement estimation of setback building. *Proceedings of International Conference on Innovative World of Structural Engineering-ICIWSE-2010"*, September 17-19, 2010, Aurangabad, Maharashtra, India.